POLITECNICO
MILANO 1863

School of Architecture Urban Planning Construction Engineering

Master of Science in Building and Architectural Engineering

A.Y. 2018 / 2019

STEEMBER

Steel and timber for a high-rise building in Queens, New York

Final thesis

Supervisor:

Prof. Gabriele Masera

Chinnici Federico - 898197

Maranesi Marco - 905512

THESIS SUMMARY

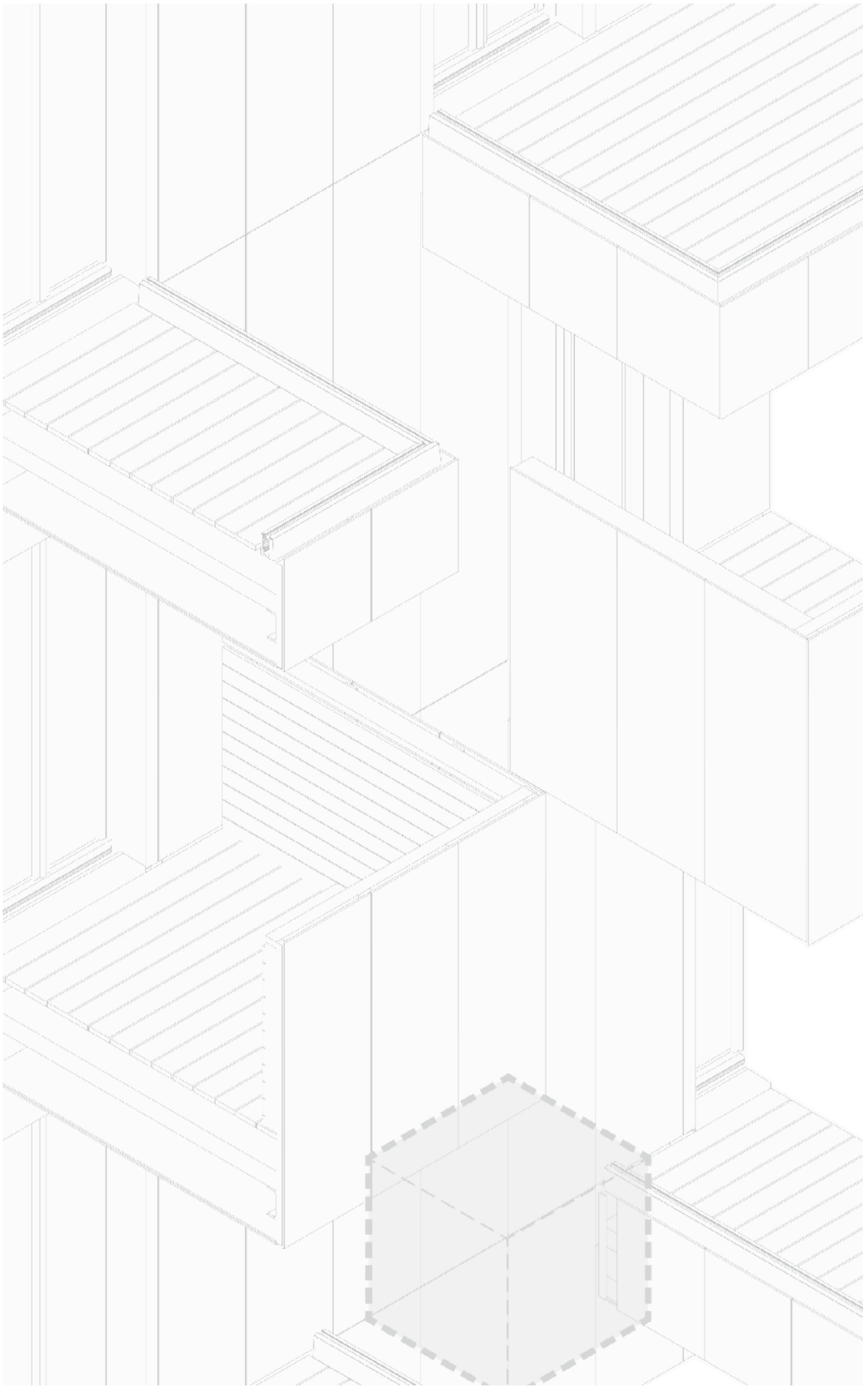

00 SINOSSI ABSTRACT

SINOSSI

Il progetto “Steember” nasce da un bando per studenti volto alla riqualificazione di un lotto abbandonato del Queens, New York.

Tale competizione architettonica viene organizzata annualmente dalla “Association of Collegiate Schools of Architecture” (ACSA) ed è intitolata “TIMBER IN THE CITY: Urban Habitats Competition”.

Il concorso nasce da una partnership tra il Binational Softwood Lumber Council (BSLC), l’Association of Collegiate Schools of Architecture (ACSA) e la School of Constructed Environments (SCE) della Parsons School of Design. Lo scopo è di coinvolgere gli studenti nell’immaginare la trasformazione delle città esistenti attraverso edifici sostenibili ed alimentati da risorse rinnovabili, offrendo una costruzione conveniente ed originale utilizzando il legno in maniera sia tradizionale che innovativa. L’obiettivo principale è l’interrelazione tra residenze e cambiamento climatico progettando ambienti di vita e di lavoro confortevoli ed accoglienti.

La competizione sfida i partecipanti a re-immaginare un lotto abbandonato sul lungofiume del Queens come un ambiente salutare, moderno ed accogliente per la popolazione della città.

Per sviluppare tale progetto si è partiti da una iniziale fase di analisi urbana per individuare le esigenze della popolazione locale, considerando che una città enorme e cosmopolita come New York è già piena di servizi e diversità. Successivamente, è stato prima organizzato e quindi implementato un programma funzionale col fine di sviluppare un planivolumetrico efficiente ed allo stesso tempo architettonicamente di pregio. L’intero progetto comprende tre edifici con tre diverse funzioni: un centro educativo per la prima infanzia, un centro sportivo comunitario e una torre residenziale, che è l’edificio principale.

Ci si è quindi concentrati sul progetto architettonico dell’edificio residenziale che è stato studiato nel dettaglio con l’obiettivo di garantire diverse tipologie di unità abitative, al fine di coprire numerosi segmenti di mercato. Il processo di progettazione ha seguito un approccio integrato, considerando insieme gli aspetti architettonici, strutturali, tecnologici ed energetici.

Grande attenzione è stata dedicata alla parte tecnologica ed energetica del progetto, con l’obiettivo di raggiungere un edificio che può essere principalmente prefabbricato e che è estremamente confortevole e sostenibile energeticamente.

Ogni aspetto del progetto è stato sistematicamente sviluppato con analisi approfondite e specifiche simulazioni. Infine, i risultati sono stati implementati secondo un approccio multidisciplinare individuando la migliore soluzione architettonica ed ingegneristica.

Politecnico di Milano, Master of Science in Building and Architectural Engineering
Steember - Steel and timber for a high rise building in Queens, New York
Chinnici Federico - **Maranesi** Marco

ABSTRACT

“Steember” is the result of study for the redevelopment and requalification of an abandoned lot situated in Queens, New York City, on Vernon Boulevard.

The guidelines are given by The Association of Collegiate Schools of Architecture (ACSA) which yearly organizes “TIMBER IN THE CITY: Urban Habitats Competition” for the 2018-2019 Academic Year.

The competition is a partnership between the Binational Softwood Lumber Council (BSLC), the Association of Collegiate Schools of Architecture (ACSA) and the School of Constructed Environments (SCE) at Parsons School of Design. The program is intended to engage students to imagine the transformation of existing cities through sustainable buildings from renewable resources, offering expedient, affordable construction, innovating with new and traditional wooden materials, and designing healthy living and working environments. The main focus is the interrelationship between housing, healthy, early childhood education and climate change.

The competition challenges participants to re-imagine a vacant waterfront site in Queens, New York as a vibrant and vanguard model of healthy, biophilic living for the future of the city.

The first part of the project started with a phase of urban analysis to pinpoint the requirements of the local population, considering that a huge and cosmopolitan city as New York is already full of functions and diversity. After this, a functional program was organized and then implemented in an urban masterplan. The whole project contains three buildings with three different functions: an early childhood education centre, a community wellness centre and the main building which is a residential high rise tower.

The architectural project of the residential building was studied with the goal to guarantee different typologies of dwelling units, in order to cover many residential market segments. The design process followed an integrated approach, considering together the architectural, structural, technological and energy aspects.

Great attention has been paid to the technological and energy part of the project, with the goal to reach a building which can be mostly prefabricated and which is extremely energy efficient.

Every aspect of the project has been systematically developed with deep analysis and specific software simulations. Then, the results have been implemented according to a multi-disciplinary approach, finding out the best architectural or engineering solution.

01 TIMBER IN CONSTRUCTION

1.1 – INTRODUCTION

Timber for construction is one of the many forest products used around the world. It is used in buildings both large and small, in particular for residential houses and villas in North Europe, Canada and the USA. There is a huge global supply for the foreseeable future, and although there is a worldwide trend towards deforestation, it is generally due to clearing land for agriculture rather than logging for timber.

While there are limitless possible designs, and construction is based on both engineering and cultural practice, timber has a high strength to weight ratio and is used most efficiently in structures where it is carrying a lot of its own self-weight.

Figure 1.1 - The timber frame of a building

In many areas of the world, building codes limit timber buildings height well below what is possible in wooden structures. Important questions relating to the service life of timber structures are also frequent, affected predominantly by their fire performance and moisture sensitivity, and how this can be extended through the modification of the natural material or using effective design details.

Construction-grade timber and engineered forest products are some of the highest value products from trees. This suggests that structural use is important for economies that rely on forestry. Furthermore, following primary use as structure, there are many secondary or tertiary uses for timber construction waste that retains its value.

The environmental benefits, such as the circular economy and the low level of CO_2 emission, have been demonstrated on some projects, but are not always easy to quantify or generalize.

1.2 – PROCESSING TIMBER PRODUCTS

The global supply chain for wood is a complex network of harvesters, processors, and distributors. In Europe, the most commonly used structural timbers are derived from sustainably managed coniferous forests.

Although typically not as dense and hard as hardwood species, softwoods are cheap and largely available in useful dimensions and can be easily engineered into timber products that optimise their structural properties. These enhanced properties equate to high strength-to-weight ratios that allow timber to compete with other more energy or carbon-intensive construction materials.

1.2.1 – THE HARVESTING OF ROUNDWOOD

The first stage of timber processing is the wood harvest. Felled trees with branches removed and trunks cut to length for transportation are commonly referred to as “Roundwood”. European, American an Canadian forests are some of the most intensively managed in the world. Depending on the topography, a common silvicultural practise typically ranges from:

- clear-felling and artificial regeneration of whole stands of plantation trees;
- natural regeneration under shelterwood;
- mixed and natural regeneration combined with selective cutting.

Clear fell harvesting with specially customised harvester heads offers the greatest efficiencies in terms of annual yield due to the regular trunk diameter of consecutive farmed trees.

Thinning and clear-cut harvesting operations are increasingly mechanised for optimum productivity. Mechanized round wood harvesting is carried out by customised cutting heads mounted on a hydraulically controlled harvester vehicle.

1.2.2. – DRY TIMBER

As a natural material, wood is susceptible to fungal degradation, but below 20% moisture content there is no issue occurring.

International standards for structural timber specify an upper limit of 20% moisture content for “dry graded” timber in order for it to receive a defined strength grading. Dried timber also provides a more receptive substrate for glueing and is lighter to transport. Moreover, timber’s durability and environmental resistance can be further enhanced by thermal and chemical treatments.

As a hygroscopic material, timber fluctuates in moisture content relative to its surrounding environment. It is therefore important to dry timber before using it in order to match the anticipated moisture content within a building environment and avoid excess movement as the timber naturally dries to its equilibrium service condition. The embodied moisture is generally represented as a percentage of the dry weight of timber, and the moisture content which wood tends towards in a given temperature and humidity is called the “equilibrium moisture content”.

Figure 1.2 - Dry wooden logs and timber

Harvested softwood can have moisture content in excess of 100%, consisting of “free water” held in the cell cavities and chemically ‘bound water’ in the cell walls. Once all free water has been removed from the cell cavities a state known as the ‘fibre saturation point’ (FSP) is reached. Timber at or above the FSP is termed “green” wood, and above the FSP, the mechanical properties of the wood are not seen to vary with moisture content. Below the FSP, there is a strong correlation of mechanical properties with moisture content, with strength and stiffness increasing with decreasing moisture content. Timber also shrinks as it dries below the FSP. Since the equilibrium moisture content in buildings is commonly around 8–12%, well below the FSP of 25–35%, depending on species, drying of the ‘bound water’ is necessary to avoid shrinkage in service. In order to improve the mechanical properties of wood and for dimensional stability in use, it is, therefore, necessary to reduce the natural moisture content with natural or accelerated drying.

There are many methods of removing moisture from timber including air, solvent, microwave and supercritical CO_2 drying, but the most common in the sawn softwood industry is convective or condensing kiln drying. Convective drying, although energy and equipment intensive, offers the most accelerated means of drying dimensional timber for the market. The “kiln” is defined as an enclosed structure, typically 30–100 m^3, that provides controlled heating, air circulation, humidification and ventilation. Heating is achieved by indirect (steam, hot water, thermal liquid, electricity) or direct means (gas/oil burner). It is common for convective kilns to enclose overhead or side fans that circulate warm or dehumidified air through and around an open stack of sawn timber. Equipment factors which can affect the efficiency of softwood drying include standards of kiln thermal insulation and the modulation of fans’ speed during different stages of the drying cycle.

Studies in the Pacific Northwest of the United States have shown that of all the manufacturing processes associated with converting roundwood into dimensional timber, kiln drying of softwood consumes the most energy accounting for up to 92% of total manufacturing energy. By contrast, harvesting and regeneration of forestry have been shown to have a minimal impact, accounting for just 5% cumulative energy use.

Structural timber is most commonly used within a dry building envelope but it can be exposed to excess moisture on-site during the construction phase. To ensure equilibrium moisture content relative to its anticipated service environment, structural timber is dried to between a 12–20% moisture content. Structural timber unprotected on-site is likely to be exposed to elevated levels of moisture. Once the timbers are enclosed within the finished building, the 20% moisture content would then decrease in situ to 12%. Service class definitions are important as excessive shrinkage in-situ can cause warping and cracking of timber, reducing its mechanical properties.

1.2.3 – DIMENSIONAL TIMBER PROCESSING

During the processing of roundwood, approximately 50% is recovered as viable board and plank products, with the remaining dust, shavings and fibre byproducts typically used as biomass fuel or as fibre in engineered timber panel products with a market value. In order to ensure that processed timber materials are able to support anticipated maximum loads as part of a structure in service, it is necessary to strength grade each piece of dimensional timber. This grading standard permits a structural engineer to specify a chosen strength class of timber and use the characteristic strength values of that class in their design calculations.

Aside from dimensional sawn timber, softwoods are also processed into structurally optimised building materials known as “engineered timber”. The benefits of these wood composites manufactured from laminated timbers, adhesives and other materials, include increased dimensional stability, more homogeneous mechanical properties and greater durability. The following are the families of these materials.

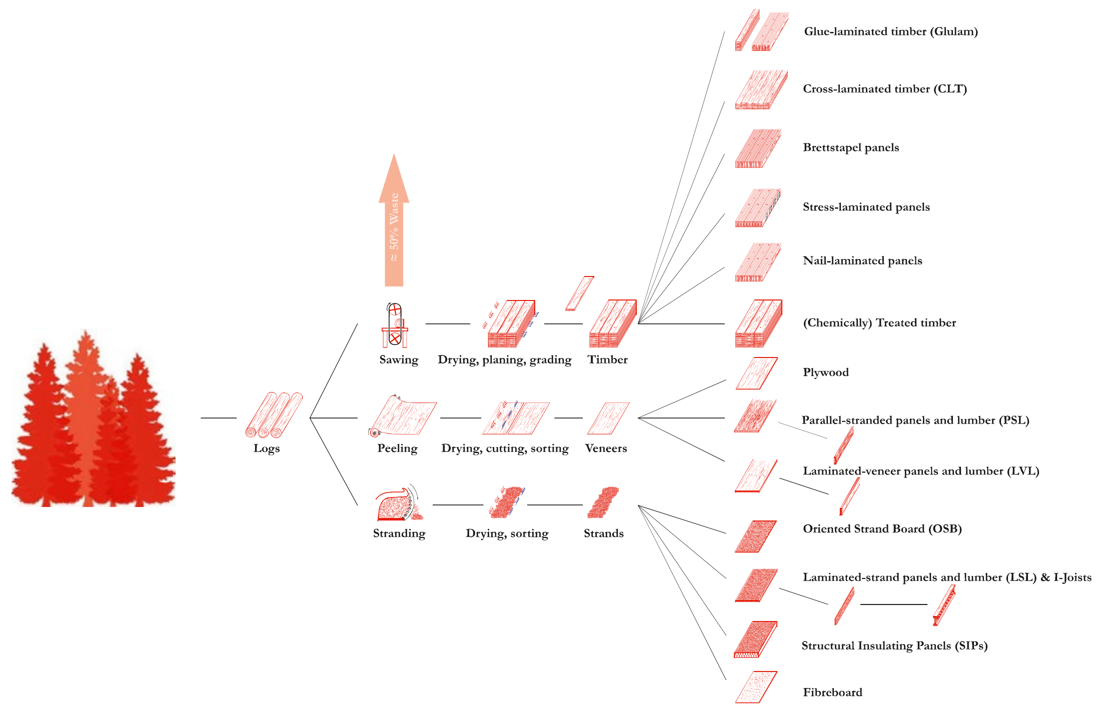

Figure 1.3 - The processing chain of engineered timber products, P.H. Fleming

GLULAM

Defined as a structural timber member composed by at least two essentially parallel laminations which may comprise of one or two boards side by side having finished thicknesses from 6 mm up to 45 mm. These are typically used to fabricate curved and long beams limited only by methods of transport. Glulam is allocated to specific strength classes defined in BS EN 14080:2013.

LAMINATED VENEER LUMBER (LVL)

A reconstituted dimensional timber that is common twice the strength of dimensional timber of the same species manufactured from rotary peeled veneers of spruce, pine or douglas fir of 3 mm thickness. Usually, the veneer grain is oriented in a single direction but cross-grained sections are also manufactured to offer tailored mechanical properties. Lengths of short veneer are jointed end-to-end with a scarf joint allowing limitless dimensional lengths.

Politecnico di Milano, Master of Science in Building and Architectural Engineering
Steember - Steel and timber for a high rise building in Queens, New York
Chinnici Federico - **Maranesi** Marco

STRUCTURAL VENEER LUMBER (SVL)

It consists of outer plies of LVL laminated together to form linear structural components. Douglas fir veneers of 2.5 mm laminated in the direction of grain parallel to the longitudinal direction of the board or beam are common.

CROSS-LAMINATED TIMBER (CLT or XLAM)

Timber panels that are made of a minimum of three layers of sawn softwood stacked on top of one another at right angles and glued to form a thickness in the range 50–500 mm suitable for floor, wall and roof elements of up to 13.5 m in length.

I-JOISTS

Whilst these are more expensive and deeper than solid timber joists for an equivalent strength and stiffness, composite IJoists are more dimensionally stable due to their homogeneous OSB web and the relatively small dimension of the solid timber or LVL flanges.

PANEL TYPES

Structural prefabricated sandwich panels consisting of an insulation layer encased between two skins of fibre or oriented strand board.

Many engineered panel products are also combined with dimensional timber frame constructions to add bracing and shear strength including Plywood, Oriented Strand Board (OSB, Medium Density Fiber Board (MDF) and Fiberboard.

Although engineered timber products have superior structural properties as compared to dimensional timber, the necessity for adhesives use, negatively impacts the embodied energy burden of these products.

1.3 – TIMBER FOR STRUCTURAL USE

1.3.1 – WHAT TO BUILD WITH TIMBER

Timber is one of the three structural materials currently used in the construction of large structures, along with steel and reinforced concrete. If timber is used in the types of building in which it is most structurally efficient then the timber we harvest can do the most to reduce the environmental impact of construction.

Hardwood is slightly stronger, and softwood slightly weaker, although timber cannot match modern high-strength concrete in compression. Timber is less stiff than concrete, and both materials are far less stiff and strong than steel, however, it has a low density compared with these other conventional structural materials.

This results in efficiency for long-span or tall structures, in which a significant part of the load to be carried by the structure is its own weight. When those loads are resisted purely in tension or compression, the strength-to-weight or elastic modulus-to-weight ratio are measures of the mass of material required to achieve a structure of a given area, height or span.

As a consequence, timber is a particularly structurally efficient material in structures, or parts of structures, in which a high proportion of the load to be resisted is the self-weight of the structure itself.

Examples are roofs, some bridges and the gravity load resisting system of tall buildings. In structures for which the load to be resisted is largely independent of the weight of the structure, such as the wind load on a tall building, the higher absolute strength of steel or reinforced concrete may make them more efficient, in terms of the amount of material required to achieve the function of the building.

In case of an earthquake, the force imposed on the structure by shaking depends strongly on its mass, with heavier structures experiencing larger seismic forces. Light timber residential buildings have therefore been seen to perform better in seismic events, compared to havier structures such as reinforced concrete or masonry ones.

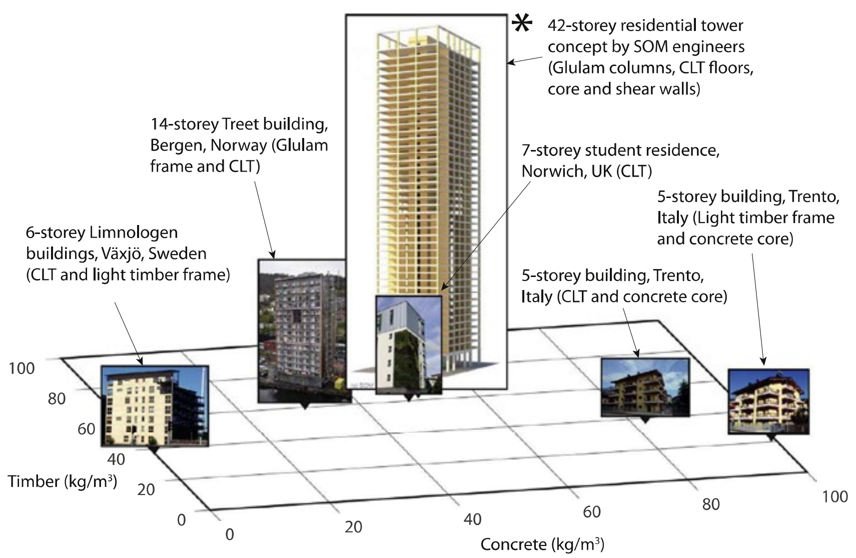

Figure 1.4 - Material usage, in terms of mass, in multi-storey timber buildings. The axes show the mass of timber and concrete used per m³ of each building.

Politecnico di Milano, Master of Science in Building and Architectural Engineering
Steember - Steel and timber for a high rise building in Queens, New York
Chinnici Federico - **Maranesi** Marco

1.3.2 – BUILDING TALL BUILDINGS WITH TIMBER

In the last decade, a handful of six-storey timber buildings and higher have been constructed, and engineers have begun to look at the possibility to build much taller with timber.

The complexity of the structure of a tall building increases with the height of the structure. In low-rise buildings, where the forces to be resisted are relatively low, it is possible to resist lateral loads by bending stresses in walls which form a vertical cantilever. This is the approach widely used in cross-laminated timber construction in buildings.

Using a frame around the perimeter of the building, rather than a core in the interior, can load all members in uniform tension and compression.

A common system for very tall buildings in concrete is a central core coupled with shear walls near the outer edges of the building by stiff link beams.

For buildings up to about six storeys, CLT uses substantially more timber to achieve the same function as a light timber frame building. For buildings over six stories, CLT together with light timber frame may require less timber than CLT alone, and for buildings taller than ten stories the only proven system to date is the external glulam frame supporting internal CLT units.

The structural material is only part of the material used in a building. Some materials, such as glazing, cladding and mechanical and electrical fittings may be unrelated to the structure. The use of wood as a structural material, however, often has the consequence of introducing other materials to achieve certain performance requirements: concrete is often used to achieve acceptable floor vibration, for example, and gypsum boards for fire resistance or concrete to achieve thermal mass results.

02 PRELIMINARY ANALYSIS

2.1 – GENERAL OVERVIEW

The object of the thesis is the development of a complete project for a new residential centre in Queens, New York City. The guidelines are given by the competition “Timber in the city” which challenges participants to re-imagine a vacant waterfront on Vernon Boulevard.

The City of New York also called either New York City (NYC) or simply New York (NY), is the most populous city in the United States. In 2018 the estimated population was of 8,398,748 distributed over a land area of about 784 km^2, this is why New York is also the most densely populated city in the United States.

Located at the southern tip of the state of New York, the city is the centre of the New York metropolitan area and one of the world’s most populous megacities. It is considered as the cultural, financial, and media capital of the world, and exerts a significant impact upon commerce, entertainment, research, technology, education, politics, tourism, art, fashion, and sports in the whole world. It is home to the headquarters of the United Nations and is also an important centre for international diplomacy.

NYC is the most ethnically and religiously diverse, famously congested, and the most attractive urban centre in the country. No other city has contributed more images to the world’s consciousness of American people and culture, becoming a symbol of the whole nation. Its own symbol is, actually, the Statue of Liberty, but the metropolis is itself an icon. New York City incorporates five boroughs, each of which is a separate county of the State of New York. These five boroughs – Brooklyn, Queens, Manhattan, The Bronx, and Staten Island – were merged into a single city in 1898.

Figure 2.1 - The flag of the city of New York

2.1.1– THE BOROUGHS

New York was formed when the independent city of Brooklyn, the portion of Westchester county called the Bronx, Staten Island, and large parts of Queens county were added to Manhattan following a referendum. Much of the new territory was still rural, and less of half of all roads in the expanded city were paved. The five boroughs, which were all soon designated counties of New York state, became the basic municipal administrative units.

The first section of the subway system opened in 1904, and soon all the boroughs were connected by anew and efficient transportation except Staten Island. The ever-growing number of bridges, tunnels, and highways were designed in those years to facilitate commerce in the city, and even nowadays these take, along with the subways, hordes of commuters into Manhattan in the morning and return them home at night.

Figure 2.2 - The five boroughs of New York City

MANHATTAN

More than 30 million tourists visit New York annually, but most of these rarely see much beyond Manhattan island, which is the smallest city borough. Divided by 12 north-south avenues and crossed by 220 east-west streets, Manhattan is easily understood and infinitely enchanting. It is the original New York, boasts the world’s largest collection of skyscrapers, and is overloaded with cultural, commercial and political institutions and places of enduring interest. Even according to residents of the other boroughs, Manhattan is “the city,” the administrative, business, and financial centre of the metropolis. In no other part of New York are there such stark contrasts between rich and poor, as it results to be the city with the highest number of billionaires in the whole world.

Figure 2.3 - The view of the Manhattan skyline

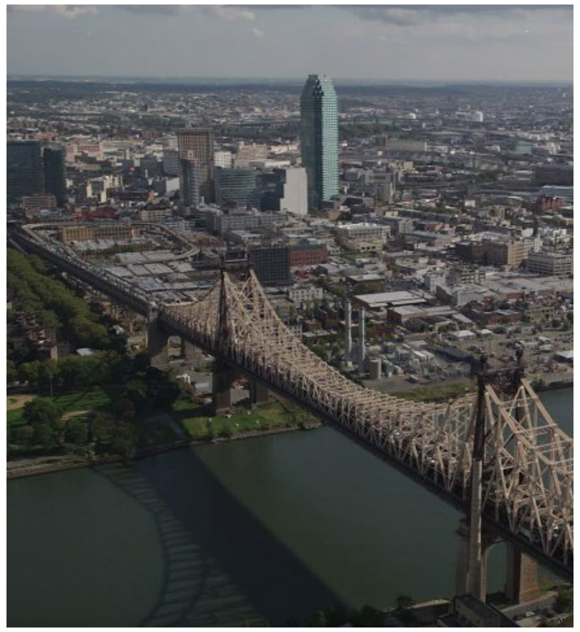

Figure 2.4 - A view of Queens and the iconic Queensboro bridge, connecting Queens to Manhattan

QUEENS

Queens county would constitute a major American city were it not a part of New York. Its land is more than one-third of the city with a primarily middle-class population owning private homes. In the 19th century, Queens had two shorelines that attracted the wealthy, and it served as the final resting place for deceased New Yorkers.

A pleasing mix of the urban and the rural environment, Queens was the centre of the silent-film industry until displaced by Hollywood in the late ‘20s. This growing borough had more than a million inhabitants even before it was linked to the Bronx by three bridges and to Manhattan by the Midtown Tunnel in 1940.

In a diverse and cosmopolitan city as New York, Queens ranks as the most ethnically varied of all the boroughs. It has no visible slum area since its residents are united in rejecting low-income housing and high-rise apartments.

THE BRONX

The Bronx is the northernmost borough and (except for a tiny sliver of Manhattan) the only part of New York on the mainland. It was first settled by farmers and for centuries remained rural, and is also the scene of many conflicts during the American Revolution, but afterwards, it became the area where wealthy politicians and merchants established summer homes.

For more than a decade after the mid-1960s, the Bronx became the scene of urban decay caused by crime, drug dealers and the strain of accepting waves of immigrants. The fires that consumed its buildings and the drug and gang wars that destroyed its young people is what created the famous bad reputation of the area. During the last quarter of the 20th century, the tide of decay reversed, and the Bronx rebounded in remarkable fashion.

BROOKLYN

The most populous borough of New York, Brooklyn, is to the east of Manhattan on the western fringe of Long Island. Early in the 19th century, it became the world's first modern commuter suburb, and Brooklyn Heights was transformed into a wealthy residential community.

Contemporary Brooklyn has the independent character of an industrial city. Although the borough has many private homes, the majority of its people live in apartments or upgraded row housing.

STATEN ISLAND

Geographically isolated at the juncture of Upper and Lower New York Bays, Staten Island is 8 km detached from Manhattan by ferry and a mile away from Brooklyn. Its surface is still the least densely populated, most rural part of the city, even though it ranks as the fastest-growing county in the state.

The construction of the Verrazano-Narrows Bridge in 1964 opened the Staten Island to quick development and made it a functional part of city life. Staten Island is the most homogeneous borough in New York; it has the lowest proportion of ethnic minorities and is the youngest and most politically conservative, such that when in 1990 U.S. Supreme Court ordered a reduction in borough power, Staten Islanders endorsed a move to study secession from New York to become an independent city.

2.1.2– THE MULTI-ETHNIC POPULATION

The shifting population base of New York remains its most dramatic story and at the end of the 20th century, representatives of some 200 national groups were counted among its people. The biggest groups are people of European ancestry, Hispanics and African Americans.

The arrival of "new" immigrants from eastern and southern Europe after 1880 again changed Manhattan. Irish and Germans, who by then held a vast proportion of political and economic power, deeply resented Italians, Greeks, Russians, Hungarians, and Poles crowding into their city. Waves of immigrants continue to reach the city also nowadays, continuously increasing these numbers. The Statue of Liberty, more than a century after its dedication in the harbour in 1886, is still the most powerful symbol of New York, as it welcomes newcomers into the city's "golden door".

Politecnico di Milano, Master of Science in Building and Architectural Engineering
Steember - Steel and timber for a high rise building in Queens, New York
Chinnici Federico - **Maranesi** Marco

2.1.3– THE CENTRE OF BUSINESS

By the beginning of the 20th century, New York was the headquarters for more than two-thirds of the top 100 American corporations, and its 25,000 factories manufactured several hundred different industrial products. It led the nation in total factory workers, a number of factories, capital valuation, and product value. New York held its leadership position and provided nearly one million industrial jobs into the '50s.

By constantly enhancing its key economic advantages, New York has remained prosperous even as it underwent change, its strength has always been lying in its diversity. The port, which lost some percentage of its shipping to other cities through the years, is still the busiest port on the East Coast and generates billions of dollars of revenue, creates thousands of jobs, and is the focus of major plans for renewal and renovation. A major portion of the country's software and computer-related industry has located itself in New York and built an urban "Silicon Alley" to mirror California's Silicon Valley. The city's continuing financial supremacy was apparent in the '90s, a decade in which the Dow Jones average quadrupled and in the process, the city became the "economic capital of the world." The vast numbers of bars, restaurants, hotels, health clubs and theatres across New York are necessary to care for and feed the millions of visitors who come to the city annually.

Figure 2.4 - A view of New York's financial district

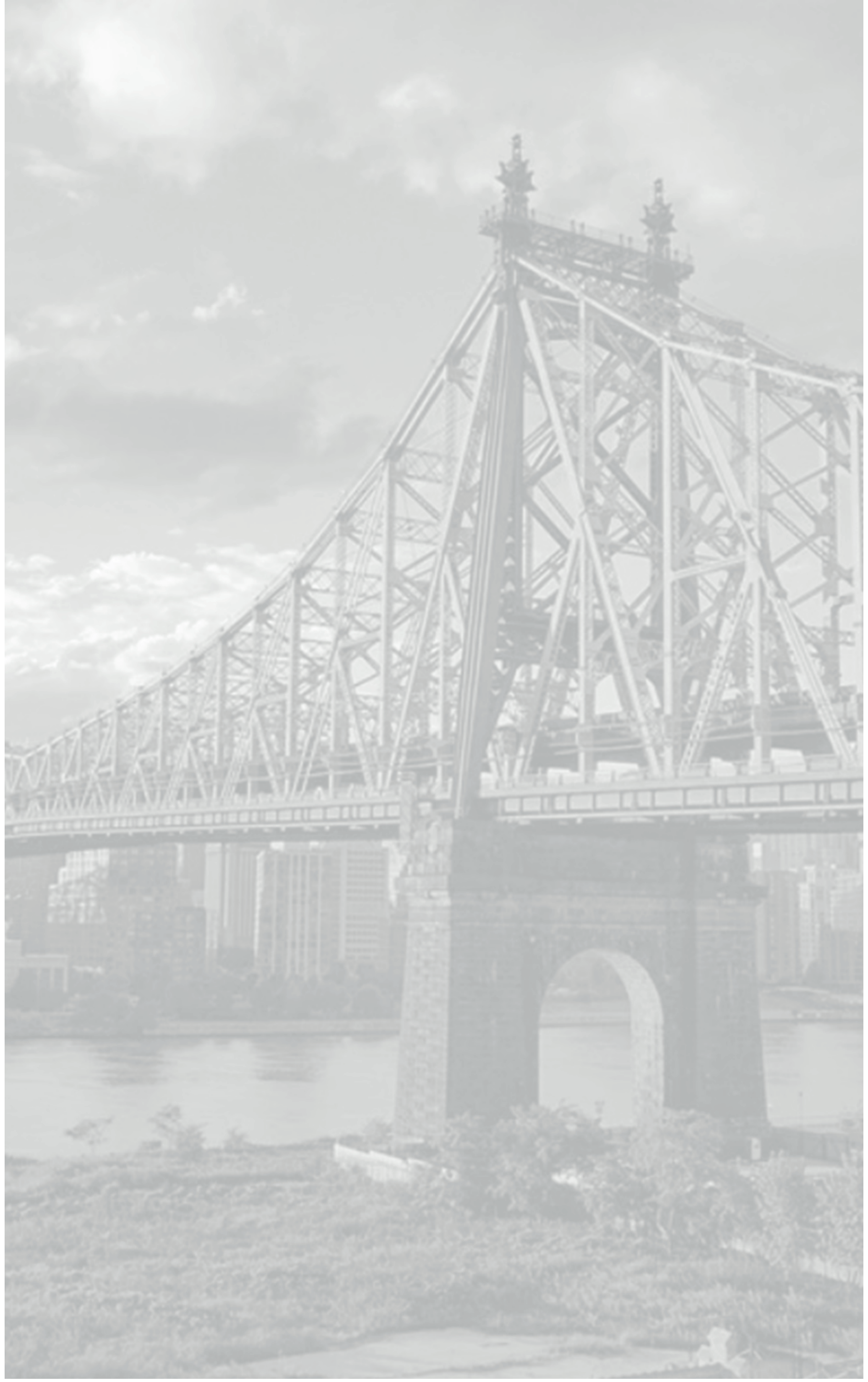

03 SITE ANALYSIS

3.1 – INTRODUCTION

The site of the competition is located at 42-02 and 42-16 Vernon Boulevard in Queens, New York, immediately at the south of the Ed Koch Queensboro Bridge and to the west of the East River overlooking Roosevelt Island. The total area is 10'200 square meters and measures approximately 40 m by 55 m.

The site currently has a flexible and expansive zoning designation that allows for mixed-use development to encourage waterfront development. This zoning allows for a FAR (Floor-to-Area Ratio) of 10 and includes residential along with commercial designations.

Figure 3.1 - The project site

Figure 3.2 - The historical New York Architectural Terracotta works building, built in 1892

Figure 3.3 - The building as it looks today

The waterfront of Queens has undergone a significant transformation over the last two decades, shifting from industrial and warehouse facilities to increasingly mixed-use and public space designations. The competition anticipates that a public waterfront for pedestrians and cyclists will run north-south, connecting Hunter's Point developments in the south up to Rainey Park and Socrates Sculpture Park in the north.

N.Y. ARCHITECTURAL TERRACOTTA WORKS BUILDING

An existing historic structure, called "New York Architectural Terra Cotta Works Building", is located on 42-16 Vernon Boulevard and it is to be kept and integrated into the design of the project. It was the operational headquarter of a once-thriving company that produced the terra cotta for buildings such as Carnegie Hall and the Ansonia Hotel.

Established in 1886, the company was the only major architectural terracotta manufacturer in New York City and, when completed, its facilities were the largest in the country. The company set up its manufacturing operations on the Long Island City waterfront in 1886 and initially kept an office at 38 Park Row in Manhattan. Six years later, its office headquarters were moved to this remarkable building, whose design served to advertise the company's considerable range and skill. According to the building's designation report, it is "the only one of its kind known to survive in the United States".

Politecnico di Milano, Master of Science in Building and Architectural Engineering
Steember - Steel and timber for a high rise building in Queens, New York
Chinnici Federico - **Maranesi** Marco

3.2 – THE I.M.M. INVESTIGATION

IMM stands for Integrated Modification Methodology and it is an innovative design methodology based on a process with the main goal of improving the CAS (Complex Adaptive Systems) energy performance, modifying its constituents and optimizing the architecture of their ligands.

Its approach is fundamentally Holistic, Multi-Layer, Multi-scale. In this methodology, the city is considered as a dynamic Complex Adaptive System comprised by the synergic integration of a number of elementary parts, which through their arrangement and the architecture of their ligands provide a certain physical and provisional arrangement of the CAS. In IMM the emergence process of interaction between elementary parts to form a synergy is named Key categories. These are the products of the synergy between elementary parts, a new organization that emerges not simply as an additive result of the proprieties of the elementary parts. When we alter the interaction between elementary parts and recombine them in a different way, different organizations emerge, but it could also get lost. This explains that added proprieties emerge just when the combination is right.

According to this view, the city is not only a mere aggregation of disconnected energy consumers and the total energy consumption of the city is different from the sum of all of the buildings' consumption.

This considerable gap between the total energy consumption of the city and the sum of all consumers is concealed from the urban morphology and urban form of the city. The IMM investigates the relationships between urban morphology energy consumption and environmental performances by focusing mostly on the 'Subsystems' characterized by physical characters and arrangements.

The main object of this design process is to address a more sustainable and better performing urban arrangement. IMM methodology is based on a multi-stage process composed of four different but fully integrated phases. It shows, through an interconnected Phasing Design Process, how incorporating a wide range of issues makes it possible to improve the metabolism of the city as well as its energy performance.

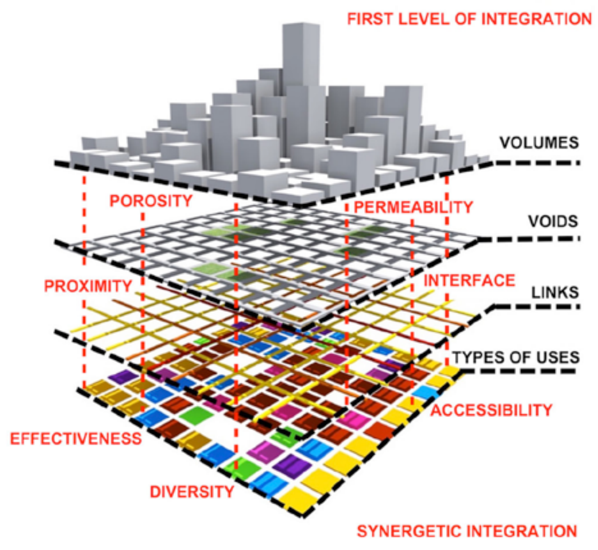

Figure 3.4 - Concept of the I.M.M. investigation

Just like any other system, the built environment is characterized by including parts and subsystems between which there are complex relationships. Accordingly, in the Investigation phase, the system is being broken into its parts. Morphologically speaking, these parts for the cities would be Urban Volume, Urban Void, Links, and Types of Uses. After analyzing the mentioned subsystems individually, the synergy between them is being investigated. Key categories are types of emergency that show how elements come to self-organize or to synchronize their states into forming a new level of organization. Emergence is something new that can't be described by the description of the parts. Emerging properties are the product of the synergies between the parts. In IMM Key Categories are namely: Porosity, Permeability, Proximity, Diversity, Interface, Accessibility, and Effectiveness. Numerous properties of the urban environment like the physical arrangement of the building blocks, car dependency, connectivity, functional arrangement and the performing manner of public transportation are being examined here.

3.2.1 - THE STUDY OF THE NEIGHBOURING AREA

IMM HORIZONTAL INVESTIGATION **VOLUMES**

IMM HORIZONTAL INVESTIGATION **VOIDS**

IMM HORIZONTAL INVESTIGATION TRANSPORTATIONS

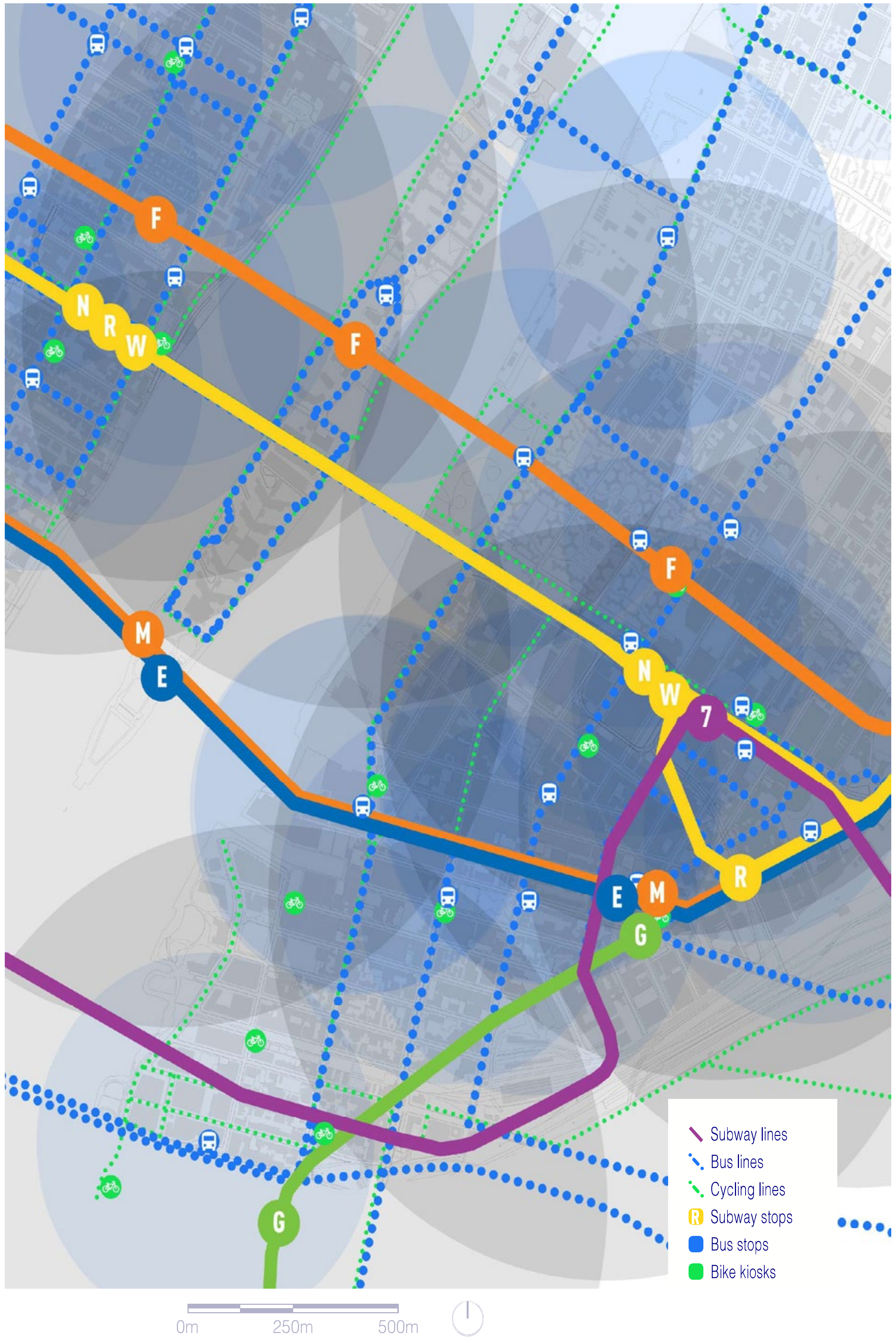

Politecnico di Milano, Master of Science in Building and Architectural Engineering
Steember - Steel and timber for a high rise building in Queens, New York
Chinnici Federico - **Maranesi** Marco

IMM HORIZONTAL INVESTIGATION FUNCTIONS

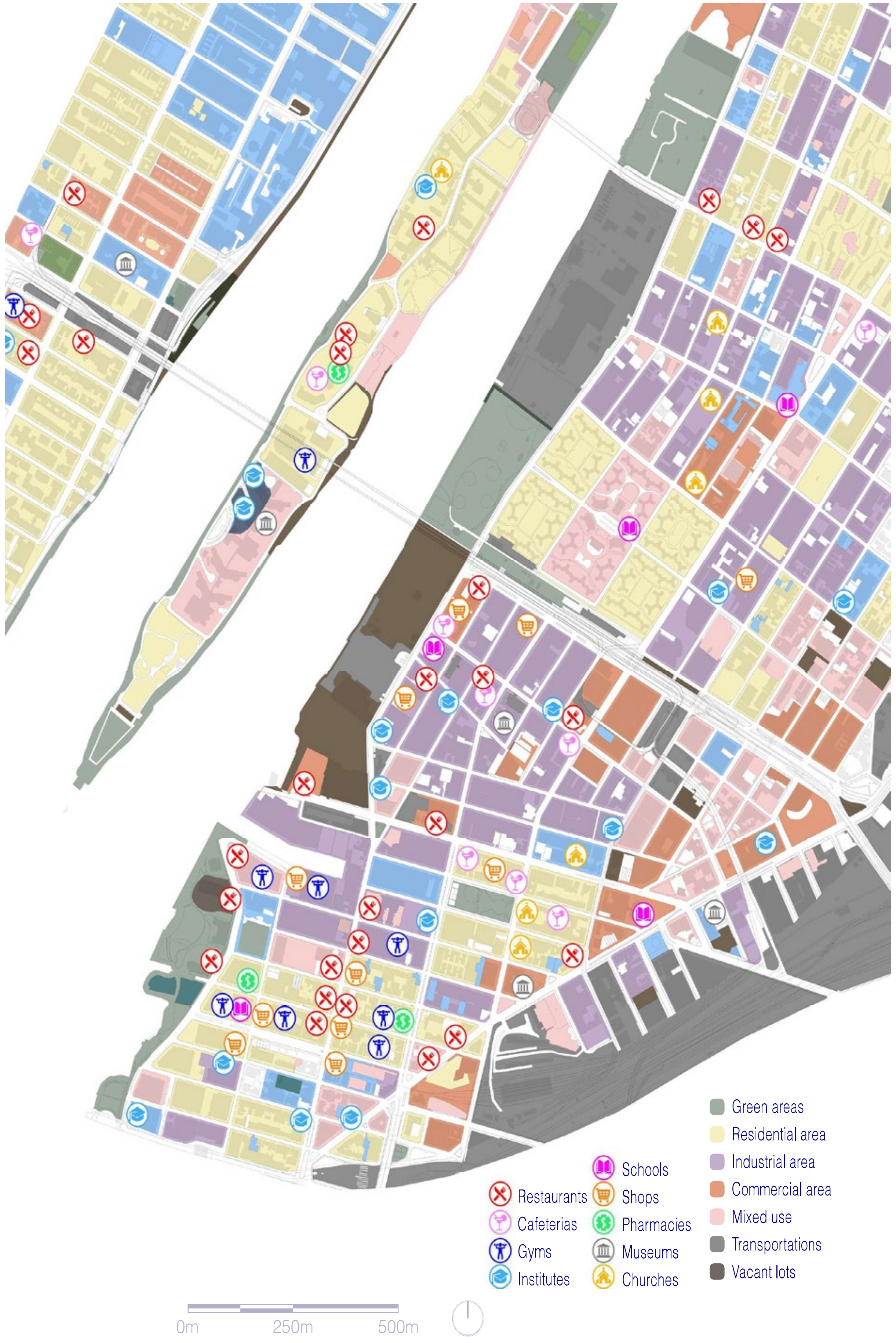

IMM VERTICAL INVESTIGATION

Volumes
Voids

POROSITY

Higher density
Lower density

0m 250m 500m

Politecnico di Milano, Master of Science in Building and Architectural Engineering
Steember - Steel and timber for a high rise building in Queens, New York
Chinnici Federico - **Maranesi** Marco

IMM VERTICAL INVESTIGATION

Volumes
Voids

PERMEABILITY

Higher permeability
Lower permeability

0m 250m 500m

IMM VERTICAL INVESTIGATION

Porosity
Permeability

COMPACTNESS

Politecnico di Milano, Master of Science in Building and Architectural Engineering
Steember - Steel and timber for a high rise building in Queens, New York
Chinnici Federico - **Maranesi** Marco

IMM VERTICAL INVESTIGATION

Functions
Voids

DIVERSITY

IMM VERTICAL INVESTIGATION + Transportations Voids **INTERFACE**

IMM VERTICAL INVESTIGATION + Diversity Interface **COMPLEXITY**

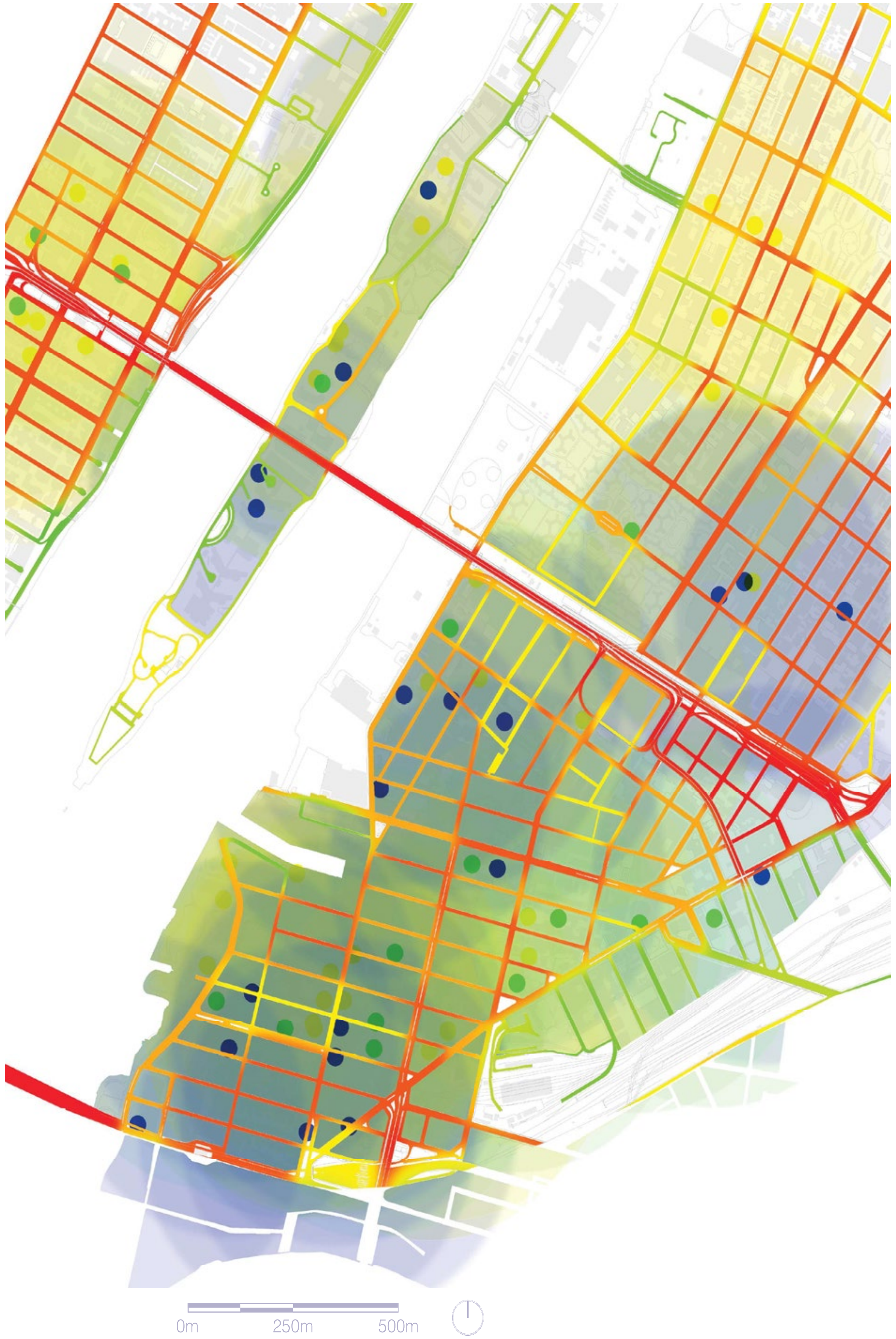

IMM VERTICAL INVESTIGATION

Volumes
Functions

PROXIMITY

Politecnico di Milano, Master of Science in Building and Architectural Engineering
Steember - Steel and timber for a high rise building in Queens, New York
Chinnici Federico - **Maranesi** Marco

IMM VERTICAL INVESTIGATION

Volumes
Transportations

EFFECTIVENESS

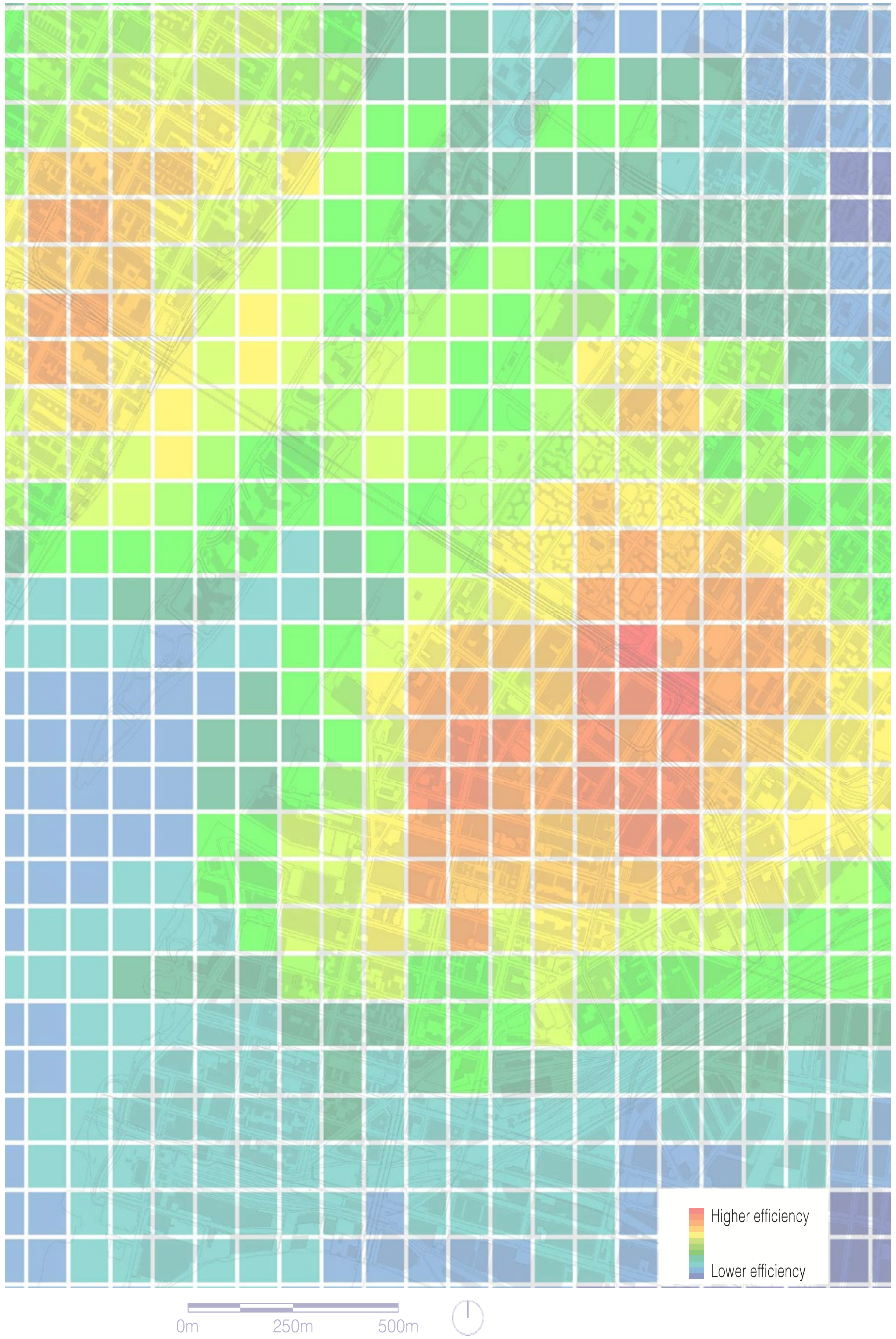

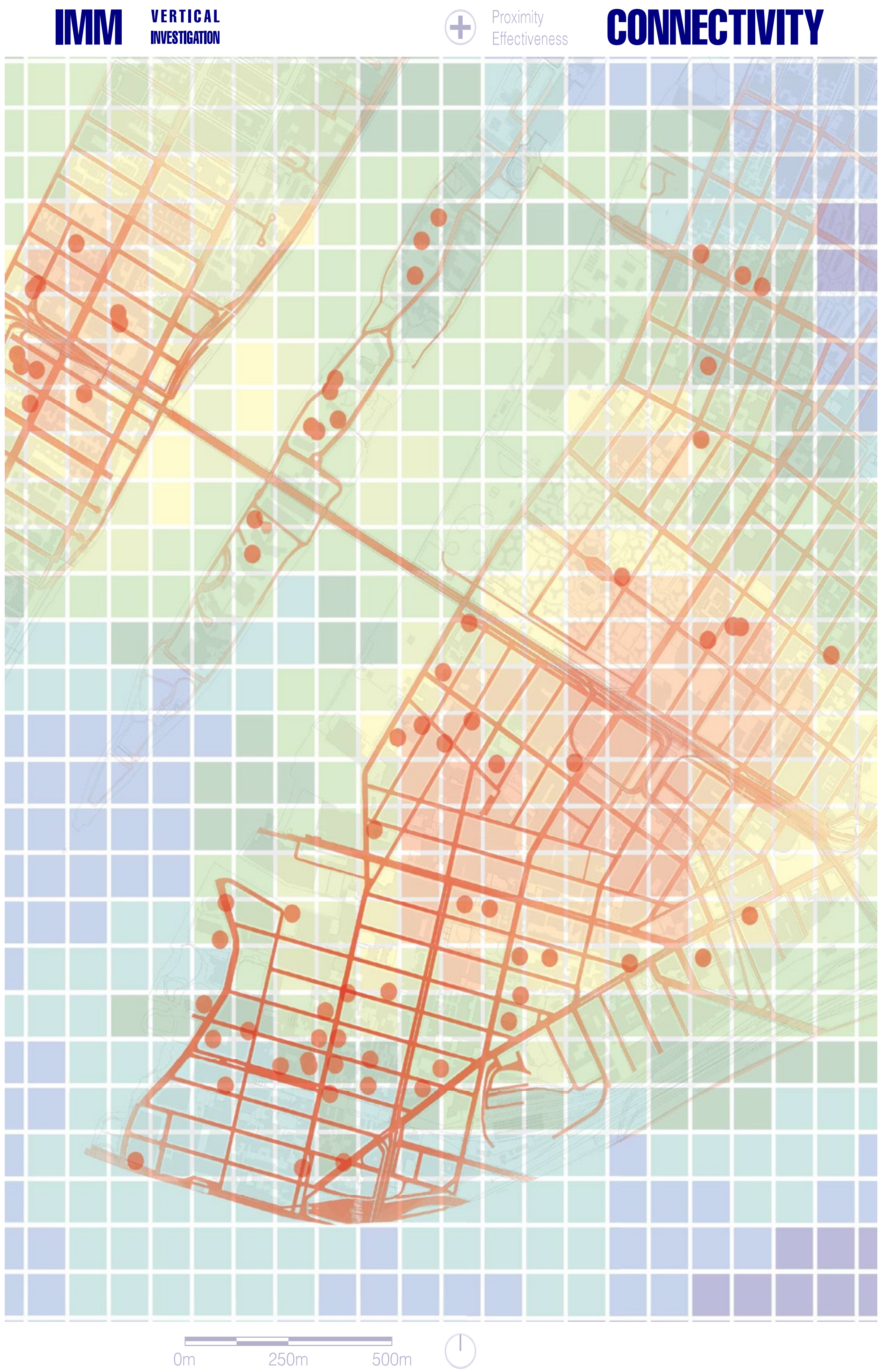

Politecnico di Milano, Master of Science in Building and Architectural Engineering
Steember - Steel and timber for a high rise building in Queens, New York
Chinnici Federico - **Maranesi** Marco

3.3 – THE SURROUNDING AREA

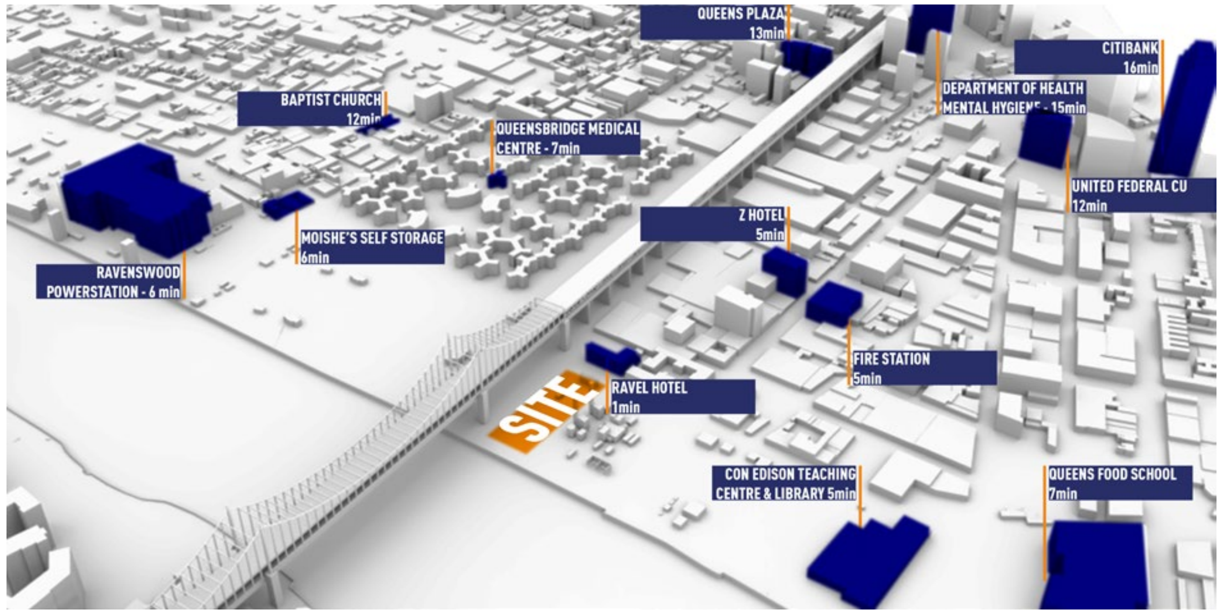

Figure 3.5 - Noticeable buildings nearby the building site

The most important road in the area of the building site is Vernon Boulevard, a street running parallel to Roosevelt Island from Socrates Sculpture Park to Hunters Point and Long Island City.

In the quarter, it is possible to notice the effect of the urban gentrification: the district is under redevelopment and what once was a set of poor and degraded buildings, is now reaching new value thanks to the construction and retrofitting of modern and functional architectures.

Just like the whole city of New York, the surrounding area of the site is a touristic attraction due to its proximity to Roosevelt Island, but most of the buildings around the vacant lot are industrial and residential. Primary and secondary functions are present and not far one from each other. The long waterfront is the object of redesign and improvement, in order to become an attraction and a liveable area useful for inhabitants and tourists.

What the city is aiming to is a complete requalification of the old industrial navy zone, as it is happening in Brooklyn, with the complete retrofitting of buildings. A clear example is the Brooklyn Navy Yard, an old shipyard and industrial complex where, in the renovated buildings, more than 330 businesses are now located, collectively employing about 7'000 people.

Figure 3.6 - The Manhattan skyline seen from Roosevelt island

Figure 3.7 - The Queens skyline seen from Roosevelt island, object of redevelopment and gentrification

3.4 – THE CLIMATE ANALYSIS

The city of New York is generally known for a humid continental climate. The weather is strongly influenced by two continental air masses: one is warm and humid and comes from the southwest, while the other one is cold and dry from the northwest.

Summers tend to be warm and humid, while winters are generally cold and snowy due to the cold air coming from the north.

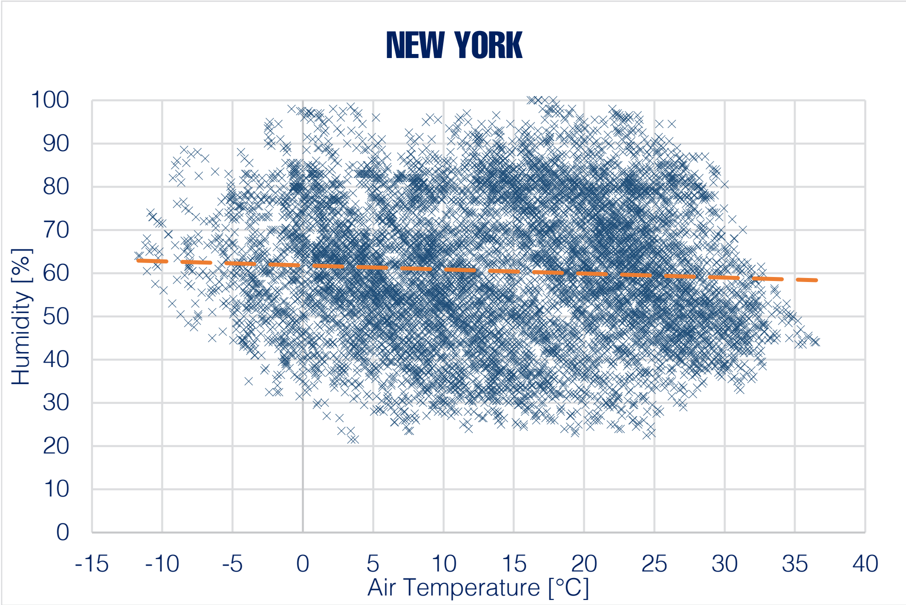

Figure 3.8 - Humidity and temperature hourly data chart

TEMPERATURE PROFILE

The temperature analysis chart reflects what the general behaviour of New York's climate is, the daily and monthly averages have a regular trend which puts the cold season from half October to March and the hot season from half May to half September. In summer it is possible to reach 35°C and higher, while in January the minimum registered temperature touches -15°C.

POLLUTION ANALYSIS

Even though New York is one of the most populated cities in the world, the quality of the air is better than what could be expected.

The particulate matter concentration in the air is lower than expected, even if the quality of the air is not so clean, obviously due to the high concentration of cars, industries and buildings.

Polluting gases like carbon monoxide (CO) and sulfur dioxide (SO_2) have a low registered concentration which is greatly far from the optimal threshold for healthy breathable air. Nitrogen dioxide (NO2) has a higher concentration if compared to the previous two gases, but also this one rarely oversteps the admitted threshold for optimal quality of the air. The gas which has a higher concentration in the air is Ozone (O_3) and this is the one that more frequently exceeds the limitations.

Anyway, thanks to the close position to the ocean and the presence of almost constant breeze and wind, the air in the detected zone of New York (less than 2 km from the site) is not unacceptable and the quality is greatly positive.

WIND ANALYSIS

Through the year the wind doesn't reach high values of speed, the maximum registered is around 13 m/s at a height of 80 meters. The most frequent direction of origin is north-west, even if the strongest winds are registered coming from south.

Politecnico di Milano, Master of Science in Building and Architectural Engineering
Steember - Steel and timber for a high rise building in Queens, New York
Chinnici Federico - **Maranesi** Marco

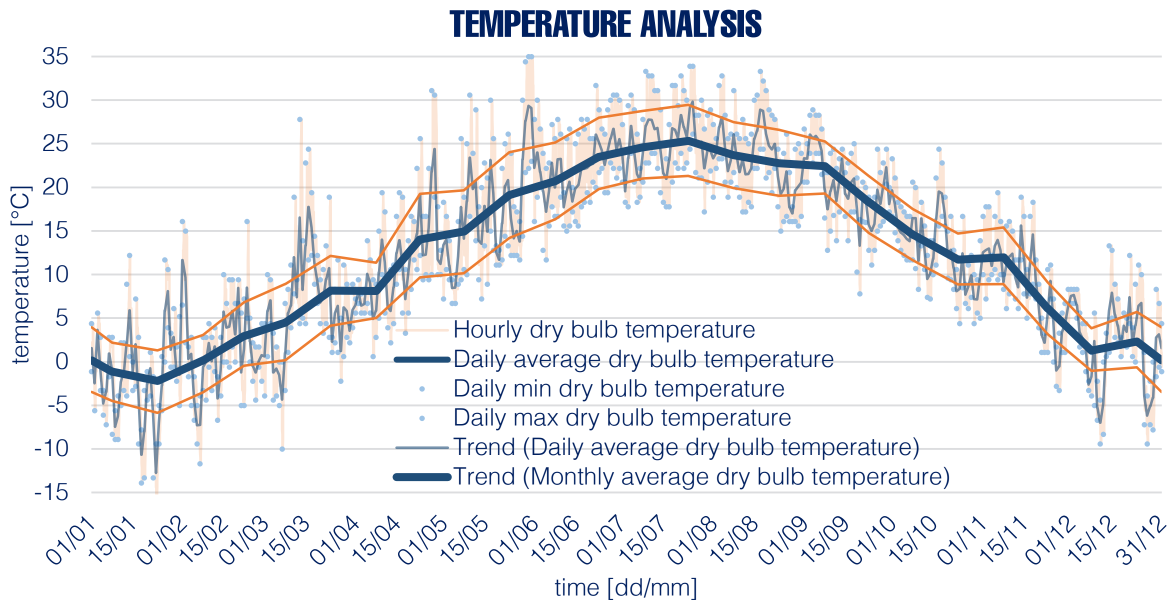

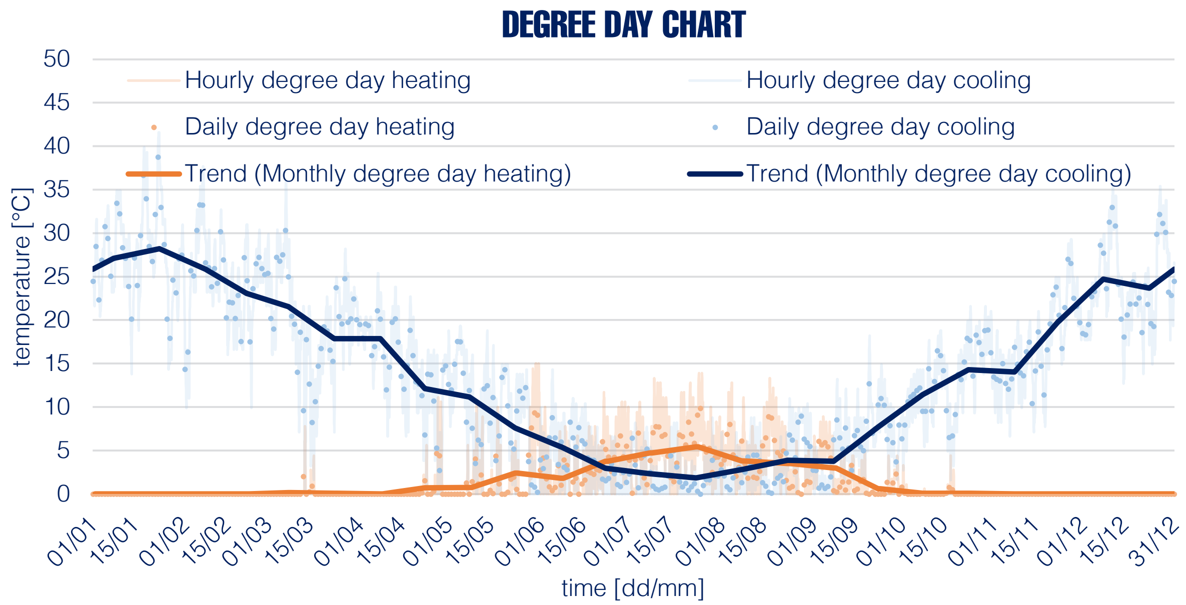

Figure 3.9 - Dry bulb Temperature and degree day hourly data chart

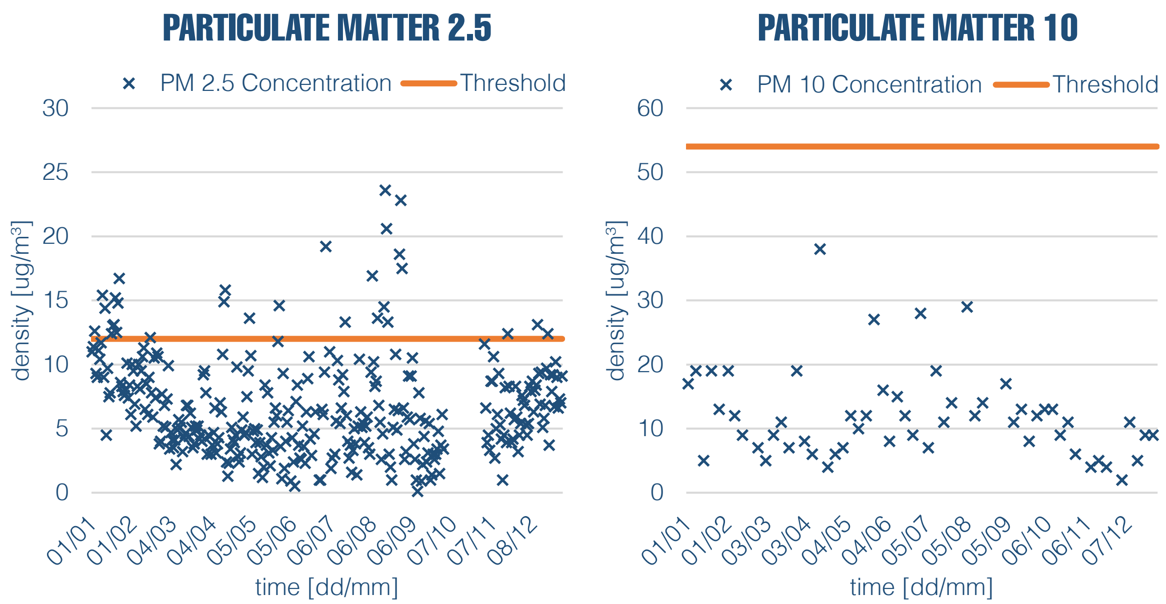

Figure 3.10 - Particulate matter concentration data chart (PM 2.5 and PM 10)

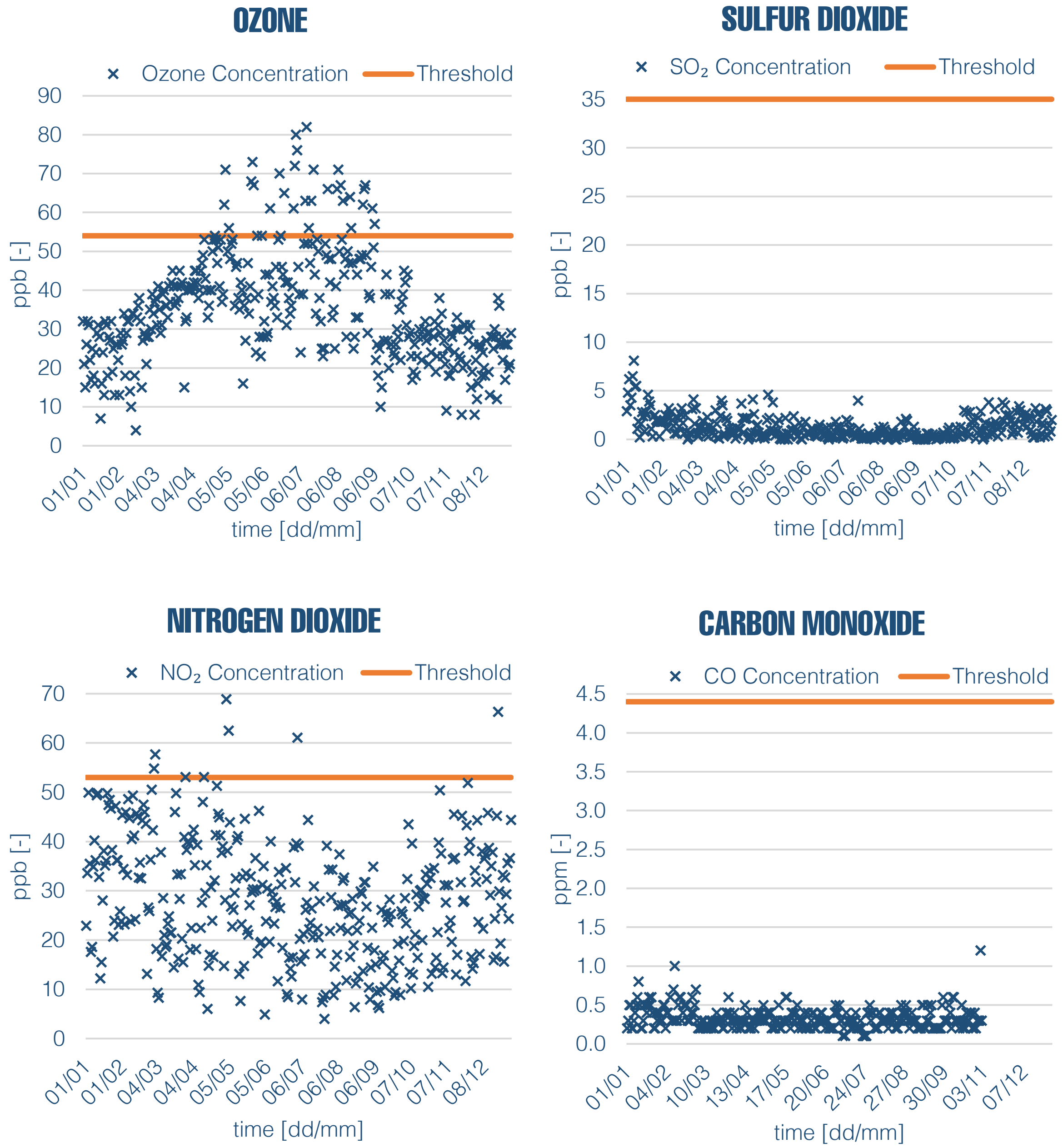

Figure 3.11 - Polluting gases concentration data chart (O_3 - SO_2 - NO_2 - CO)

Politecnico di Milano, Master of Science in Building and Architectural Engineering
Steember - Steel and timber for a high rise building in Queens, New York
Chinnici Federico - **Maranesi** Marco

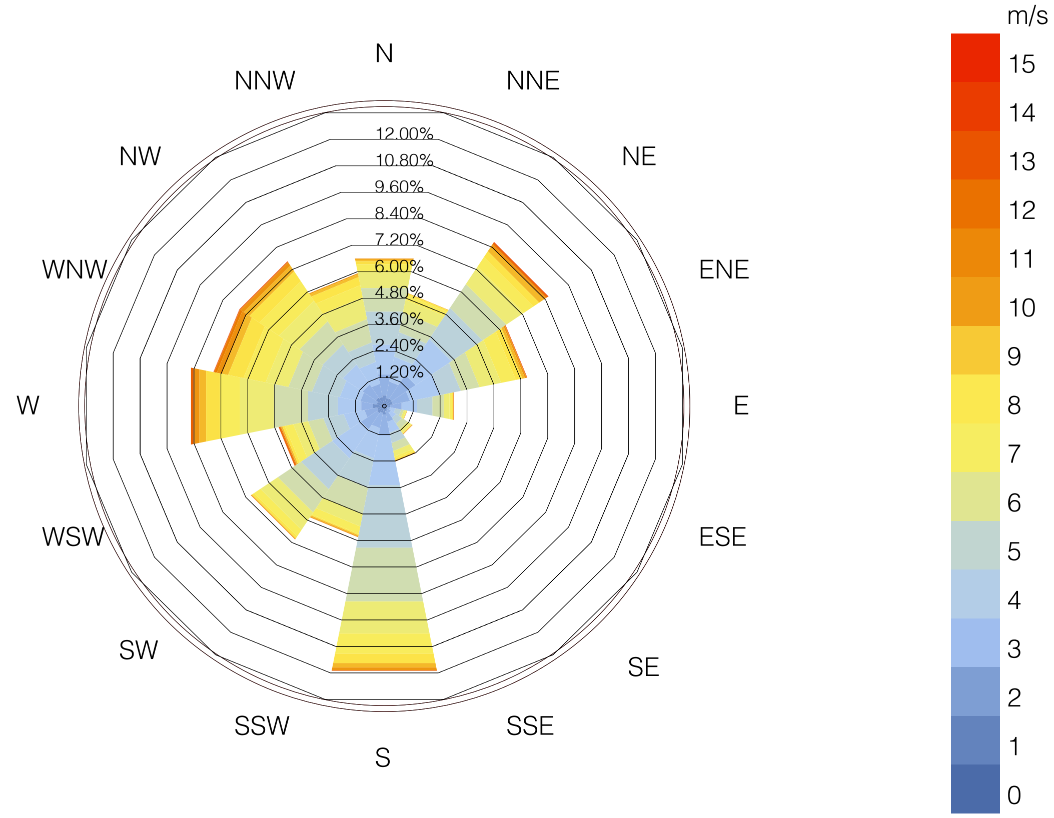

Figure 3.12 - Wind rose data chart

CARPET DIAGRAM

In the below carpet diagram, the distribution of the temperatures through the year is shown. In particular, the graph underlines that New York is in a heating-dominated climate.

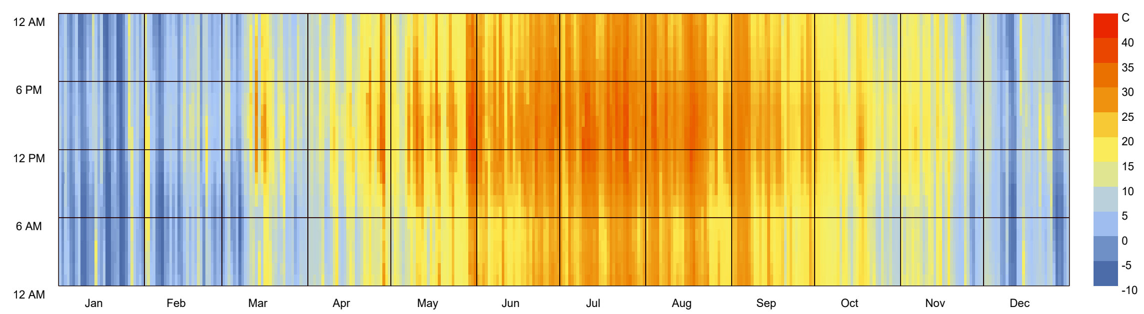

Figure 3.13 - Carpet radiation diagram

04 MASTERPLAN DESIGN

4.1 – THE SITE ANALYSIS

As requested in the competition's guidelines, the three main functions area residential, educational and wealthy. It has been chosen to keep these functions disconnected, due to the particular requirements each function foresees, resulting in three different buildings but linked by a common architectural language. In particular, the two-level kindergarten and the complex shape of the sports centre are dominated by the residential building, a 23-floor tower.

In order to position the buildings in a better way, the area has been studied in terms of solar radiation, projected shadows and wind, so that they would not create any issue for each other.

Fortunately, the site is not surrounded by excessively high buildings and the only tall element nearby is the Queensboro bridge. Being it on the north side, it does not create shadows on the land and, as a consequence, it is not a solar obstacle for winter solar gains. As it happens, the solar radiation hitting the site's surface has a constant high value, around 1'500 kWh/m^2, letting the designers consider the solar power as an opportunity to take advantage of. On the south of the site, at the moment, there is an old factory with two high chimneys, and these are the only elements that project shadows on the flat surface of the lot. Since these two elements are thin and tall, it is studied that they only create a shadow issue in winter for not more than seven or eight hours a day in the most southern region of the lot, resulting in not being a considerable obstacle. Neither the wind needs to be considered as a dangerous or hazardous element since the climatic data did not register high speed and there are no surrounding obstacles which could create turbulences.

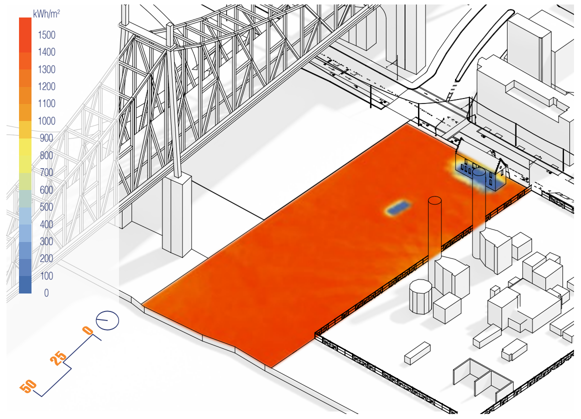
Figure 4.1 - Solar radiation analysis

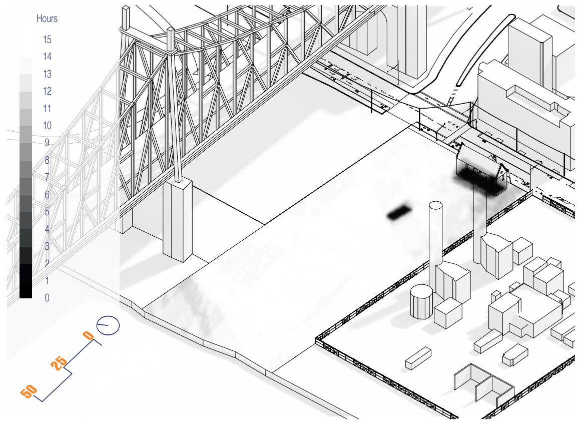
Figure 4.2 - Shadows analysis - summer

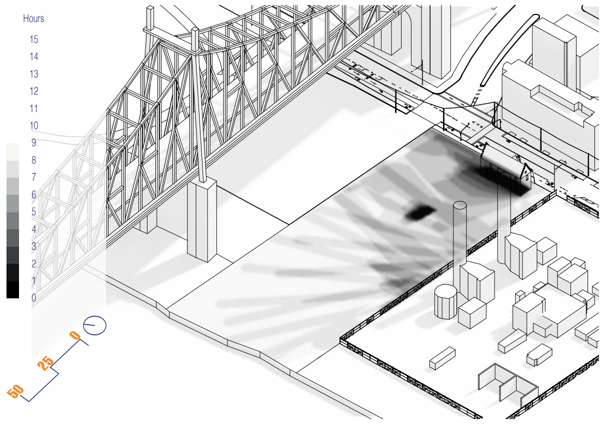
Figure 4.3 - Shadows analysis - winter

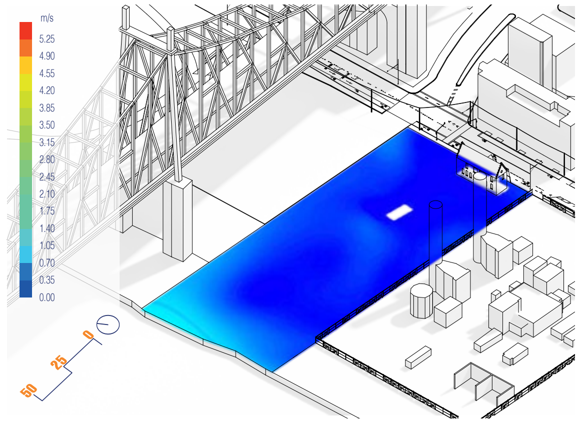
Figure 4.4 - Wind analysis - summer

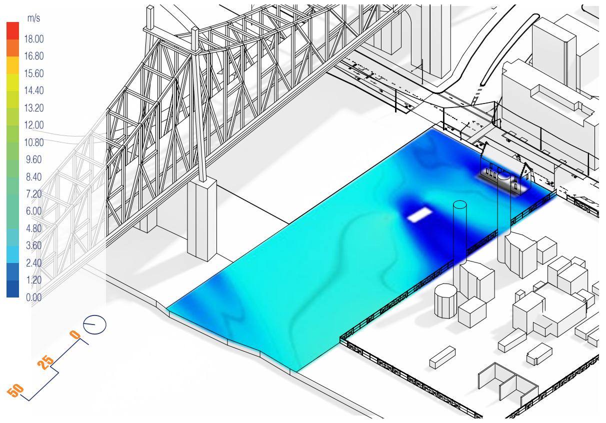
Figure 4.5 - Wind analysis - winter

Politecnico di Milano, Master of Science in Building and Architectural Engineering
Steember - Steel and timber for a high rise building in Queens, New York
Chinnici Federico - **Maranesi** Marco

4.2 – THE MASTERPLAN CREATION

After placing the buildings, designing and developing their surrounding area is important to create a harmonious and balanced environment between new constructions, land in the site and the rest of surrounding city, making it fascinating and beautiful but, at the same time, functional and practical.

THE DRIVEWAY ACCESSES

The first decision is to keep the public parking under the bridge, as it is now. These would be useful for the whole surrounding area and, in particular, for the new sports centre. On the side of the entrance of this parking, there are two vehicle ramps which enable the inhabitants of the residential tower to reach the two underground private parking levels. In this way, one only driveway access on Vernon Boulevard is in service of the residential building and the public parking.The educational centre has, instead, its own access 40 m distant from the previous one. This access leads to a small internal parking and the internal courtyard, where it is possible to have a quick stop for parents who need to leave the kids and to park for the kindergarten teachers.

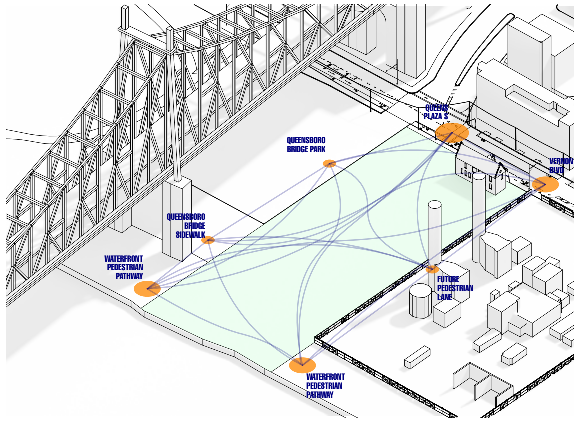
Figure 4.6 - Points of interest

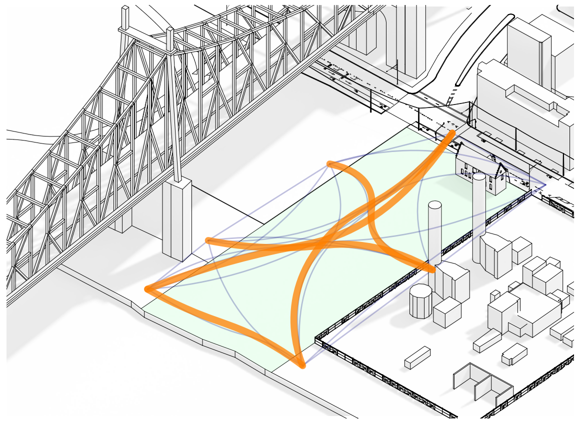
Figure 4.7 - Connections between the attractions

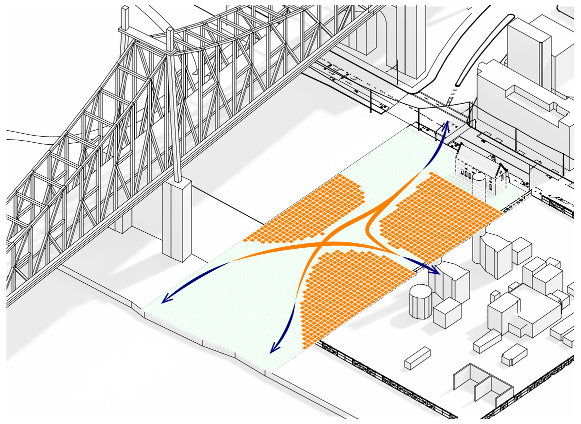
Figure 4.8 - Definition of the buildings' position

THE INTERNAL PATHS

The green open space within the buildings is crossed by internal paved paths. The main one creates a linear axis which links the main road, Vernon Boulevard, to the waterfront. In this way, also from the road, it is possible to have a view on the river and on Manhattan's skyline. Other secondary paths link the main one to the buildings and to the open parking under the bridge. The paths, in particular the main one, are carriageable, so that cars and trucks can drive over it. This is due to the lawn maintenance by gardeners and to the movement of food trucks which will populate the area under the bridge and the waterfront, to create a fix but changing attraction.

THE GREEN

All around the buildings, and in particular between the sports centre and bridge, the area is to be kept as green as possible. The lawn is everywhere, with high trees and flower brushes to give movement and colours to the open public park. Toward the basketball court of the sports centre, there's an escarpment with flowers and brushes, while all around the lawn there are scattered trees that go from the main road to the waterfront.

THE WATERFRONT

As required by the competition and by the general project of redevelopment of the city, the existing waterfront has been given new value. Previously, it just was an extension of the green space that is on the other side of the bridge. Now, it matches green, attraction, functions and a new pedestrian and cyclable path.

At the end of the lawn, in fact, there is first the cyclable path following the river from north to south. After it, a staircase which leads to the water level which, with a game of higher and lower steps, welcomes trees and brushes scattered through the waterfront.

In this way, the river walk has more than a level, allowing people to walk at the same height as the lawn or closer to the water. Thanks to this particularity, this waterfront, which is not just in front of this site but runs from north to south in front of Roosevelt Island, can become an attraction for tourists and locals.

THE ATTRACTIONS

The whole area will not be useful only for the inhabitants of the residential building, but it will be open to all the New Yorkers and all the tourists. This is why, in order to make the area more attractive and liveable, other open functions are present.

Under the bridge, for example, at the end of the public parking, there is a big paved rectangle. Half of it is occupied by a skate park, while the other half of the area is used by food truck drivers to stop and work there, according to licenses and permissions. Another food truck can be placed at the end of the principal path, close to the waterfront.

4.3 – THE POSITION OF THE BUILDINGS

Following these studies on the area, alongside with the enhancement of existing and potential pathways, the result is a reasoned and optimized position in the masterplan.

In particular, the residential building, which is the highest of the three, is set close to the bridge and on the north side of the site, so that it won't create any shadow on the other two constructions. The children education centre, which is going to be a two-storey building, will be in front of the residential tower on the south side. Moreover, it is going to be linked to the existing "New York Architectural Terra Cotta Works Building", and it can be considered as a big and modern enlargement of this one, even if with a different architectural aspect which is done on purpose, in order to better distinguish the newly added part from the original building. Regarding the sports centre, it is placed on the south side, together with the kindergarten, but closer to the river. Being it a low rise building, it will project some shadow on the north, but it will just affect the green area expected in the middle of the site.

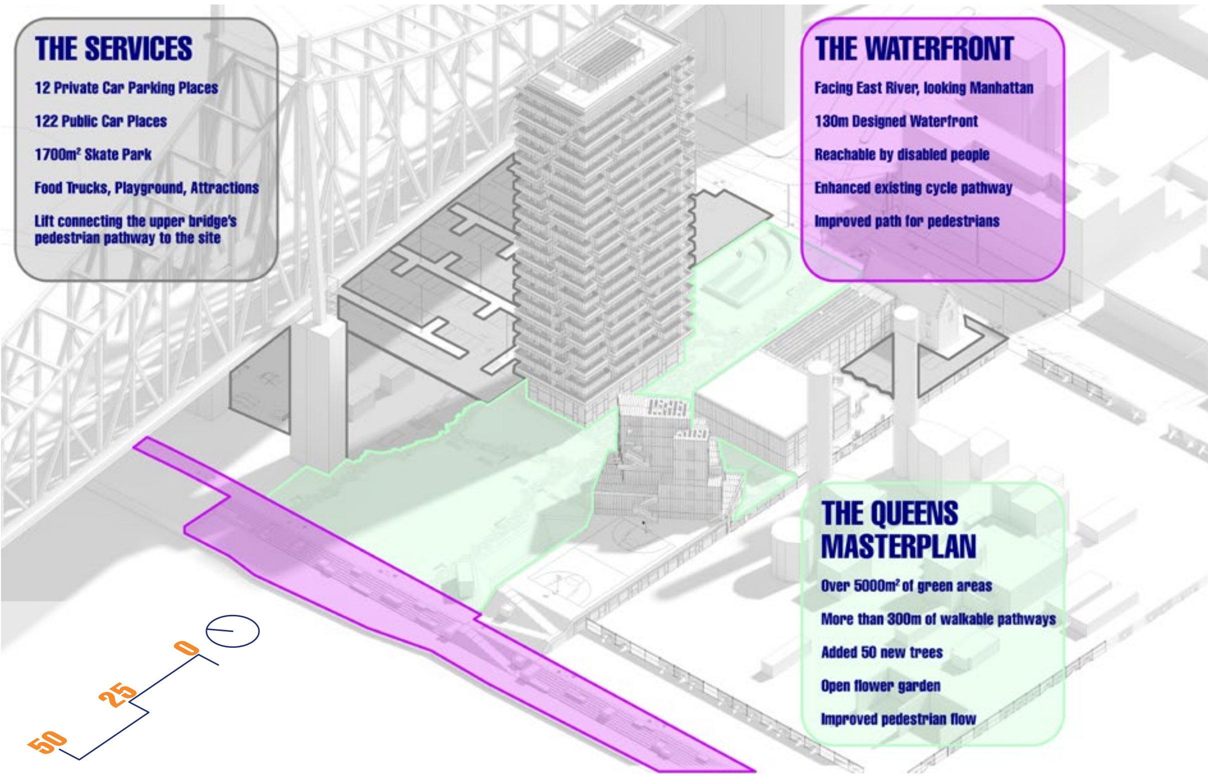

Figure 4.9 - The outdoor spaces

Politecnico di Milano, Master of Science in Building and Architectural Engineering
Steember - Steel and timber for a high rise building in Queens, New York
Chinnici Federico - **Maranesi** Marco

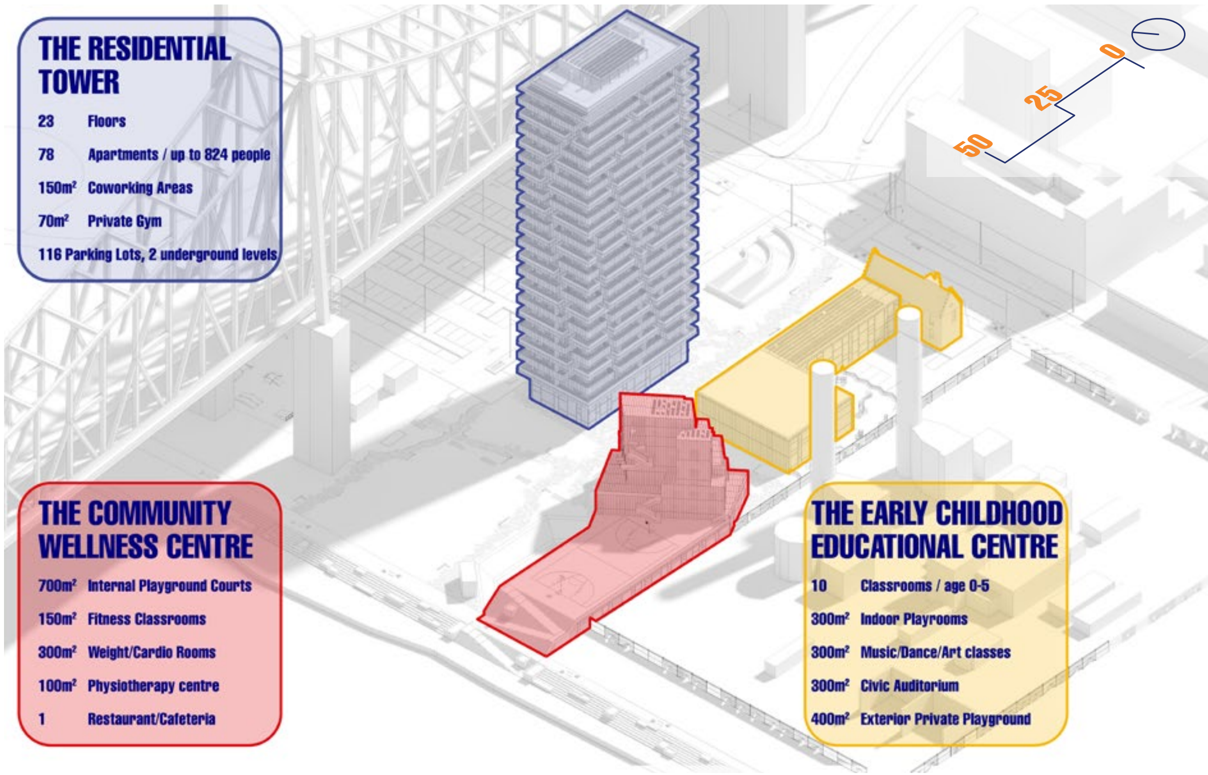

Figure 4.10 - The three main buildings

Figure 4.11 - 3D view of the masterplan

Politecnico di Milano, Master of Science in Building and Architectural Engineering
Steember - Steel and timber for a high rise building in Queens, New York
Chinnici Federico - **Maranesi** Marco

Figure 4.12 - Final 3D view of the designed masterplan

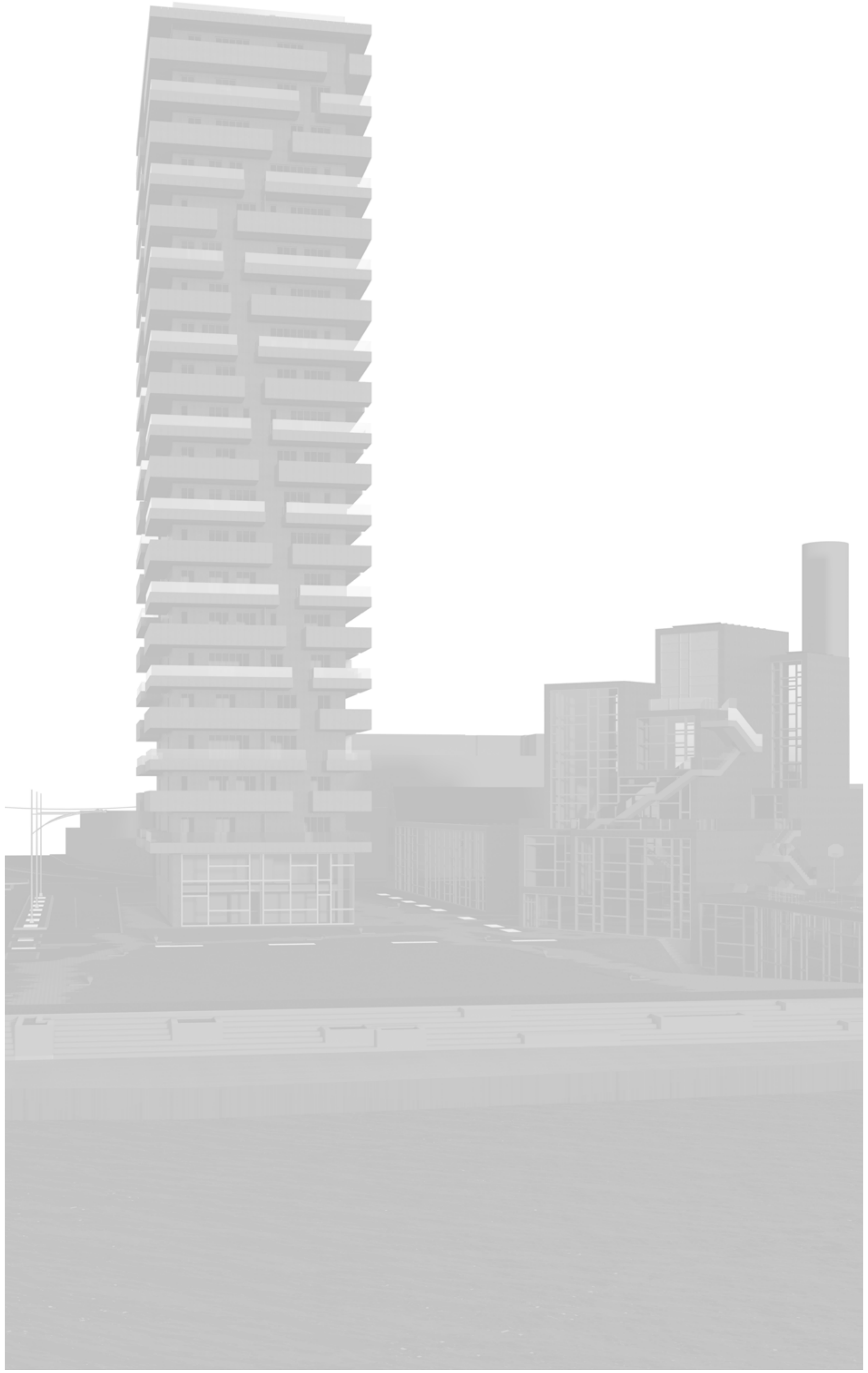

05 ARCHITECTURAL DESIGN

5.1 – INTRODUCTION

The three different buildings have big differences in shape and aspect, but they are anyway linked by a stylistic and external harmony, which create, despite the contrasts, a unique architectural language.

5.2 – THE EARLY CHILDHOOD EDUCATION CENTRE

The education centre building is to be considered as a timber structure enlargement of the existing historic building called "New York Architectural Terra Cotta Works Building".

It is sized to host until 130 children between the ages of 6 weeks and 5 years, so from infants through prekindergarten. It is linked to the original building through a corridor which serves the classrooms of the new structure, leading to the auditorium placed at the end. The rooms are normal classrooms, or specially equipped rooms for music and art activities, together with playrooms, both internal and external.

It develops on two levels, so that, according to the local regulations, there is enough room at ground floor for infants (from 6 weeks to 24 months), while older children can stay at the second level. Also, in this way, the total height of the new addition of the building is not taller than the existing one. In fact, the horizontal roof of the new part touches the old structure exactly where the original pitched roof starts.

The enlargement basically has two bodies: a long and thin one, with one row of rooms and the corridor, and a large one at the end of the previous one. This is where the corridor ends, leading to the biggest rooms and the auditorium. In this way, together with the "New York Architectural Terra Cotta Works Building", the whole building has a C shape that creates a private courtyard.

This courtyard is divided into two sections by a fence and it has two functions. The half closer to the road is parking, where the parents can shortly stop to bring inside the kids and where the workers can park their car for the day. The other half is an external private playground for kindergarten kids.

The south and north facades of the building have the same curtain wall. This has timber mullions and transoms which follow, both vertically and horizontally, a modular scheme: their distance is always a multiple of 120 cm (120, 240, 360), creating a regular disorder which gives movements but, at the same time, simplicity, to the walls. In this way, this curtain wall, which faces north and gives natural light to the classrooms, maximises the entrance in these rooms of diffuse light, so that glaring effect for children and teachers is null.

The roof is green with grass on it and it is half covered by PV panels. The access to the roof is directly from the pitch of the old building's roof, therefore, the internal vertical connection does not need to reach the roof level.

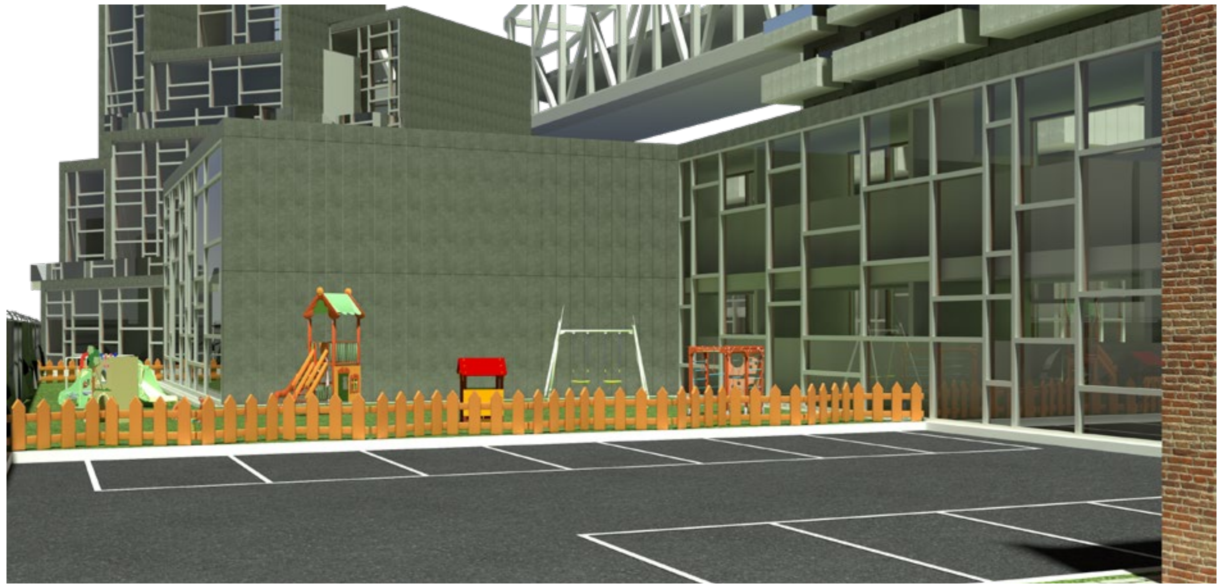

Figure 5.1 - 3D view of the early childhood education centre

Politecnico di Milano, Master of Science in Building and Architectural Engineering
Steember - Steel and timber for a high rise building in Queens, New York
Chinnici Federico - **Maranesi** Marco

5.3 – THE SPORTS WELLNESS CENTRE

The sports wellness centre is a mid-rise timber building with different functions.

The volume is divided into two main bodies: a flat and half underground one and a mid-rise body that looks composed by overlapping cubes.

The flat area is half underground and hosts two basketball courts: an indoor one at level -1 and an outdoor one on the roof. The overground body has many other functions, in particular, all the fitness rooms (cardio area, weightlifting room, CrossFit room, courses room), the locker rooms, the staff offices and, at ground level, a physiotherapy centre and a restaurant. All these functions are thought to create a healthy attraction for people that, coming here, can devote attention to their bodies, considering sport as a source of the body and mental wellness.

The whole building has a particularity: the walls facing north and south are glass facades, while the ones facing east and west are completely opaque. The inspiration for this architectural effect and for the entire building volume has been taken from the Kashiyama Daikanyama building by Nendo, a new commercial complex in Tokyo. The curtain walls of the glass facades have the same modular texture of mullions and transoms of the educational centre so that it can appear having continuity with the building on its side.

The cubes which create the mid-rise part of the building are inclined one with respect to the other. This inclination and the position of every single cube has been optimized with energy simulation, in order to find the best solution in terms of energy demand. In this way, the shape and the position of this composed volume allow to maximize the solar gains and minimize the annual energy demand for heating and cooling.

The cubes that form this complex volume are externally linked by staircases connecting the formed terraces. These stairs give movement and naturalism to a structure that would be, otherwise, too static and rigid. The volume projects its shadows on the green public area, being a source of refreshment in hot summer days, without being an obstacle for other buildings.

All the cubes have different height and flat roof. This game of heights creates a movement which is recognizable also from the top view, where the opaque roof is partially visible and it camouflages with PV panels and staircases.

The outdoor basketball court is linked by a big stair to the surrounding green area and to the waterfront. This means that every terrace is connected to the park, creating one only big and multilevel welcoming space.

One last particular aspect of this building is that, due to its inclination and its differences in height, if seen from Vernon boulevard, it recalls the visual effect of many different skyscrapers seen from a distance, and it perfectly matches the Manhattan skyline in the background view. In this way, from the road, the skyline view is not hidden but it is, instead, enhanced and embellished.

Figure 5.2 - 3D view of the sports wellness centre

5.4 – THE RESIDENTIAL TOWER

The third and last building is a residential high rise tower. This building is the more in-depth studied since every aspect of it has been deepened, from the exterior appearance to the structure and the technology.

5.3.1 – THE INTERNAL DISTRIBUTION

The building has a rectangular shape (30 m x 15 m), with the longer side parallel to the Queensboro Bridge.

THE CENTRAL CORE AND THE VERTICAL CONNECTION

The tower has a central reinforced concrete core which structurally gives strength and inertia to the whole building. It is composed of thick walls which bear the horizontal forces due to wind and earthquakes. Within these walls, there are two stairwells, three elevators and two systems cavities.

All the three elevators are big enough to host up until eight people to avoid lines and long waits in the peak hours. Alternatively, the two stairwells are available, but only the central one goes down until the two underground levels. The position of the fire doors is studied in order to create a safe filter and so that every vertical connection is secured by smoke.

THE FLOOR PLANS

The two underground levels have basically the same plan. They are linked to the outdoor by two ramps for vehicles which are parallel. The parking develops all around the tower with forty-five open parking spaces per floor, guaranteeing ninety parking spaces for the residents. The central core keeps the same plan that it has in the other floors, while under the surface of the tower there are many cellars, for a total surface of 180 m^2 per floor. These are linked to the apartments so that people can have storage rooms if they need additional space. A big technical room is to be set in both the two underground levels, in order to host all the needed mechanical systems. Considering the central stairwell as a safety exit, there is another one in the furthest corner of the parking, its exit is outside in the open public parking under the bridge. The other safety exit is the ramp itself since it is open. The whole underground level is surrounded by a crawl space, necessary for the natural ventilation required for fire safety reasons.

The ground level hosts different functions for the residents. There is a big entrance hall from where it is possible to access the central core and, from here, it is possible to get to the other functions and floors. There is a big laundry room, open to every dweller of the building, and a garbage room. These two are close to the ramps so that they can easily be accessible for vehicles. On the other side of the central core, there is bicycle storage for residents' normal and electrical bikes, with also recharge stations. The rest of the surface is occupied by a playroom and a coworking area where people can meet to hang out or to work together.

The first level is the only one which is smaller than the other ones since the coworking and the entrance hall on the ground floor have a double-height. The portion on the right of the central core is a gym, while the one on the left is a silent work/study room. They both face the below environment only closed with an internal glass wall. Both the ground and the first level are surrounded by a curtain wall which has the same modular texture of the kindergarten and of the sports centre. This choice was made to have the same architectural language in every building and to have the maximum possible light entering in these common spaces in the basement of the tower. Another common area is the roof, which is open to all the inhabitants who wish to enjoy the view with some friends on the green grass placed on the flat covering.

The upper floors are the ones that host the apartments. There different typologies of floor plans in which many kind and dimensions of flats alternate themselves. The units go from the studio, with one only room working as a living room and bedroom together, to the biggest which is the attic, placed up at the last two floors. In between, various apartments with one, two and three bedrooms are planned, combined together to create five different typologies of floor plans. Every floor has a balcony running around almost the totality of the building, with the exception of some holes on the south, east and west sides, and the correspondence with the elevators in the central core.

Politecnico di Milano, Master of Science in Building and Architectural Engineering
Steember - Steel and timber for a high rise building in Queens, New York
Chinnici Federico - **Maranesi** Marco

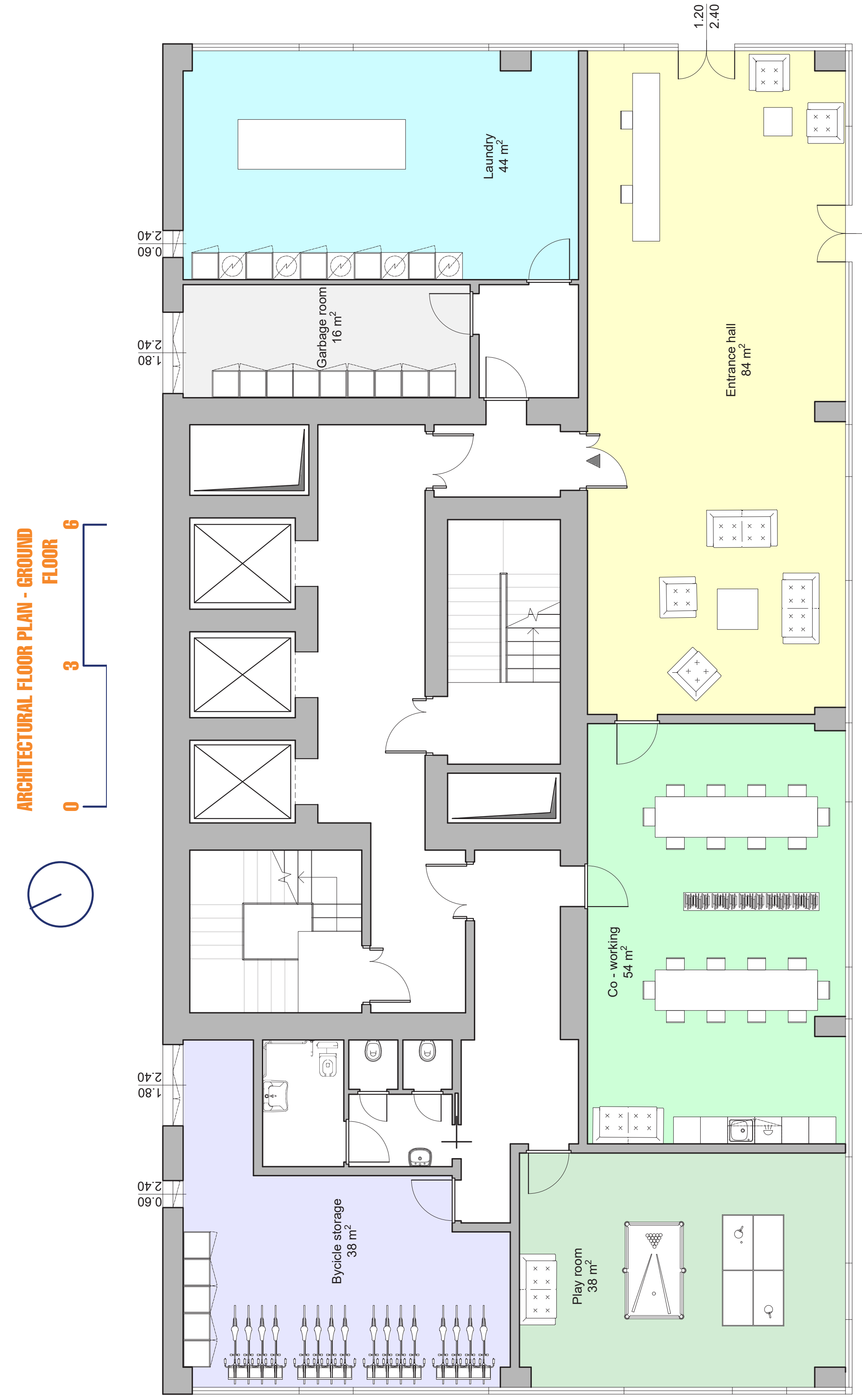

ARCHITECTURAL FLOOR PLAN - FIRST FLOOR

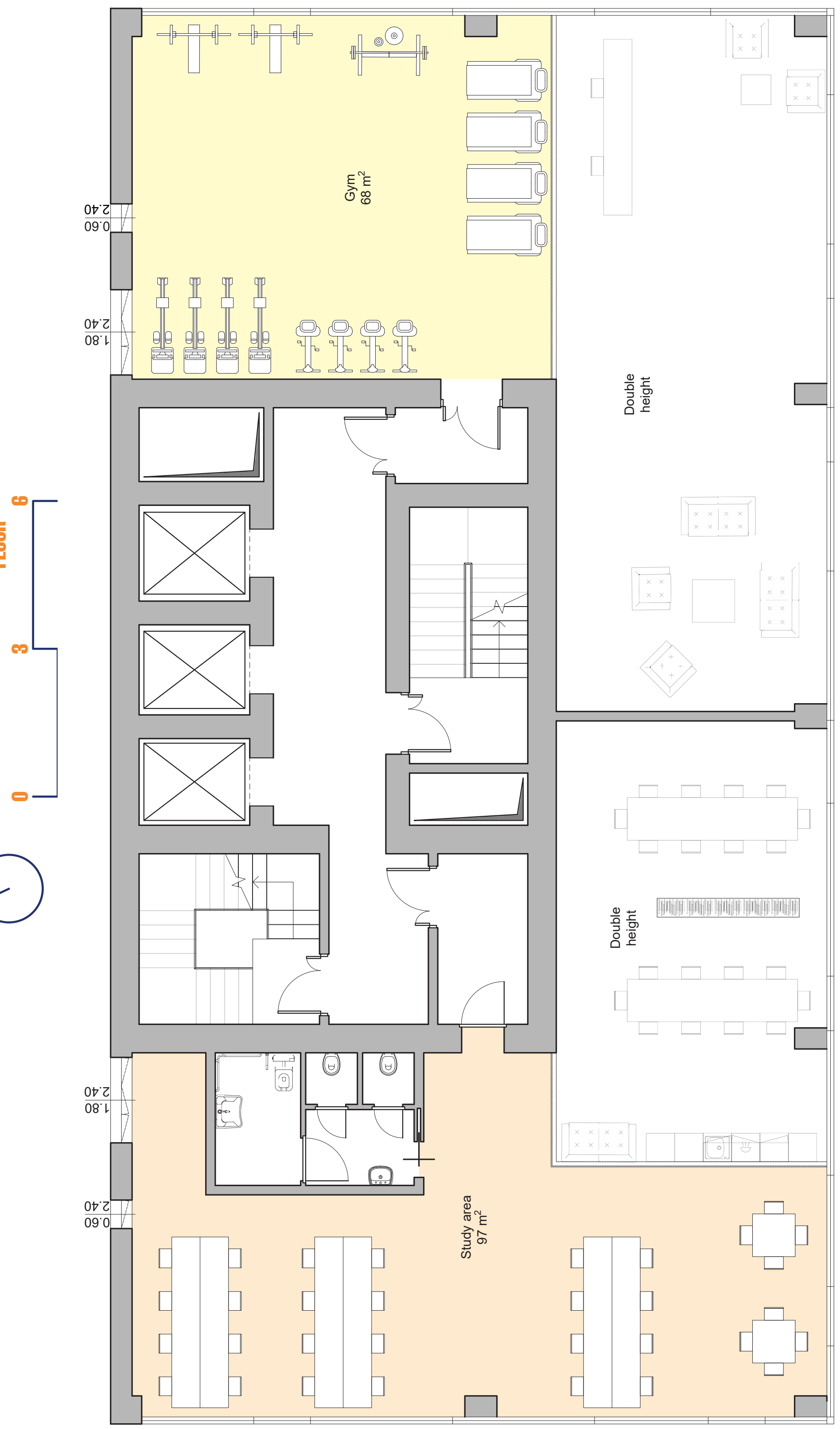

Politecnico di Milano, Master of Science in Building and Architectural Engineering
Steember - Steel and timber for a high rise building in Queens, New York
Chinnici Federico - **Maranesi** Marco

ARCHITECTURAL FLOOR PLAN - TYPE A

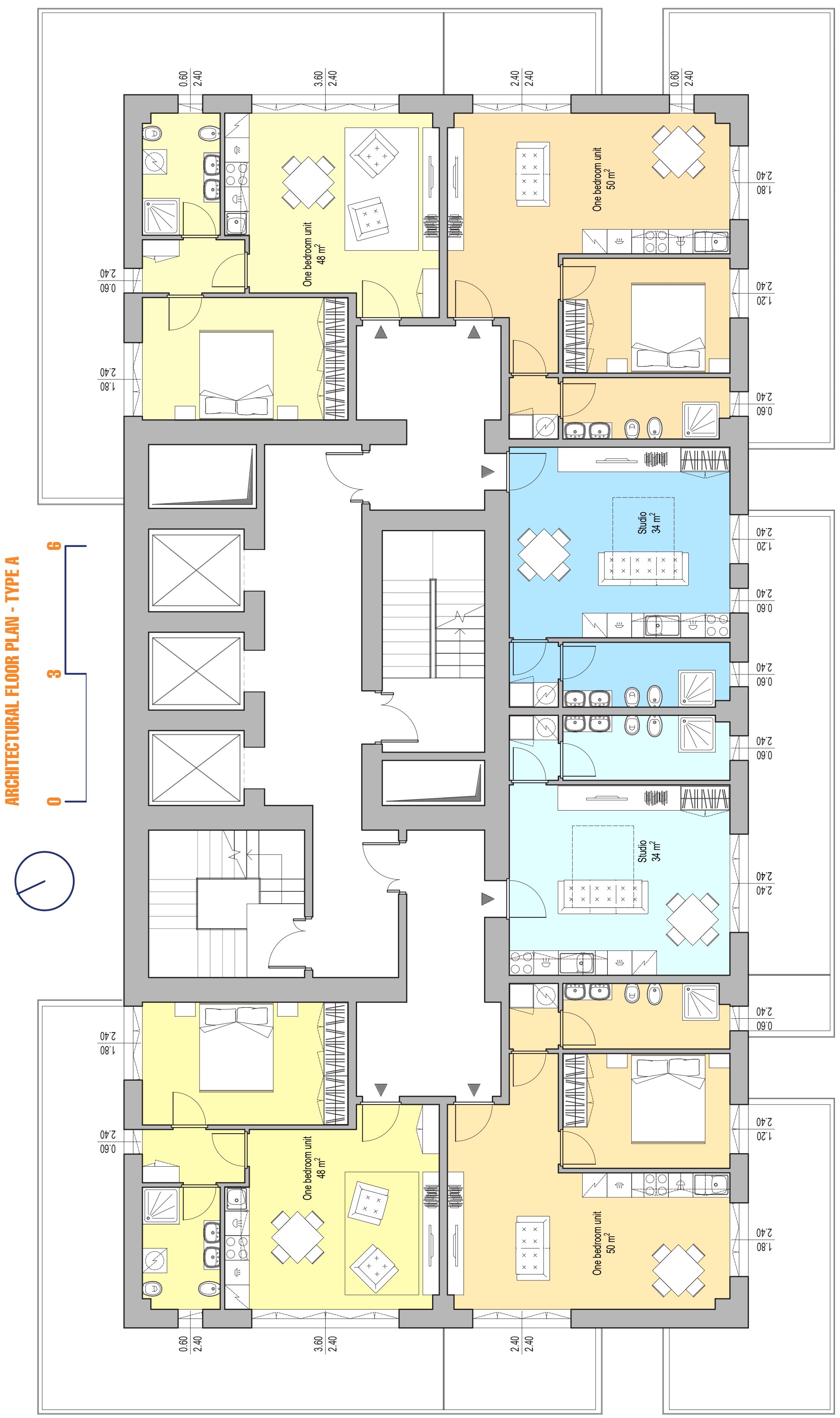

ARCHITECTURAL FLOOR PLAN - TYPE B

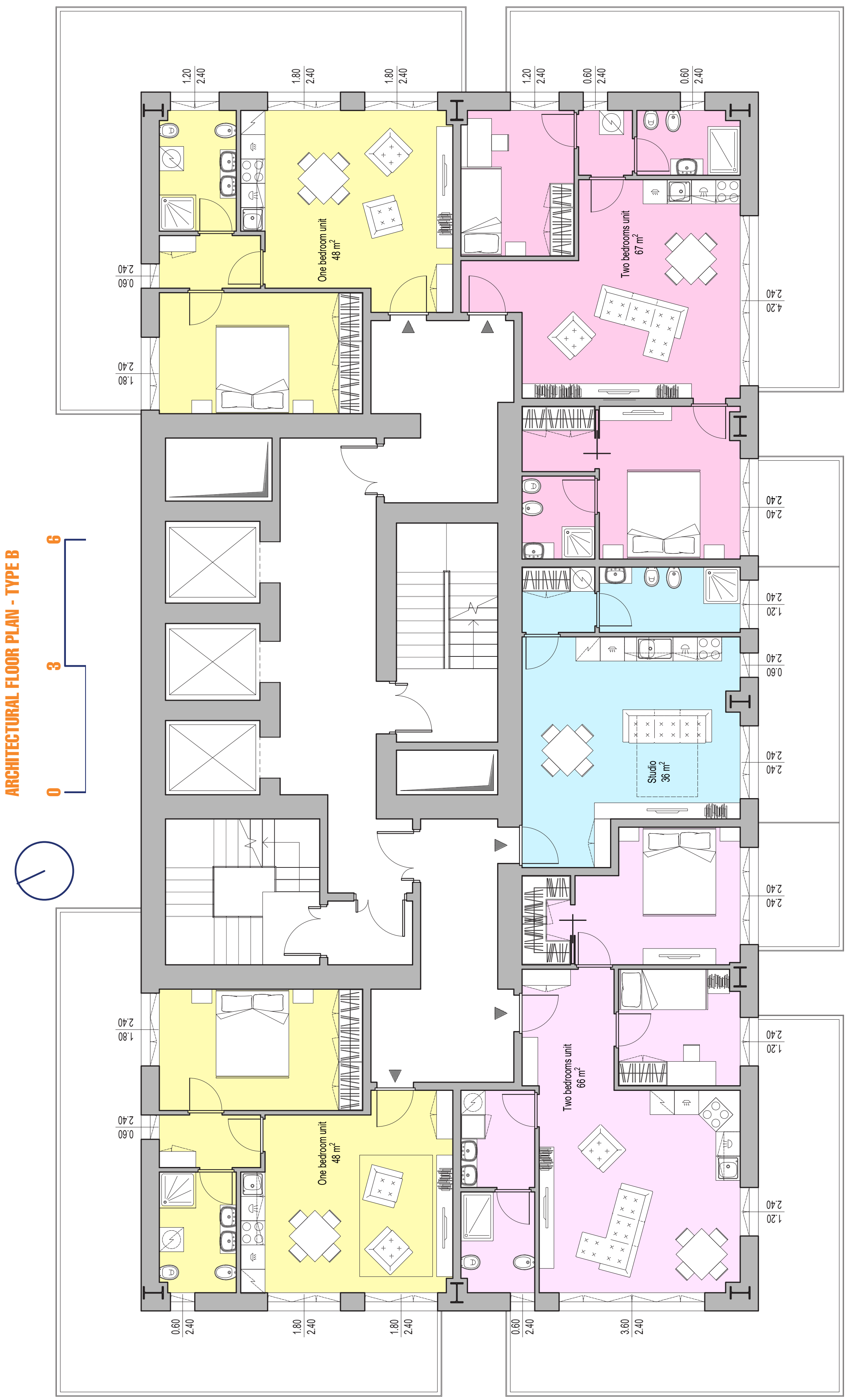

ARCHITECTURAL FLOOR PLAN - TYPE C

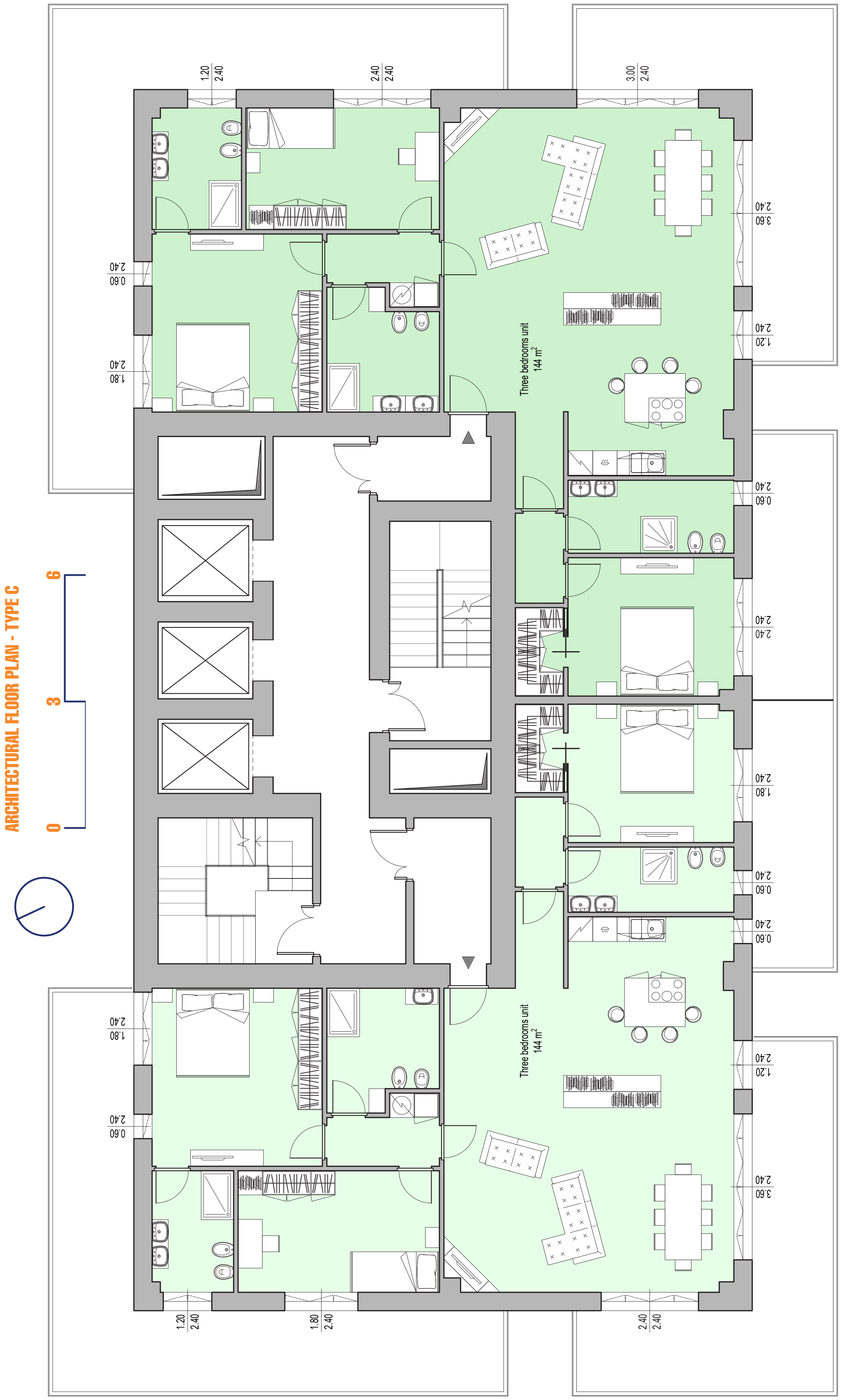

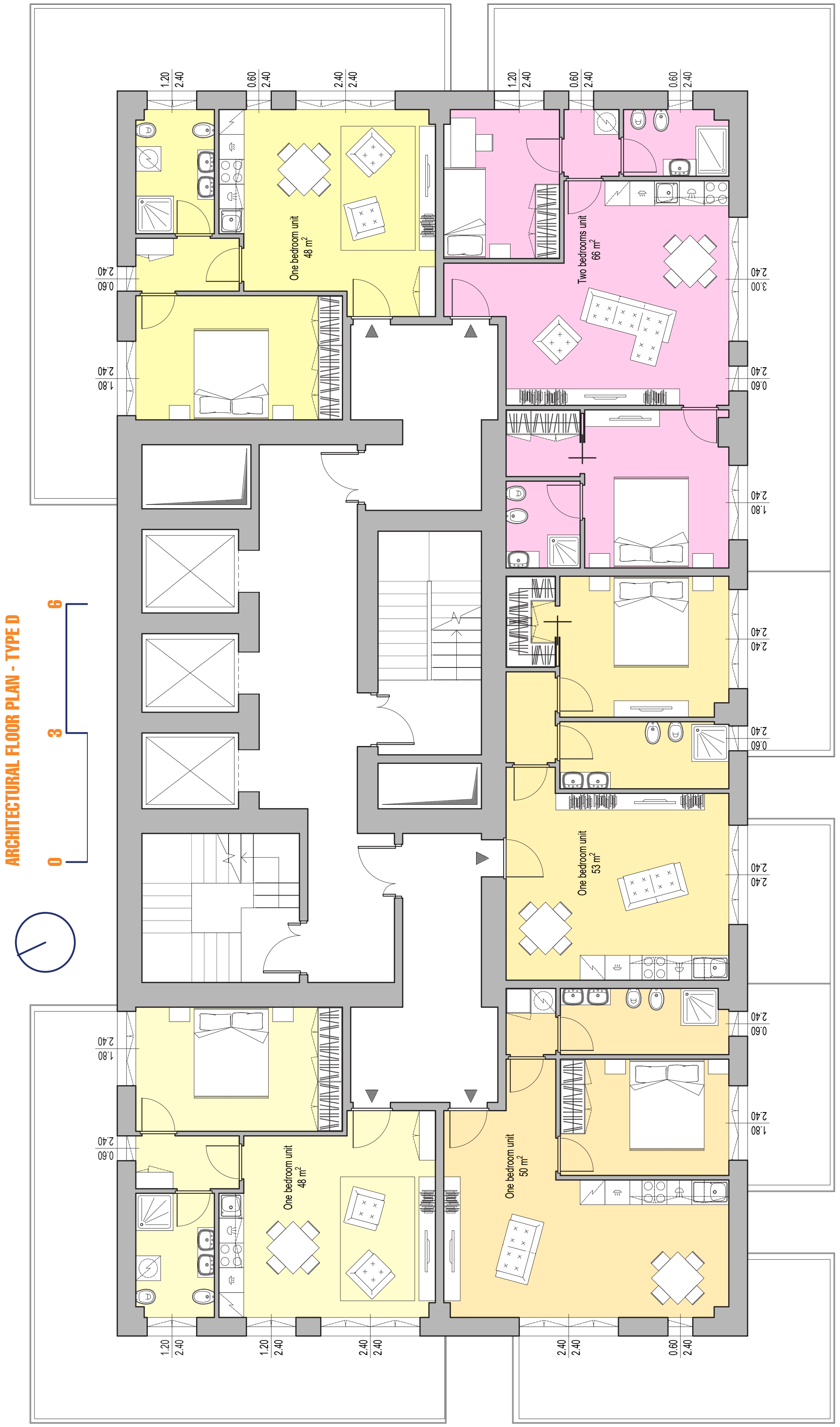

Politecnico di Milano, Master of Science in Building and Architectural Engineering
Steember - Steel and timber for a high rise building in Queens, New York
Chinnici Federico - **Maranesi** Marco

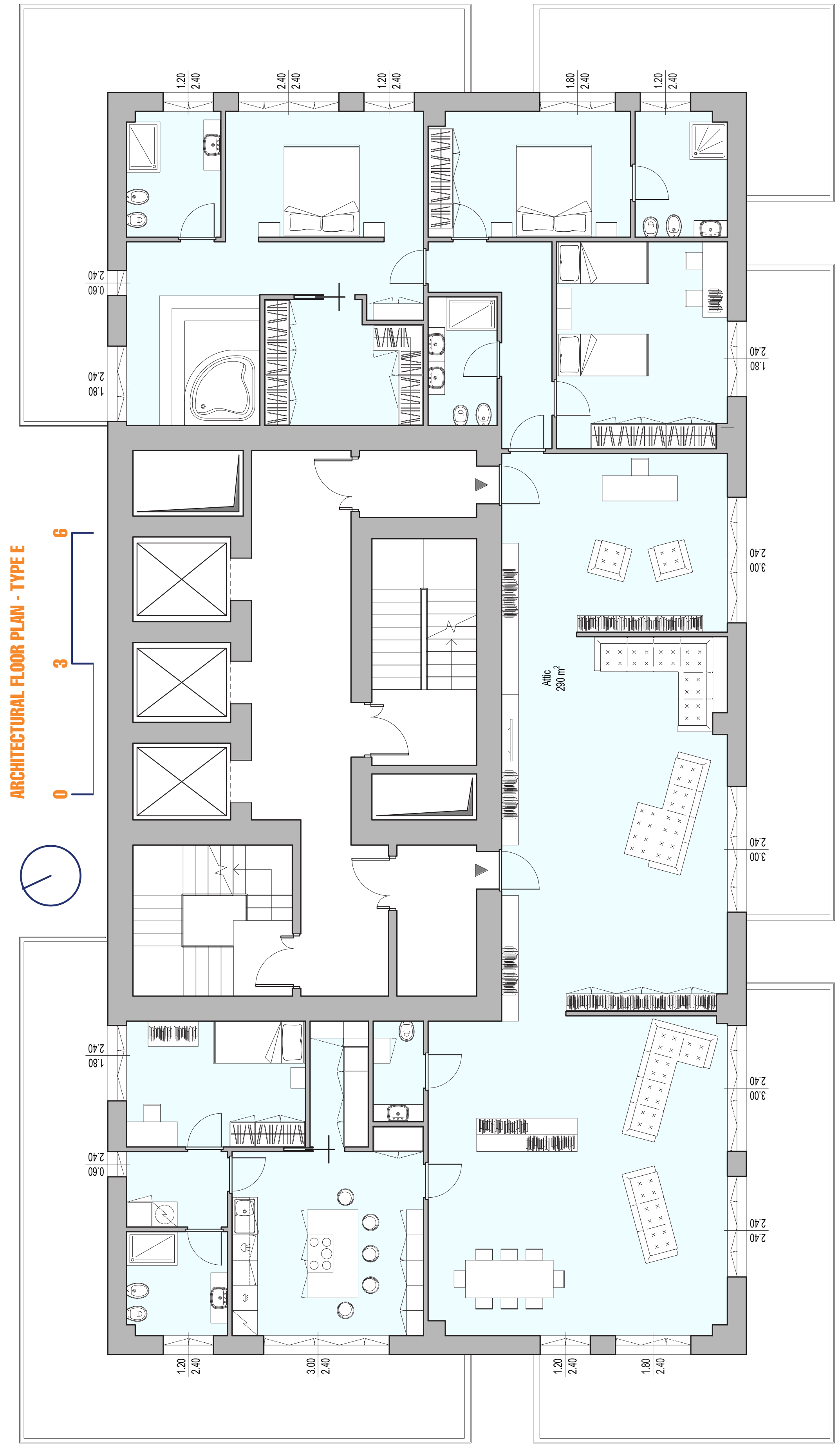

ARCHITECTURAL FLOOR PLAN - LEVEL -1

0 3 6

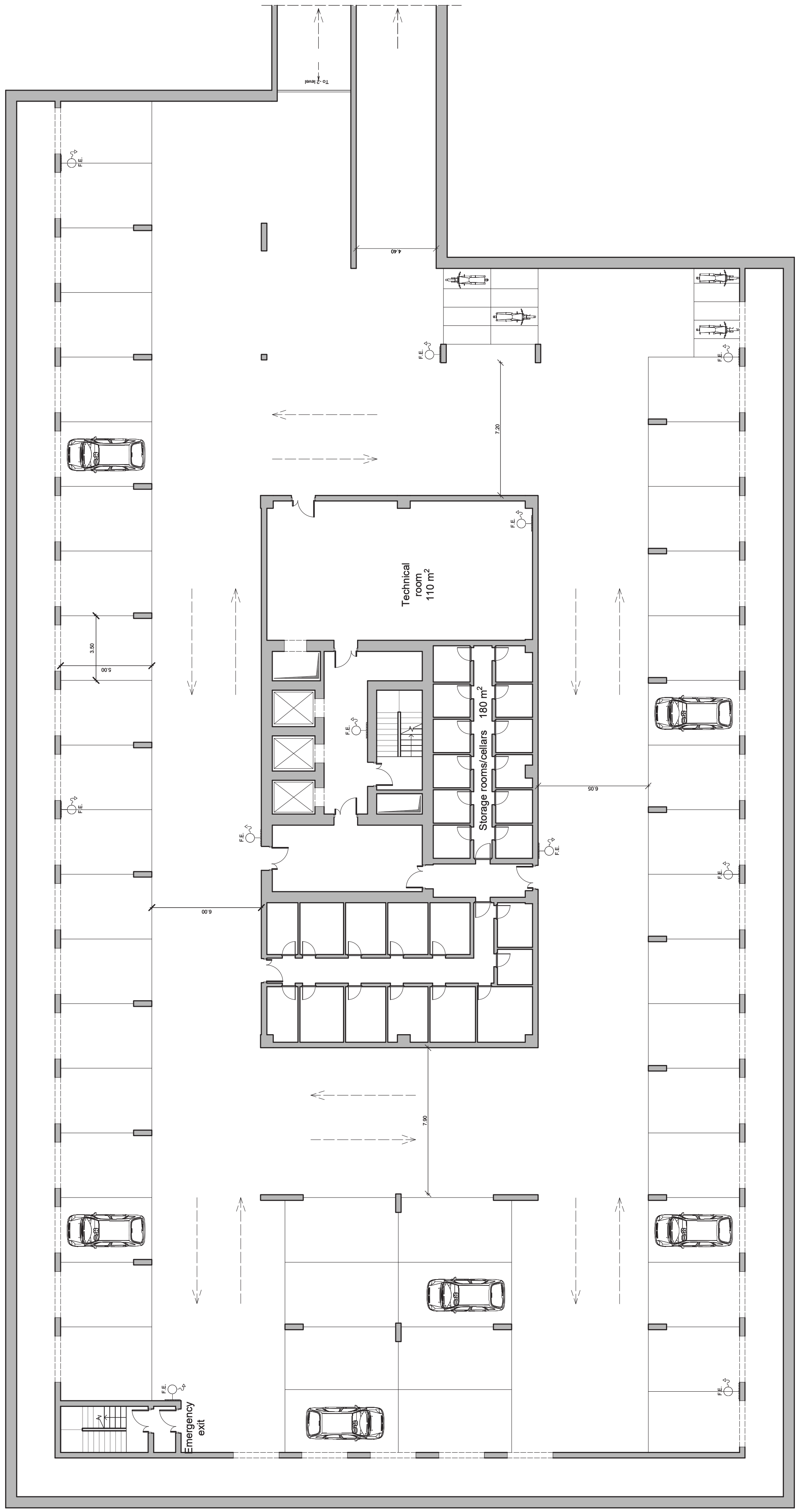

ARCHITECTURAL FLOOR PLAN - LEVEL -2

0 3 6

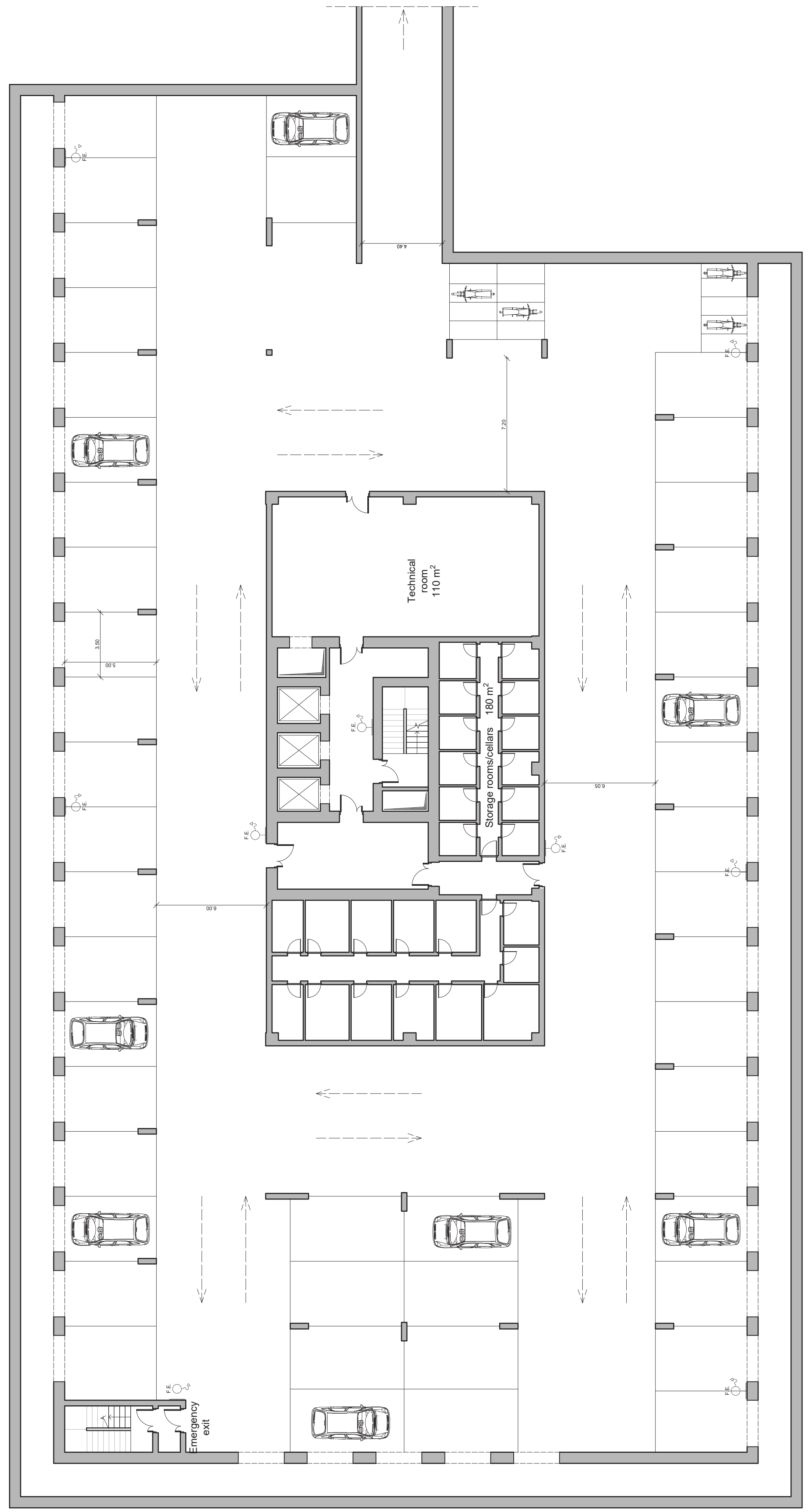

5.3.2 – THE ELEVATIONS

THE CURTAIN WALL

At the ground and on the first floor there is a timber curtain wall which is equal to the one used in the other two buildings. The timber mullions and transoms create a regular and modular texture since they have an interaxis distance which is always a multiple of 120 cm. The alternation is not regular so that they can create wider and smaller transparent rectangles that alternate on the façade.

THE CLADDING AND THE WINDOWS

The elevations of the building are very tall, so in order not to have a monotone solid element, it is important to create a pattern with cladding panels and windows. In particular, these elements are always 60 centimetres wide and they create a module that alternates on the façade. The windows are combined to have big transparent elements composed by up to seven window sashes; in this way, there is an alternation of opaque and transparent modules of 60, 120, 180 cm and so on. The northern side has a flat part with no balconies in correspondence of the elevators. This part of the elevation can be used to fix some advertisement panels due to its position: it is in front of the highway of the Queensboro Bridge. This could be a way for the owner of the building to have an income to be used for the maintenance of the building.

THE BALCONY

The balcony is a continuous element running from one side to the other, but it is interrupted by a 180 cm hole which is present on every floor. The length of the overhang has been optimized with energy simulations in order to find the optimal measure: the result is 2 meters. With this dimension the balcony works perfectly as a shading element in summer but, at the same time, it allows enough light to enter the building in winter for sufficient solar gains. Furthermore, with this length, the natural light is the best compromise between the well-lit and the overlit ratio of the internal environment. These holes create one or more lines on the facades, elements that give movement to the building and create a distinctive element on the elevations. In particular, the North-West facade and the South-East have the same pattern and appearance. Moreover, the railings are of two different kinds and they alternate vertically at every floor: one is a glass transparent element and so it won't almost be seen, while the other one is opaque and it is made with the same material of the cladding, just the colour changes, going from a lighter to a darker shade of the same one.

ARCHITECTURAL ELEVATION - NORTH-WEST

Politecnico di Milano, Master of Science in Building and Architectural Engineering
Steember - Steel and timber for a high rise building in Queens, New York
Chinnici Federico - **Maranesi** Marco

ARCHITECTURAL ELEVATION - NORTH-EAST

5.3.3 – THE ARCHITECTURAL RENDERINGS

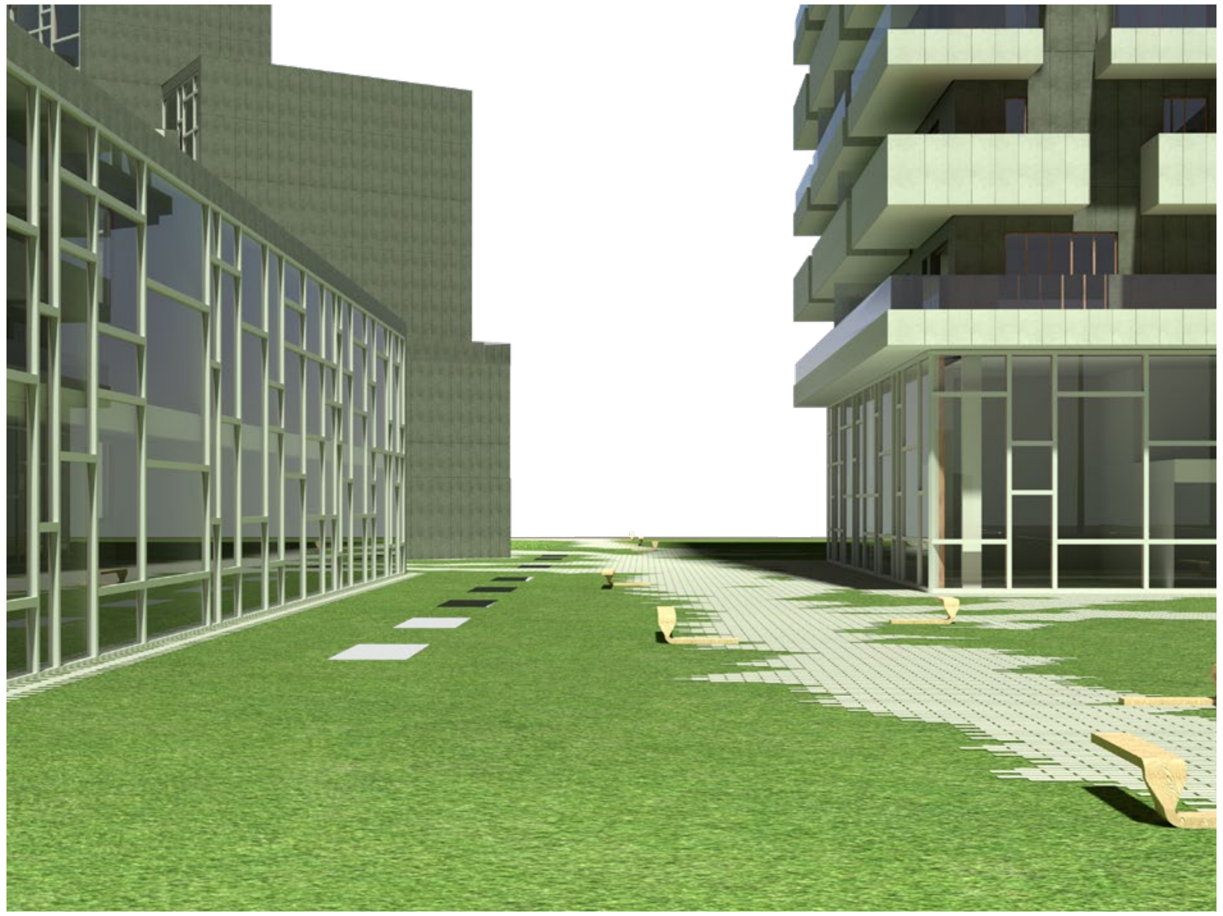

Figure 5.3 - Architectural rendering, view 1

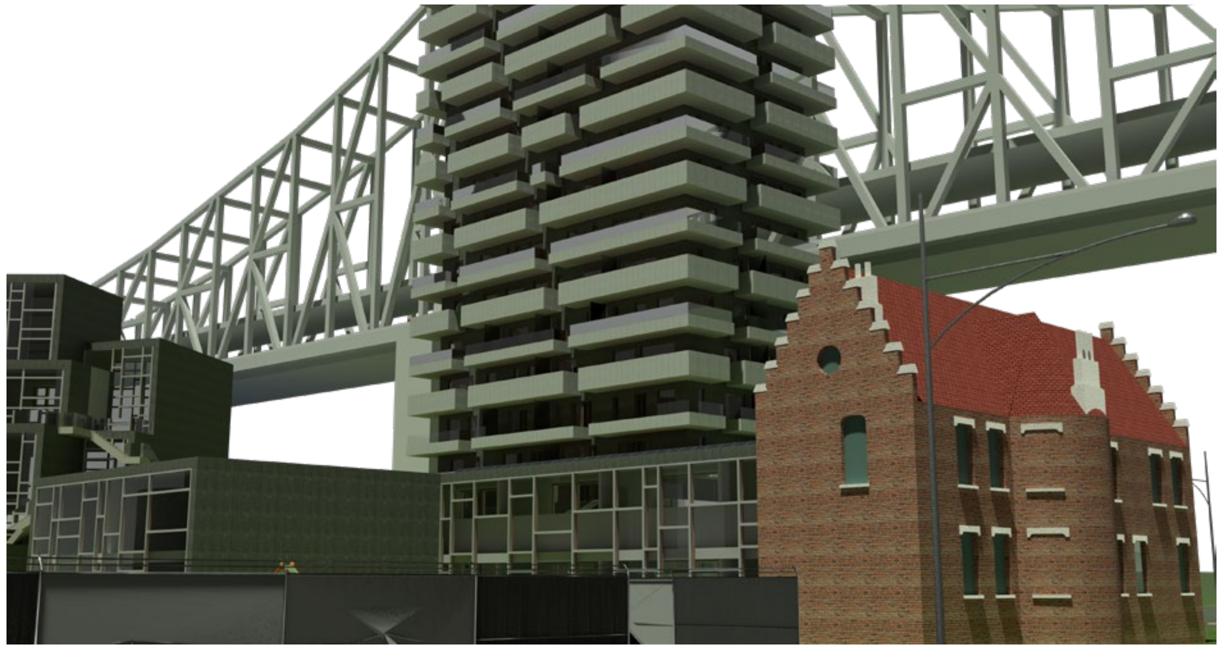

Figure 5.4 - Architectural rendering, view 2

Politecnico di Milano, Master of Science in Building and Architectural Engineering
Steember - Steel and timber for a high rise building in Queens, New York
Chinnici Federico - **Maranesi** Marco

Figure 5.5 - Architectural rendering, view 3

06 STRUCTURAL DESIGN

6.1 – MATERIAL DESCRIPTION

6.1.1 – DEFINITION

The development of dry-built technologies has increased a lot over the last decades; alongside with the growing resistance provided by higher-performant materials, it allows the combination of greater spans and higher-rise buildings, with thinner elements. On the other hand, joint techniques are always more affordable and more common in daily-practice use. Everything goes in the direction of the prefabrication, for greater management in terms of performances, quality execution and general speed of the construction process.

In the analysed building, the main effort has been done on the dimensioning and the calculations of cross-laminated timber and steel members. With this, we underline how much the prefabrication concept has in the analysed project, with a careful design and drawing of each constructing element.

6.1.2 – TIMBER

Timber, used as a bidimensional board, represents the base for a complete cross-laminated timber element. This "engineered" timber looks like practical, economical and easy to build up. From a generic point of view, CLT panels are used for load-bearing applications, working as a solid bidimensional element. It is made of odd layers and assembled orthogonally among themselves, having thus the symmetrical behaviour under the permanent and variable actions to constrain.

Boards are generally sorted by the provided resistance to bending moment; commonly, we face resistances that go from 24N/mm² to 36N/mm². Boards, previously planned, are joined by means of finger joints, in order to ensure the structural continuity between the sheets that make up the individual layers.

These panels are built inside controlled factory conditions and delivered to the site with all the layers already assembled, ready to be set in the proper positions. This technology provides both great performances in terms of energy efficiency and high-quality elements, reducing the needed onsite time, therefore the overall cost.

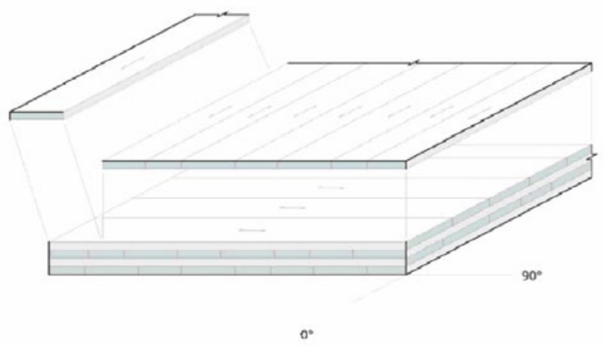

Figure 6.1 - CLT element

6.1.3 – CALCULATION PROCEDURE

CLT TECHNICAL BEHAVIOUR

The way to calculate CLT, as a combination of laminated timber boards and orthogonally crossed at each level, the finite panel has both longitudinal layers and crossed layers. The main direction of the layer corresponds to the ideal way of the loading path (from the panel, it goes in the beams, and so on), and it has a greater stiffness of the beam.

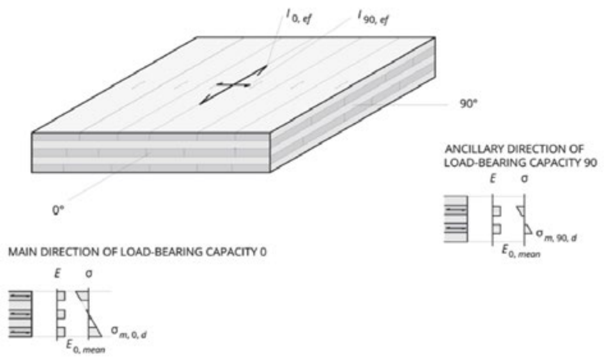

Figure 6.2 - Shear behaviour

In order to compute the effective resistance of the beam, only the panels ordered in the main direction will be computed, because of the null Young modulus assumption for transverse fibres ($E_{90} = 0$). Furthermore, a shear action, defined as "rolling shear" will appear on these above-mentioned transverse layers; consequently, these layers are intended more as spacers for the longitudinal ones, in order to get a higher inertia moment for the final verification to deflection.

CODE PRESCRIPTIONS

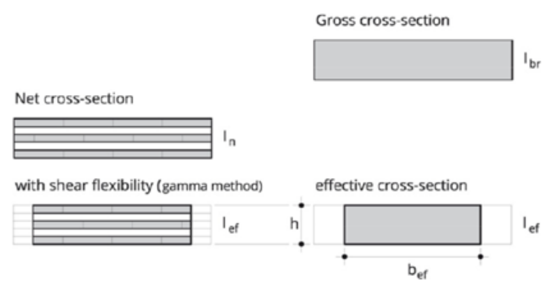

Figure 6.3 - Net cross-section vs. gross cross-section

Because of the lack of information that American standards have regarding the CLT technology prescription, and due to the embedded academic purpose this project has, the choice went for the use of the Eurocode 5. At its inside, the used method is the Gamma theory, which has been approved for the CLT technology panels. The calculation of their inertia has been reduced by a γ factor, which means a reduction of the resisting cross-section area for the calculations of verification at the Serviceability Limit State.

6.2 – CASE STUDY

6.2.1 – INTRODUCTION

The case study consists of 25 floors: 23 of them are above ground, while 2 are completely underground. Following dry-assembled concepts, the idea was to use as much as possible fastening elements, like CLT panels for initial load-bearing slabs, and steel-frame members for beams and columns.

The computed elements regard, consequently, all the members included in the tower, and more specifically:

- CLT panels for rooftop;
- CLT panels for a typical slab;
- Cantilever steel member, having a fixed-end constrain to be welded;
- Secondary steel member, acting in the middle of the span space;
- Secondary steel member, set on the outer face of the central core;
- Primary steel member;
- Border beam element, subjected to the action of the primary beam;
- Border beam element, subjected to the action of the slab itself;
- Steel column member;
- Concrete beam at the ground floor, calculated for the specific purpose of bearing a glass-façade.

For the purpose of the thesis, the above-mentioned elements have been computed in order to match the feasibility of the specific vertical and horizontal joints, aiming for a complete study of the technological field it has been addressed.

6.2.2 – STRUCTURAL SCHEME

As shown in the above image, the building is mainly based on a central concrete core, and on a simple frame made of steel.

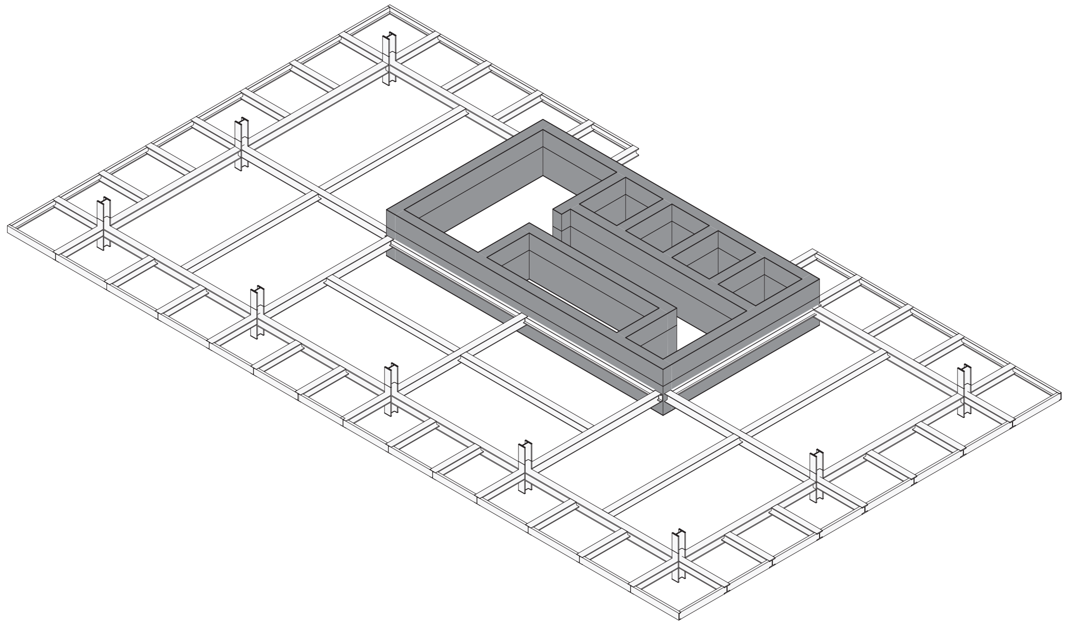

Figure 6.4 - 3D view of the typical structural scheme

Shear walls are represented by a central core, made of concrete. It acts like a windward element in case of building's torsion due to wind force, constraining the arisen momentum, but also provides security in case of a fire incident. It covers a span of 13.60 metres in the longer direction of the tower, and it has a length of a single span in the shorter direction of 7.50 metres. The slabs set at the inside are assumed as made of concrete, due to the specific aim that it must provide with respect to the fire prescriptions; this is the only place designed to resist in case of fire propagation. It includes three lifts and two stairwells, secured by filter spaces at the edge of it.

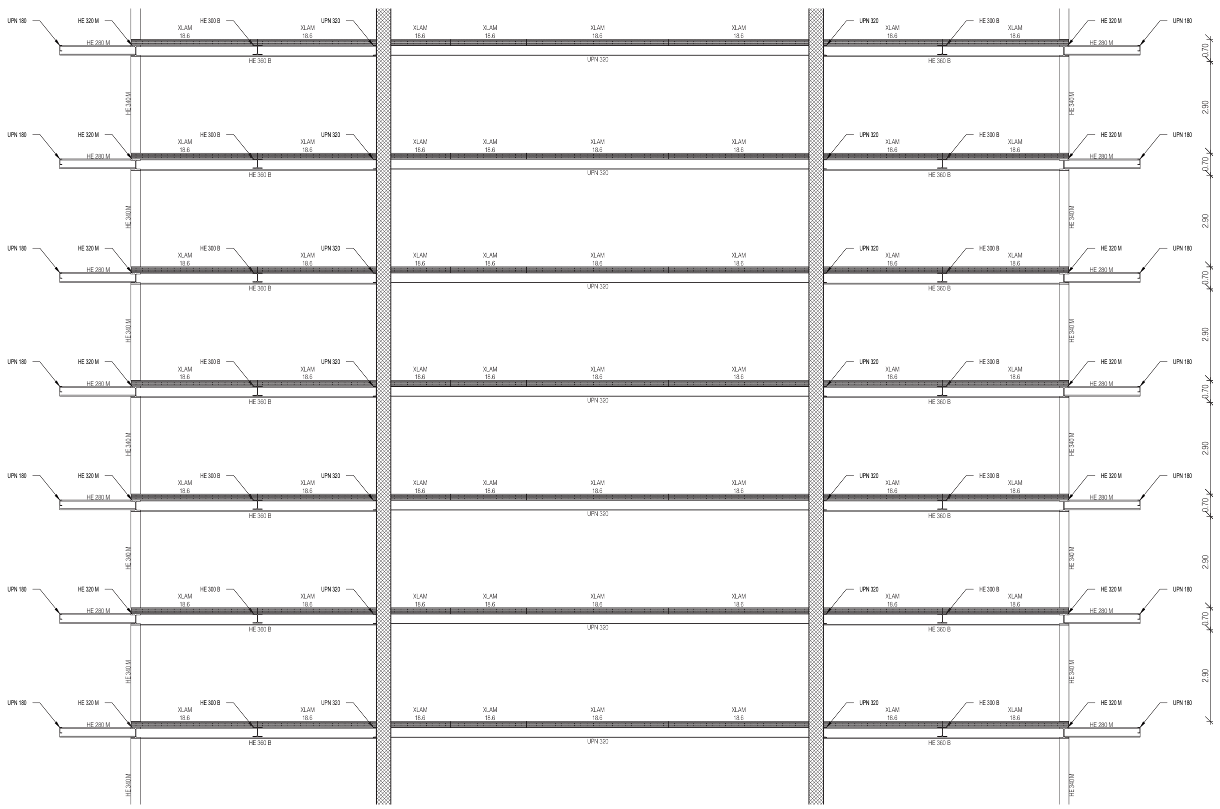

Figure 6.5 - Partial structural section of the building

Due to the severe functionality, the core must deal with, structural girders and columns have been designed in order to comply with the given spans of the concrete elements. In order to facilitate the static behaviour of the building, a regular scheme has been adopted; spans are approximately 6 to 8 metres long, and they follow the first grid the core has. The connection of the beams to the concrete is made through stiffeners plates and anchoring elements passing through the secondary beam and reaching the concrete element.

Consequently, the structural grid covers an area of 3 rows in the shorter span and 5 in the longer direction. Because of the foreseen thickness of the total slab, it has been decided to order secondary beams in the shorter direction for each loading area, so that it was possible to have slightly reduced thicknesses with respect to the other solution. Since the building has a regular vertical subdivision (double-height floors have been avoided) without the use of multi-panel door-windows over a regular height, the greater size border beams have is not impacting on the defined architectural choice. Due to these considerations, CLT panels were ordered in the orthogonal direction of the above-mentioned position of secondary beams.

6.2.3 – TECHNOLOGY

As anticipated, the use of CLT panels and lumber elements could output as the main conclusion a lightweight construction. The layer assembling of customised elements, membranes and panels, also considers the mid-long spans the building has: therefore, lighter stratigraphy could help for a reduced load acting on the structure so that the selection of steel element might go for a thinner member. In this way, the reduced space reserved for structural elements can go for a greater commercial area of apartments, increasing the overall value of the building.

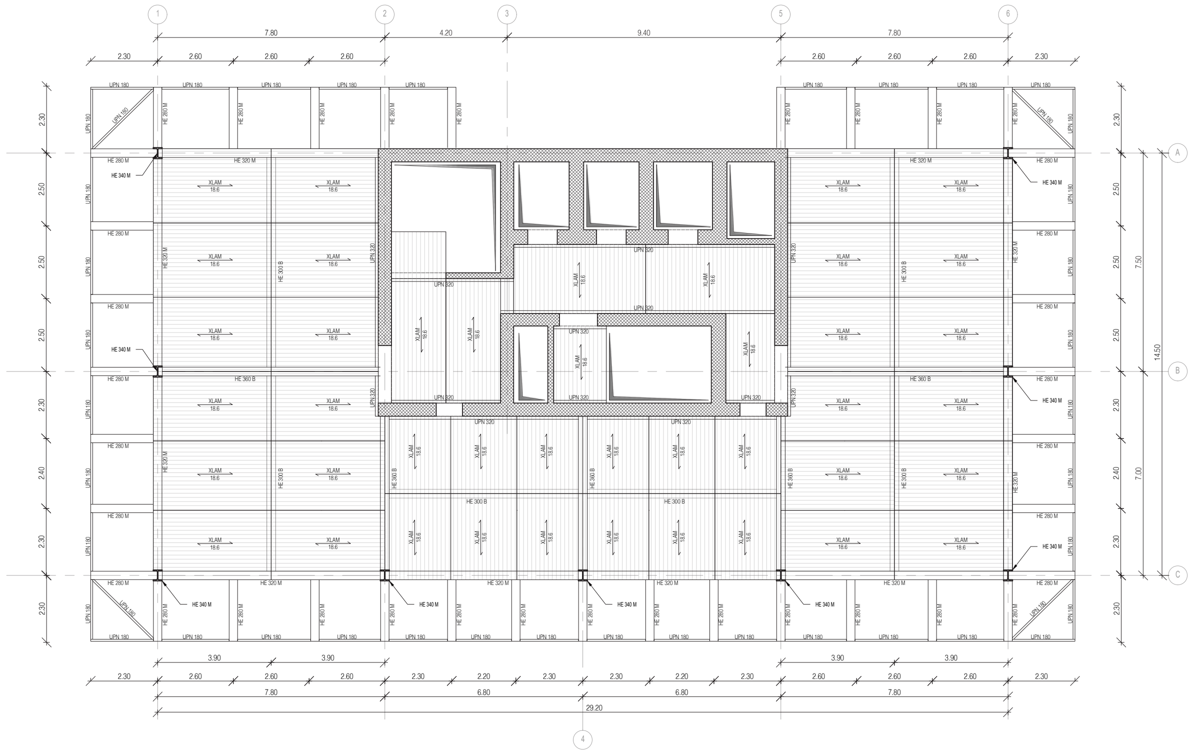

Figure 6.6 - Structural plan of the typical floor

6.2.4 – CODES

The following list includes the code used for the definition of general and specific prescriptions of all the structural elements:

- "Eurocode 1: Actions on structures"
- "Eurocode 2: Design of concrete structures"
- "Eurocode 3: Design of steel structures"
- "Eurocode 5: Design of timber structures"
- "ASCE 7: Minimum Design Loads for Buildings and Other Structures"

Because of the limited availability of data for the project site, it has been decided to rely completely on the Eurocodes for the design of the structures for each specific element.

6.2.5 – MATERIALS

The following subchapter shows, for each material, the properties of the chosen material. Later, the reasons the choice for the specific class will be explained, by looking into the detail of the calculation procedure.

CROSS LAMINATED TIMBER PANELS

- Class		GL36h
- Characteristic bending strength	$f_{m,k}$	32.00 N/mm²
- Operative bending strength	$f_{m,k*}$	28.80 N/mm²
- Partial safety coefficient for CLT	γ_M	1.25
- Characteristic shear strength	$f_{v,k}$	4.30 N/mm²
- Operative shear strength	$f_{v,k*}$	3.44 N/mm²
- Operative compressive strength along the grain	$f_{c,0,d}$	31.00 N/mm²
- Young Modulus	$E_{g,,mean}$	14 700 N/mm²
- Operative Young Modulus	$E_{g,,mean,fin}$	4 900 N/mm²
- Coefficient due to humidity exposure (class 1)	k_{def}	0.60
- Coefficient due to humidity exposure (class 3)	k_{def}	2.00
- Coefficient of shape affecting moment verification	k_{sys}	1.13 vs. 1.23
- Characteristic traction // to fibres	$f_{t,0,g,k}$	25.60 N/mm²
- Rolling shear modulus	$G_{r,g,mean}$	51.20 N/mm²

STEEL – CANTILEVER BEAMS

- Class		S355
- Characteristic yielding strength	$f_{y,k}$	355.0 N/mm²
- Operative bending strength	$f_{m,k*}$	338.1 N/mm²
- Partial safety coefficient for structural steel	γ_{ss}	1.05
- Admissible operative tangent tensional stress	τ_d	195.2 N/mm²
- Young Modulus	$E_{g,,mean}$	210 kN/mm²

STEEL – SECONDARY AND PRIMARY BEAMS

- Class		S235
- Characteristic yielding strength	$f_{y,k}$	235.0 N/mm²
- Operative bending strength	$f_{m,k*}$	223.8 N/mm²
- Partial safety coefficient for structural steel	γ_{ss}	1.05
- Admissible operative tangent tensional stress	τ_d	129.2 N/mm²
- Young Modulus	$E_{g,,mean}$	210 kN/mm²

STEEL – BORDER BEAMS

- Class		S275
- Characteristic yielding strength	$f_{y,k}$	275.0 N/mm²
- Operative bending strength	$f_{m,k*}$	261.9 N/mm²
- Partial safety coefficient for structural steel	γ_{ss}	1.05
- Admissible operative tangent tensional stress	τ_d	151.2 N/mm²
- Young Modulus	$E_{g,,mean}$	210 kN/mm²

STEEL – COLUMNS

- Class		S550MC
- Characteristic yielding strength	$f_{y,k}$	550.0 N/mm²
- Operative bending strength	$f_{m,k*}$	523.8 N/mm²
- Partial safety coefficient for structural steel	γ_{ss}	1.05
- Admissible operative tangent tensional stress	τ_d	302.4 N/mm²
- Young Modulus	$E_{g,,mean}$	210 kN/mm²

CONCRETE – BORDER BEAMS

- Class		C37/45
- Characteristic cubic compressive strength	$R_{c,k}$	45.00 N/mm²
- Characteristic cylinder compressive strength	$f_{c,k}$	37.50 N/mm²
- Compressive resistance strength	$f_{c,d}$	21.25 N/mm²
- Operative compressive resistance strength	$f'_{c,d}$	17.00 N/mm²
- Operative tensional stress of concrete	σ_c	22.50 N/mm²
- Average tensional compressive cylindric res.	$f_{c,m}$	45.50 N/mm²
- Average tensional cylindric resistance	f_{ctm}	3.36 N/mm²
- Characteristic traction resistance	f_{ctk}	2.35 N/mm²
- Concrete/steel Young Modulus ratio	α_e	15
- Speed of development for concrete resistances	β_b	2.25

STEEL – REINFORCEMENT OF BORDER BEAMS

- Class B450C
- Characteristic yielding strength $f_{y,k}$ 450.0 N/mm²
- Operative bending strength f_{m,k^*} 391.3 N/mm²
- Partial safety coefficient for structural steel γ_{ss} 1.15
- Admissible operative tensional stress σ_c 360.0 N/mm²
- Young Modulus $E_{g,,mean}$ 210 kN/mm²

6.3 – LOAD ANALYSIS

6.3.1 – PERMANENT LOADS

In the following pages, there are tables of recaps of the permanent loads applied on the different elements composing the technological part acting on the structure. Those loads are subdivided into the category G1 (permanent load-bearing layers) and G2 (permanent non-load-bearing layers).

ROOF

	Layers	ρ [kN/m³]	t [m]	q [kN/m²]
G2	Soil	14.64	0.150	2.20
	Filtering membrane	0.00	0.004	0.00
	Stock/dryer layer	0.25	0.082	0.02
	Lightweight screed	4.00	0.075	0.30
	Waterproof membrane	20.00	0.002	0.04
	OSB panel	6.25	0.013	0.08
	Wooden fibre	1.60	0.160	0.26
G1	Xlam slab	4.00	0.332	1.33
G2	Water vapour barrier	11.00	0.003	0.03
	Wooden fibre	0.70	0.050	0.04
	Gypsumfibre sheet	11.50	0.013	0.14
	Gypsumfibre sheet	11.50	0.013	0.14
			0.818	4.69
Q	SNOW	C_e [-]	C_t [-]	
		0.90	0.85	
		I_{snow} [-]	p_g [kN/m²]	q_s [kN/m²]
		1.10	0.96	0.57
	CATEGORY A			2.00
				7.26

INTERMEDIATE SLAB

	Layers	ρ [kN/m³]	t [m]	q [kN/m²]
G2	Internal partitions			1.34
	Wooden tiles	9.20	0.010	0.09
	Gypsumfibre sheet	11.50	0.013	0.14
	Lightweight screed	15.00	0.045	0.68
	Wooden fibre insulation	2.50	0.020	0.05
	Lightweight screed	4.00	0.080	0.32
	Protective membrane	3.50	0.002	0.01
	Clomping insulation	7.00	0.013	0.09
G1	Xlam slab	4.00	0.186	0.74
G2	Wooden fibre insulation	0.70	0.050	0.04
	Gypsumfibre sheet	11.50	0.013	0.14
	Gypsumfibre sheet	11.50	0.013	0.14
	Gypsum plaster	12.00	0.010	0.12
			0.454	3.90
Q	CATEGORY A			2.00
				5.90

BALCONY

	Layers	ρ [kN/m³]	t [m]	q [kN/m²]
G1	Wooden boards	10.00	0.030	0.30
	Lightweight concrete	20.00	0.110	2.20
			0.320	2.54
Q	CATEGORY 5			2.50
				5.04

PAVEMENT SLAB

	Layers	ρ [kN/m³]	t [m]	q [kN/m²]
G2	Internal partitions			1.34
	Tiles	20.00	0.015	0.30
	Lightweight screed	4.00	0.080	0.32
	Waterproof membrane	20.00	0.002	0.04
	Wooden fibre insulation	1.60	0.160	0.26
G1	Xlam slab	4.00	0.186	0.74
G2	Wooden fibre insulation	0.70	0.050	0.04
	Gypsumfibre sheet	11.50	0.013	0.14
	Gypsumfibre sheet	11.50	0.013	0.14
			0.493	3.03
Q	CATEGORY A			2.00
				5.03

GARDEN

	Layers	ρ [kN/m³]	t [m]	q [kN/m²]
	Soil	14.64	0.150	2.20
	Filtering membrane	0.00	0.001	0.00
G2	Stock/dryer layer	0.25	0.082	0.02
	Protective membrane	10.50	0.004	0.04
	Screed	14.00	0.100	1.40
G1	Cast Concrete	25.00	0.050	1.25
	Imafor H320 alveolare	12.75	0.320	4.08
			0.470	8.99
Q	CATEGORY 4			5.00
				13.99

EXTERNAL WALLS

	Layers	ρ [kN/m³]	t [m]	q [kN/m²]
	Wooden cladding	3.80	0.020	0.08
	Gypsumfibre sheet	11.50	0.013	0.14
	Wooden fibre insulation	1.60	0.080	0.13
	Gypsumfibre sheet	11.50	0.013	0.14
	Wooden frame	3.80	0.160	0.08
	Wooden fibre insulation	1.60		0.22
	Gypsumfibre sheet	11.50	0.013	0.14
	Water vapour barrier	5.50	0.020	0.11
	Gypsumfibre sheet	11.50	0.013	0.14
	Gypsum plaster	12.00	0.010	0.12
			0.340	1.31
			h_{floor} [m]	$g_{ext.\ wall}$ [kN/m]
IND. TYPE			3.60	4.72

INTERNAL PARTITIONS

	Layers	ρ [kN/m³]	t [m]	q [kN/m²]
	Ceramic tile	20.00	0.010	0.20
	Gypsum plaster	12.00	0.010	0.12
	Gypsumfibre sheet	11.50	0.013	0.14
	Gypsumfibre sheet	11.50	0.013	0.14
	Wooden frame	3.80	0.120	0.06
	Insufflate cellulose insulation	0.38		0.04
	Gypsumfibre sheet	11.50	0.013	0.14
	Gypsumfibre sheet	11.50	0.013	0.14
	Gypsum plaster	12.00	0.010	0.14
	Ceramic tile	20.00	0.010	0.20
			0.21	1.34

CURTAIN WALL

	Layers	ρ [kN/m³]	t [m]	q [kN/m²]
	Glass wall	10.80	0.05	0.53
			h_{floor} [m]	$g_{curtain\ wall}$ [kN/m]
			6.80	3.60

6.3.2 – VARIABLE LOADS

CATEGORIES FOR RESIDENTIAL USE

Regarding the main function of this project, residential use is highlighted as the one and only function of the building. According to the EC 1991-1-1, the selected categories are A as the main variable load inside the building and H as the load acting on the roof.

Category	Specific Use	Example
A	Areas for domestic and residential activities	Rooms in residential buildings and houses; bedrooms and wards in hospitals; bedrooms in hotels and hostels kitchens and toilets.
B	Office areas	
C	Areas where people may congregate (with the exception of areas defined under category A, B, and D[1])	**C1**: Areas with tables, etc. e.g. areas in schools, cafés, restaurants, dining halls, reading rooms, receptions. **C2**: Areas with fixed seats, e.g. areas in churches, theatres or cinemas, conference rooms, lecture halls, assembly halls, waiting rooms, railway waiting rooms. **C3**: Areas without obstacles for moving people, e.g. areas in museums, exhibition rooms, etc. and access areas in public and administration buildings, hotels, hospitals, railway station forecourts. **C4**: Areas with possible physical activities, e.g. dance halls, gymnastic rooms, stages. **C5**: Areas susceptible to large crowds, e.g. in buildings for public events like concert halls, sports halls including stands, terraces and access areas and railway platforms.
D	Shopping areas	**D1**: Areas in general retail shops **D2**: Areas in department stores

[1] Attention is drawn to 6.3.1.1(2), in particular for C4 and C5. See EN 1990 when dynamic effects need to be considered. For Category E, see Table 6.3

NOTE 1 Depending on their anticipated uses, areas likely to be categorised as C2, C3, C4 may be categorised as C5 by decision of the client and/or National annex.

NOTE 2 The National annex may provide sub categories to A, B, C1 to C5, D1 and D2

NOTE 3 See 6.3.2 for storage or industrial activity

Figure 6.7 - Categories of use for residential, social, commercial and administration areas

Categories of loaded area	Specific Use
H	Roofs not accessible except for normal maintenance and repair.
I	Roofs accessible with occupancy according to categories A to $\boxed{AC_1}$ G $\boxed{AC_1}$
K	Roofs accessible for special services, such as helicopter landing areas

Figure 6.8 - Categorisation of roofs

Categories of loaded areas	q_k [kN/m²]	Q_k [kN]
Category A		
- Floors	1,5 to2,0	2,0 to 3,0
- Stairs	2,0 to4,0	2,0 to 4,0
- Balconies	2,5 to 4,0	2,0 to 3,0
Category B	2,0 to 3,0	1,5 to 4,5
Category C		
- C1	2,0 to 3,0	3,0 to 4,0
- C2	3,0 to 4,0	2,5 to 7,0 (4,0)
- C3	3,0 to 5,0	4,0 to 7,0
- C4	4,5 to 5,0	3,5 to 7,0
- C5	5,0 to 7,5	3,5 to 4,5
category D		
- D1	4,0 to 5,0	3,5 to 7,0 (4,0)
- D2	4,0 to 5,0	3,5 to 7,0

Figure 6.9 - Imposed loads on floors, balconies and stairs in buildings

SNOW LOAD

The calculation of the snow load is performed according to "ASCE 7: Minimum Design Loads for Buildings and Other Structures". This is due to the availability of data from the New York code building because the Eurocode allows the use of national annexes for its computation.

According to the (Eq. 7-1), we have:

$$q_s = 0.7 * c_e * c_t * I * p_g$$

Where:

C_e = exposure coefficient;

C_t = thermal coefficient;

I = importance factor;

S_k = characteristic value of snow load on the ground.

C_e can be computed as the below-shown table, where it is a function of the terrain category (B for urban and suburban areas), and of the fully exposed building (defined as "Roofs exposed on all sides with no shelter, afforded by terrain, higher structures, or trees"):

Terrain Category	Fully Exposed	Exposure of Roof* Partially Exposed	Sheltered
A (see Section 6.5.6)	N/A	1.1	1.3
B (see Section 6.5.6)	0.9	1.0	1.2
C (see Section 6.5.6)	0.9	1.0	1.1
D (see Section 6.5.6)	0.8	0.9	1.0
Above the treeline in windswept mountainous areas.	0.7	0.8	N/A
In Alaska, in areas where trees do not exist within a 2-mile (3 km) radius of the site.	0.7	0.8	N/A

The terrain category and roof exposure condition chosen shall be representative of the anticipated conditions during the life of the structure. An exposure factor shall be determined for each roof of a structure.

Figure 6.10 - Exposure coefficient C_e

Politecnico di Milano, Master of Science in Building and Architectural Engineering
Steember - Steel and timber for a high rise building in Queens, New York
Chinnici Federico - **Maranesi** Marco

C_t is a function of the warmness of the rooftop: since it can be considered as a warm element (with a transmittance lower than 0.40 W/m²K), we can get the coefficient from the below table, and from the extract of the referent national annexe:

Thermal Condition*	C_t
All structures except as indicated below	1.0
Structures kept just above freezing and others with cold, ventilated roofs in which the thermal resistance (R-value) between the ventilated space and the heated space exceeds 25 F°·hr·sq ft/Btu (4.4 K·m²/W)	1.1
Unheated structures and structures intentionally kept below freezing	1.2
Continuously heated greenhouses** with a roof having a thermal resistance (R-value) less than 2.0 F°·hr·ft²/Btu(0.4 K·m²/W)	0.85

*These conditions shall be representative of the anticipated conditions during winters for the life of the structure.

**Greenhouses with a constantly maintained interior temperature of 50°F (10°C) or more at any point 3 ft above the floor level during winters and having either a maintenance attendant on duty at all times or a temperature alarm system to provide warning in the event of a heating failure.

Figure 6.11 - Thermal coefficient C_t

It follows an extract that defines the exposure class for the snow coefficient.

"Exposure B: Exposure B shall apply where the ground surface roughness condition, as defined by Surface Roughness B, prevails in the upwind direction for a distance of at least 2630 ft (800 m) or 10 times the height of the building, whichever is greater. Exception: For buildings whose, mean roof height is less than or equal to 30 ft (9.1 m), the upwind distance may be reduced to 1500 ft (457 m).

Exposure C: Exposure C shall apply for all cases where exposures B or D do not apply.

Exposure D: Exposure D shall apply where the ground surface roughness, as defined by surface roughness D, prevails in the upwind direction for a distance at least 5000 ft (1524 m) or 10 times the building height, whichever is greater. Exposure D shall extend inland from the shoreline for a distance of 660 ft (200 m) or 10 times the height of the building, whichever is greater".

The important factor I is a function of the building's category; our building is the category III, as shown in the below tables:

Nature of Occupancy	Category
Buildings and other structures that represent a low hazard to human life in the event of failure including, but not limited to: Agricultural facilities Certain temporary facilities Minor storage facilities	I
All buildings and other structures except those listed in Categories I, III, and IV	II
Buildings and other structures that represent a substantial hazard to human life in the event of failure including, but not limited to: Buildings and other structures where more than 300 people congregate in one area Buildings and other structures with day care facilities with capacity greater than 150 Buildings and other structures with elementary school or secondary school facilities with capacity greater than 250 Buildings and other structures with a capacity greater than 500 for colleges or adult education facilities Health care facilities with a capacity of 50 or more resident patients but not having surgery or emergency treatment facilities Jails and detention facilities Power generating stations and other public utility facilities not included in Category IV Buildings and other structures not included in Category IV (including, but not limited to, facilities that manufacture, process, handle, store, use, or dispose of such substances as hazardous fuels, hazardous chemicals, hazardous waste, or explosives) containing sufficient quantities of hazardous materials to be dangerous to the public if released. Buildings and other structures containing hazardous materials shall be eligible for classification as Category II structures if it can be demonstrated to the satisfaction of the authority having jurisdiction by a hazard assessment as described in Section 1.5.2 that a release of the hazardous material does not pose a threat to the public.	III
Buildings and other structures designated as essential facilities including, but not limited to: Hospitals and other health care facilities having surgery or emergency treatment facilities Fire, rescue, ambulance, and police stations and emergency vehicle garages Designated earthquake, hurricane, or other emergency shelters Designated emergency preparedness, communication, and operation centers and other facilities required for emergency response Power generating stations and other public utility facilities required in an emergency Ancillary structures (including, but not limited to, communication towers, fuel storage tanks, cooling towers, electrical substation structures, fire water storage tanks or other structures housing or supporting water, or other fire-suppression material or equipment) required for operation of Category IV structures during an emergency Aviation control towers, air traffic control centers, and emergency aircraft hangars Water storage facilities and pump structures required to maintain water pressure for fire suppression Buildings and other structures having critical national defense functions Buildings and other structures (including, but not limited to, facilities that manufacture, process, handle, store, use, or dispose of such substances as hazardous fuels, hazardous chemicals, hazardous waste, or explosives) containing extremely hazardous materials where the quantity of the material exceeds a threshold quantity established by the authority having jurisdiction. Buildings and other structures containing extremely hazardous materials shall be eligible for classification as Category II structures if it can be demonstrated to the satisfaction of the authority having jurisdiction by a hazard assessment as described in Section 1.5.2 that a release of the extremely hazardous material does not pose a threat to the public. This reduced classification shall not be permitted if the buildings or other structures also function as essential facilities.	IV

Figure 6.12 - Classification of buildings for flood, wind, snow, earthquake and ice loads

Category*	I
I	0.8
II	1.0
III	1.1
IV	1.2

*See Section 1.5 and Table 1-1.

Figure 6.13 - Classification of buildings for flood, wind, snow, earthquake and ice loads

P_g is a given value for the roof's slope under 5°.

Consequently, the final load is:

$$q_s = 0.7 * 0.90 * 0.85 * 1.10 * 0.96 = 0.57\ kN/m^2$$

WIND LOAD

The calculation of the snow load is performed according to the Eurocode 1-4 prescriptions for wind actions. Because of the high number of coefficients that need to be computed, it has been decided to show a few steps for the definition of the wind load.

For its calculations, it has been decided to evaluate the parapet only under the effect of the wind load; wind forces acting on external walls, curtain walls and roof have been neglected.

As a starting point, the value of the initial wind speed was taken according to the class of the building (class III, as coded in the "ASCE 7: Minimum Design Loads for Buildings and Other Structures") and the variation of the wind height has been reached, with the following formula:

$$v_{m(z)} = c_{r(z)} * c_{o(z)} * v_b = 1.04 * 1.00 * 53.55 = 55.61\ m/s$$

Where:

$v_{m(z)}$ = mean wind velocity;

$c_{r(z)}$ = roughness factor, accounts for the variability of the mean wind velocity at the site of the structure due to the height above ground level and the ground roughness of the terrain upwind of the structure in the wind direction considered. In the procedure, a total height of 84.1 metres has been considered as the highest values of the balcony, on the last floor;

$c_{o(z)}$ = terrain orthography, wherein the absence of characteristic situations, can be assumed as 1;

v_b = basic wind velocity, given in the National Annex.

After the computation of the mean wind, it is now the step of calculating the eventual wind turbulence Iv, as a basic step for the following peak velocity pressure.

$$I_{v(z)} = \frac{\sigma_v}{v_{m(z)}} = \frac{13.03}{55.61} = 0.23$$

Where:

σ_v = standard deviation of the mean velocity;

$v_{m(z)}$ = mean wind velocity.

Once the turbulence intensity is defined, the next step is the peak velocity pressure $q_{p(z)}$ at height z, which includes mean and short-term velocity fluctuations. The formula is the following:

$$q_{p(z)} = \left(1 + 7 * I_{v(z)}\right) * \frac{1}{2} * \rho * v_{m(z)}^2 = (1 + 7 * 0.23) * 0.50 * 1.25 * 55.61^2$$
$$= 5.10\ kN/m^2$$

Where:

I_v = wind turbulence factor;

ρ = density of the air (coded as 1.25 kg/m³);

$v_{m(z)}$ = mean wind velocity.

The final calculation regards directly the wind pressure, acting on a surface. Here, codes prescribe the use of the highest value between external pressure and internal pressure, as the driving coefficient for the definition of the final wind force.

$$w_e = q_{p(z)} * c_{pe} = 5.10 * 1.60 = 8.17\ kN/m^2$$

Where:

w_e = wind pressure acting on the external surfaces;

$q_{p(z)}$ = peak velocity pressure;

c_{pe} = is the pressure coefficient for the external pressure.

6.4 – ELEMENTS' DESIGN

6.4.1 – STEEL CANTILEVER BEAM

LOAD CALCULATION

Given the permanent load (2.54 kN/m²) and the variable load (2.50 kN/m²), we can compute the kN/m value by using the highest length a single beam has to bear due to the slab weight.

$$g' = g * l = 2.54 * 3.75 = 9.54\ kN/m$$

$$q' = q * l = 2.50 * 3.75 = 9.38\ kN/m$$

$$g' + q' = 9.54 + 9.38 = 18.91\ kN/m$$

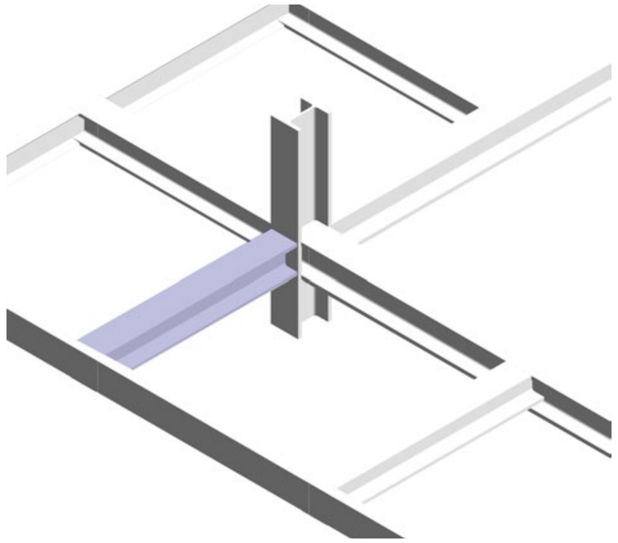

Figure 6.14 - The cantilever beam

Due to the presence of the parapet, we have a pointed load set on the extremity of the balcony.

$$P = \rho * s_{th.} * h_{rail} * l * \gamma_g = 35 * (2 * 0.012) * 1.10 * 3.75 * 1.35 = 4.68\ kN$$

The parapet provides also bending moment on the top end of the structure, which will be considered as negative due to the reverse action.

$$M_w = w_e * l * \frac{h_{rail}^2}{2} = 8.17 * 3.75 * \frac{1.10^2}{2} = 18.53\ kNm$$

ULS - M_{max}

Following the superimposition of the schematic schemes, as shown in the below images, we can compute the maximum bending moment at the ultimate limit state.

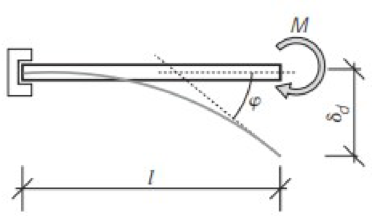

$M = \text{costante} \quad V = 0 \quad \varphi = +\frac{Ml}{EI} \quad \delta_d = +\frac{Ml^2}{2EI}$

Figure 6.15 - Isostatic scheme: fixed-end constrain and moment force

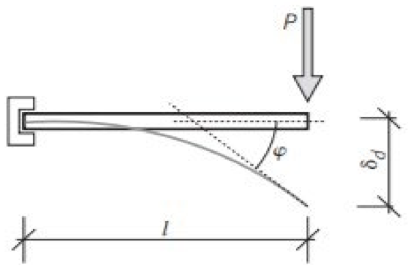

$M_{max} = Pl \quad V = P \quad \varphi = +\frac{Pl^2}{2EI} \quad \delta_d = +\frac{Pl^3}{3EI}$

Figure 6.16 - Isostatic scheme: fixed-end constrain and concentrated load on opposite extreme

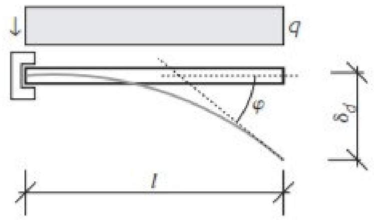

$$M_{max} = \frac{ql^2}{2} \quad V_{max} = ql \quad \varphi = +\frac{ql^3}{6EI} \quad \delta_d = \frac{ql^4}{8EI}$$

Figure 6.17 - Isostatic scheme: fixed-end constrain and distributed load over the span

Eurocode prescriptions refer to use of some safety partial coefficients for permanent and variable loads. At the ULS, those coefficients are:

$$\gamma_g = 1.35$$

$$\gamma_q = 1.50$$

Proceeding with the moment actions:

$$M_{ed,dis} = (\gamma_g * g' + \gamma_q * q') * \frac{l^2}{2} = (1.35 * 9.54 + 1.50 * 9.38) * \frac{2.30^2}{2} = 71.24\ kNm$$

$$M_{ed,con} = \gamma_g * P * l = 1.35 * 4.68 * 2.30 = 14.52\ kNm$$

$$M_w = 18.53\ kNm$$

The final moment will be:

$$M_{ed} = M_{ed,distr} + M_{ed,con} + M_w = 71.24 + 14.52 - 18.53 = 67.24\ kNm$$

The final step, thus, is to find the minimum module resistance due to the bending moment.

$$W_{x,min} = \frac{M_{ed}}{f_{y,k}} = \frac{72.24}{338.10} = 199\ cm^3$$

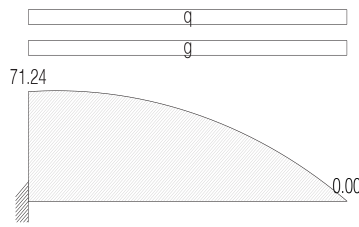

Figure 6.18 - Moment diagram of the distributed load

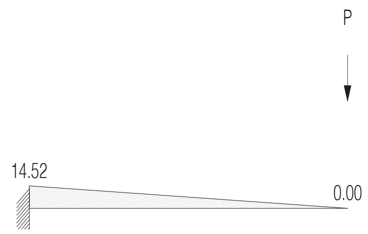

Figure 6.19 - Moment diagram of the concentrated load

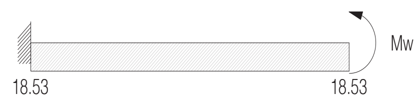

Figure 6.20 - Moment diagram of the moment wind force

SLS – δ_{max}

The code prescribes which is the worst combination between the variable loads only (at the SLS state), with an allowed deflection of l/150 for cantilever beams, and the complete load (permanent + variable) with an allowed deflection of l/125, intended as getting half of the values with respect to isostatic beams with hinged-rolled constrains.

Condizioni	Limiti (vedere fig. 4.1)	
	δ_{max}	δ_2
Coperture in generale	L/200	L/250
Coperture praticate frequentemente da personale diverso da quello della manutenzione	L/250	L/300
Solai in generale	L/250	L/300
Solai o coperture che reggono intonaco o altro materiale di finitura fragile o tramezzi non flessibili	L/250	L/350
Solai che supportano colonne (a meno che lo spostamento sia stato incluso nella analisi globale per lo stato limite ultimo)	L/400	L/500
Dove δ_{max} può compromettere l'aspetto dell'edificio	L	/250

Figure 6.21 - Table of the limit values for deflection

Calculations are:

$$comb.1 = \frac{q'}{\delta'_{max}} = \frac{9.38}{\frac{2.30}{150}} = 611\ kN$$

$$comb.2 = \frac{g' + q'}{\delta''_{max}} = \frac{9.54 + 9.38}{\frac{2.30}{125}} = 1\ 028\ kN$$

Using the worst combination, it is now possible to proceed by looking at the minimum inertia the beam must provide. The superimposition of the effects leads to the result. In order to get it, we should compute the final Young modulus, which is susceptible to the above-mentioned service class of the beam.

$$I_{x,min,distr.} = (g' + q') * \frac{l^4}{8 * E_s * \delta''_{max}} = (9.54 + 9.38) * \frac{2.30^4}{8 * 210\ 000 * \left(\frac{2.30}{125}\right)} = 1\ 712\ cm^4$$

$$I_{x,min,con.} = P * \frac{l^3}{3 * E_s * \delta''_{max}} = 4.68 * \frac{2.30^3}{3 * 210\ 000 * \left(\frac{2.30}{100}\right)} = 491\ cm^4$$

$$I_{x,min,w} = M_w * \frac{l^2}{2 * E_s * \delta''_{max}} = 18.53 * \frac{2.30^2}{2 * 210\ 000 * \left(\frac{2.30}{100}\right)} = 1\ 268\ cm^4$$

The final minimum inertia will be:

$$I_{x,min} = I_{x,min,distr.} + I_{x,min,con.} - I_{x,min,w} = 1\ 712 + 491 - 1\ 268 = 935\ cm^4$$

BEAM CHOICE

Because of the minimum resistant module and the minimum inertia, it has been selected a proper beam in order to verify these two above-mentioned restrictions. The selection goes for a HE 280 M, needed for the verification due to torsion moment.

$$h = 31\ cm; \qquad A = 240\ cm^2$$

$$b = 29\ cm; \qquad \rho_{g,k} = 1.89\ \frac{kN}{m}$$

$$t_w = 0.019\ cm; \qquad W_x = 2\ 551\ cm^3$$

$$t_f = 0.033\ cm; \qquad I_x = 39\ 550\ cm^4$$

Thus:

$$W_{x,} > W_{x,min} \rightarrow 2\ 551\ cm^3 > 300\ cm^3$$

$$I_x > I_{x,min} \rightarrow 39\ 550\ cm^4 > 935\ cm^4$$

SLS - M_{max}

With the superimposition of the combination, it is now possible to compute the maximum bending moment at the SLS. The used formulas are the above-mentioned ones.

$$M_{ed,distr.} = \left(\rho_{g,k} + g' + q'\right) * \frac{l^2}{2} = (1.89 + 9.54 + 9.38) * \frac{2.30^2}{2} = 55.02\ kNm$$

$$M_{ed,conc.} = P * l = 4.68 * 2.30 = 10.76\ kNm$$

$$M_w = 18.53\ kNm$$

Therefore:

$$M_{ed} = M_{ed,distr.} + M_{ed,conc.} - M_w = 55.02 + 10.76 - 18.53 = 47.25\ kNm$$

The resisting moment is computed as:

$$M_{rd} = f_{y,k} * \frac{W_x}{\delta_M} = 375.00 * \frac{2\ 551}{1.05} = 862.48\ kNm$$

So:

$$M_{ed} < M_{rd} \rightarrow 47.25\ kNm < 862.48\ kNm \rightarrow utilisation\ 5\%$$

ULS - V_{max}

With the superimposition of the combination, it is now possible to compute the maximum shear at the ULS, with its relative coefficients. The used formulas are the above-mentioned ones.

$$V_{max,distr.} = \left(\gamma_g * \left(\rho_{g,k} + g'\right) + \gamma_q * q'\right) * L = (1.35 * (1.89 + 9.54) + 1.50 * 9.38) * 2.30 = 67.82\ kN$$

$$V_{max,conc.} = \gamma_g * P = 1.35 * 4.68 = 6.31\ kN$$

Since there is no shear effect due to wind actions, the effective shear at the ULS.

$$V_{max} = V_{max,distr.} + V_{max,conc.} = 67.82 + 6.31 = 74.13\ kN$$

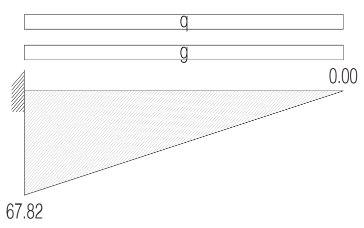

Figure 6.21 - Shear diagram of the distributed load

Figure 6.22 - Shear diagram of the concentrated load

The resisting shear is computed as:

$$V_{rd} = \tau_d * \frac{A_w}{\gamma_M} = \frac{\frac{355.00}{1.05}}{\sqrt{3}} * \frac{(0.31 * 0.019)}{1.05} = 1\,066.16\ kN$$

Consequently:

$$V_{ed} < V_{rd} \rightarrow 74.13\ kN < 1\,066.16\ kN \rightarrow utilisation\ 7\%$$

SLS – δ_{max}

With the superimposition of the combination, it is now possible to compute the deflection at the SLS. The used formulas are the above-mentioned ones. Eurocode defines the way to compute the deflection due to the load-bearing slab with some partial coefficients due to the intensity of the action (permanent, semi-permanent, accidental, etc.), according to the load type (people, snow, wind).

In addition, a creep phenomenon is considered, by multiplying the coefficient of class (subjected to humidity exposure) to the permanent load only, as an adding force for the deflection verification.

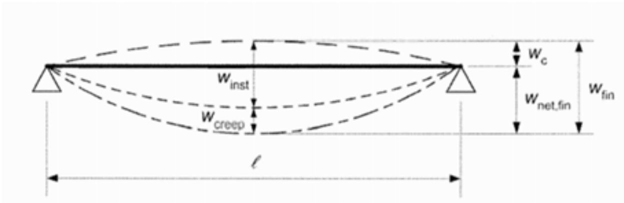

Figure 6.23 - Coefficients due to variable load types

$$\delta_{beam,g} = \left(\rho_{g,k} + g'\right) * \frac{l^4}{8 * E_s * I_x} = (0.715 + 9.54) * \frac{2.45^4}{8 * 210\,000 * 39\,550} = 0.000\ m$$

$$\delta_{beam,g} = \left(\rho_{g,k} + g' + q'\right) * \frac{l^4}{8 * E_s * I_x} = (0.715 + 9.54 + 9.38) * \frac{2.45^4}{8 * 210\,000 * 39\,550} = 0.001\ m$$

The allowed deflection for a fixed-end beam due to permanent load only is:

$$\delta_{max} = \frac{l}{\frac{350}{2}} = \frac{2.30}{\frac{350}{2}} = 0.013\ m$$

While for a beam loaded of both permanent and variable loads, the maximum allowed deflection is:

$$\delta_{max} = \frac{l}{\frac{300}{2}} = \frac{2.30}{\frac{300}{2}} = 0.015\ m$$

Consequently:

$$\delta_{beam,g} < \delta_{max} \rightarrow 0.000\ m < 0.013\ m \rightarrow utilisation\ 4\%$$

Consequently:

$$\delta_{beam,g+q} < \delta_{max} \rightarrow 0.001\ m < 0.015\ m \rightarrow utilisation\ 6\%$$

Politecnico di Milano, Master of Science in Building and Architectural Engineering
Steember - Steel and timber for a high rise building in Queens, New York
Chinnici Federico - **Maranesi** Marco

SLS – τ_{max}

Another effect given to the cantilever beam is due torsion moment. Because the distribution load is not set on the exact axis of the beam, in some cases it is needed to go through a further verification of the bending moment due to torsion.

In order to compute this, at first it is needed to check the torsion moment, intended as a distributed load acting on its middle, multiplied by its lever arm:

$$M_{tor} = (g' + q') * l * (l - \frac{l_{prim.}}{3 * 2}) = (9.54 + 9.38) * 2.30 * (2.30 - \frac{7.80}{3 * 2}) = 43.49\ kNm$$

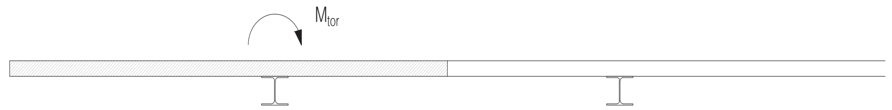

Figure 6.24 - Longitudinal section of the balcony and torsion effect

The outcome of the tensional tangent stress will be:

$$\tau_{max} = 3 * M_{tor} * \frac{t_f}{\sum_{i=1}^{i=3}(2 * b * t_f^3 + (h - 2 * t_f) * t_w^3} = 3 * 43.49 * \frac{33}{(2 * 220 * 33^3 + (310 - 2 * 33) * 19^3} = 193.57 \frac{N}{mm^2}$$

While the resisting force due to torsion is:

$$\tau_{tor} = \frac{f_{yd}}{\sqrt{3}} = \frac{338.10}{\sqrt{3}} = 195.20 \frac{N}{mm^2}$$

Therefore:

$$\tau_{max} < \tau_{tor} \rightarrow 193.57 \frac{N}{mm^2} < 195.20 \frac{N}{mm^2} \rightarrow utilisation\ 99\%$$

6.4.2 – XLAM - INTERMEDIATE SLAB

INTRODUCTION

Before computing the load analysis, a proper computation on the CLT needs to be done. As mentioned in the early part of the chapter, the extreme layers are the ones who need to resist the bending action. The ones set in the middle are considered as "spacers", in order to achieve a great inertia moment, able to provide a lower deflection of the panel.

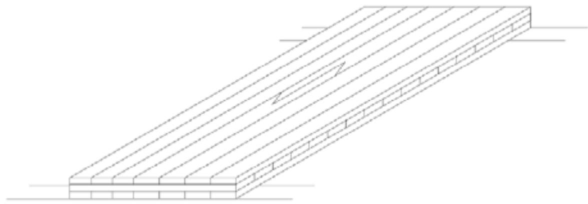

Figure 6.25 - Mono/dimensional XLAM slab

For the calculation of the load-bearing panel, it has been decided to show the most frequent action where panels are set. Since we have one rooftop level, while the rest are all slabs, the below-shown procedure counts for the slab computation only. By changing the initial loads acting on the rooftop rather than the intermediate slabs, the number of layers for the roof level will change. However, the procedure for their calculation is always the same; in addition to the loads, it changes just some coefficient for the service class of the timber.

GEOMETRY

The calculation of the number of layers composing the finite panel refers to the first step.

$$L_{ref} = \frac{l_{prim.}}{2} = \frac{7.80}{2} = 3.90\ m$$

$$b = \frac{l_{sec.}}{3} = \frac{7.50}{3} = 2.50\ m$$

Once defined the two measures of the single board, it is now time to evaluate the inertia the single layer has:

$$J_1 = b * \frac{th_1^3}{12} = 2.50 * \frac{0.040^3}{12} = 1\,333.33\ cm^4$$

$$J_2 = b * \frac{th_2^3}{12} = 2.50 * \frac{0.033^3}{12} = 748.69\ cm^4$$

Because of the gamma theory prescription, the final effective inertia moment of the panel will be computed by means of a corrective γ coefficient:

$$\gamma_{i,1} = 1 \Big/ 1 + \left(\pi^2 * E_{mean} * \frac{(b * th_1)}{L_{ref}^2} * \frac{th_1}{b * G_{rg,mean}}\right) = (1 + \left(\pi^2 * 14\,700 * \frac{2.50 * 0.040}{3.90^2} * \frac{0.040}{2.50 * 51.20}\right))^{-1} = 0.77$$

Given the coefficient (where Grg, mean is the rolling shear resistance, defined as redoubling the shear resistance), it is now possible to go forward with the definition of the highest inertia moment of the board. At first, a lever arm of the uppermost panel needs to be done, with respect to the centre of the xlam element itself:

$$a_1 = \frac{(n_{layers,th.1} * th_1 + n_{layers,th.2} * th_2)}{2} - \frac{th_1}{2} = \frac{3 * 0.040 + 2 * 0.033}{2} - \frac{0.040}{2} = 0.073\ m$$

$$J_{1,eff} = J_1 + (\gamma_{i,1} * (b * th_1) * a_1^2 = 1\,333.33 + (0.77 * (2.50 * 0.040) * 0.040^2 = 42\,386\ cm^4$$

The reason why only the uppermost layer has been computed is that the resistant module counts for the highest inertia moment of the single board, and it is:

$$W_{o,net} = \frac{J_{1,eff}}{a_1} = \frac{42\,386}{0.073} = 5\,806\ cm^3$$

For the shear verification, the resistance module due to rolling shear needs to be calculated as well:

$$S_{r,net} = b * th_1 * a_1 = 2.50 * 0.040 * 0.073 = 7\,300\ cm^3$$

LOADS

Given the permanent load (3.90 kN/m²) and the variable load (2.00 kN/m²), we can compute the kN/m value by using the maximum span between two secondary beams supporting the xlam board.

$$g' = g * b = 3.90 * 2.50 = 9.76\ kN/m$$

$$q' = q * b = 2.00 * 2.50 = 5.00\ kN/m$$

$$g' + q' = 9.76 + 5.00 = 14.76\ kN/m$$

ULS - M_{max}

Following the superimposition of the schematic schemes, as shown in the below images, we can compute the maximum bending moment at the ultimate limit state.

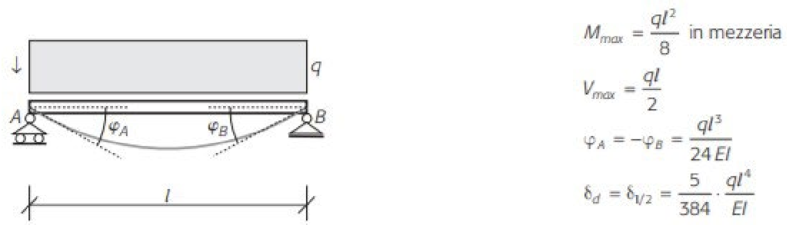

Figure 6.26 - Isostatic scheme with roller/hinge and distributed load

Proceeding with the moment actions:

$$M_{ed} = \left(\gamma_g * g' + \gamma_q * q'\right) * \frac{l^2}{8} = (1.35 * 9.36 + 1.50 * 5.00) * \frac{3.90^2}{8} = 39.30\ kNm$$

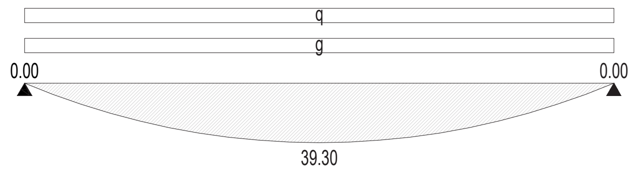

Figure 6.27 - Moment diagram of the distributed load

The maximum tensions due to bending moment are:

$$\sigma_{m,d} = \frac{M_{ed}}{W_{0,net}} = \frac{39.30}{5\,806} = 6.77 \frac{N}{mm^2}$$

While the resisting moment provided by the board is:

$$f_{m,k}^* = \frac{f_{m,k}}{\gamma_M} = \frac{36.00}{1.25} = 28.80 \frac{N}{mm^2}$$

Consequently:

$$\sigma_{m,d} < f_{m,k}^* \rightarrow 6.77 \frac{N}{mm^2} < 28.80 \frac{N}{mm^2} \rightarrow utilisation\ 24\%$$

ULS - V_{max}

At the same time, we can compute the action given by shear forces:

$$V_{max} = \left(\gamma_g * g' + \gamma_q * q'\right) * L/2 = (1.35 * 9.36 + 1.50 * 5.00) * 3.90/2 = 40.31\ kN$$

The maximum tangent tensional stresses will be computed as:

$$\tau_{v,d} = V_{ed} * \frac{S_{r,net}}{J_{1,eff} * b} = 40.31 * \frac{7\,300}{42\,386 * 2.50} = 0.28 \frac{N}{mm^2}$$

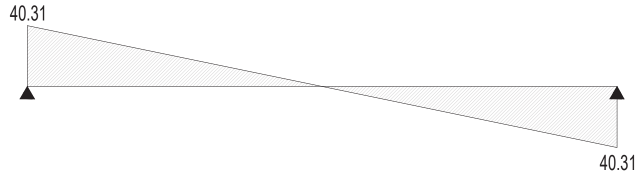

Figure 6.28 - Shear diagram of the distributed load

Here, the resistant module due to rolling shear has been considered, since it has a greater value. The verification, for xlam elements, should be done both to shear actions and rolling shear forces.

Due to Eurocode prescriptions, the service class of the timber will influence the resistance of the resisting shear. Because the computed xlam slab is set in an indoor environment, the used coefficient is 0.60.

$$f_{v,d}^{**} = \frac{f_{v,d}}{\gamma_M} * k_{def} = \frac{4.30}{1.25} * 0.60 = 2.06\ \frac{N}{mm^2}$$

$$f_{vr,d}^{*} = f_{vr,d} * k_{def} = 1.20 * 0.60 = 0.72\ \frac{N}{mm^2}$$

Thus:

$$\tau_{vd} < f_{v,d}^{*} \rightarrow 0.28 \frac{N}{mm^2} < 2.06 \frac{N}{mm^2} \rightarrow utilisation\ 14\%$$

$$\tau_{vd} < f_{vr,d}^{*} \rightarrow 0.28 \frac{N}{mm^2} < 0.72 \frac{N}{mm^2} \rightarrow utilisation\ 39\%$$

SLS - M_{max}

It is now possible to compute the maximum bending moment at the SLS. The used formulas are the above-mentioned ones.

$$M_{ed} = (g' + q') * \frac{l^2}{8} = (9.36 + 5.00) * \frac{3.90^2}{8} = 28.05\ kNm$$

Afterwards, it is needed to calculate the maximum acting due to bending moment:

$$\sigma_{m,d} = \frac{M_{ed}}{W_{0,net}} = \frac{28.05}{5\,806} = 4.83 \frac{N}{mm^2}$$

While the resisting moment provided by the board at the SLS is the combination of the operative resisting stress, corrected by two more coefficients, mentioned earlier in the wooden cantilever beam.

$$f_{m,k}^{*} = \frac{f_{m,k}}{\gamma_M} = \frac{36.00}{1.25} = 28.80 \frac{N}{mm^2}$$

$$k_{def} = 0.60$$

$$k_{sys} = 1 + 0.025 * \left(n_{layers,th.1} + n_{layers,th.2}\right) = 1 + 0.025 * (3 + 2) = 1.13$$

Then:

$$f_{m,d} = f_{m,k} * k_{def} * k_{sys} = \frac{36.00}{1.25} * 0.60 * 1.13 = 19.44 \frac{N}{mm^2}$$

Consequently:

$$\sigma_{m,d} < f_{m,d} \rightarrow 4.83 \frac{N}{mm^2} < 19.44 \frac{N}{mm^2} \rightarrow utilisation\ 25\%$$

SLS – δ_{max}

It is now possible to compute the deflection at the SLS. The used formulas are the above-mentioned ones. Eurocode defines the way to compute the deflection due to the load-bearing slab with some partial coefficients due to the intensity of the action (permanent, semi-permanent, accidental, etc.), according to the load type (people, snow, wind).

In addition, a creep phenomenon is considered, by multiplying the coefficient of class (subjected to humidity exposure) to the permanent load only, as an adding force for the deflection verification.

XLAM slabs should be verified in two different ways: the first one foresees the verification under the condition of a quasi-permanent design situation, while the second one refers to an initial and an end deformation.

$$\delta_{inst.} = \frac{5}{384} * \left(g' + \psi_{0,var.} * q'\right) * \frac{l^4}{E_{mean,fin} * J_{max,eff}}$$
$$= \frac{5}{384} * (9.76 + 0.70 * 5.00) * \frac{3.90^4}{9\,188 * 42\,386} = 0.010\ m$$
$$\delta_{creep} = k_{def} * \frac{5}{384} * g' * \frac{l^4}{8 * E_{mean,fin} * J_{max,eff}} = 0.60 * \frac{5}{384} * 9.76 * \frac{3.90^4}{9\,188 * 42\,386}$$
$$= 0.005\ m$$

The outcome is going to be:

$$\delta_{beam} = \delta_{inst.} + \delta_{creep} = 0.010 + 0.005 = 0.015\ m$$

The allowed deflection is:

$$\delta_{max} = \frac{l}{250} = \frac{3.90}{250} = 0.016\ m$$

Consequently:

$$\delta_{beam} < \delta_{max} \rightarrow 0.015\ m < 0.016\ m \rightarrow utilisation\ 94\%$$

And:

$$\delta_{inst.} = \frac{5}{384} * (g' + q') * \frac{l^4}{E_{mean,fin} * J_{max,eff}} = \frac{5}{384} * (9.76 + 5.00) * \frac{3.90^4}{9\,188 * 42\,386}$$
$$= 0.011\ m$$
$$\delta_{creep} = k_{def} * \frac{5}{384} * g' * \frac{l^4}{8 * E_{mean,fin} * J_{max,eff}} = 0.60 * \frac{5}{384} * 9.76 * \frac{3.90^4}{9\,188 * 42\,386}$$
$$= 0.005\ m$$

So:

$$\delta_{beam} = \delta_{inst.} + \delta_{creep} = 0.011 + 0.005 = 0.016\ m$$

The allowed deflection at the initial state is:

$$\delta_{max} = \frac{l}{300} = \frac{3.90}{300} = 0.013\ m$$

Consequently:

$$\delta_{inst} < \delta_{max} \rightarrow 0.011\ m < 0.013\ m \rightarrow utilisation\ 85\%$$

While the allowed deflection at the initial state is:

$$\delta_{max} = \frac{l}{200} = \frac{3.90}{200} = 0.020\ m$$

Therefore:

$$\delta_{beam} < \delta_{max} \rightarrow 0.016\ m < 0.020\ m \rightarrow utilisation\ 80\%$$

6.4.3 – XLAM - ROOF

Because of the same procedure between the xlam board of the rooftop and the xlam board of the intermediate slab, it has been decided to avoid a merely carbon copy of the previous calculations. The only changing variables are represented by the different loads (permanent and variable), with the snow and wind load addition (and their relative partial coefficients regarding the load durability). Consequently, no calculation report has been added to the thesis. However, panels set on the rooftop have been computed in order to complete the work, drawing the exact layering composition for the effective representation of the technological joints described later in the thesis book.

After the calculations, differently from the intermediate floor XLAM slab, which results in a 18,4 cm thick slab, composed by 5 layers, the roof XLAM panels needed are 33,2 cm thick and composed by 9 layers.

Politecnico di Milano, Master of Science in Building and Architectural Engineering
Steember - Steel and timber for a high rise building in Queens, New York
Chinnici Federico - **Maranesi** Marco

6.4.4 – STEEL SECONDARY BEAM - HE SHAPE

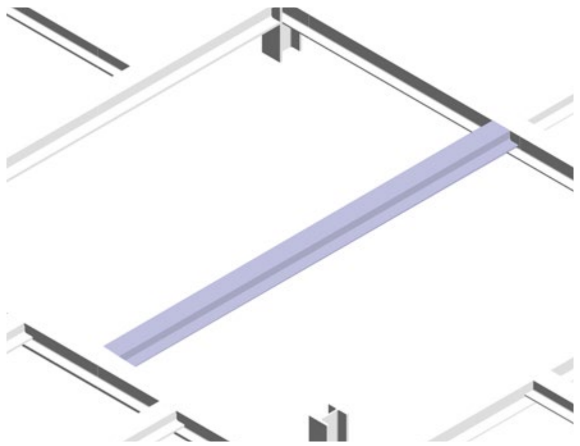

Figure 6.29 - The secondary beam

LOAD CALCULATIONS

Given the permanent load (3.90 kN/m²) and the variable load (2.00 kN/m²), we can compute the kN/m value by using the highest length a secondary beam has in our project.

$$g' = g * l = 3.90 * 3.875 = 15.12\ kN/m$$

$$q' = q * l = 2.00 * 3.875 = 7.75\ kN/m$$

$$g' + q' = 15.12 + 7.75 = 22.87\ kN/m$$

ULS - M_{max}

Following the superimposition of the schematic schemes, as shown in the below images, we can compute the maximum bending moment at the ultimate limit state.

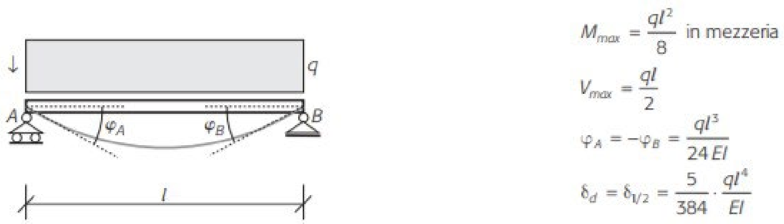

Figure 6.30 - Isostatic scheme with roller/hinge and distributed load

Proceeding with the moment actions:

$$M_{ed} = (\gamma_g * g' + \gamma_q * q') * \frac{l^2}{8} = (1.35 * 15.12 + 1.50 * 7.75) * \frac{7.50^2}{8} = 225.27\ kNm$$

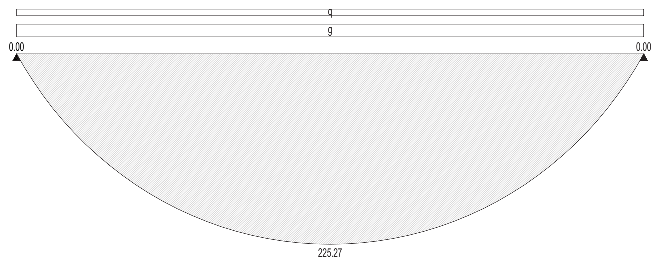

Figure 6.31 - Moment diagram of the distributed load

The next step is the calculation of the minimum module resistance the beam must load. The operative resistance to bending moment will be:

$$W_{x,min} = \frac{M_{ed}}{f_{yd}} = \frac{225.27}{(\frac{235}{1.05})} = 1\ 007\ cm^3$$

SLS – δ_{max}

The code prescribes which is the worst combination between the variable loads only (at the SLS state), with an allowed deflection of l/350 for rolled-hinged beams, and the complete load (permanent + variable) with an allowed deflection of l/300.

Condizioni	Limiti (vedere fig. 4.1)	
	δ_{max}	δ_2
Coperture in generale	L/200	L/250
Coperture praticate frequentemente da personale diverso da quello della manutenzione	L/250	L/300
Solai in generale	L/250	L/300
Solai o coperture che reggono intonaco o altro materiale di finitura fragile o tramezzi non flessibili	L/250	L/350
Solai che supportano colonne (a meno che lo spostamento sia stato incluso nella analisi globale per lo stato limite ultimo)	L/400	L/500
Dove δ_{max} può compromettere l'aspetto dell'edificio	L	/250

Figure 6.32 - Table of the limit values for deflection

Calculations are:

$$comb.1 = \frac{g' + q'}{\delta''_{max}} = \frac{15.12 + 7.75}{\frac{7.50}{200}} = 915\ kN$$

$$comb.2 = \frac{q'}{\delta'_{max}} = \frac{7.75}{\frac{7.50}{250}} = 362\ kN$$

Using the worst combination, it is now possible to proceed by looking at the minimum inertia the beam must provide. The superimposition of the effects leads to the result.

$$I_{x,min} = \frac{5}{384} * (g' + q') * \frac{l^4}{E_s * \delta''_{max}} = \frac{5}{384} * (15.12 + 7.75) * \frac{7.50^4}{210\ 000 * \left(\frac{7.50}{200}\right)} = 11\ 965\ cm^4$$

BEAM CHOICE

Because of the minimum resistant module and the minimum inertia, a proper beam has been selected in order to verify these two above-mentioned restrictions.

The selection went for the HE 300 B, able to provide sufficient inertia with a lower weight, important in the cases of multi-storey residential constructions, where the slab height should get lightened as much as possible. In this way, the later computation of the column could take advantage due to a lighter column height and a greater performance on the instability verification.

$$h = 30\ cm;$$

$$t_w = 1.10\ cm;$$

$$A = 149\ cm^2$$

$$\rho_{g,k} = 1.170 \frac{kN}{m}$$

$$W_x = 1\ 678\ cm^3$$

$$I_x = 25\ 170\ cm^4$$

Thus:

$$W_x > W_{x,min} \rightarrow 1\ 678\ cm^3 > 1\ 007\ cm^3$$

$$I_x > I_{x,min} \rightarrow 25\ 170\ cm^4 > 11\ 965\ cm^4$$

SLS - M_{max}

With the superimposition of the combinations, it is now possible to compute the maximum bending moment at the SLS. The used formulas are the above-mentioned ones.

$$M_{ed} = \left(\rho_{g,k} + g' + q'\right) * \frac{l^2}{8} = (1.170 + 15.12 + 7.75) * \frac{7.50^2}{8} = 169.04\ kNm$$

The resisting moment is computed as:

$$M_{rd} = f_{yk} * \frac{W_x}{\delta_M} = 235.00 * \frac{1\ 678}{1.05} = 375.55\ kNm$$

So:

$$M_{ed} < M_{rd} \rightarrow 169.04\ kNm < 375.55\ kNm \rightarrow utilisation\ 45\%$$

ULS - V_{max}

With the superimposition of the combination, it is now possible to compute the maximum shear at the ULS, with its relative coefficients. The used formulas are the above-mentioned ones.

$$V_{ed} = \left(\gamma_g * \left(\rho_{g,k} + g'\right) + \gamma_q * q'\right) * \frac{L}{2} = (1.35 * (1.170 + 15.12) + 1.50 * 7.75) * \frac{7.50}{2} = 126.07\ kN$$

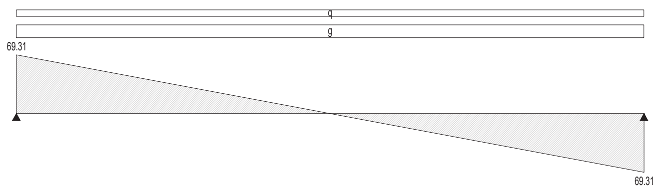

Figure 6.33 - Shear diagram of the distributed load

The resisting shear is computed as:

$$V_{rd} = \tau_d * \frac{A_w}{\gamma_M} = \frac{\frac{235.00}{1.05}}{\sqrt{3}} * \frac{0.30 * 0.011}{1.05} = 406.11\ kN$$

Consequently:

$$V_{ed} < V_{rd} \rightarrow 126.07\ kN < 406.11\ kN \rightarrow utilisation\ 31\%$$

SLS – δ_{max}

With the superimposition of the combination, it is now possible to compute the deflection at the SLS. The used formulas are the above-mentioned ones.

$$\delta_{beam,g} = \frac{5}{384} * \left(\rho_{g,k} + g'\right) * \frac{l^4}{E_s * I_x} = \frac{5}{384} * (1.170 + 15.12) * \frac{7.50^4}{210\ 000 * 25\ 170} = 0.013\ m$$

$$\delta_{beam,g+q} = \frac{5}{384} * \left(\rho_{g,k} + g' + q'\right) * \frac{l^4}{E_s * I_x} = \frac{5}{384} * (1.170 + 15.12 + 7.75) * \frac{7.50^4}{210\ 000 * 25\ 170} = 0.019\ m$$

The allowed deflection for a rolled-hinged beam due to permanent load only is:

$$\delta_{max} = \frac{l}{350} = \frac{7.50}{350} = 0.021\ m$$

While for a beam loaded of both permanent and variable loads, the maximum allowed deflection is:

$$\delta_{max} = \frac{l}{300} = \frac{7.50}{300} = 0.025\ m$$

Consequently:

$$\delta_{beam,g} < \delta_{max} \rightarrow 0.013\ m < 0.021\ m \rightarrow utilisation\ 62\%$$

And:

$$\delta_{beam,g+q} < \delta_{max} \rightarrow 0.019\ m < 0.025\ m \rightarrow utilisation\ 76\%$$

6.4.5 – STEEL SECONDARY BEAM - UPN SHAPE

As far as the previous situation, where XLAM panels of both intermediate slab and rooftop have the same procedure, here there is a change in the beam shape. For some secondary beams, it is needed to use a UPN profile, because they are placed on the core concrete wall's face, anchoring these beams with screws and bolts to the main support. In addition, a torsion moment set on the beam should be verified, due to the non-centralised load acting on the beam.

Moreover, a reduced span acts on this beam, downgrading the resisting moment it has to provide at the ULS and SLS.

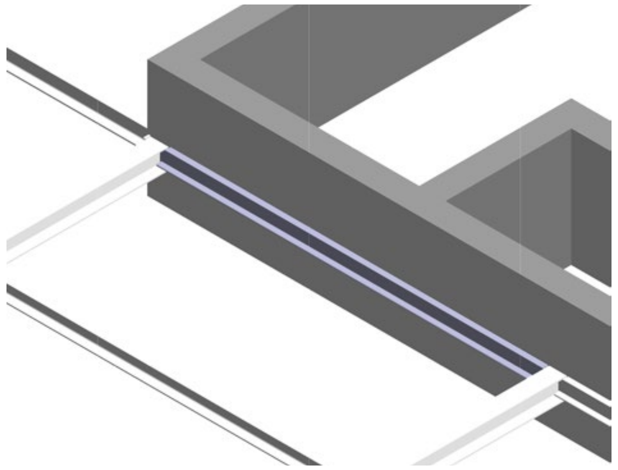

Figure 6.34 - The secondary UPN beam - C profile

LOAD CALCULATIONS

Given the permanent load (3.90 kN/m²) and the variable load (2.00 kN/m²), we can compute the kN/m value by using the highest length a secondary beam has in our project.

$$g' = g * l = 3.90 * 1.94 = 7.56\ kN/m$$

$$q' = q * l = 2.00 * 1.94 = 3.88\ kN/m$$

$$g' + q' = 7.56 + 3.88 = 11.44\ kN/m$$

ULS - M_{max}

Following the superimposition of the schematic schemes, as shown in the below images, we can compute the maximum bending moment at the ultimate limit state.

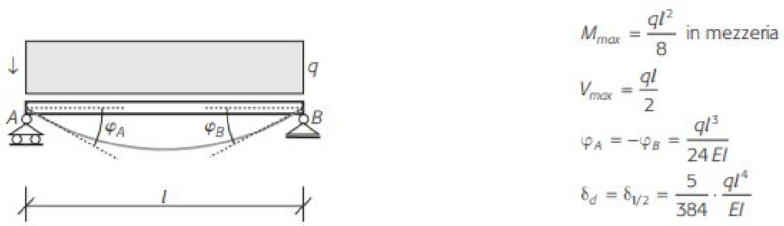

Figure 6.35 - Isostatic scheme with roller/hinge and distributed load

Proceeding with the moment actions:

$$M_{ed} = (\gamma_g * g' + \gamma_q * q') * \frac{l^2}{8} = (1.35 * 7.56 + 1.50 * 3.88) * \frac{7.50^2}{8} = 112.63\ kNm$$

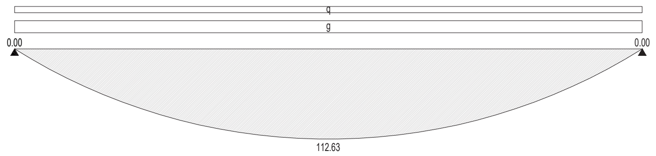

Figure 6.36 - Moment diagram of the distributed load

As foreseen, the moment at the ULS is acting with a half value due to the reduced span.

The next step is the calculation of the minimum module resistance the beam must load. The operative resistance to bending moment will be:

$$W_{x,min} = \frac{M_{ed}}{f_{yd}} = \frac{112.63}{\left(\frac{235}{1.05}\right)} = 503\ cm^3$$

SLS – δ_{max}

The code prescribes which is the worst combination between the variable loads only (at the SLS state), with an allowed deflection of l/350 for rolled-hinged beams, and the complete load (permanent + variable) with an allowed deflection of l/300.

Condizioni	Limiti (vedere fig. 4.1)	
	δ_{max}	δ_2
Coperture in generale	L/200	L/250
Coperture praticate frequentemente da personale diverso da quello della manutenzione	L/250	L/300
Solai in generale	L/250	L/300
Solai o coperture che reggono intonaco o altro materiale di finitura fragile o tramezzi non flessibili	L/250	L/350
Solai che supportano colonne (a meno che lo spostamento sia stato incluso nella analisi globale per lo stato limite ultimo)	L/400	L/500
Dove δ_{max} può compromettere l'aspetto dell'edificio	L	/250

Figure 6.37 - Table of the limit values for deflection

Calculations are:

$$comb.1 = \frac{g' + q'}{\delta_{max}^{"}} = \frac{7.56 + 3.38}{\frac{7.50}{200}} = 305\ kN$$

$$comb.2 = \frac{q'}{\delta_{max}'} = \frac{3.38}{\frac{7.50}{250}} = 129\ kN$$

Using the worst combination, it is now possible to proceed by looking at the minimum inertia the beam must provide.

$$I_{x,min} = \frac{5}{384} * (g' + q') * \frac{l^4}{E_s * \delta_{max}^{"}} = \frac{5}{384} * (7.56 + 3.38) * \frac{7.50^4}{210\ 000 * \left(\frac{7.50}{200}\right)} = 5\ 983\ cm^4$$

BEAM CHOICE

Because of the minimum resistant module and the minimum inertia, a proper beam has been selected in order to verify these two above-mentioned restrictions.

The selection went for the UPN 320, able to provide the minimum allowed inertia.

$$h = 32\ cm;$$

$$b = 10\ cm;$$

$$t_w = 1.40\ cm;$$

$$t_f = 1.75\ cm;$$

$$A = 77.30\ cm^2$$

$$\rho_{g,k} = 0.606 \frac{kN}{m}$$

$$W_x = 679\ cm^3$$

$$I_x = 10\,870\ cm^4$$

Thus:

$$W_x > W_{x,min} \rightarrow 679\ cm^3 > 503\ cm^3$$

$$I_x > I_{x,min} \rightarrow 10\,870\ cm^4 > 5\,983\ cm^4$$

SLS - M_{max}

With the superimposition of the combinations, it is now possible to compute the maximum bending moment at the SLS. The used formulas are the above-mentioned ones.

$$M_{ed} = (\rho_{g,k} + g' + q') * \frac{l^2}{8} = (0.606 + 7.56 + 3.88) * \frac{7.50^2}{8} = 84.67\ kNm$$

The resisting moment is computed as:

$$M_{rd} = f_{yk} * \frac{W_x}{\delta_M} = 235.00 * \frac{679}{1.05} = 151.97\ kNm$$

So:

$$M_{ed} < M_{rd} \rightarrow 84.67\ kNm < 151.97\ kNm \rightarrow utilisation\ 56\%$$

ULS - V_{max}

With the superimposition of the combination, it is now possible to compute the maximum shear at the ULS, with its relative coefficients. The used formulas are the above-mentioned ones.

$$V_{ed} = (\gamma_g * (\rho_{g,k} + g') + \gamma_q * q') * \frac{L}{2} = (1.35 * (0.606 + 7.56) + 1.50 * 3.38) * \frac{7.50}{2} = 63.14\ kN$$

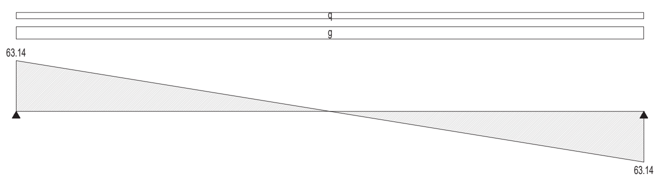

Figure 6.38 - Shear diagram of the distributed load

Politecnico di Milano, Master of Science in Building and Architectural Engineering
Steember - Steel and timber for a high rise building in Queens, New York
Chinnici Federico - **Maranesi** Marco

The resisting shear is computed as:

$$V_{rd} = \tau_d * \frac{A}{\gamma_M} = \frac{\frac{235.00}{1.05}}{\sqrt{3}} * \frac{0.30 * 0.014}{1.05} = 551.32\ kN$$

Consequently:

$$V_{ed} < V_{rd} \rightarrow 63.14\ kN < 551.32\ kN \rightarrow utilisation\ 11\%$$

SLS – δ_{max}

With the superimposition of the combination, it is now possible to compute the deflection at the SLS. The used formulas are the above-mentioned ones.

$$\delta_{beam,g} = \frac{5}{384} * (\rho_{g,k} + g') * \frac{l^4}{E_s * I_x} = \frac{5}{384} * (0.686 + 7.56) * \frac{7.50^4}{210\,000 * 10\,870} = 0.015\ m$$

$$\delta_{beam,g+q} = \frac{5}{384} * (\rho_{g,k} + g' + q') * \frac{l^4}{E_s * I_x} = \frac{5}{384} * (0.686 + 7.56 + 3.88) * \frac{7.50^4}{210\,000 * 10\,870} = 0.022\ m$$

The allowed deflection for a rolled-hinged beam due to permanent load only is:

$$\delta_{max} = \frac{l}{350} = \frac{7.50}{350} = 0.021\ m$$

While for a beam loaded of both permanent and variable loads, the maximum allowed deflection is:

$$\delta_{max} = \frac{l}{300} = \frac{7.50}{300} = 0.025\ m$$

Consequently:

$$\delta_{beam,g} < \delta_{max} \rightarrow 0.015\ m < 0.021\ m \rightarrow utilisation\ 71\%$$

And:

$$\delta_{beam,g+q} < \delta_{max} \rightarrow 0.022\ m < 0.025\ m \rightarrow utilisation\ 88\%$$

6.4.6 – STEEL PRIMARY BEAM

LOAD CALCULATIONS

Given the shear value of the secondary HE beams and added to the shear value of another HE secondary beam (this time with 7.00 metres of span instead of 7.50 metres), it is possible to go directly at the maximum ULS moment and the SLS deflection.

$$P_{sec.7.50m} = 126.07\ kN$$

$$P_{sec.7.00m} = 117.66\ kN$$

$$\boldsymbol{P = P_{sec.7.50m} + P_{sec.7.00m} = 126.07 + 117.66 = 243.73\ kN}$$

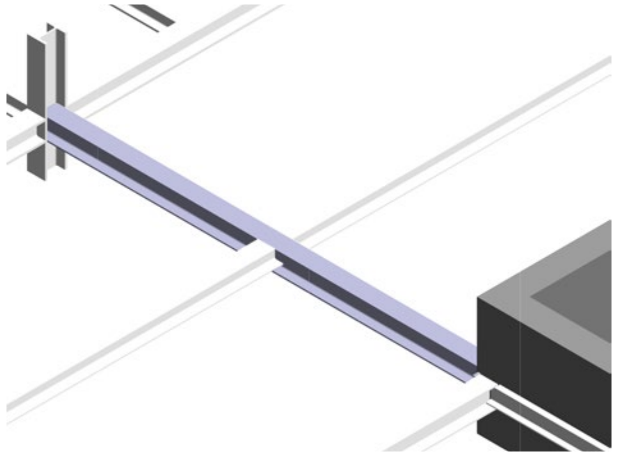

Figure 6.39 - The primary steel beam

ULS - M_{max}

Following the superimposition of the schematic schemes, as shown in the below images, we can compute the maximum bending moment at the ultimate limit state.

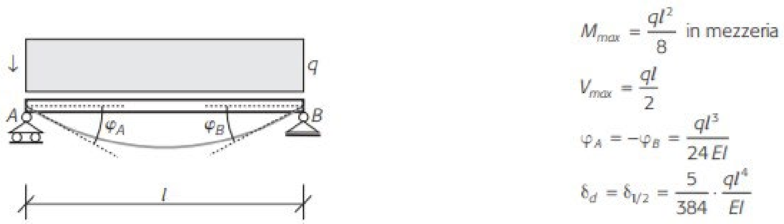

Figure 6.40 - Isostatic scheme with roller/hinge and distributed load

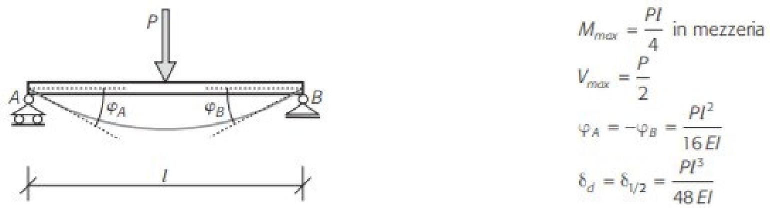

Figure 6.41 - Isostatic scheme with roller/hinge and concentrated load

Proceeding with the moment actions:

$$M_{ed} = P * \frac{l}{4} = 247.37 * \frac{7.80}{4} = 482.38\ kNm$$

The next step is the calculation of the minimum module resistance the beam must load. The operative resistance to bending moment will be:

$$W_{x,min} = \frac{M_{ed}}{f_{yd}} = \frac{482.38}{(\frac{235}{1.05})} = 2\ 155\ cm^3$$

SLS – δ_{max}

It is now possible to proceed by looking at the minimum inertia the beam must provide.

$$I_{x,min} = \frac{P * l^3}{48 * E_s * \delta''_{max}} = \frac{243.73 * 7.80^3}{48 * 210\ 000 * \left(\frac{7.80}{250}\right)} = 36\ 777\ cm^4$$

BEAM CHOICE

Because of the minimum resistant module and the minimum inertia, a proper beam has been selected in order to verify these two above-mentioned restrictions.

The selection went for the HE 360 B, able to provide sufficient inertia with a lower weight, important in the cases of multi-storey residential constructions, where the slab height should get lightened as much as possible. In this way, the later computation of the column could take advantage due to a lighter column height and a greater performance on the instability verification.

$$h = 36\ cm;$$

$$t_w = 1.20\ \text{cm};$$

$$t_f = 2.30\ cm;$$

$$A = 181\ cm^2$$

$$\rho_{g,k} = 1.420\frac{kN}{m}$$

$$W_x = 2\ 400\ cm^3$$

$$I_x = 43\ 190\ cm^4$$

Thus:

$$W_x > W_{x,min} \rightarrow 2\ 400\ cm^3 > 2\ 155\ cm^3$$

$$I_x > I_{x,min} \rightarrow 43\ 190\ cm^4 > 36\ 777\ cm^4$$

SLS - M_{max}

With the superimposition of the combinations, it is now possible to compute the maximum bending moment at the SLS. The used formulas are the above-mentioned ones.

$$M_{ed,conc.} = P * \frac{l}{4} = 174.30 * \frac{7.80}{4} = 339.88\ kNm$$

$$M_{ed,distr.} = \rho_{p,k} * \frac{l^2}{8} = 1.420 * \frac{7.80^2}{8} = 18.10\ kNm$$

The summation of the two effects is:

$$\boldsymbol{M_{ed} = M_{ed,conc.} + M_{ed,distr.} = 339.88 + 18.10 = 350.68\ kNm}$$

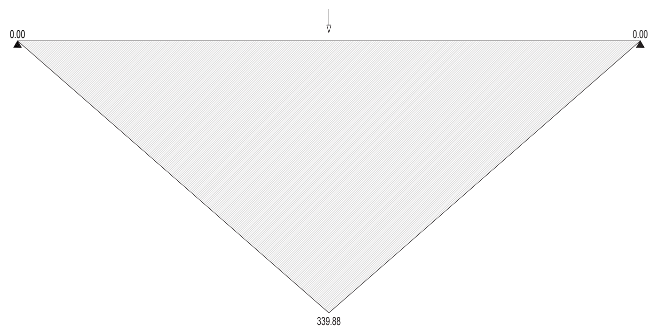

Figure 6.42 - Moment diagram of the concentrated load

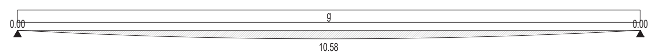

Figure 6.43 - Moment diagram of the distributed load

The resisting moment is computed as:

$$M_{rd} = f_{yk} * \frac{W_x}{\delta_M} = 235.00 * \frac{2\,400}{1.05} = 537.14\ kNm$$

So:

$$M_{ed} < M_{rd} \rightarrow 350.68\ kNm < 537.14\ kNm \rightarrow utilisation\ 65\%$$

ULS - V_{max}

With the superimposition of the combination, it is now possible to compute the maximum shear at the ULS, with its relative coefficients. The used formulas are the above-mentioned ones.

$$V_{ed,conc.} = \frac{P}{2} = \frac{243.73}{2} = 121.86\ kN$$

$$V_{ed,distr.} = (\gamma_g * \rho_{g,k}) * \frac{L}{2} = (1.35 * 1.420) * \frac{7.80}{2} = 7.48\ kN$$

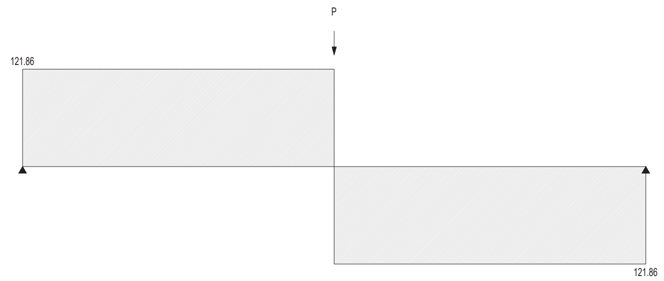

Figure 6.44 - Shear diagram of the concentrated load

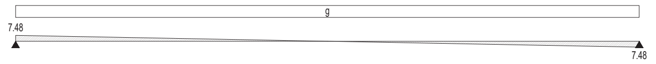

Figure 6.45 - Shear diagram of the distributed load

The summation of the two effects is:

$$V_{ed} = V_{ed,conc.} + V_{ed,distr.} = 121.86 + 7.48 = 129.34\ kN$$

The resisting shear is computed as:

$$V_{rd} = \tau_d * \frac{A}{\gamma_M} = \frac{\frac{235.00}{1.05}}{\sqrt{3}} * \frac{0.36 * 0.012}{1.05} = 531.63\ kN$$

Consequently:

$$V_{ed} < V_{rd} \rightarrow 129.34\ kN < 531.63\ kN \rightarrow utilisation\ 24\%$$

SLS – δ_{max}

With the superimposition of the combination, it is now possible to compute the deflection at the SLS. The used formulas are the above-mentioned ones.

$$\delta_{beam,conc.} = P * \frac{l^3}{48 * E_s * I_x} = 174.30 * \frac{7.80^3}{48 * 210\,000 * 43\,190} = 0.019\ m$$

$$\delta_{beam,distr.} = \frac{5}{384} * \rho_{g,k} * \frac{l^4}{E_s * I_x} = \frac{5}{384} * 1.420 * \frac{7.80^4}{210\,000 * 43\,190} = 0.001\ m$$

The summation of the two effects is:

$$\delta_{beam} = \delta_{beam,conc.} + \delta_{beam,distr.} = 0.019 + 0.001 = 0.020\ m$$

The allowed deflection for a rolled-hinged beam is:

$$\delta_{max} = \frac{l}{350} = \frac{7.80}{300} = 0.026\ m$$

Consequently:

$$\delta_{beam} < \delta_{max} \rightarrow 0.020\ m < 0.026\ m \rightarrow utilisation\ 77\%$$

6.4.7 – STEEL BORDER BEAM - SECONDARY BEAM LOAD

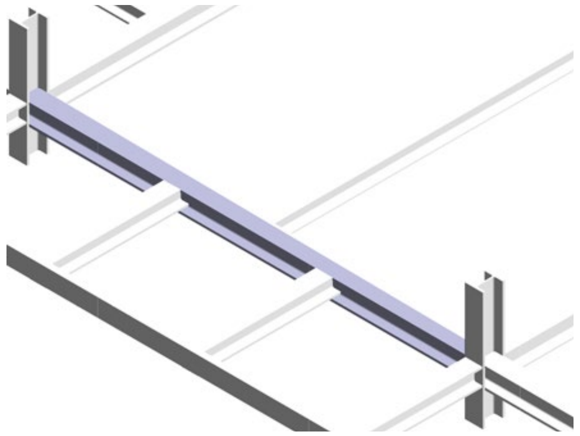

Figure 6.46 - The border steel beam

In the following pages, we go through the calculation of two different types of border beams: one is subjected to a load of the secondary beam, set in the middle of the border beam itself. The second one instead is subjected to the load of the slab, where its length influence is counted as half of it, as it was for the secondary UPN beam.

This will lead to different loads of combinations, and different levels of moment, shear, deflection and torsion. That is why in the case, the computational procedure, even if they are equivalent, will be both explained.

LOAD CALCULATIONS

Given the shear value of the cantilever beam (counting twice, each border beam will bear two cantilevers) and added to the shear value of the HE secondary beam (with a total length of 7.50 metres), it is possible to go directly at the maximum ULS moment and the SLS deflection.

This time it is not possible, to sum up, the two loads since they are acting on three different cross-sections on the beam.

$$P_{cant.2.30m} = 74.13\ kN$$

$$P_{sec.7.50m} = 126.07\ kN$$

Furthermore, the distributed load represented by the external wall should be added to the total load that the border beam must bear; its value is:

$$q_{ext.wall} = 4.72\ kN/m$$

ULS - M_{max}

Following the superimposition of the schematic schemes, as shown in the below images, we can compute the maximum bending moment at the ultimate limit state.

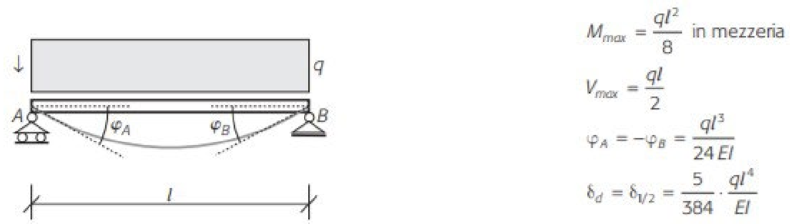

Figure 6.47 - Isostatic scheme with roller/hinge and distributed load

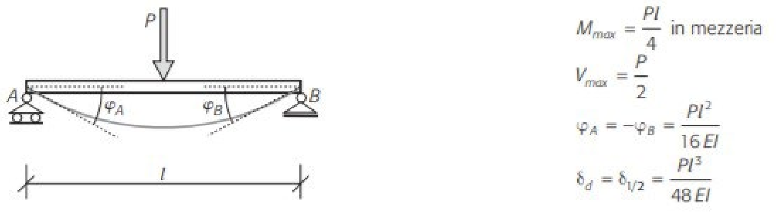

Figure 6.48 - Isostatic scheme with roller/hinge and concentrated load

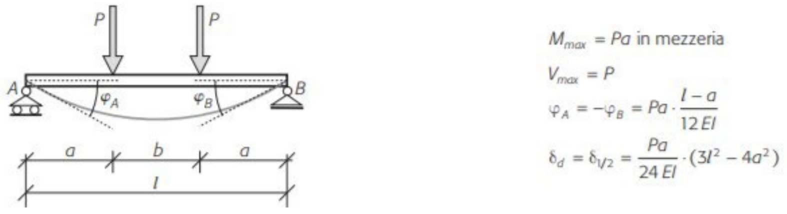

Figure 6.49 - Isostatic scheme with roller/hinge and double concentrated load

Proceeding with the moment actions:

$$M_{ed,wall} = (\gamma_g * g_{ext.wall}) * \frac{l^2}{8} = (1.35 * 4.72) * \frac{7.80^2}{8} = 48.42\ kNm$$

$$M_{ed,sec.7.50m} = P_{sec} * \frac{l}{4} = 126.07 * \frac{7.80}{4} = 245.83\ kNm$$

$$M_{ed,cant.2.30m} = P_{cant.} * \frac{l}{3} = 74.13 * \frac{7.80}{3} = 192.75\ kNm$$

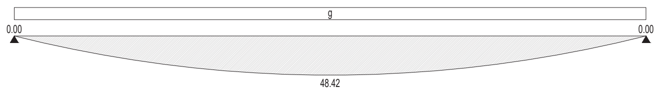

Figure 6.50 - Moment diagram of the distributed load

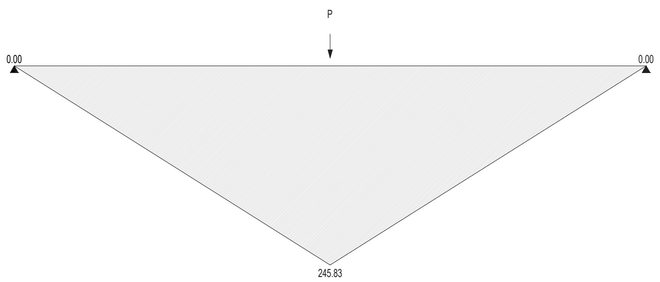

Figure 6.51 - Moment diagram of the concentrated load

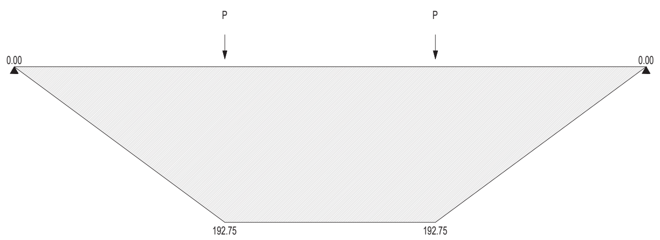

Figure 6.52 - Moment diagram of the double concentrated load

Summing up the three values:

$$M_{ed} = M_{ed,wall} + M_{ed,sec.7.50m} + M_{ed,cant.2.30m} = 48.42 + 245.83 + 192.75 = 487.00\ kNm$$

Politecnico di Milano, Master of Science in Building and Architectural Engineering
Steember - Steel and timber for a high rise building in Queens, New York
Chinnici Federico - **Maranesi** Marco

The next step is the calculation of the minimum module resistance the beam must load. The operative resistance to bending moment will be:

$$W_{x,min} = \frac{M_{ed}}{f_{yd}} = \frac{487.00}{\left(\frac{275}{1.05}\right)} = 1\,859\ cm^3$$

SLS – δ_{max}

It is now possible to proceed by looking at the minimum inertia the beam must provide. The superimposition of the effects leads to the result.

$$I_{x,min,wall} = \frac{5}{384} * q_{ext.wall} * \frac{l^4}{E_s * \delta_{max}} = \frac{5}{384} * 4.72 * \frac{7.80^4}{210\,000 * \left(\frac{7.80}{250}\right)} = 3\,469\ cm^4$$

$$I_{x,min,sec.7.50m} = P_{sec} * \frac{l^3}{48 * E_s * \delta_{max}} = 90.15 * \frac{7.80^3}{48 * 210\,000 * \left(\frac{7.80}{250}\right)} = 13\,603\ cm^4$$

$$I_{x,min,cant.2.30m} = P_{cant} * \frac{\frac{l}{3}}{24 * E_s * \delta_{max}} * \left(3 * l^2 - 4 * \frac{l}{3}^2\right)$$
$$= 52.52 * \left(\frac{7.80}{3}\right) / \left(24 * 210\,000 * \left(\frac{7.80}{250}\right) * \left(3 * 7.80^2 - 4 * \left(\frac{7.80}{3}\right)^2\right)\right)$$
$$= 13\,501\ cm^4$$

The final minimum inertia will be:

$$I_{x,min} = I_{x,min,wall} + I_{x,min,sec.\ 7.50m} + I_{x,min,cant.\ 2.45m} = 3\,469 + 13\,603 + 13\,501 = 30\,574\ cm^4$$

BEAM CHOICE

Because of the minimum resistant module and the minimum inertia, a proper beam has been selected in order to verify these two above-mentioned restrictions.

The selection went for the HE 320 M, high as the primary beam, in order to save space enough to a reduced thickness of the slab, allowing the possibility of having higher indoor spaces and permit the positioning of the pre-assembled wall, which has a greater high due to small handles. Furthermore, due to the torsion moment provided by the cantilever beam, greater resistance of the internal web and flanges is needed for its verification.

$$b = 30.90\ cm;$$

$$h = 35.90\ cm;$$

$$t_w = 2.10\ \text{cm};$$

$$t_f = 4.00\ cm;$$

$$A = 312\ cm^2$$

$$\rho_{g,k} = 2.450 \frac{kN}{m}$$

$$W_x = 3\,796\ cm^3$$

$$I_x = 68\,130\ cm^4$$

Thus:

$$W_{x,} > W_{x,min} \rightarrow 3\,796\ cm^3 > 1\,859\ cm^3$$

$$I_x > I_{x,min} \rightarrow 68\,130\ cm^4 > 40\,636\ cm^4$$

SLS - M_{max}

With the superimposition of the combinations, it is now possible to compute the maximum bending moment at the SLS. The used formulas are the above-mentioned ones.

$$M_{ed,beam} = \rho_{p,k} * \frac{l^2}{8} = 2.450 * \frac{7.80^2}{8} = 18.63\ kNm$$

$$M_{ed,wall} = q_{ext.wall} * \frac{l^2}{8} = 4.72 * \frac{7.80^2}{8} = 35.87\ kNm$$

$$M_{ed,sec.7.50m} = P_{sec} * \frac{l}{4} = 90.15 * \frac{7.80}{4} = 175.80\ kNm$$

$$M_{ed,cant.2.30m} = P_{cant} * \frac{l}{3} = 52.52 * \frac{7.80}{3} = 136.55\ kNm$$

The summation of the four effects is:

$$M_{ed} = M_{ed,beam} + M_{ed,wall} + M_{ed,sec.7.50m} + M_{ed,cant.2.45m} = 18.63 + 35.87 + 175.80 + 136.55 = 366.85\ kNm$$

The resisting moment is computed as:

$$M_{rd} = f_{yk} * \frac{W_x}{\delta_M} = 275.00 * \frac{3\ 796}{1.05} = 994.19\ kNm$$

So:

$$M_{ed} < M_{rd} \rightarrow 359.24\ kNm < 994.19\ kNm \rightarrow utilisation\ 36\%$$

ULS - V_{max}

With the superimposition of the combination, it is now possible to compute the maximum shear at the ULS, with its relative coefficients. The used formulas are the above-mentioned ones.

$$V_{ed,beam} = (\gamma_g * \rho_{g,k}) * \frac{L}{2} = (1.35 * 2.450) * \frac{7.80}{2} = 12.90\ kN$$

$$V_{ed,wall} = (\gamma_g * q_{ext.wall}) * \frac{L}{2} = (1.35 * 4.72) * \frac{7.80}{2} = 24.83\ kN$$

$$V_{ed,sec.7.50m} = \frac{P_{sec}}{2} = \frac{126.07}{2} = 63.03\ kN$$

$$V_{ed,cant.2.30m} = P_{cant} = 74.13\ kN$$

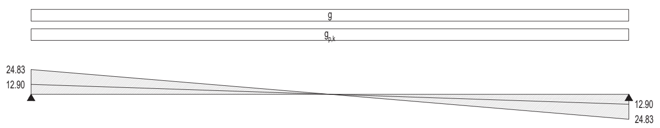

Figure 6.53 - Shear diagram of the distributed load

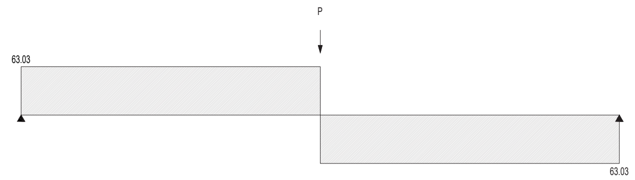

Figure 6.54 - Shear diagram of the concentrated load

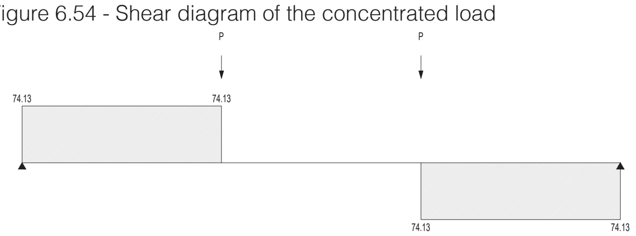

Figure 6.55 - Shear diagram of the double concentrated load

The summation of the four effects is:

$$V_{ed} = V_{ed,beam} + V_{ed,wall} + V_{ed,sec.7.50m} + V_{ed,cant.2.30m} = 12.90 + 24.83 + 63.03 + 74.13 = 174.90\ kN$$

The resisting shear is computed as:

$$V_{rd} = \tau_d * \frac{A_w}{\gamma_M} = \frac{\frac{275.00}{1.05}}{\sqrt{3}} * \frac{0.359 * 0.021}{1.05} = 1\ 085.69\ kN$$

Consequently:

$$V_{ed} < V_{rd} \rightarrow 174.90\ kN < 1\ 085.69\ kN \rightarrow utilisation\ 16\%$$

SLS – δ_{max}

With the superimposition of the combination, it is now possible to compute the deflection at the SLS. The used formulas are the above-mentioned ones.

$$\delta_{beam} = \frac{5}{384} * \rho_{g,k} * \frac{l^4}{E_s * I_x} = \frac{5}{384} * 2.450 * \frac{7.80^4}{210\ 000 * 68\ 130} = 0.001\ m$$

$$\delta_{wall} = \frac{5}{384} * q_{ext.wall} * \frac{l^4}{E_s * I_x} = \frac{5}{384} * 4.72 * \frac{7.80^4}{210\ 000 * 68\ 130} = 0.002\ m$$

$$\phi_{sec.7.50m} = P_{sec} * \frac{l^3}{48 * E_s * I_x} = 90.15 * \frac{7.80^3}{48 * 210\ 000 * 68\ 130} = 0.006\ m$$

$$\delta_{cant.2.45m} = P_{cant} * \frac{\frac{l}{3}}{24 * E_s * I_x} * \left(3 * l^2 - 4 * \frac{l}{3}^2\right) = 52.52 * \frac{\frac{7.80}{3}}{24 * 210\ 000 * 68\ 130} * \left(3 * 7.80^2 - 4 * \left(\frac{7.80}{3}\right)^2\right) = 0.006\ m$$

The summation of the four effects is:

$$\delta_{beam} = \delta_{beam} + \delta_{wall} + \delta_{sec.7.50m} + \delta_{cant.2.30m} = 0.001 + 0.003 + 0.006 + 0.006 = 0.015\ m$$

The allowed deflection for a rolled-hinged beam is:

$$\delta_{max} = \frac{l}{300} = \frac{7.80}{300} = 0.026\ m$$

Consequently:

$$\delta_{beam} < \delta_{max} \rightarrow 0.015\ m < 0.026\ m \rightarrow utilisation\ 58\%$$

SLS – τ_{max}

As previously mentioned, another effect given to the beam is due torsion moment.

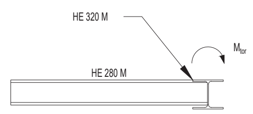

Figure 6.56 - Longitudinal section of the cantilever loading the border beam

In order to compute this, at first, it is needed to check the torsion moment. One only is the torsion moment affecting the border beam, in two different sections. This torsion moment is provided by the cantilever beam, using the fixed-end moment earlier computed:

$$M_{tor} = M_{cant} = 47.25\ kNm$$

The outcome of the tensional tangent stress will be:

$$\tau_{max} = 3 * M_{tor} * \frac{t_f}{\sum_{i=1}^{i=3}(2 * b * t_f^3 + (h - 2 * t_f) * t_w^3}$$
$$= 3 * 47.25 * \frac{40}{(2 * 309 * 40^3 + (359 - 2 * 40) * 21^3} = 134.56 \frac{N}{mm^2}$$

While the resisting force due to torsion is:

$$\tau_{tor} = \frac{f_{yd}}{\sqrt{3}} = \frac{261.90}{\sqrt{3}} = 151.21 \frac{N}{mm^2}$$

Therefore:

$$\tau_{max} < \tau_{tor} \rightarrow 134.56 \frac{N}{mm^2} < 151.21 \frac{N}{mm^2} \rightarrow utilisation\ 89\%$$

6.4.8 – STEEL BORDER BEAM - SLAB'S LOAD

LOAD CALCULATIONS

Given the shear value of the cantilever beam (counting twice, each border beam will bear two cantilevers), it is possible to go directly at the maximum ULS moment and the SLS deflection.

This time it is not possible to sum up the two loads since they are acting on three different cross-sections on the beam.

$$P_{cant.\ 2.30m} = 74.13\ kN$$

Given the permanent load (3.90 kN/m^2) and the variable load (2.00 kN/m^2), we can compute the kN/m value by using the highest length the border beam has in the project.

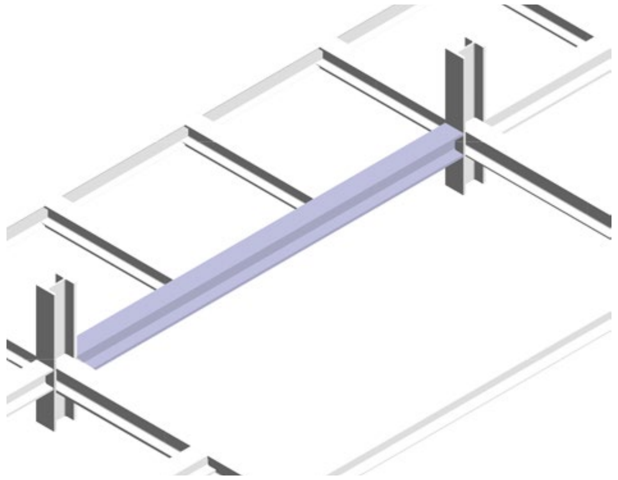

Figure 6.57 - The secondary steel beam

$$g' = g * l = 3.90 * 1.94 = 7.56\ kN/m$$

$$q' = q * l = 2.00 * 1.94 = 3.88\ kN/m$$

$$g' + q' = 7.56 + 3.88 = 11.44\ kN/m$$

Furthermore, the distributed load represented by the external wall should be added to the total load that the border beam must bear; its value is:

$$q_{ext.wall} = 4.72\ kN/m$$

ULS - M_{max}

Following the superimposition of the schematic schemes, as shown in the below images, we can compute the maximum bending moment at the ultimate limit state.

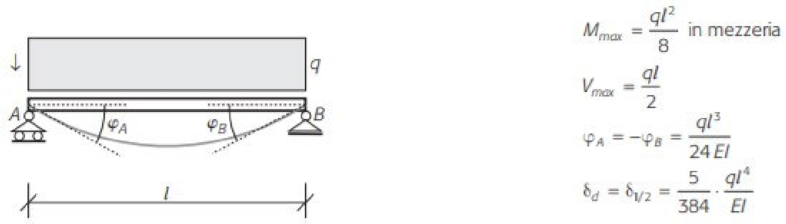

Figure 6.58 - Isostatic scheme with roller/hinge and distributed load

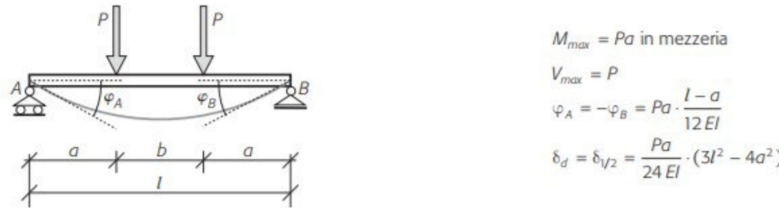

Figure 6.59 - Isostatic scheme with roller/hinge and double concentrated load

Proceeding with the moment actions:

$$M_{ed,slab} = (\gamma_g * g' + \gamma_q * q') * \frac{l^2}{8} = (1.35 * 7.56 + 1.50 * 3.88) * \frac{7.50^2}{8} = 112.63\ kNm$$

$$M_{ed,wall} = (\gamma_g * g_{ext.wall}) * \frac{l^2}{8} = (1.35 * 4.72) * \frac{7.50^2}{8} = 44.77\ kNm$$

$$M_{ed,cant.2.30m} = P_{cant.} * \frac{l}{3} = 74.13 * \frac{7.80}{3} = 185.34\ kNm$$

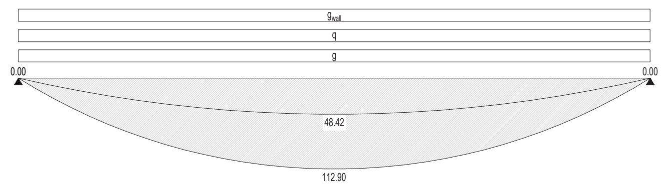

Figure 6.60 - Moment diagram of the distributed load

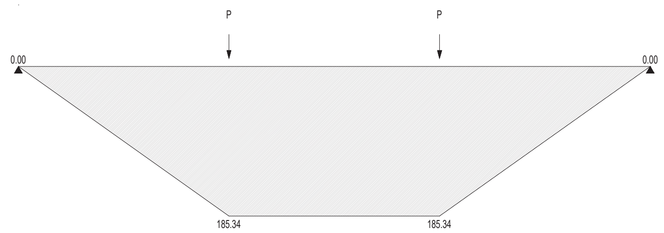

Figure 6.61 - Moment diagram of the double concentrated load

Summing up the three values:

$$M_{ed} = M_{ed,slab} + M_{ed,wall} + M_{ed,cant.2.30m} = 112.63 + 44.77 + 185.34 = 342.74\ kNm$$

The next step is the calculation of the minimum module resistance the beam must load. The operative resistance to bending moment will be:

$$W_{x,min} = \frac{M_{ed}}{f_{yd}} = \frac{342.74}{(\frac{275}{1.05})} = 1\ 309\ cm^3$$

SLS – δ_{max}

It is now possible to proceed by looking at the minimum inertia the beam must provide. The superimposition of the effects leads to the result.

Condizioni	Limiti (vedere fig. 4.1)	
	δ_{max}	δ_2
Coperture in generale	L/200	L/250
Coperture praticate frequentemente da personale diverso da quello della manutenzione	L/250	L/300
Solai in generale	L/250	L/300
Solai o coperture che reggono intonaco o altro materiale di finitura fragile o tramezzi non flessibili	L/250	L/350
Solai che supportano colonne (a meno che lo spostamento sia stato incluso nella analisi globale per lo stato limite ultimo)	L/400	L/500
Dove δ_{max} può compromettere l'aspetto dell'edificio	L	/250

Figure 6.62 - Table of the limit values for deflection

$$comb.1 = \frac{g' + q'}{\delta''_{max}} = \frac{7.56 + 3.38}{\frac{7.50}{250}} = 381\ kN$$

$$comb.2 = \frac{q'}{\delta'_{max}} = \frac{3.38}{\frac{7.50}{300}} = 155\ kN$$

Using the worst combination, it is now possible to proceed by looking at the minimum inertia the beam must provide.

$$I_{x,min,slab} = \frac{5}{384} * (g' + q') * \frac{l^4}{E_s * \delta''_{max}} = \frac{5}{384} * (7.56 + 3.38) * \frac{7.50^4}{210\,000 * \left(\frac{7.50}{300}\right)} = 7\,478\ cm^4$$

$$I_{x,min,wall} = \frac{5}{384} * q_{ext.wall} * \frac{l^4}{E_s * \delta_{max}} = \frac{5}{384} * 4.72 * \frac{7.50^4}{210\,000 * \left(\frac{7.50}{300}\right)} = 3\,084\ cm^4$$

$$I_{x,min,cant.2.30m} = P_{\ cant} * \frac{\frac{l}{3}}{24 * E_s * \delta_{max}} * \left(3 * l^2 - 4 * \frac{l}{3}^2\right)$$
$$= 52.52 * \frac{\frac{7.50}{3}}{24 * 210\,000 * \left(\frac{7.50}{300}\right)} * \left(3 * 7.50^2 - 4 * \left(\frac{7.50}{3}\right)^2\right) = 12\,483\ cm^4$$

The final minimum inertia will be:

$$I_{x,min} = I_{x,min,slab} + I_{x,min,wall} + I_{x,min,cant.\ 2.30m} = 7\,478 + 3\,084 + 12\,483 = 23\,045\ cm^4$$

BEAM CHOICE

Because of the minimum resistant module and the minimum inertia, a proper beam has been selected in order to verify these two above-mentioned restrictions.

The selection went for the HE 320 M, high as the primary beam, in order to save space enough to a reduced thickness of the slab, allowing the possibility of having higher indoor spaces and permit the positioning of the pre-assembled wall, which has a greater high due to small handles. Furthermore, due to the torsion moment provided by the cantilever beam, greater resistance of the internal web and flanges is needed for its verification.

$b = 30.90\ cm;$ $A = 312\ cm^2$

$h = 35.90\ cm;$ $\rho_{g,k} = 2.450 \frac{kN}{m}$

$t_w = 2.10\ cm;$ $W_x = 3\,796\ cm^3$

$t_f = 4.00\ cm;$ $I_x = 68\,130\ cm^4$

Thus:

$$W_x > W_{x,min} \rightarrow 3\,796\ cm^3 > 1\,307\ cm^3$$

$$I_x > I_{x,min} \rightarrow 68\,130\ cm^4 > 23\,045\ cm^4$$

SLS - M_{max}

With the superimposition of the combinations, it is now possible to compute the maximum bending moment at the SLS. The used formulas are the above-mentioned ones.

$$M_{ed,beam} = \rho_{p,k} * \frac{l^2}{8} = 2.450 * \frac{7.50^2}{8} = 17.23\ kNm$$

$$M_{ed,slab} = (\rho_{g,k} + g' + q') * \frac{l^2}{8} = (2.450 + 7.56 + 3.88) * \frac{7.50^2}{8} = 97.63\ kNm$$

$$M_{ed,wall} = q_{ext.wall} * \frac{l^2}{8} = 4.72 * \frac{7.50^2}{8} = 33.16\ kNm$$

$$M_{ed,cant.2.30m} = P_{cant} * \frac{l}{3} = 52.52 * \frac{7.50}{3} = 131.30\ kNm$$

The summation of the four effects is:

$$M_{ed} = M_{ed,beam} + M_{ed,slab} + M_{ed,wall} + M_{ed,cant.2.30m} = 17.23 + 97.63 + 33.16 + 131.30$$
$$= 279.32\ kNm$$

The resisting moment is computed as:

$$M_{rd} = f_{yk} * \frac{W_x}{\delta_M} = 275.00 * \frac{3\,796}{1.05} = 946.85\ kNm$$

So:

$$M_{ed} < M_{rd} \rightarrow 279.32\ kNm < 946.85\ kNm \rightarrow utlisation\ 29\%$$

ULS - V_{max}

With the superimposition of the combination, it is now possible to compute the maximum shear at the ULS, with its relative coefficients. The used formulas are the above-mentioned ones.

$$V_{ed,beam} = (\gamma_g * (\rho_{g,k} + g') + \gamma_q * q') * \frac{L}{2} = (1.35 * (2.450 + 7.56) + 1.50 * 3.38) * \frac{7.50}{2}$$
$$= 72.47\ kN$$

$$V_{ed,wall} = (\gamma_g * q_{ext.wall}) * \frac{L}{2} = (1.35 * 4.72) * \frac{7.80}{2} = 23.88\ kN$$

$$V_{ed,cant.2.30m} = P_{cant} = 74.13\ kN$$

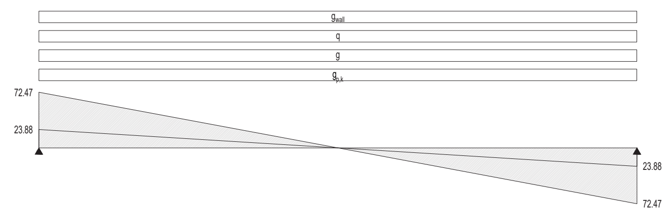

Figure 6.63 - Shear diagram of the distributed load

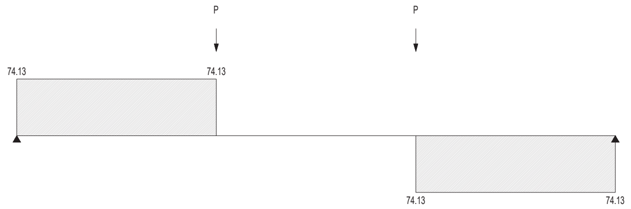

Figure 6.64 - Shear diagram of the double concentrated load

The summation of the four effects is:

$$V_{ed} = V_{ed,beam} + V_{ed,wall} + V_{ed,cant.2.30m} = 72.47 + 23.88 + 73.92 = 170.49\ kN$$

The resisting shear is computed as:

$$V_{rd} = \tau_d * \frac{A}{\gamma_M} = \frac{\frac{275.00}{1.05}}{\sqrt{3}} * \frac{0.36 * 0.021}{1.05} = 1\,085.69\ kN$$

Consequently:

$$V_{ed} < V_{rd} \rightarrow 170.49\ kN < 1\,085.69\ kN \rightarrow utilisation\ 16\%$$

SLS – δ_{max}

With the superimposition of the combination, it is now possible to compute the deflection at the SLS. The used formulas are the above-mentioned ones.

$$\delta_{beam} = \frac{5}{384} * \left(\rho_{g,k} + g' + q'\right) * \frac{l^4}{E_s * I_x}$$
$$= \frac{5}{384} * (2.450 + 7.56 + 3.88) * \frac{7.50^4}{210\,000 * 68\,130} = 0.004\ m$$

$$\delta_{wall} = \frac{5}{384} * q_{ext.wall} * \frac{l^4}{E_s * I_x} = \frac{5}{384} * 4.72 * \frac{7.50^4}{210\,000 * 68\,130} = 0.001\ m$$

$$\delta_{cant.2.30m} = P_{cant} * \frac{\frac{l}{3}}{24 * E_s * I_x} * \left(3 * l^2 - 4 * \frac{l}{3}^2\right)$$
$$= 69.39 * \frac{\frac{7.50}{3}}{24 * 210\,000 * 68\,130} * \left(3 * 7.50^2 - 4 * \left(\frac{7.50}{3}\right)^2\right) = 0.005\ m$$

The summation of the four effects is:

$$\delta_{beam} = \delta_{beam} + \delta_{wall} + \delta_{cant.2.30m} = 0.004 + 0.001 + 0.005 = 0.011\ m$$

The allowed deflection for a rolled-hinged beam is:

$$\delta_{max} = \frac{l}{300} = \frac{7.50}{300} = 0.025\ m$$

Consequently:

$$\delta_{beam} < \delta_{max} \rightarrow 0.011\ m < 0.025\ m \rightarrow utilisation\ 44\%$$

SLS – τ_{max}

As previously mentioned, another effect given to the beam is due torsion moment.

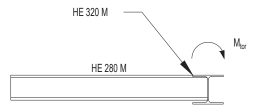

Figure 6.65 - Longitudinal section of
the cantilever loading the border beam

In order to compute this, at first, it is needed to check the torsion moment. Two are the torsion moments affecting the border beam, in three different sections. Their torsion moment is provided by the cantilever beam, using the fixed-end moment earlier computed, and by the slab acting on the border beam itself:

$$M_{tor,cant} = M_{cant} = 47.25\ kNm$$

The outcome of the tensional tangent stress will be:

$$\tau_{max} = 3 * M_{tor} * \frac{t_f}{\sum_{i=1}^{i=3}(2 * b * t_f^3 + \left(h - 2 * t_f\right) * t_w^3}$$
$$= 3 * 47.25 * \frac{40}{(2 * 309 * 40^3 + (359 - 2 * 40) * 21^3} = 134.56 \frac{N}{mm^2}$$

While the resisting force due to torsion is:

$$\tau_{tor} = \frac{f_{yd}}{\sqrt{3}} = \frac{261.90}{\sqrt{3}} = 151.21 \frac{N}{mm^2}$$

Therefore:

$$\tau_{max} < \tau_{tor} \rightarrow 134.56 \frac{N}{mm^2} < 151.21 \frac{N}{mm^2} \rightarrow utilisation\ 89\%$$

6.4.9 – STEEL COLUMN

Once designed all the structural beams, it is now time to go on with the computation of the most loaded column, in order to verify both the compression forces and the arisen moment from the cantilever beams.

The following step is to compute the total load acting at the base of the pillar, with a later-determined HEM profile. Regarding the total bending moment, there is no influence due to the column, since it does not provide any further bending moment.

An additional note is that all the floors have been considered with the same weight, in order to be on the safe side for the entire column's calculation process.

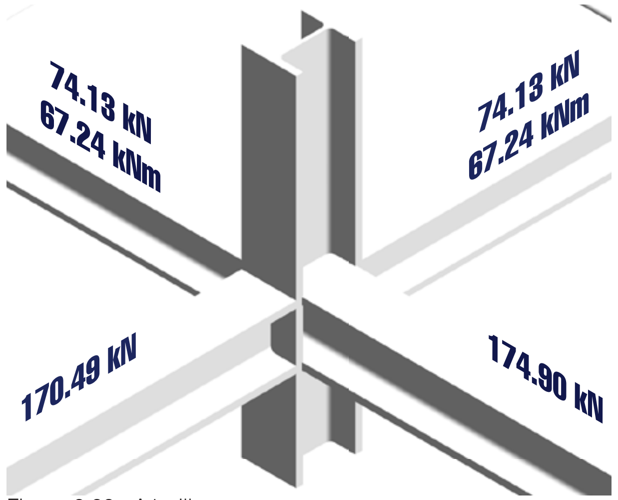

Figure 6.66 - A1 pillar
2x cantilever beams + border-secondary loaded-beam + border-slab loaded-beam

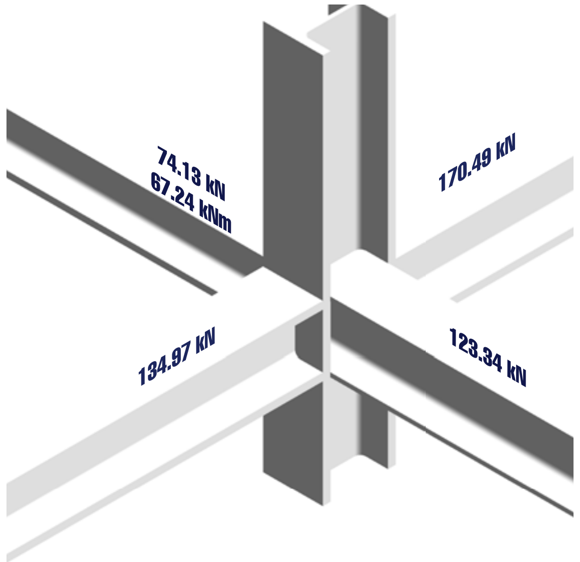

Figure 6.67 - B1 pillar
Cantilever beam + 2x border-slab loaded-beams + primary beam

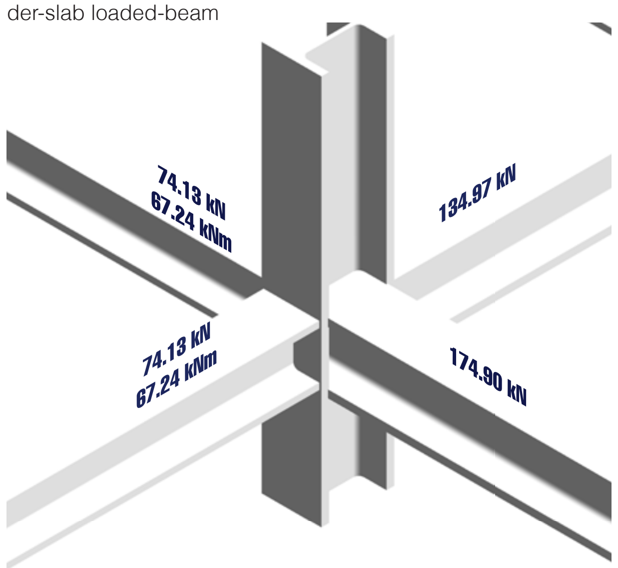

Figure 6.68 - C1 pillar
2x cantilever beams + border-secondary loaded-beam + border-slab loaded-beam)

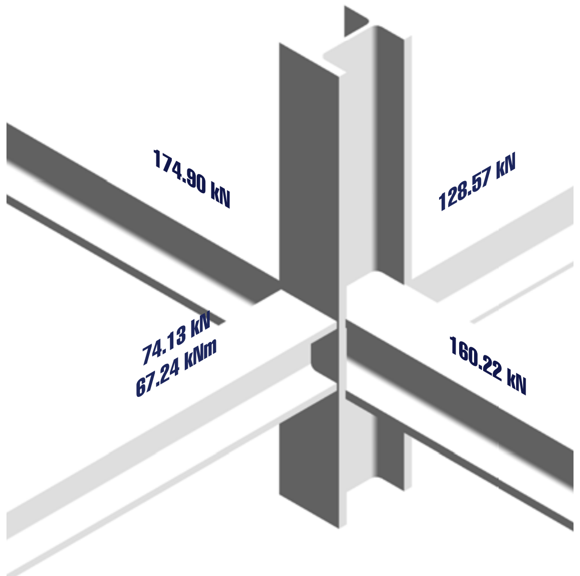

Figure 6.69 - C2 pillar
Cantilever beam + 2x border-secondary loaded-beams + primary beam

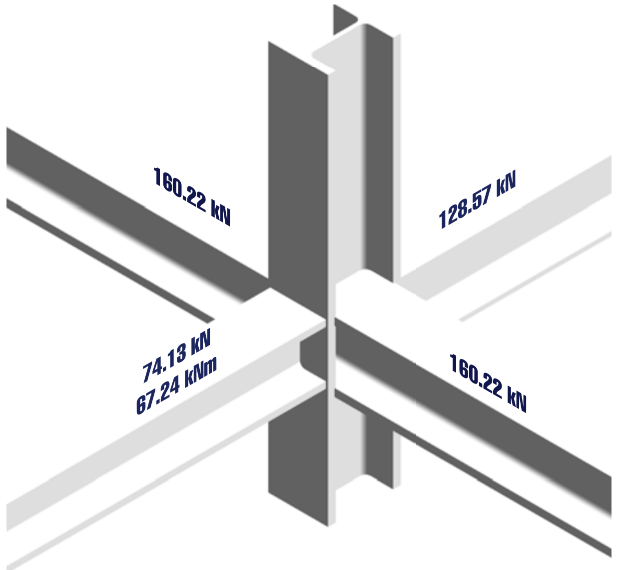

Figure 6.70 - C2 pillar
Cantilever beam + 2x border-secondary loaded-beams + primary beam

Politecnico di Milano, Master of Science in Building and Architectural Engineering
Steember - Steel and timber for a high rise building in Queens, New York
Chinnici Federico - **Maranesi** Marco

LOADS

Because of the elevated compression resistance, the column should provide, it has been selected the use of a high-strength steel class.

Shear forces and bending moments at the ULS have been considered for the computation of the pillars.

COLUMN A1

The loads due to the shear forces provided by the beams are:

$$N_{ed.A1} = P_{cant.2.30m} + P_{cant.2.30m} + P_{border\ sec.7.80m} + P_{border\ slab\ 7.50m}$$
$$= 74.13 + 74.13 + 174.68 + 170.49 = 493.65\ kN$$

$$M_{ed.A1} = M_{cant.2.30m} + M_{cant.2.30m} + M_{border\ sec.7.80m} + M_{border\ slab\ 7.50m}$$
$$= 67.24 + 67.24 + 0.00 + 0.00 = 134.48\ kNm$$

Thus:

$$N_{ed,tot,A1} = N_{ed,A1} * n_{floors} + \rho_{g,k} * h_{floors} * n_{floors}$$
$$= 493.65 * 23 - 2 * (74.13 + 74.13) + 1.720 * 3.60 * 23 = 11\ 199.89\ kN$$

$$M_{ed,tot,A1} = M_{ed,A1} * n_{floors} = 134.48 * 23 - 2 * (67.24 + 67.24) = 2\ 258.04\ kNm$$

In this case, a HE 260 M has been considered for the self-weight of the beam:

$$A_{min,ed\ A1} = \frac{N_{ed\ A1}}{f_{yd}} = \frac{11\ 199.89}{523.81} = 213.82\ cm^2$$

$$W_{min,ed\ A1} = \frac{M_{ed\ A1}}{f_{yd}} = \frac{2\ 824.14}{523.81} = 53.92\ cm^3$$

Computing its verifications:

$$A = 220\ cm^2 > 213.82\ cm^2$$

$$W_x = 2\ 159\ cm^3 > 53.92\ cm^3$$

COLUMN B1

The loads due to the shear forces provided by the beams are:

$$N_{ed.B1} = P_{cant.2.30m} + P_{primary\ 7.80m} + P_{border\ slab\ 7.50m} + P_{border\ slab\ 7.00m}$$
$$= 74.13 + 129.34 + 170.49 + 134.97 = 508.93\ kN$$

$$M_{ed.B1} = M_{cant.2.30m} + M_{primary\ 7.80m} + M_{border\ slab\ 7.50m} + M_{border\ slab\ 7.00m}$$
$$= 67.24 + 0.00 + 0.00 + 0.00 = 67.24\ kNm$$

Thus:

$$N_{ed,tot,B1} = N_{ed,B1} * n_{floors} + \rho_{g,k} * h_{floors} * n_{floors}$$
$$= 508.93 * 23 - 2 * 74.13 + 1.720 * 3.60 * 23 = 11\ 713.66\ kN$$

$$M_{ed,tot,B1} = M_{ed,B1} * n_{floors} = 67.24 * 23 - 2 * (67.24 + 67.24) = 1\ 412.07\ kNm$$

In this case, a HE 280 M has been considered for the self-weight of the beam:

$$A_{min,ed\ B1} = \frac{N_{ed\ B1}}{f_{yd}} = \frac{11\ 713.66}{523.81} = 223.62\ cm^2$$

$$W_{min,ed\ B1} = \frac{M_{ed\ B1}}{f_{yd}} = \frac{1\ 412.07}{523.81} = 26.96\ cm^3$$

Computing its verifications:

$$A = 240\ cm^2 > 223.62\ cm^2$$

$$W_x = 2\ 551\ cm^3 > 26.96\ cm^3$$

COLUMN C1

The loads due to the shear forces provided by the beams are:

$$N_{ed.C1} = P_{cant.2.30m} + P_{cant.2.30m} + P_{border\ sec.7.80m} + P_{border\ slab\ 7.00m} = 74.13 + 74.13 + 174.90 + 134.97 = 458.14\ kN$$

$$M_{ed.C1} = M_{cant.2.30m} + M_{cant.2.30m} + M_{border\ sec.7.80m} + M_{border\ slab\ 7.00m} = 67.24 + 67.24 + 0.00 + 0.00 = 134.48\ kNm$$

Thus:

$$N_{ed,tot,C1} = N_{ed,C1} * n_{floors} + \rho_{g,k} * h_{floors} * n_{floors} = 458.14 * 23 - 2 * (74.13 + 74.13) + 1.570 * 3.60 * 23 = 10370.67\ kN$$

$$M_{ed,tot,C1} = M_{ed,C1} * n_{floors} = 134.48 * 23 - 2 * (67.24 + 67.24) = 2\ 824.14\ kNm$$

In this case, a HE 240 M has been considered for the self-weight of the beam:

$$A_{min,ed\ C1} = \frac{N_{ed\ C1}}{f_{yd}} = \frac{10\ 370.67}{523.81} = 197.99\ cm^2$$

$$W_{min,ed\ C1} = \frac{M_{ed\ C1}}{f_{yd}} = \frac{2\ 824.14}{523.81} = 53.92\ cm^3$$

Computing its verifications:

$$A = 200\ cm^2 > 197.99\ cm^2$$

$$W_x = 1\ 799\ cm^3 > 53.92\ cm^3$$

COLUMN C2

The loads due to the shear forces provided by the beams are:

$$N_{ed.C2} = P_{cant.2.30m} + P_{primary\ 7.00m} + P_{border\ sec\ 7.80m} + P_{border\ sec\ 6.80m} = 74.13 + 128.57 + 174.90 + 160.22 = 537.83\ kN$$

$$M_{ed.C2} = M_{cant.2.30m} + M_{primary\ 7.80m} + M_{border\ sec\ 7.80m} + M_{border\ sec\ 6.80m} = 67.24 + 0.00 + 0.00 + 0.00 = 67.24\ kNm$$

Thus:

$$N_{ed,tot,C2} = N_{ed,B1} * n_{floors} + \rho_{g,k} * h_{floors} * n_{floors} = 537.83 * 23 - 2 * 74.13 + 1.890 * 3.60 * 23 = 12\ 378.25\ kN$$

$$M_{ed,tot,C2} = M_{ed,C2} * n_{floors} = 67.24 * 23 - 2 * 67.24 = 1\ 412.07\ kNm$$

In this case, a HE 280 M has been considered for the self-weight of the beam:

$$A_{min,ed\ C2} = \frac{N_{ed\ C2}}{f_{yd}} = \frac{12\ 378.25}{523.81} = 236.31\ cm^2$$

$$W_{min,ed\ B1} = \frac{M_{ed\ C2}}{f_{yd}} = \frac{1\ 412.07}{523.81} = 26.96\ cm^3$$

Computing its verifications:

$$A = 240\ cm^2 > 223.62\ cm^2$$

$$W_x = 2\ 551\ cm^3 > 26.96\ cm^3$$

COLUMN C4

The loads due to the shear forces provided by the beams are:

$$N_{ed.C4} = P_{cant.2.30m} + P_{primary\ 7.00m} + P_{border\ sec\ 6.80m} + P_{border\ sec\ 6.80m} = 74.13 + 128.57 + 160.22 + 160.22 = 523.15\ kN$$

$$M_{ed.C4} = M_{cant.2.30m} + M_{primary\ 7.80m} + M_{border\ sec\ 6.80m} + M_{border\ sec\ 6.80m} = 67.24 + 0.00 + 0.00 + 0.00 = 67.24\ kNm$$

Thus:

$$N_{ed,tot,C4} = N_{ed,C4} * n_{floors} + \rho_{g,k} * h_{floors} * n_{floors} = 537.83 * 23 - 2 * 74.13 + 1.890 * 3.60 * 23 = 12\ 040.70\ kN$$

$$M_{ed,tot,C4} = M_{ed,C4} * n_{floors} = 67.24 * 23 - 2 * 67.24 = 2\ 824.14\ kNm$$

In this case, a HE 280 M has been considered for the self-weight of the beam:

$$A_{min,ed\ B1} = \frac{N_{ed\ B1}}{f_{yd}} = \frac{12\ 040.70}{523.81} = 229.87\ cm^2$$

$$W_{min,ed\ B1} = \frac{M_{ed\ B1}}{f_{yd}} = \frac{2\ 824.14}{523.81} = 53.92\ cm^3$$

Computing its verifications:

$$A = 240\ cm^2 > 223.62\ cm^2$$

$$W_x = 2\ 551\ cm^3 > 26.96\ cm^3$$

After the load calculation for each element, we discovered that the C2 column is the pillar most subjected to compression actions (two out of the four beams support part of the slab), while for A1 and C1 the bending moment given by two cantilever beams reaches the maximum value.

We can go now through the minimum resistance due to compressive actions. Bending moment checking will be neglected in this calculation report since it is clearly obvious that compressions actions are more burdensome that bending moment.

ULS – N_{max}/M_{max}

The calculation of the minimum area able to support the load is:

$$A_{min,ed} = \frac{N_{ed,max}}{f_{yd}} = \frac{12\,378.25}{\frac{550.00}{1.05}} = 236.31\ cm^2$$

While the minimum resistant module is computed as:

$$W_{x,min,ed} = \frac{M_{ed,max}}{f_{yd}} = \frac{2\,824.14}{\frac{550.00}{1.05}} = 53.92\ cm^3$$

The above-mentioned HE 400 M column verifies the two minimum requirements:

$$A > A_{min,ed} \rightarrow 315.80\ cm^2 > 236.31\ cm^2$$

$$W_x > W_{x,min,ed} \rightarrow 4\,052\ cm^3 > 53.92\ cm^3$$

$$W_y > W_{y,min,ed} \rightarrow 1\,276\ cm^3 > 53.92\ cm^3$$

BEAM CHOICE

As a recap, here the values regarding the HE 340 M beam are shown again, working as an easier comprehension for the following stages.

$$h = 37.70\ cm;$$

$$b = 30.90\ cm;$$

$$t_w = 2.10\ \text{cm};$$

$$t_f = 4.00\ cm;$$

$$r = 2.70\ cm;$$

$$i_x = 15.55\ cm;$$

$$i_y = 7.90\ cm;$$

$$A = 315.80\ cm^2$$

$$\rho_{g,k} = 2.480\frac{kN}{m}$$

$$W_x = 4\,052\ cm^3$$

$$W_y = 1\,276\ cm^3$$

$$I_x = 76\,370\ cm^4$$

$$I_y = 19\,710\ cm^4$$

ULS – N_{max}

As the Eurocode prescribes, it is important to verify the stability of the column along its main two axes, the x-x inertial and the y-y inertial axis, at the Ultimate Limit State.

The first step is to select the so-called imperfection coefficient for the instability curve of the pillar. It must respect specific geometrical rules, according to the selected profile, and they are mentioned in the below image.

Politecnico di Milano, Master of Science in Building and Architectural Engineering
Steember - Steel and timber for a high rise building in Queens, New York
Chinnici Federico - **Maranesi** Marco

Curva di instabilità	*a*	*b*	*c*	*d*
Coefficiente di imperfezione α	0,21	0,34	0,49	0,76

Figure 6.71 - Imperfection coefficients

Sezione trasversale	Limiti	Instabilità attorno all'asse	Curva di instabilità
Sezioni laminate ad I 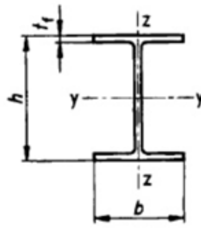	$h/b > 1{,}2$:		
	$t_f \leq 40$ mm	y-y z-z	a b
	40 mm $< t_f \leq 100$ mm	y-y z-z	b c
	$h/b \leq 1{,}2$:		
	$t_f \leq 100$ mm	y-y z-z	b c
	$t_f > 100$ mm	y-y z-z	d d

Figure 6.72 - Curve instability selection for cross-section profiles

Consequently, since:

$$\frac{h}{b} = \frac{37.70}{30.90} \geq 1.20$$

And

$$t_f \leq 4.00\ cm$$

We can go through the "a" coefficient for the x-x axis and "b" coefficient y-y axis.

So:

$$\alpha_{x-x} = 0.21$$

$$\alpha_{y-y} = 0.34$$

The following step is to compute the slenderness coefficient, given as:

$$\lambda_x = \frac{h_{floor}}{i_x} = \frac{360}{15.55} = 23.15$$

$$\lambda_y = \frac{h_{floor}}{i_y} = \frac{360}{7.90} = 45.57$$

To compute the a-dimensional slenderness, it is important to use yielding stress able to resist to the following verifications.

$$\overline{\lambda_x} = \frac{\lambda_x}{\lambda_1} = \frac{23.15}{\pi^2 * \sqrt{\frac{E_s}{f_{yk}}}} = \frac{23.15}{\pi^2 * \sqrt{\frac{210\,000}{550.00}}} = 0.38$$

$$\overline{\lambda_y} = \frac{\lambda_y}{\lambda_1} = \frac{45.57}{\pi^2 * \sqrt{\frac{E_s}{f_{yk}}}} = \frac{45.57}{\pi^2 * \sqrt{\frac{210\,000}{550.00}}} = 0.74$$

A further Φ coefficient is needed to go through the calculations, defined as:

$$\phi_x = 0.5 * \left(1 + \alpha_{x-x} * \left(\overline{\lambda_x} - 0.2\right) + \overline{\lambda_x}^{\,2}\right) = 0.5 * (1 + 0.21 * (0.38 - 0.2) + 0.38^2) = 0.59$$

$$\phi_y = 0.5 * \left(1 + \alpha_{y-y} * \left(\overline{\lambda_y} - 0.2\right) + \overline{\lambda_y}^{\,2}\right) = 0.5 * (1 + 0.34 * (0.74 - 0.2) + 0.74^2) = 0.87$$

The final reductive coefficient for permanent instability will be:

$$\chi_x = \frac{1}{\phi_x + \sqrt{\phi_x^{\,2} - \overline{\lambda_x}^{2}}} = \frac{1}{0.59 + \sqrt{0.59^2 - 0.38^2}} = 0.96$$

$$\chi_y = \frac{1}{\phi_y + \sqrt{\phi_y^{\,2} - \overline{\lambda_y}^{2}}} = \frac{1}{0.87 + \sqrt{0.87^2 - 0.74^2}} = 0.76$$

The final resistance due to compression instability can be computed. At first, it is needed to show the cross-section class, that depends on the geometry, on the selected profiles and on the steel class. If the below formula is verified, the element under investigation will be asseverated in class 1.

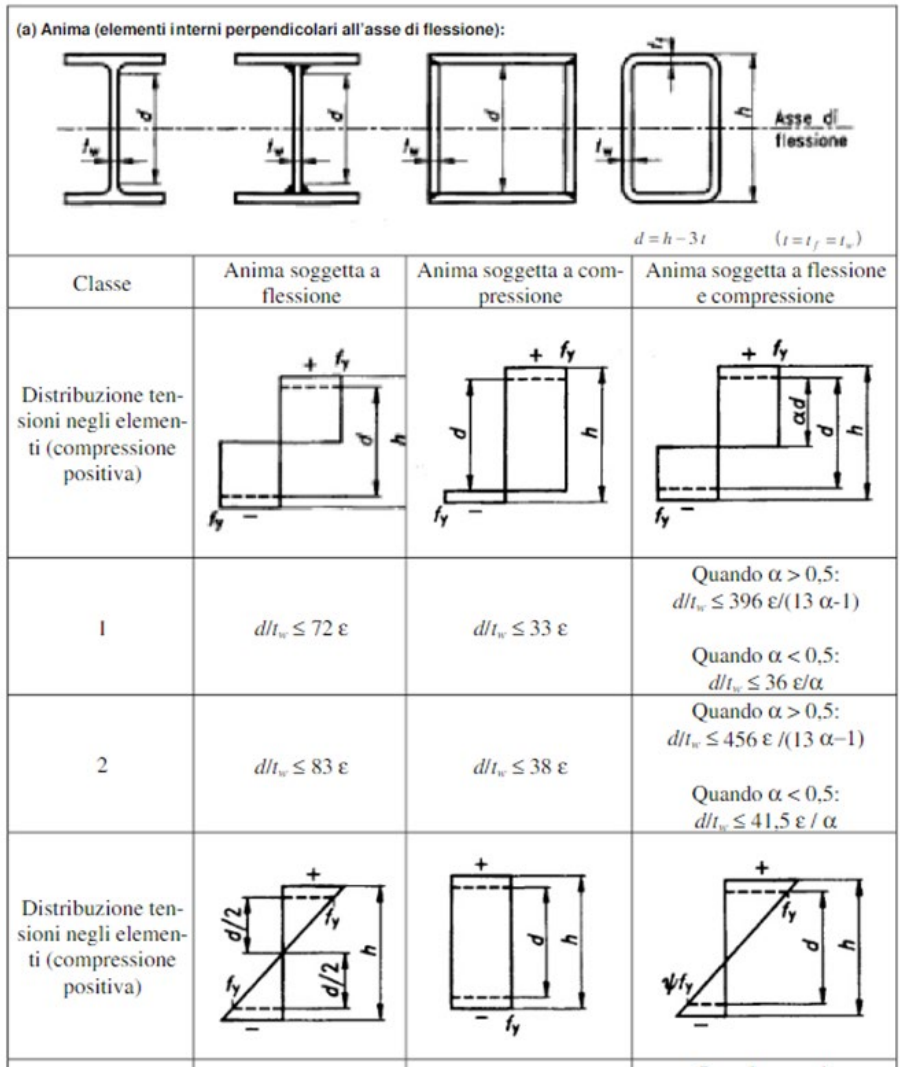

(a) Anima (elementi interni perpendicolari all'asse di flessione):

Classe	Anima soggetta a flessione	Anima soggetta a compressione	Anima soggetta a flessione e compressione
Distribuzione tensioni negli elementi (compressione positiva)			
1	$d/t_w \le 72\,\varepsilon$	$d/t_w \le 33\,\varepsilon$	Quando $\alpha > 0{,}5$: $d/t_w \le 396\,\varepsilon/(13\,\alpha-1)$ Quando $\alpha < 0{,}5$: $d/t_w \le 36\,\varepsilon/\alpha$
2	$d/t_w \le 83\,\varepsilon$	$d/t_w \le 38\,\varepsilon$	Quando $\alpha > 0{,}5$: $d/t_w \le 456\,\varepsilon/(13\,\alpha-1)$ Quando $\alpha < 0{,}5$: $d/t_w \le 41{,}5\,\varepsilon/\alpha$
Distribuzione tensioni negli elementi (compressione positiva)			

Figure 6.73 - Service classes of steel

$$\frac{h - 2 * (t_f + r)}{t_w} \le 72 * \sqrt{\frac{E_s}{f_{yk}}}$$

$$\frac{37.70 - 2 * (4.00 + 2.70)}{2.10} \le 72 * \sqrt{\frac{210\,000}{550}}$$

For sections of class 1,2 and 3, the β_α can be assumed as 1.

Consequently:

$$N_{rd,x} = \chi_x * \beta_a * A * f_{yd} = 0.96 * 1 * 315.80 * 523.81 = 15\,858.85\ kN$$

And:

$$N_{ed,max} < N_{rd,x} \rightarrow 12\,378.25\ kN < 15\,858.85\ kN \rightarrow utilisation\ 78\%$$

$$N_{ed,max} < N_{rd,y} \rightarrow 12\,378.25\ kN < 12\,559.87\ kN \rightarrow utilisation\ 99\%$$

COMBINED COMPRESSIVE AND BENDING STRESS VERIFICATION

Additional verification is due to the combined action of bending moment and compressive forces.

In order to compute this, two more coefficients should be solved, having the following limitation:

$$k_x \le 1.50\ and\ k_y \le 1.50$$

Thus:

$$k_x = 1 - \frac{\mu_x * N_{ed}}{\chi_x * A * f_{yd}} = 1 - \frac{0.90 * 12\,378.25}{0.96 * 315.80 * 523.81} = 0.30$$

$$k_y = 1 - \frac{\mu_y * N_{ed}}{\chi_y * A * f_{yd}} = 1 - \frac{0.90 * 12\,378.25}{0.76 * 315.80 * 523.81} = 0.11$$

Where μ_x and μ_y are taken as the maximum allowed value in Eurocode (equal to 0.90), in order to be on the safe side.

Consequently, we can calculate the overall relation:

$$\frac{N_{ed,max}}{\chi_{min} + A * f_{yd}} + \frac{k_x * M_{ed,max}}{W_x * f_{yd}} + \frac{k_y * M_{ed,max}}{W_y * f_{yd}} \le 1$$

$$\rightarrow \frac{12\,378.25}{0.76 * 326 * 523.81} + \frac{0.30 * 2\,258.04}{4\,052 * 523.81} + \frac{0.11 * 2\,258.04}{1\,276 * 523.81} = 0.99$$

Thus:

$$0.99 < 1.00$$

6.4.10 – CONCRETE MIX DESIGN

The very last element computed in this thesis project is the concrete beam. Due to an architectural choice of having a glass façade passing in front of the steel frame, a greater beam's base was needed, in order that both columns and glass façade could load on the beam, without any other supporting plate.

The only way to reach the set target was the consideration and the use of concrete, able to be designed in a more flexible way with respect to other materials. Steel beams are not suitable, because the pre-determined shape can lead to bases not greater than 30 cm. On the other way around, wooden beams are not enough to resist to compression forces provided by steel columns.

Therefore, a more proper structural solution was decided to complete the structural design.

Brief mix design has been done, in order to select a proper concrete class, able to respect the below-exposed environmental prescriptions. These resistant classes should pass through the UNI EN 206 -2006, that defines a minimum concrete class with respect to the exposure to the aggressivity of the environment.

No risk of corrosion or attack:

- X0;
- Minimum resistant class: C12/15;

Corrosion induced by carbonation:

- XC1
- Dry or permanently wet: w/c_{max} = 0,60;
- Minimum concrete dosage (kg/m^3) = 300;
- Minimum resistant class: C25/30;

- XC2
- Wet, rarely dry: w/c_{max} = 0,60;
- Minimum concrete dosage (kg/m^3) = 300;
- Minimum resistant class: C25/30;

- XC3
- Moderate humidity: w/c_{max} = 0,55;
- Minimum concrete dosage (kg/m^3) = 320;
- Minimum resistant class: C28/35;

- XC4
- Cyclic wet and dry: w/c_{max} = 0,50;
- Minimum concrete dosage (kg/m^3) = 340;
- Minimum resistant class: C32/40;

Corrosion induced by chlorides:

- XD1

- Moderate humidity: w/c_{max} = 0,55;
- Minimum concrete dosage (kg/m^3) = 320;
- Minimum resistant class: C28/35;

- XD2
- Wet, rarely dry: w/c_{max} = 0,50;
- Minimum concrete dosage (kg/m^3) = 340;
- Minimum resistant class: C32/40;

- XD3
- Cyclic wet and dry: w/c_{max} = 0,45;
- Minimum concrete dosage (kg/m^3) = 360;
- Minimum resistant class: C35/45;

Corrosion induced by chlorides from sea water:

- XS1
- Exposed to airborne salt but not in direct contact with sea water: w/c_{max} = 0,45;
- Minimum concrete dosage (kg/m^3) = 340;
- Minimum resistant class: C32/40;

- XS2 - Permanently submerged: w/c_{max} = 0,45;
- Minimum concrete dosage (kg/m^3) = 360;
- Minimum resistant class: C35/45;

- XS3
- Tidal, splash and spray zones: w/c_{max} = 0,45;
- Minimum concrete dosage (kg/m^3) = 360;
- Minimum resistant class: C35/45;

Freeze/Thaw attack:

- XF1
- Moderate water saturation, without de-icing agent: w/c_{max} = 0,50;
- Minimum concrete dosage (kg/m^3) = 320;
- Minimum resistant class: C32/40;

- XF2
- Moderate water saturation, with de-icing agent w/c_{max} = 0,50;
- Minimum concrete dosage (kg/m^3) = 340;
- Minimum resistant class: C25/30;

- XF3
- High water saturation, without de-icing agents: $w/c_{max} = 0,50$;
- Minimum concrete dosage (kg/m^3) = 340;
- Minimum resistant class: C25/30;

- XF4
- High water saturation with de-icing agents or sea water: $w/c_{max} = 0,45$;
- Minimum concrete dosage (kg/m^3) = 360;
- Minimum resistant class: C28/35;

Chemical attack:

- XA1
- Slightly aggressive chemical environment: $w/c_{max} = 0,55$;
- Minimum concrete dosage (kg/m^3) = 320;
- Minimum resistant class: C28/35;

- XA2
- Moderately aggressive chemical environment: $w/c_{max} = 0,50$;
- Minimum concrete dosage (kg/m^3) = 340;
- Minimum resistant class: C32/40;

- XA3
- Highly aggressive chemical environment: $w/c_{max} = 0,45$;
- Minimum concrete dosage (kg/m^3) = 360;
- Minimum resistant class: C35/45.

The proposed target is to select the maximum value among each category class. Because the beam, set at the ground floor, is:

- inside the buildings with moderate or high air humidity →**XC3**;
- exposed to airborne chlorides →**XD1**;
- near to or on the coast →**XS1**;
- exposed to rain and agent freezing →**XF1**;
- set in a high-aggressive chemical environment →**XA3**;

It is possible to state the minimum class of resistance due to exposure will be the C35/45; the highest parameter was the aggressiveness of the environment. We can assume the high aggressiveness is due to the presence of a former factory building next to the site and, more in general, set in the centre of a high-dense industrial activity zone as the Queens is.

6.4.11 – CONCRETE BEAM - SLAB'S LOAD

GEOMETRICAL PRE-DESIGN

Concrete pre-design elements should be checked too many parameters influencing already at the early stage of its design.

Given the base and the height dimensions, the beam should verify that:

$$h > \frac{l}{25}$$

Given the length of the beam, as previously calculated, and since:

$$h = 70\ cm$$

We have

$$70\ cm > 31\ cm$$

The minimum cover for the steel rebars is:

$$d_{cover,nom} = MAX(\phi_{bars}; 15\ mm) + 10\ mm$$

The selected bars are:

$$\phi = 28\ mm$$

So, the minimum cover is:

$$d_{cover,nom} = 28 + 10 = 38\ mm$$

Consequently, the effective height will be:

$$d_{max} = h - h_{cover,nom} - \frac{\phi}{2} = 70 - 3.80 - \frac{2.80}{2} = 64.80\ cm$$

The effective distance between the concrete tensioned face and the barycentre of the steel reinforcement is designed as:

$$d = 45\ cm$$

So

$$d < d_{max} \rightarrow 45\ cm < 64.80\ cm$$

The base should be set in the following range:

$$b > MAX\left(20\ cm; \frac{h}{4}\right)$$
$$b < MIN(h + d; 2 * d)$$

Since:

$$b = 70\ cm$$

We have:

$$b_{min} < b < b_{max} \rightarrow 20\ cm < 70\ cm < 90\ cm$$

LOAD ANALYSIS

The load analysis considers both the self-weight of the beam and the curtain wall lying on it. The total load at the ULS is:

$$\frac{\rho}{2} = \rho' * b * h = 25 * 0.70 * 0.70 = 6.13 \frac{kN}{m}$$

Given the permanent load (3.03 kN/m²) and the variable load (2.00 kN/m²), we can compute the kN/m value by using the highest length a single beam has to bear due to the slab weight and curtain wall weight.

Thus:

$$g' + q' = (g + q) * l_{infl} + \frac{\rho}{2} = (3.03 + 2.00) * 3.75 + 6.13 = 24.99 \frac{kN}{m}$$

$$g_{curt.wall} = 3.60 \frac{kN}{m}$$

$$Q_{tower} = g' + q' + g_{curt.wall} = 24.99 + 3.60 = 28.59 \frac{kN}{m}$$

At the same time, the concrete beam needs to support the relative influenced area of the adjacent garden. The slab's weight counts for 8.99 kN/m², while the variable load is equal to 5.00 kN/m², as prescribed by the Eurocode.

A regular structural grid of 6x6 metres of the underground floor counts to the beam an influenced area equal to 3 metres.

$$Q_{garden} = (g + q) * l + \frac{\rho}{2} = (8.99 + 5.00) * 3.00 + 6.13 = 48.09 \frac{kN}{m}$$

At the Ultimate Limit State, the calculation is:

$$\begin{aligned} Q &= \left(\gamma_g * g + \gamma_q * q\right) * l_{infl} + \gamma_g * \frac{\rho}{2} + \left(\gamma_g * g + \gamma_q * q\right) * l_{infl} + \gamma_g * \frac{\rho}{2} + \gamma_g * g_{curt.wall} \\ &= (1.35 * 3.03 + 1.50 * 2.00) * 3.75 + 1.35 * 6.13 \\ &+ (1.35 * 8.99 + 1.50 * 5.00) * 3.00 + 1.35 * 6.13 + 1.35 * 3.60 \\ &= 106.90 \frac{kN}{m} \end{aligned}$$

ULS - M_{max}

Following the superimposition of the schematic schemes, as shown in the below images, we can compute the maximum bending moment at the ultimate limit state. A secondary beam acts on the concrete member.

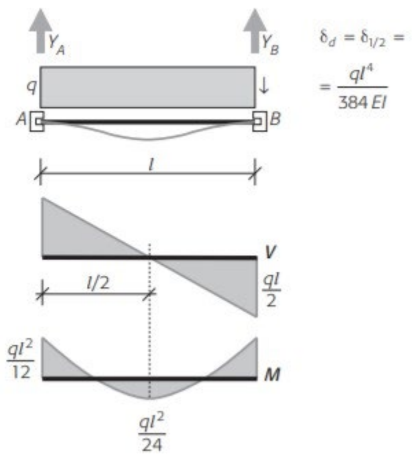

Figure 6.74 - Hyper-static scheme with double fixed-end constraints and distributed load

Politecnico di Milano, Master of Science in Building and Architectural Engineering
Steember - Steel and timber for a high rise building in Queens, New York
Chinnici Federico - **Maranesi** Marco

Proceeding with the moment actions:

$$M_{ed,distr,mid} = Q * \frac{l^2}{24} = 106.90 * \frac{7.50^2}{24} = 250.54 \text{ kNm}$$

While for extreme cross-sections:

$$M_{ed,slab,extr} = Q * \frac{l^2}{12} = 106.90 * \frac{7.50^2}{12} = 501.08\ kNm$$

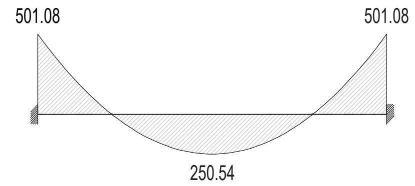

Figure 6.75 - Moment diagram of the distributed load

REINFORCEMENT DESIGN

The next step is to determine the minimum area for steel reinforcement. According to the Eurocode, the minimum quantity should not be less than:

$$A_{steel,min} = MAX(\frac{M_{ed}}{0.90 * d * f_{yd}}; 6.16\ cm^2; 0.26 * \frac{f_{ctm}}{f_{yd}} * b * d; 0.003 * f_{yk})$$

$$A_{steel,min} = MAX\left(\frac{501.08\ vs. 250.54}{0.90 * 45 * 391.30}; 6.16; 0.26 * \frac{3.36}{391.30} * 70 * 45; 0.003 * 450\right)$$

$$A_{steel,min,mid} = 13.17\ cm^2$$

$$A_{steel,min,extr} = 26.35\ cm^2$$

Moreover, a further prescription states that the overall quantity of reinforcement should not be less than:

$$\rho_{min} = 0.0013\% * b * d = 0.0013\% * 70 * 45 = 4.10\%$$

And not more than:

$$\rho_{max} = 0.0078\% * f_{yk} = 0.0078\% * 450 = 4.21\%$$

Due to this result, 22 rebars have been selected on the tensional side, and 11 more are set in the compressional side. As mentioned before, the diameter size of the rebars is 28 mm.

Thus:

$$A_{steel} = \left(n_{long.bars,tens} + n_{long.bars,comp}\right) * \pi^2 * \frac{\phi}{4} = (22 + 11) * \pi^2 * \frac{28}{4} = 203.20\ cm^2$$

And:

$$\rho = \frac{A_{steel}}{b * h} = \frac{203.20}{70 * 70} = 4.15\%$$

Consequently:

$$A_{steel} > A_{steel,min,mid} \rightarrow 203.20\ cm^2 > 13.17\ cm^2$$

$$A_{steel} > A_{steel,min,extr} \rightarrow 203.20\ cm^2 > 26.35\ cm^2$$

And:

$$\rho_{min} < \rho < \rho_{max} \rightarrow 4.10\% < 4.15\% < 4.29\%$$

Moreover, the Eurocode states a further verification on the longitudinal reinforcement, according to the compressive area, with respect to the tensional one. This happens in case of a great quantity of reinforcement, in case the minimum quantity of rebars are not enough to respect the above-mentioned formula:

$$\rho'_{s+} \geq 0.25 * \rho_{s+}$$

$$\rho'_{s+} \geq 0.25 * \rho_{s-}$$

$$\rho'_{s-} \geq 0.50 * \rho_{s-}$$

Thus:

$$\rho'_{s+} = \frac{A_{steel}}{b * h} = \frac{11 * \pi^2 * \phi/4}{70 * 70} = 1.38\%$$

$$\rho'_{s-} = \frac{A_{steel}}{b * h} = \frac{11 * \pi^2 * \phi/4}{70 * 70} = 1.38\%$$

$$\rho_{s+} = \frac{A_{steel}}{b * h} = \frac{22 * \pi^2 * \phi/4}{70 * 70} = 2.76\%$$

$$\rho_{s-} = \frac{A_{steel}}{b * h} = \frac{22 * \pi^2 * \phi/4}{70 * 70} = 2.76\%$$

Therefore:

$$\rho'_{s+} \geq 0.25 * \rho_{s+} \rightarrow 1.38\% \geq 0.69\%$$

$$\rho'_{s-} \geq 0.25 * \rho_{s-} \rightarrow 1.38\% \geq 0.69\%$$

$$\rho'_{s-} \geq 0.50 * \rho_{s-} \rightarrow 1.38\% \geq 1.38\%$$

ANCHORAGE LENGTH

The anchorage length of the rebars to the concrete pillars set below the steel columns depends on different factors and coefficients:

$$l_b = \frac{\phi_{long\ bars} * f_{yd}}{4 * f_{ctk} * \frac{\beta_b}{\gamma_c}} = \frac{28 * 391.30}{4 * 2.35 * \frac{2.25}{1.50}} = 93.14\ cm$$

ULS - M_{max}

As the first step for the bending moment verification, it is needed to check the neutral axis of the beam.

Given the reinforcement area in both the tensional and the compressional sides, as:

$$A_{s,tens} = n_{long.bars,tens} * \pi^2 * \frac{\phi}{4} = 22 * \pi^2 * \frac{28}{4} = 135.47\ cm^2$$

$$A_{s,comp} = n_{long.bars,comp} * \pi^2 * \frac{\phi}{4} = 11 * \pi^2 * \frac{28}{4} = 67.73\ cm^2$$

It is possible to compute the neutral axis position:

$$x = \alpha_e * \frac{A_{s,tens} + A_{s,comp}}{b} * \left(-1 + \sqrt{1 + \frac{2 * b}{\alpha_e * (A_{s,tens} + A_{s,comp})} * (d * A_{s,tens}) + \frac{(h-d) * A_{s,comp}}{A_{s,tens} + A_{s,comp}}}\right) =$$

$$= 15 * \frac{135.47 + 67.73}{70} * \left(-1 \sqrt{1 + 2 * \frac{70}{15 * 135.47 * 67.73} * 45 * 135.47 + ((70-45) * 67.73)/(135.47 + 67.73)}\right) = 28.81\ cm$$

The final resisting moment is:

$$M_{rd} = A_{s,tens} * f_{yd} * (d - 0.4 * x) = 135.47 * 391.30 * (45 - 0.4 * 28.81) = 2\,129.52\ kNm$$

So:

$$M_{ed,mid} < M_{rd} \rightarrow 250.54\ kNm < 2\,129.52\ kNm \rightarrow utilisation\ 12\%$$

$$M_{ed,extr} < M_{rd} \rightarrow 501.08\ kNm < 2\,129.52\ kNm \rightarrow utilisation\ 24\%$$

ULS - V_{max}

With the superimposition of the combination, it is now possible to compute the maximum shear at the ULS, with its relative coefficients. The used formulas are the above-mentioned ones.

$$V_{ed} = Q * \frac{l}{2} = 107.34 * \frac{7.50}{2} = 400.87\ kN$$

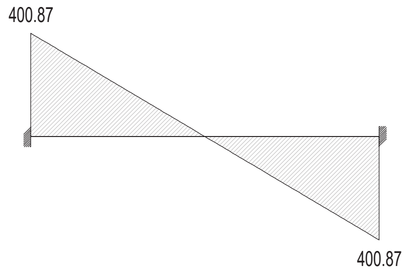

Figure 6.76 - Shear diagram of the distributed load

The resisting shear is computed as:

$$V_{rd} = \frac{C_{rd,c}}{\gamma_c} * \left(1 + \sqrt{\frac{b}{d}}\right) * (\rho_s * f_{ck})^{\frac{1}{3}} * b * d$$

$$= \frac{0.18}{1.50} * \left(1 + \sqrt{\frac{70}{45}}\right) + (0.0415 * 45)^{\frac{1}{3}} * 70 * 45 = 456.80\ kN$$

Consequently:

$$V_{ed} < V_{rd} \rightarrow 400.87\ kN < 456.80\ kN \rightarrow utilisation\ 88\%$$

SLS - M_{max}

With the superimposition of the combination, it is now possible to compute the bending moment at the SLS. The neutral axis, since it depends on the geometry of the beam and the reinforcement quantity, is already set.

The bending moment is:

$$M_{ed,SLS,mid} = \left((g'+q')*l+\frac{\rho}{2}+g_{curt.wall}\right)*\frac{l^2}{24}+\left((g'+q')*l+\frac{\rho}{2}\right)*\frac{l^2}{24}$$
$$= \left((3.03+2.00)*3.90+6.13+3.60\right)*\frac{7.50^2}{24}$$
$$+\left((8.99+5.00+)*3.00+6.13\right)*\frac{7.50^2}{24} = 179.73\ kNm$$

$$M_{ed,SLS,extr} = \left((g'+q')*l+\frac{\rho}{2}+g_{curt.wall}\right)*\frac{l^2}{12}+\left((g'+q')*l+\frac{\rho}{2}\right)*\frac{l^2}{12}$$
$$= \left((3.03+2.00)*3.90+6.13+3.60\right)*\frac{7.50^2}{12}$$
$$+\left((8.99+5.00+)*3.00+6.13\right)*\frac{7.50^2}{12} = 359.45\ kNm$$

The bending moment computed at the SLS is given by means of the stresses acting on the beam, rather than the final value; knowing the neutral axis earlier computed, they are calculated as:

$$\sigma'_c = M_{ed,SLS,mid}*\frac{2}{b*x*d-\frac{x}{3}} = 179.73*\frac{2}{70*28.81*45-\frac{28.81}{3}} = 5.04\frac{N}{mm^2}$$

$$\sigma"_c = M_{ed,SLS,extr}*\frac{2}{b*x*d-\frac{x}{3}} = 359.454*\frac{2}{70*28.81*45-\frac{28.81}{3}} = 10.07\frac{N}{mm^2}$$

Since the operative tensional stress of concrete is:

$$\sigma_c = 0.60*f_{ck} = 0.60*37.50 = 22.50\frac{N}{mm^2}$$

Therefore:

$$\sigma'_c < \sigma_c \rightarrow 5.04\frac{N}{mm^2} < 22.50\frac{N}{mm^2} \rightarrow utilisation\ 22\%$$

$$\sigma"_c < \sigma_c \rightarrow 10.07\frac{N}{mm^2} < 22.50\frac{N}{mm^2} \rightarrow utilisation\ 45\%$$

STIRRUPS' DESIGN

Due to the presence of the shear stress, it is needed to increase the amount of steel by means of stirrups set embracing the longitudinal reinforcement.

The code prescribes a minimum size of the stirrup diameter:

$$\phi_{st,min} = MAX(6\ mm; 0.09*b) = 6.30\ mm$$

Consequently:

$$\phi_{st} = 8\ mm$$

And:

$$\phi_{st} > \phi_{st,min} \rightarrow 8\ mm > 6.30\ mm$$

The stirrup needs a specific hook length, coded as:

$$d_{hook,min} = MAX\left(10; 10*2\phi_{long\ bars}\right) = MAX(10; 10*2.80) = 28\ cm$$

The designed hook is:

$$d_{hook} = 30\ cm$$

Thus:

$$d_{hook} > d_{hook,min} \rightarrow 30\ cm < 28\ cm$$

The distance between the stirrups depends on their position on the beam itself. When we are dealing with the beam core (set in the centre), the distance should be designed less than:

$$d_{st,cor,max} = MIN(60; 0.75*d) = MIN(60; 0.75*45) = 33.75\ cm$$

So:

$$d_{st,cor} = 30\ cm$$

Thus:

$$d_{st,cor} < d_{st,cor,min} \rightarrow 33\ cm < 33.75\ cm$$

Regarding the critical distance, the designed distance should be less than:

$$d_{st,cr,max} = MIN\left(\frac{h-d_{cover}}{4}; 22.50; 8*\phi_{long\ bars}; 24*\phi_{st}\right)$$
$$= \left(\frac{70-22.80}{4}; 22.50; 8*2.80; 24*0.80\right) = 11.80\ cm$$

So:

$$d_{st,cr} = 10\ cm$$

Thus:

$$d_{st,cr} < d_{st,cr,min} \rightarrow 10\ cm < 11.80\ cm$$

The number of stirrups set for each linear metre should be not less than:

$$n_{st.} = \frac{100}{MAX\left(d_{st,cor}; d_{st,cr}\right)} = \frac{100}{33; 10} = 3$$

The computed area for the stirrups, set on the longitudinal section, is:

$$A_{st} = n_{st.} * n_{st.bars} * \pi^2 * \frac{\phi}{4} = 3 * 4 * \pi^2 * \frac{8}{4} = 6.09 \frac{cm^2}{m}$$

While the minimum prescription is:

$$A_{st,min} = MAX\left(0.09\% * b; 0.08 * \frac{\sqrt{f_{ck}}}{f_{yk}}\right) = MAX\left(0.09\% * 70; 0.08 * \frac{\sqrt{37.50}}{450}\right)$$
$$= 0.06 \frac{cm^2}{m}$$

Thus:

$$A_{st} > A_{st,min} \rightarrow 6.09 \frac{cm^2}{m} > 0.06 \frac{cm^2}{m}$$

Before calculating the ratio, we should evaluate the maximum allowed distance between the legs of the stirrups, that is:

$$d_{st,legs,max} = MIN(30; 0.80 * d) = MIN(30; 0.80 * 45) = 30\ cm$$

$$d_{st,legs} = 25\ cm$$

Thus:

$$d_{st,legs} < d_{st,legs,max} \rightarrow 23\ cm < 30\ cm$$

The ratio that corresponds to the stirrup area is:

$$\rho_{s,st} = \frac{A_s}{b * d_{st,legs}} = \frac{6.09}{70 * 25} = 0.35\%$$

And it should be not less than:

$$\rho_{s,st,min} = 0.09\%$$

Thus:

$$\rho_{s,st} > \rho_{s,st,min} \rightarrow 0.35\% < 0.09\%$$

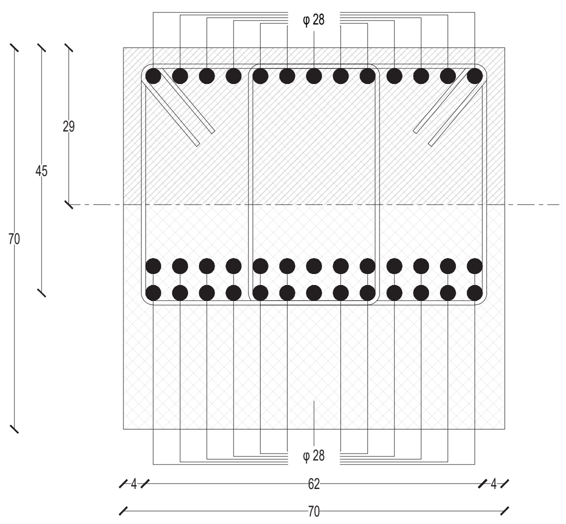

Figure 6.77 - Cross-section of the beam

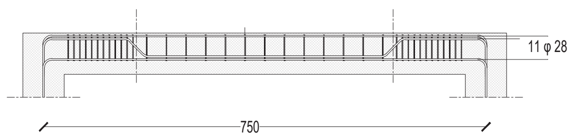

Figure 6.78 - Longitudinal section of the beam

Politecnico di Milano, Master of Science in Building and Architectural Engineering
Steember - Steel and timber for a high rise building in Queens, New York
Chinnici Federico - **Maranesi** Marco

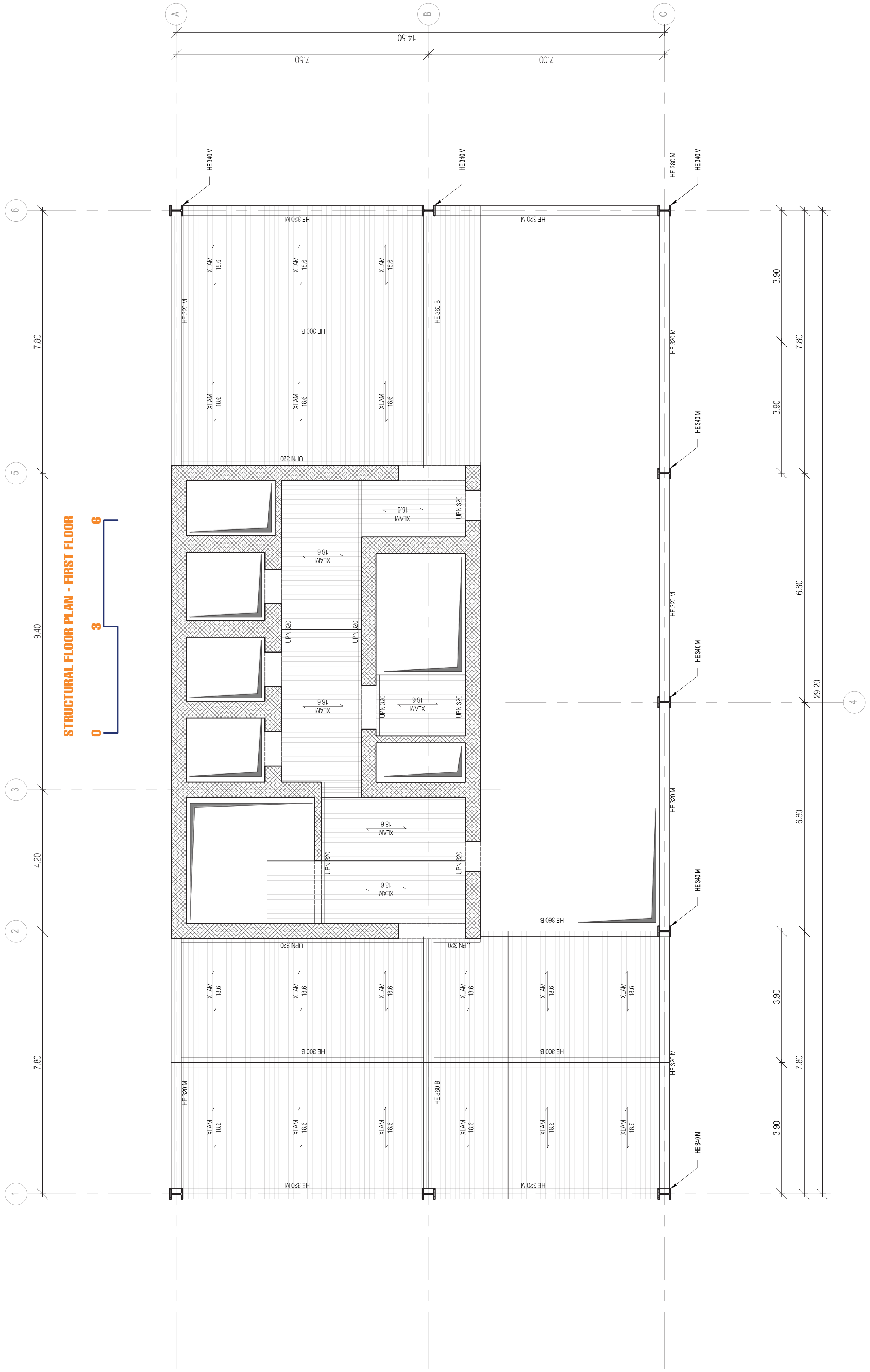

Politecnico di Milano, Master of Science in Building and Architectural Engineering
Steember - Steel and timber for a high rise building in Queens, New York
Chinnici Federico - **Maranesi** Marco

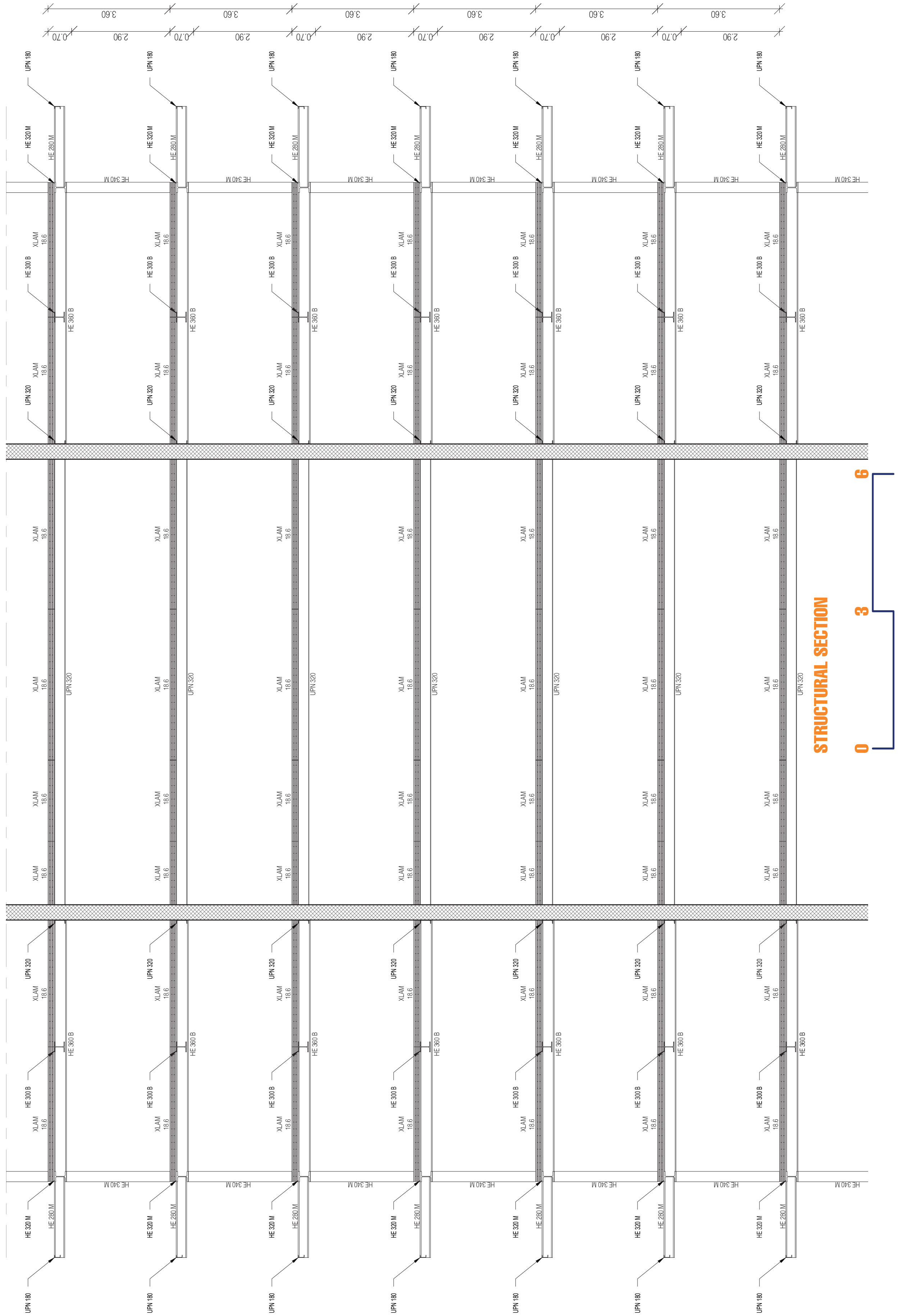

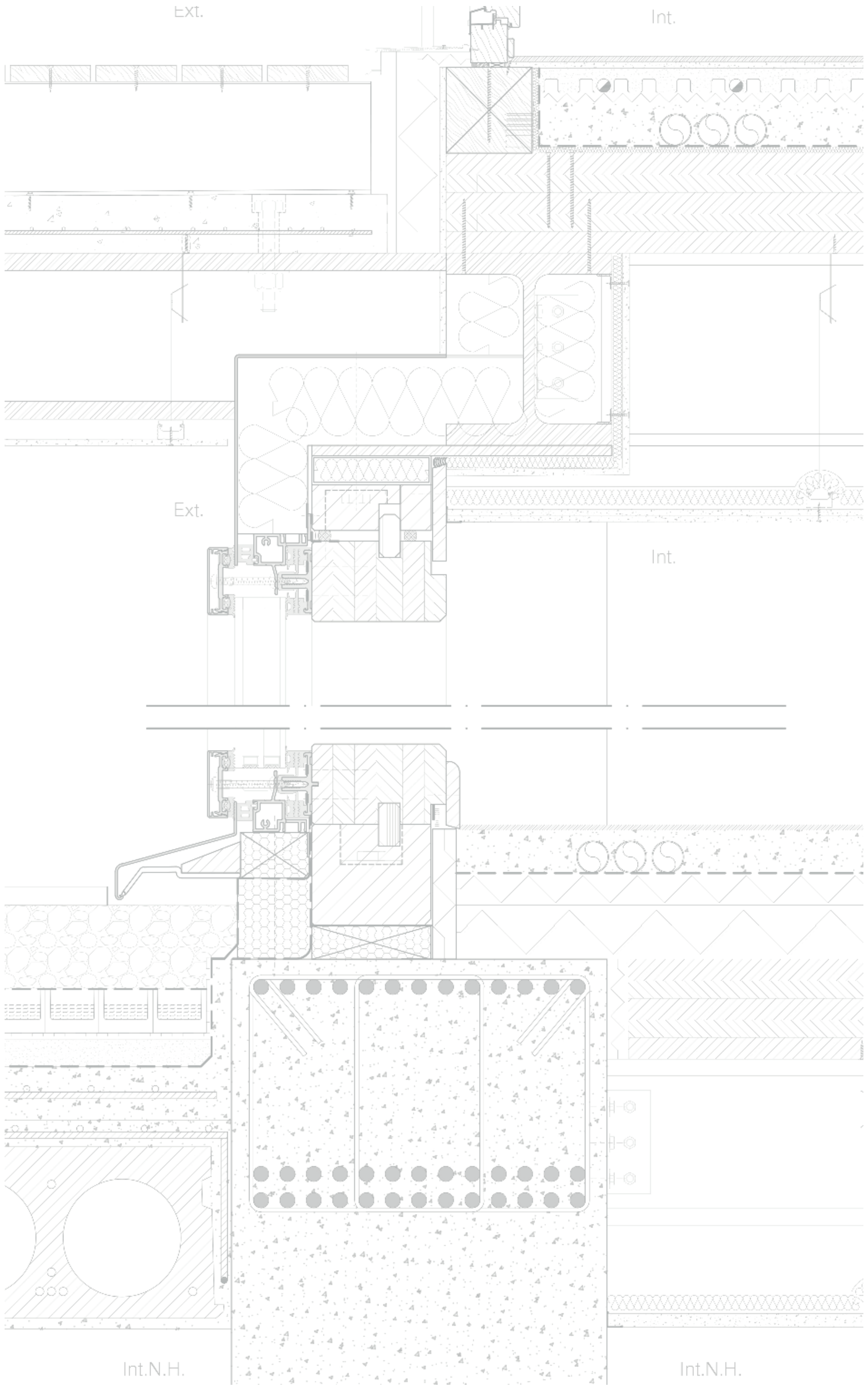

07 TECHNOLOGICAL DESIGN

7.1 – INTRODUCTION

The technological elements of the building are all lightweight members which can be put in place in an easy and fast way. One of the goals is to have most of the elements prefabricated, in order to have less manufacture possible on site. Such elements would just need to be supplied and installed, leaving just the internal and external finishing to the site carpenters.

The main used materials are steel for the structure of the building frame, and timber for the slabs and for the external and internal walls. These materials allow having wide freedom of shape and personalization, in order to make the installation of the prefabricated elements easier and faster. In particular, the walls have a timber frame structure with gypsum fibre panels, while the slabs are composed by cross-laminated timber panels, over which there will be the facilities screed and the radiant floor. This choice permits to have the enclosure completely built up in laboratory with the maximum dimensions obliged by the transportation limits. Moreover, the balcony is composed by a prefabricated concrete slab. The concrete is casted into a load-bearing corrugated sheet which works as a disposable formwork. This slab can arrive to the building site already waterproofed, with installed flooring and parapet, ready to be anchored to the steel cantilevers.

The choice of steel and timber as main materials is due to extreme prefabrication level that they offer and to light weight that these elements have. A precise and detailed construction process as also the aim to demonstrate how timber structures are ideal elements in many different types of buildings and, in particular, in high rise buildings as well.

Finally, timber was also chosen because is renewable, sustainable and ecological. The many trees used will be, in fact, automatically substituted by new ones even without human intervention if harvesting happens accordingly to the autoregeneration of forests.

Using timber can have an additional positive environmental impact because trees absorb carbon dioxide through photosynthesis and lock it away as carbon, thus removing it from the atmosphere. Therefore, timber can be considered as a carbon negative material. It is however important to remember that the sequestered carbon will be released at the end of life of the timber product, unless it is reused or recycled.

Politecnico di Milano, Master of Science in Building and Architectural Engineering
Steember - Steel and timber for a high rise building in Queens, New York
Chinnici Federico - **Maranesi** Marco

7.2 – THE STRATIGRAPHIES AND THEIR THERMAL PROPERTIES

First of all, the perimetral elements have been studied in order to select optimal materials at each layer reaching the best thermal properties. The considered parameters are the U values and the presence of interstitial condensation using the Glaser-method.

The used internal and external convective heat transfer coefficients are:

h_i = 8 W/m²K h_e = 23 W/m²K

7.2.1 – THE STUDY OF THE THERMAL PROPERTIES

- The external wall

U = 0,148 W/m²K **Ms = 77,72 kg/m²**

Layers	t [m]	λ [W/mK]	ρ [kg/m³]	C [J/kgK]
Convective internal heat transfer coefficient	/	/	/	/
Gypsumfibre board	0.013	0.320	1100	1100
Water vapour barrier	0.003	0.400	500	1800
Gypsumfibre board	0.013	0.320	1100	1100
Cellulose	0.160	0.038	45	2100
Gypsumfibre board	0.013	0.320	1100	1100
Wooden fibre insulation	0.080	0.040	160	2100
Air cavity	/	/	/	/
Fibre cement board	0.013	0.350	1150	2600
Convective external heat transfer coefficient	/	/	/	/

Layers	δ [kg/(smPa)]	r [(sm²Pa)/kg]	P_{sj} [Pa]	P_{vj} [Pa]]	
Convective internal heat transfer coefficient	/	/	2268	1474	✓
Gypsumfibre board	1.44×10^{-11}	8.69×10^{8}	2247	1473	✓
Water vapour barrier	2.49×10^{-15}	1.60×10^{12}	2241	409	✓
Gypsumfibre board	1.44×10^{-11}	8.69×10^{8}	2221	408	✓
Cellulose	4.68×10^{-11}	3.42×10^{9}	826	404	✓
Gypsumfibre board	1.44×10^{-11}	8.69×10^{8}	818	403	✓
Wooden fibre insulation	9.35×10^{-12}	4.28×10^{9}	460	391	✓
Convective external heat transfer coefficient	/	/	401	361	✓

- The green roof

U = 0,086 W/m²K **Ms = 442,33 kg/m²**

Layers	t [m]	λ [W/mK]	ρ [kg/m³]	C [J/kgK]
Convective external heat transfer coefficient	/	/	/	/
Soil	0.150	0.200	1464	840
Filtering membrane	0.004	0.220	0.00	0.00
Stock/dryer layer	0.082	0.034	25	1200
Lightweight screed	0.075	0.090	380	2500
Waterproof membrane	0.002	0.220	2000	840
OSB panel	0.013	0.130	650	1600
Wooden fibre insulation	0.160	0.040	160	2100
Xlam slab	0.332	0.120	400	1600
Water vapour barrier	0.003	0.400	500	1800
Wooden fibre insulation	0.050	0.040	160	2100
Gypsumfibre board	0.013	0.320	1100	1100
Gypsumfibre board	0.013	0.320	1100	1100
Convective internal heat transfer coefficient	/	/	/	/

Layers	δ [kg/(smPa)]	r [(sm²Pa)/kg]	P_{si} [Pa]	P_{vi} [Pa]	
Convective external heat transfer coefficient	/	/	401	361	✓
Soil	$1.87x10^{-10}$	$8.02x10^{8}$	404	361	✓
Filtering membrane	$1.56x10^{-12}$	$5.26x10^{10}$	447	361	✓
Stock/dryer layer	$9.35x10^{-15}$	$4.28x10^{11}$	678	386	✓
Lightweight screed	$9.38x10^{-11}$	$5.33x10^{8}$	680	585	✓
Waterproof membrane	$9.35x10^{-15}$	$2.14x10^{11}$	741	585	✓
OSB panel	$4.68x10^{-12}$	$2.67x10^{9}$	742	684	✓
Wooden fibre insulation	$9.35x10^{-12}$	$1.71x10^{10}$	753	685	✓
Xlam slab	$2.67x10^{-12}$	$1.24x10^{11}$	1355	693	✓
Water vapour barrier	$2.49x10^{-15}$	$1.60x10^{12}$	1989	751	✓
Wooden fibre insulation	$9.35x10^{-12}$	$4.28x10^{9}$	1996	1496	✓
Gypsumfibre board	$1.44x10^{-11}$	$8.69x10^{8}$	2282	1498	✓
Gypsumfibre board	$1.44x10^{-11}$	$8.69x10^{8}$	2294	1499	✓
Convective internal heat transfer coefficient	/	/	2306	1499	✓

Politecnico di Milano, Master of Science in Building and Architectural Engineering
Steember - Steel and timber for a high rise building in Queens, New York
Chinnici Federico - **Maranesi** Marco

- The ground floor

U = 0,133 W/m²K **Ms = 229,13 kg/m²**

Layers	t [m]	λ [W/mK]	ρ [kg/m³]	C [J/kgK]
Convective internal heat transfer coefficient	/	/	/	/
Tiles	0.015	1.000	2079	840
Lightweight screed	0.075	0.090	380	2500
Waterproof membrane	0.002	0.220	2000	840
Wooden fibre insulation	0.160	0.040	160	2100
Xlam slab	0.186	0.120	400	1600
Wooden fibre insulation	0.040	0.040	160	2100
Gypsumfibre board	0.013	0.320	1100	1100
Gypsumfibre board	0.013	0.320	1100	1100
Convective external heat transfer coefficient	/	/	/	/

Layers	δ [kg/(smPa)]	r [(sm²Pa)/kg]	P_{si} [Pa]	P_{vi} [Pa]	
Convective internal heat transfer coefficient	/	/	2277	1480	✓
Tiles	$4.68x10^{-12}$	$3.12x10^{9}$	2270	1469	✓
Lightweight screed	$9.38x10^{-11}$	$8.53x10^{9}$	1896	1465	✓
Waterproof membrane	$9.35x10^{-15}$	$2.14x10^{11}$	1892	698	✓
Wooden fibre insulation	$9.35x10^{-12}$	$1.71x10^{10}$	798	636	✓
Xlam slab	$2.67x10^{-12}$	$6.96x10^{10}$	550	387	✓
Wooden fibre insulation	$9.35x10^{-12}$	$4.28x10^{9}$	419	371	✓
Gypsumfibre board	$1.44x10^{-11}$	$8.69x10^{8}$	415	368	✓
Gypsumfibre board	$1.44x10^{-11}$	$8.69x10^{8}$	410	365	✓
Convective external heat transfer coefficient	/	/	406	365	✓

7.2.2 – THE STRATIGRAPHIES

THE EXTERNAL WALL

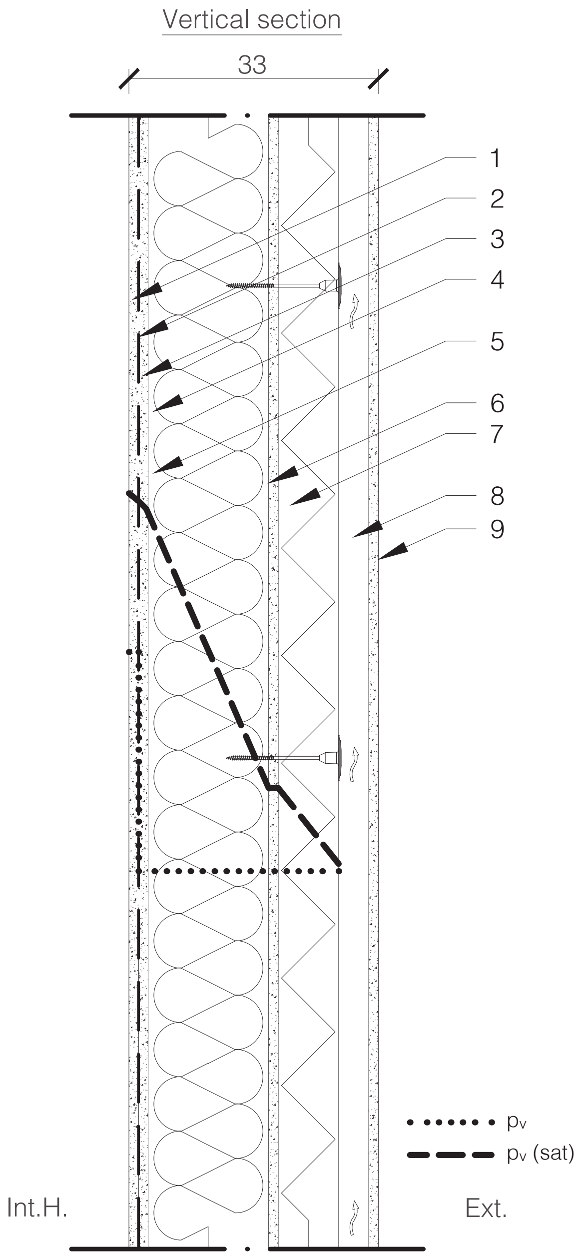

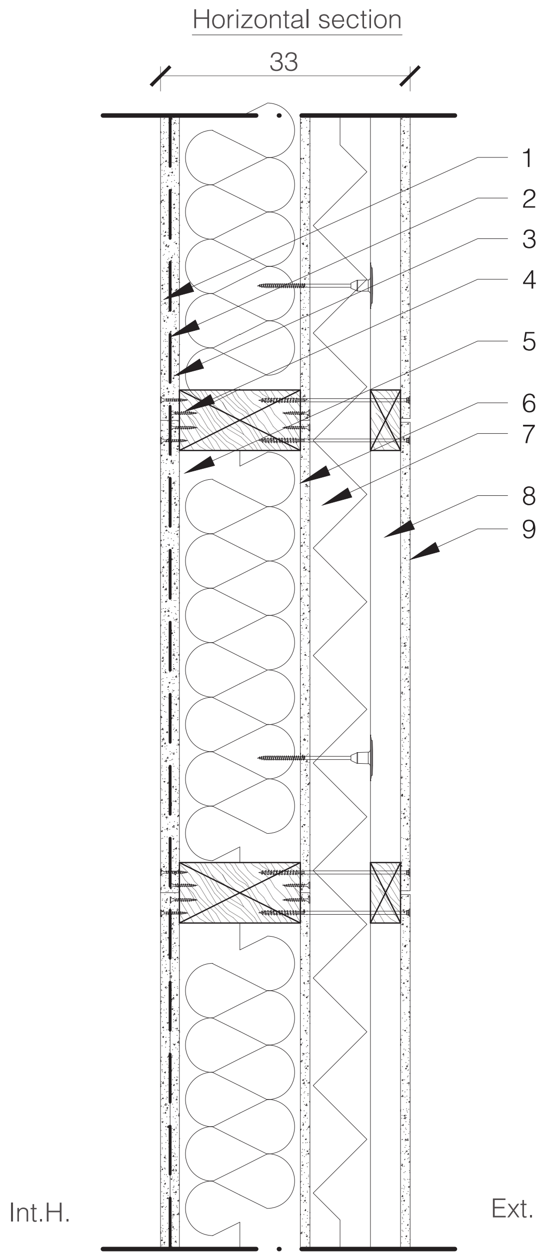

1	Fermacell Gypsum fiberboard, (th: 1.25 cm)
2	Water vapour barrier Riwega DS 48 2200 TOP SK, density: 1100 kg/m³, λ = 0.17 W/m²K, (th: 0.2 cm)
3	Fermacell Gypsum fiberboard, (th: 1.25 cm)
4	Laminated spruce wood beam, structure of the frame wall, 8 x16 cm (th: 16 cm)
5	Wooden fiber insulation Gutex Thermowall, 125x59cm, λ = 0.040 W/m²K, (th: 16 cm)
6	Fermacell Powerpanel H_2O fiberboard, (th: 1.25 cm)
7	Wooden fiber insulation Gutex Thermowall, 83x60 cm, λ = 0.040 W/m²K, (th: 8 cm)
8	Air cavity (th: 4 cm)
9	External cladding in fiber cement panels, (th: 1.25 cm)

Politecnico di Milano, Master of Science in Building and Architectural Engineering
Steember - Steel and timber for a high rise building in Queens, New York
Chinnici Federico - **Maranesi** Marco

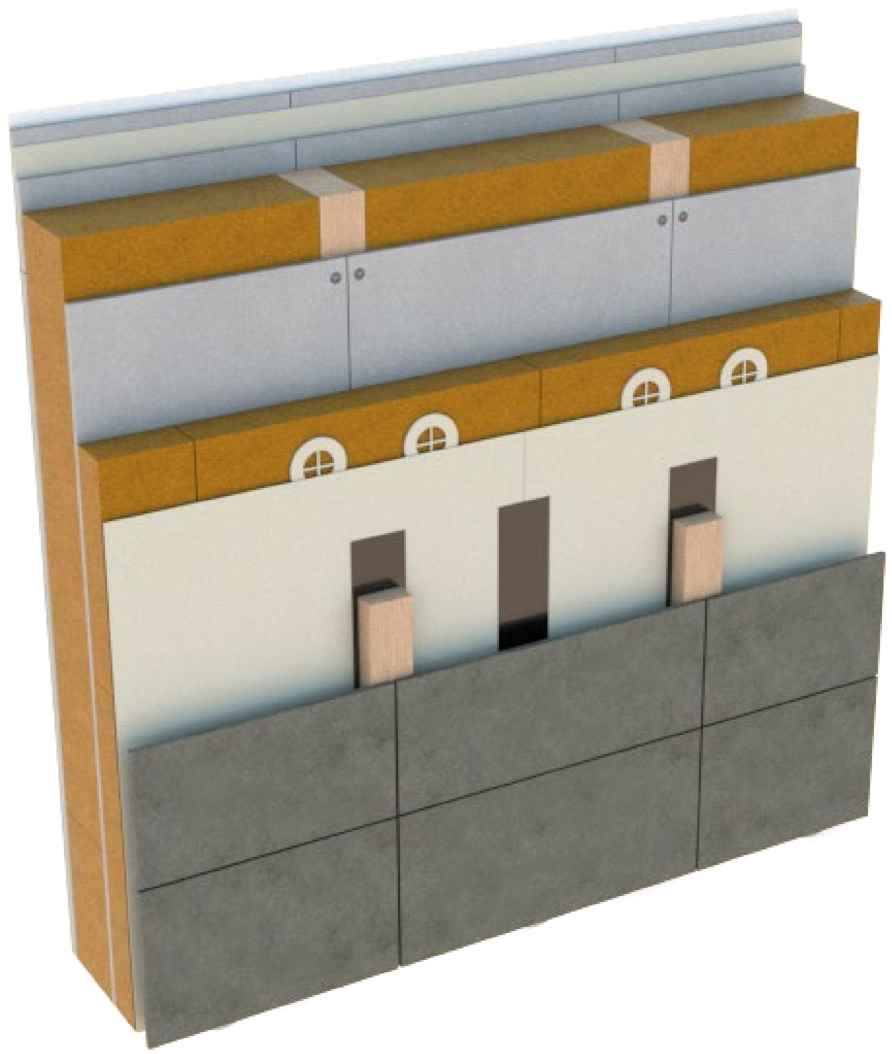

THE GREEN ROOF

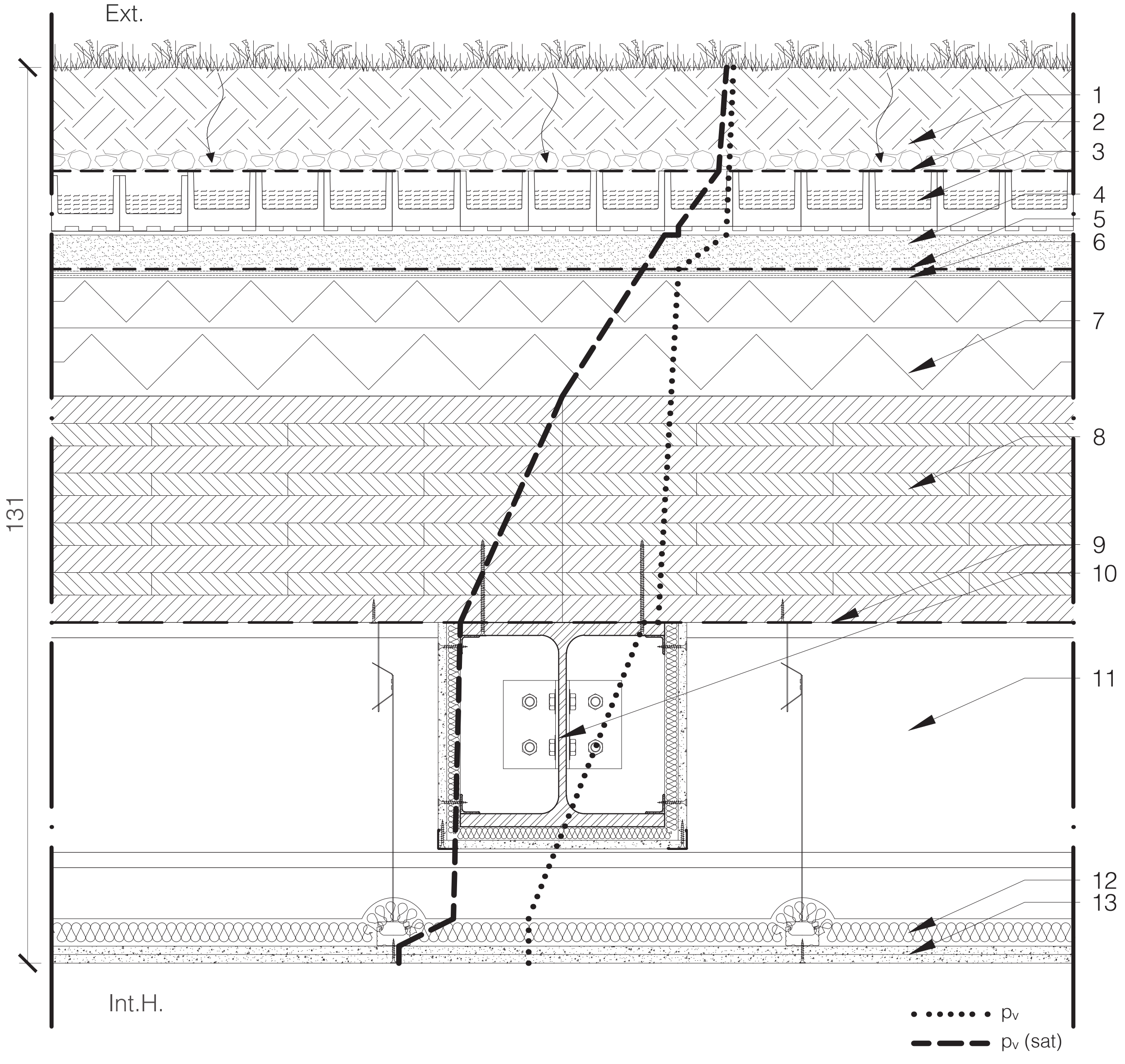

1	Filling gravel and soil for grass (th: 15 cm)
2	Anti root polypropylene-fiber tissue, (th: 0.4 cm)
3	Water collection polystyrene panels, 125x100cm, λ = 0.034 W/mK, (th: 8.2cm) (DiaDrain type) with mechanical protection membrane Armodillo Index in polyester
4	Dry assembled lightweight mortar screed Pavileca, density 400 kg/m^3, λ = 0.09 W/mK, (th: 5cm minimum), slope 1%
5	Adhesive waterproofing sheath Monoself FV 2 MM P (th: 0.2 cm)
6	OSB panel (th: 1.25 cm)
7	Wooden fiber insulation FiberThermBase 250, 135x60cm, λ = 0.040 W/mK, (th: 10 + 6 cm)
8	9-layer spruce wooden boards -XLAM- bearing slab, λ = 0.12 W/mK, (th: 33.2 cm)
9	Water vapour adhesive barrier Riwega DS 48 2200 TOP SK, density: 1100 kg/m^3, λ = 0.17 W/m^2K, (th: 0.3cm)
10	Secondary load bearing steel beam HEB 300
11	Primary load bearing steel beam HEB 360
12	Acoustic wooden fiber panel insulation, 140x60cm, density 70 kg/m^3, λ = 0.040 W/mK, (th: 5cm)
13	2 x Fermacell Gypsum fiberboard, density 1150 kg/m^3, λ = 0.32 W/mK, (th: 1.25 + 1.25cm)

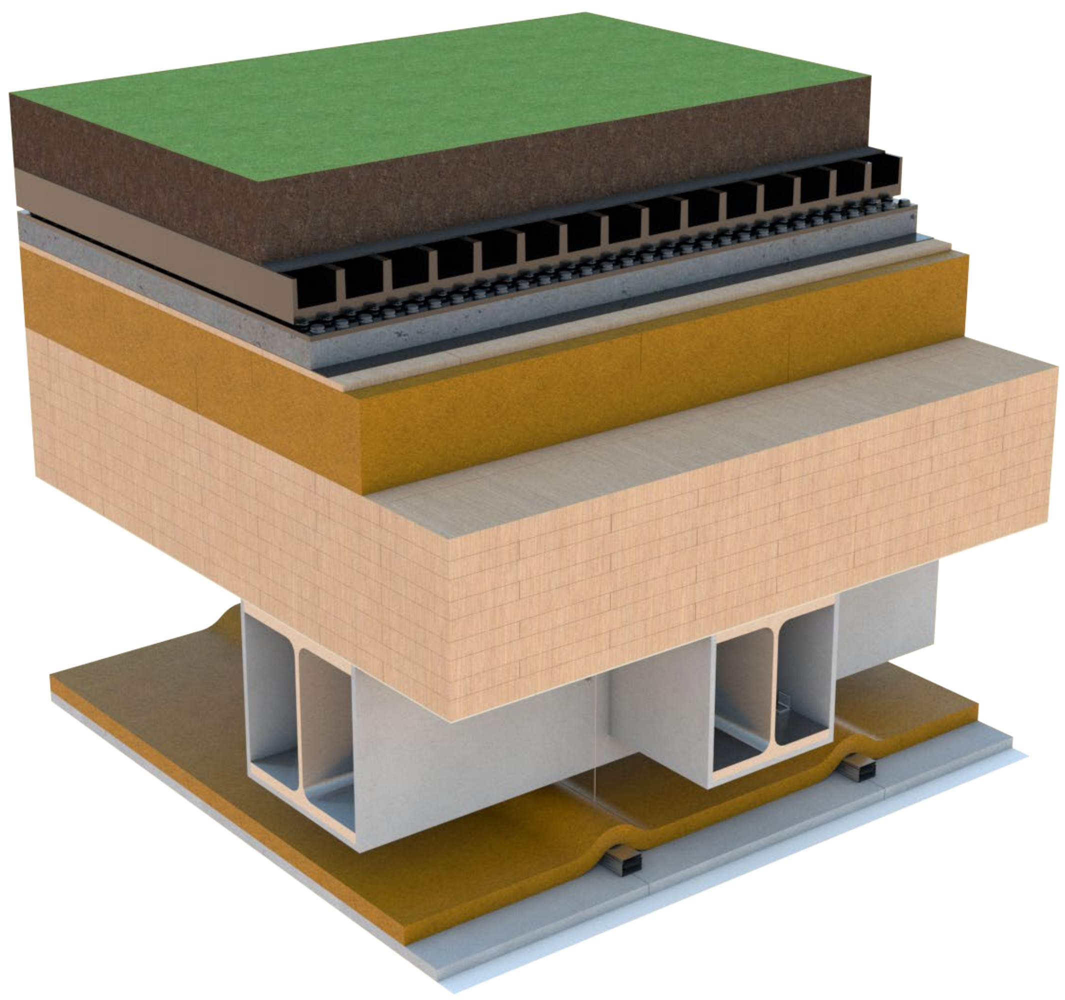

THE GROUND FLOOR SLAB

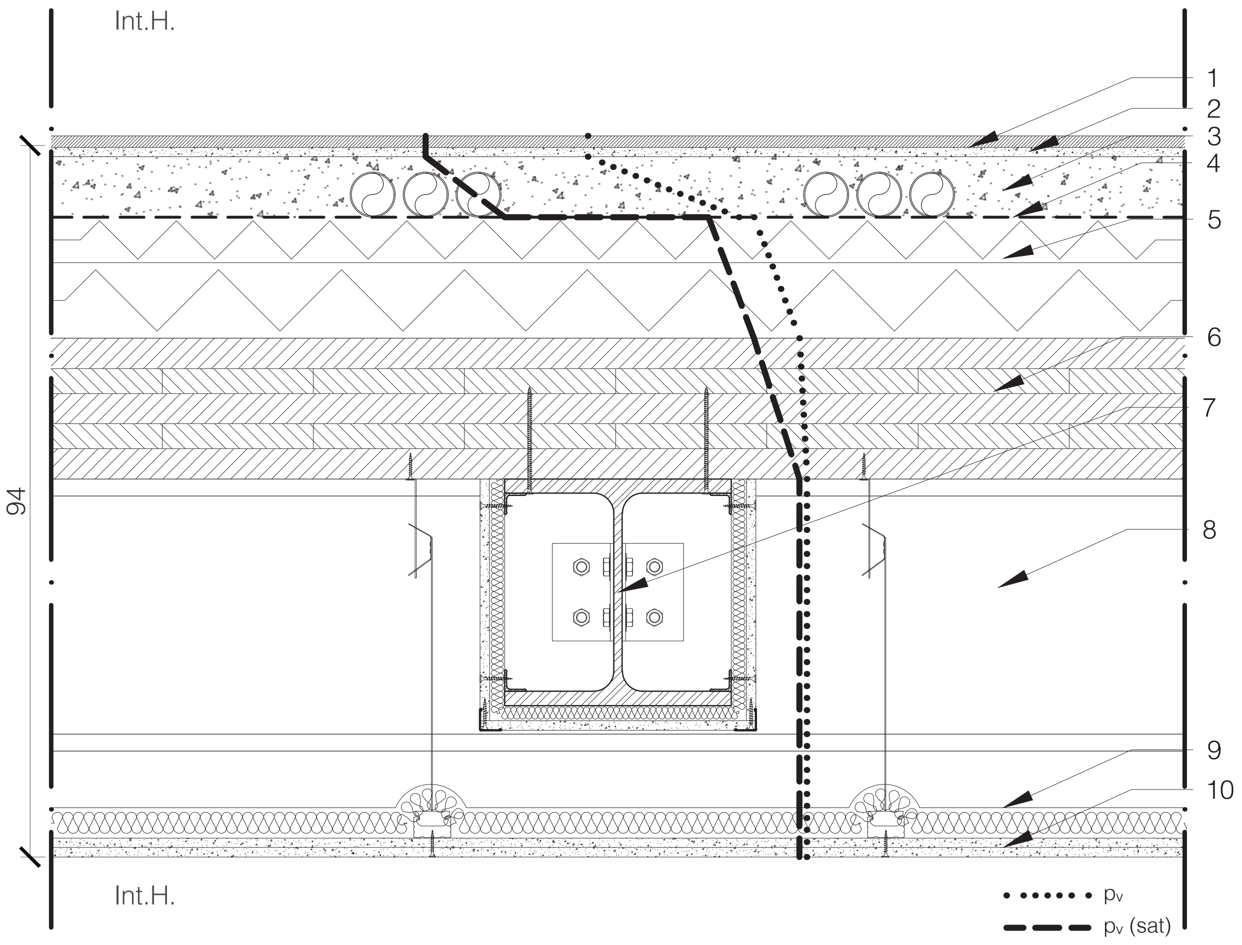

1	Porcelain stoneware tiles, 40x40cm, (th.1,5 cm), placed with a double-component adhesive, class S1, (th: 0.3 cm)
2	Fermacell Gypsum fiberboard, (th: 1.25 cm)
3	Facilities integration dry lightweight mortar screed Pavileca, density 400 kg/m^3, λ = 0.09 W/mK, (th: 8 cm)
4	Adhesive waterproofing sheath Monoseff FV 2 MM P (th: 0.2 cm)
5	Wooden fiber insulation FiberThermBase 250, 135x60cm, λ = 0.040 W/m^{2}K, (th: 10 + 6 cm)
6	5-layer spruce wooden boards -XLAM- bearing slab, λ = 0.12 W/mK, (th: 18.6 cm)
7	Secondary load bearing steel beam HEM 240
8	Primary load bearing steel beam HEM 280
9	Acoustic double glass wool panel insulation, 140x60cm, density 70kg/m^3, λ = 0.038 W/mK, (th: 5cm)
10	2 x Fermacell Gypsum fiberboard, (th: 1.25+1.25cm)

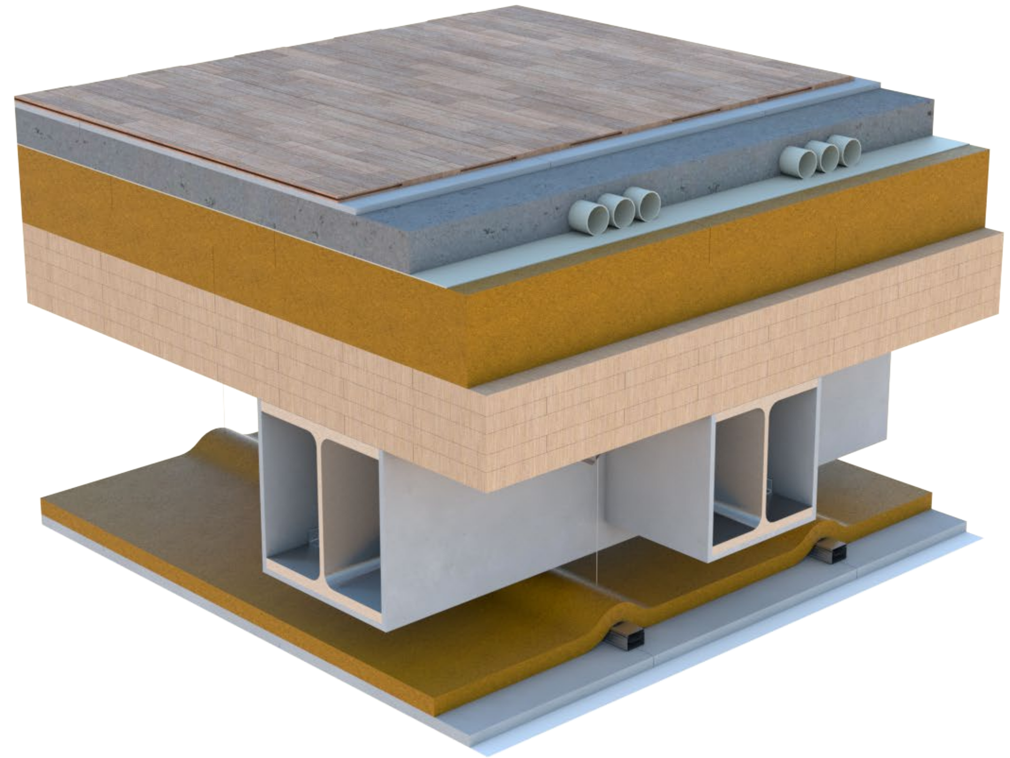

THE INTERMEDIATE SLAB

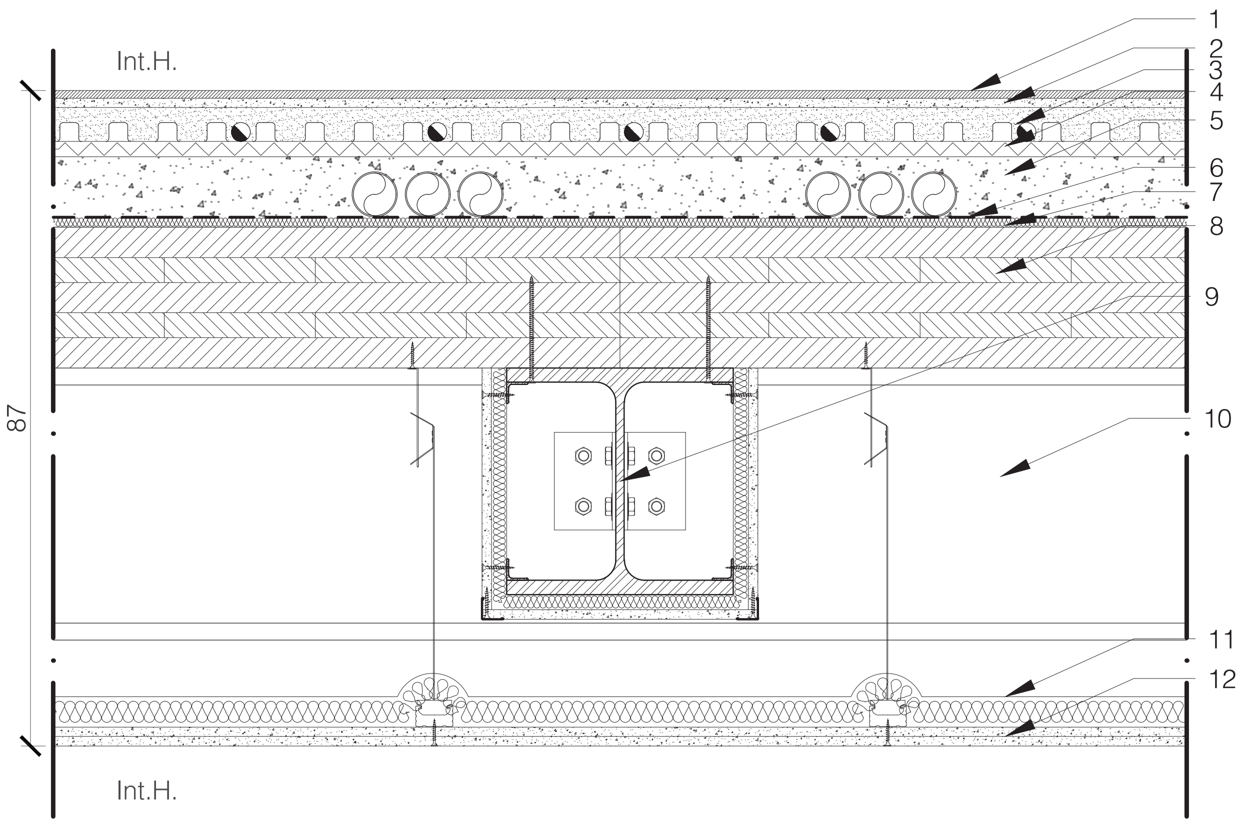

1	Wooden tiles finishing (th: 1 cm)
2	Fermacell Gypsum fiberboard, (th: 1.25 cm)
3	Heat-sealing mortar screed, density: 1500 kg/m^3; prefab radiant heating panels in polystyrene, 120x60cm (th: 4.5cm)
4	Polystyrene panel with metallic thermo-conduction sheet, λ = 0.032 W/m2K (th: 2cm)
5	Facilities integration dry lightweight mortar screed Pavileca, density 400 kg/m^3, λ = 0.09 W/mK, (th: 8 cm)
6	Adhesive waterproofing sheath Monoself FV 2 MM P (th: 0.2 cm)
7	Clomping insulation rubber and bitumen paper panel, 100x100cm, density 700kg/m^3, λ = 0.033 W/mK, (th. 1.3cm)
8	5-layer spruce wooden boards -XLAM- bearing slab, λ = 0.12 W/mK, (th: 18.6 cm)
9	Secondary load bearing steel beam HEB 300
10	Primary load bearing steel beam HEB 360
11	Acoustic wooden fiber panel insulation, 140x60cm, density 70 kg/m^3, λ = 0.040 W/mK, (th: 5cm)
12	2 x Fermacell Gypsum fiberboard, (th: 1.25 + 1.25cm)

Politecnico di Milano, Master of Science in Building and Architectural Engineering
Steember - Steel and timber for a high rise building in Queens, New York
Chinnici Federico - **Maranesi** Marco

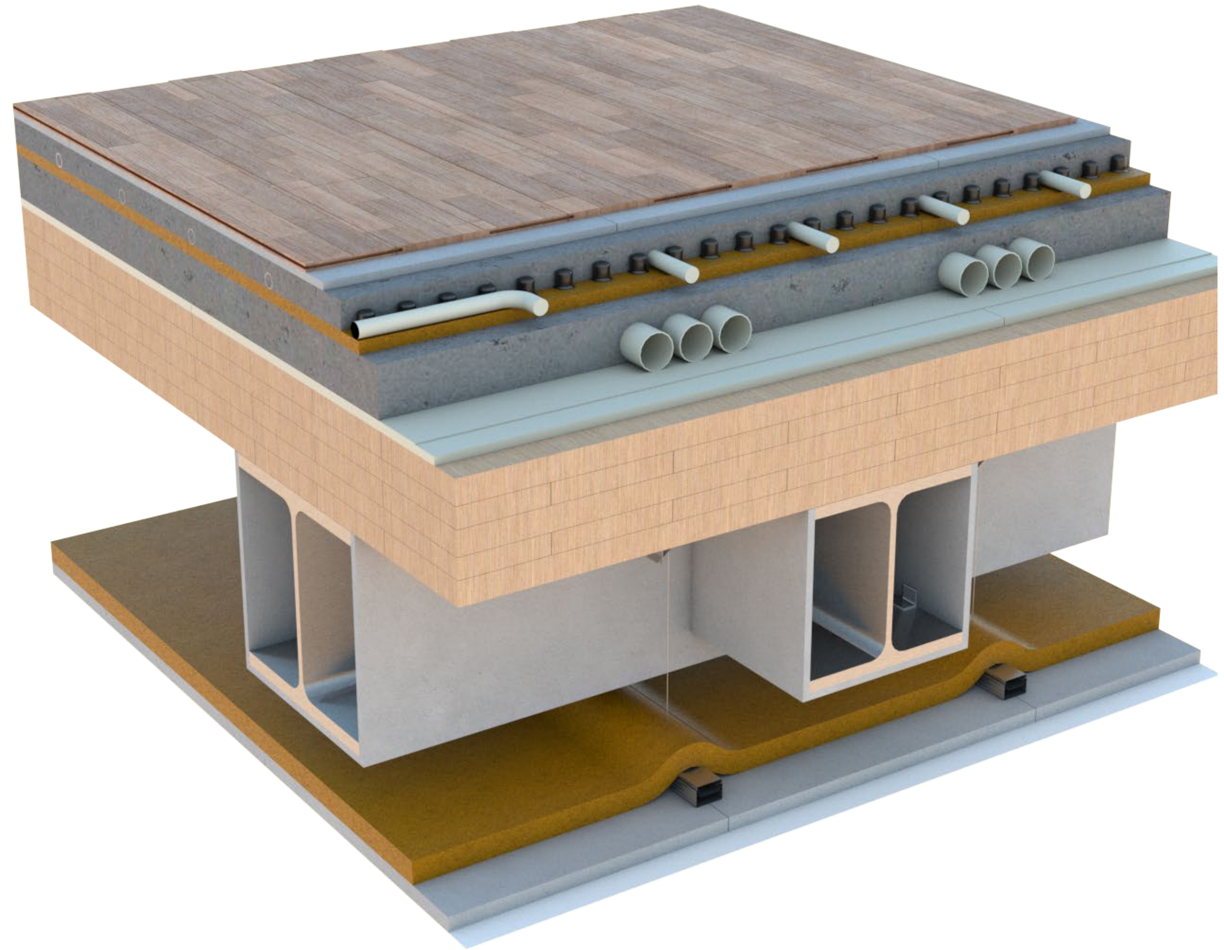

THE INTERNAL PARTITION

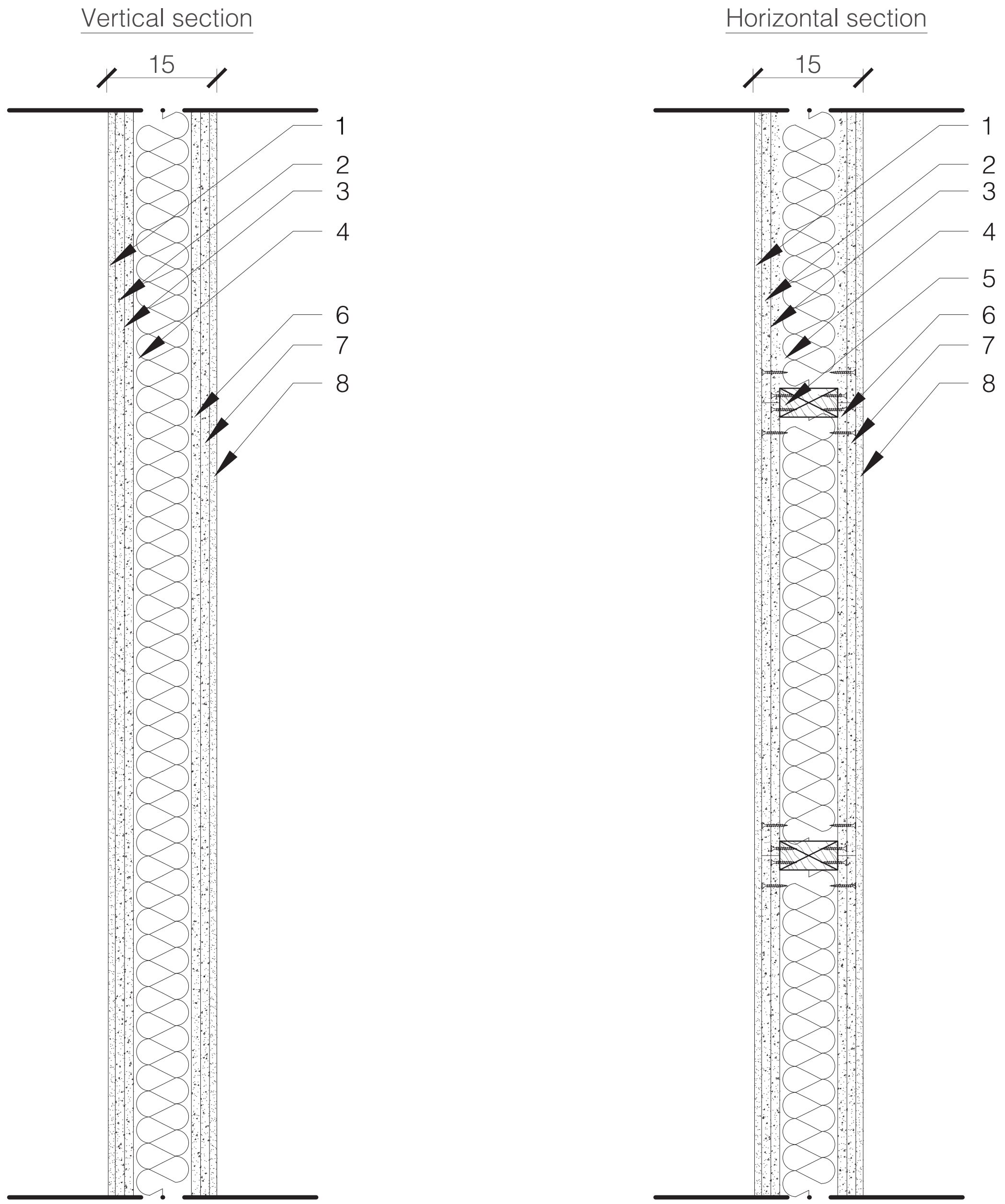

1	Internal finish in painted gypsum plaster (th: 1 cm)
2	Fermacell Gypsum fiberboard, (th: 1.25 cm)
3	Fermacell Gypsum fiberboard, (th: 1.25 cm)
4	Blown cellulose Climacell S, density 55 kg/m^3, λ = 0.038 W/m^{2}K (th: 8 cm)
5	Laminated spruce wood beam, structure of the frame wall, 8x4 cm (th: 8 cm)
6	Fermacell Gypsum fiberboard, (th: 1.25 cm)
7	Fermacell Gypsum fiberboard, (th: 1.25 cm)
8	Internal finish in painted gypsum plaster (th: 1 cm)

THE BALCONY

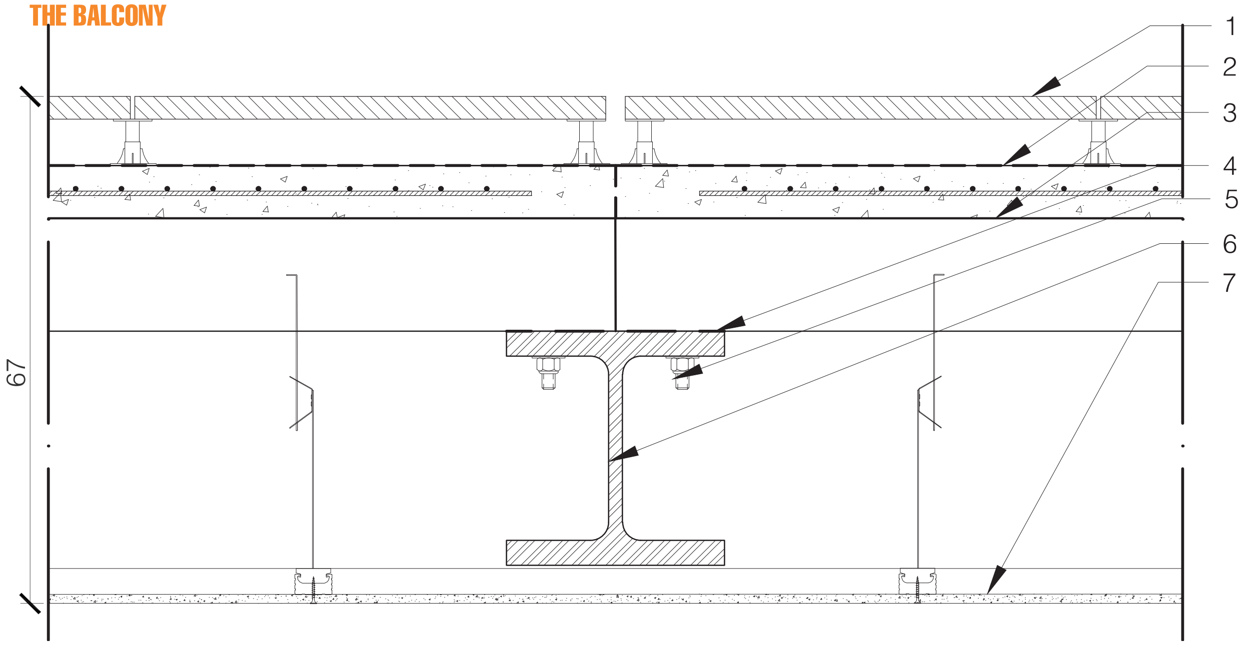

1	External floating floor pavement, 6 cm cavity (th: 9 cm)
2	Adhesive waterproofing sheath Monoself FV 2 MM P (th: 0.2 cm)
3	Prefab. slab: lightweight concrete pre-cast in a metal sheet being a disposable formwork, slope 1% SAND150 corrugated load bearing sheet, h = 15 cm (th: 1,5 mm) Lightweight concrete with electro-welded mesh (th: 6 cm)
4	Neoprene waterproofing and vibration pad between steel beam and concrete
5	Bolt drowned in concrete casting for the anchoring of the slab to the steel beam
6	Steel cantilever beam HE 280 M
7	Outdoor Aquapanel board for countertop (th: 1,25 cm)

THE OUTDOOR CARRIAGEABLE SLAB

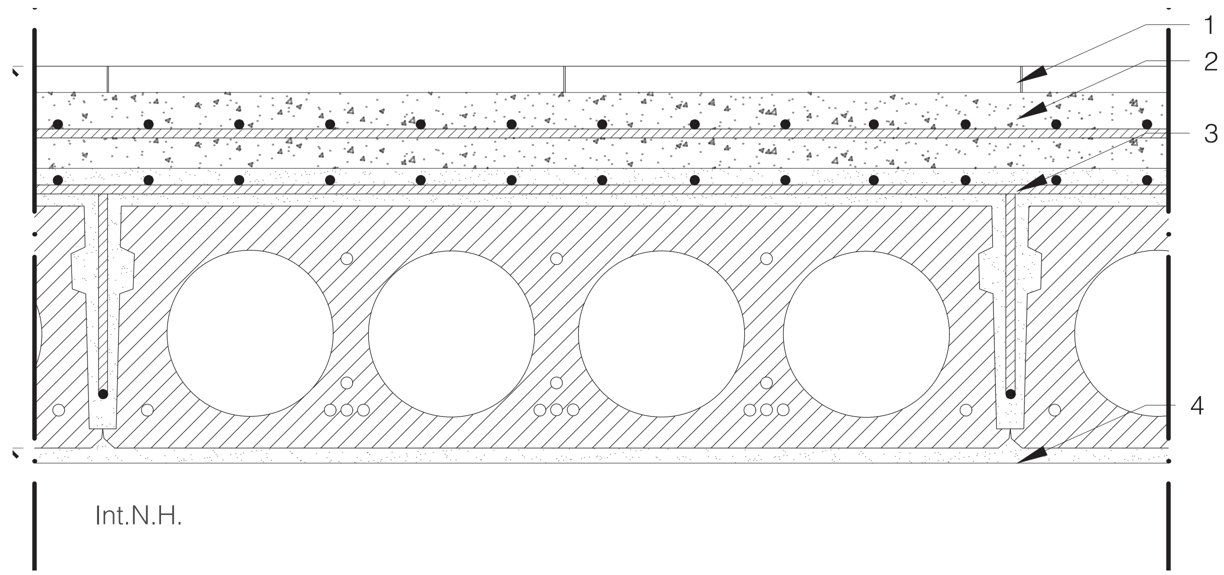

1	External stone tiles, (th.3 cm)
2	Double collaborating cast concrete with electro-welded mesh, Φ12, (th: 15 cm)
3	Hollow core prefabricated concrete slab IMAFOR H320, weight: 408 kg/m^2 (th: 32 cm)
4	Fire protection mortar made by gypsum, concrete and vermiculite KF4 Fassa Bortolo (th: 0.2 cm)

7.3 – THE TECHNOLOGICAL JOINTS

VERTICAL JOINT - INTERMEDIATE SLAB + EXTERNAL WALL

SCALE 1:10

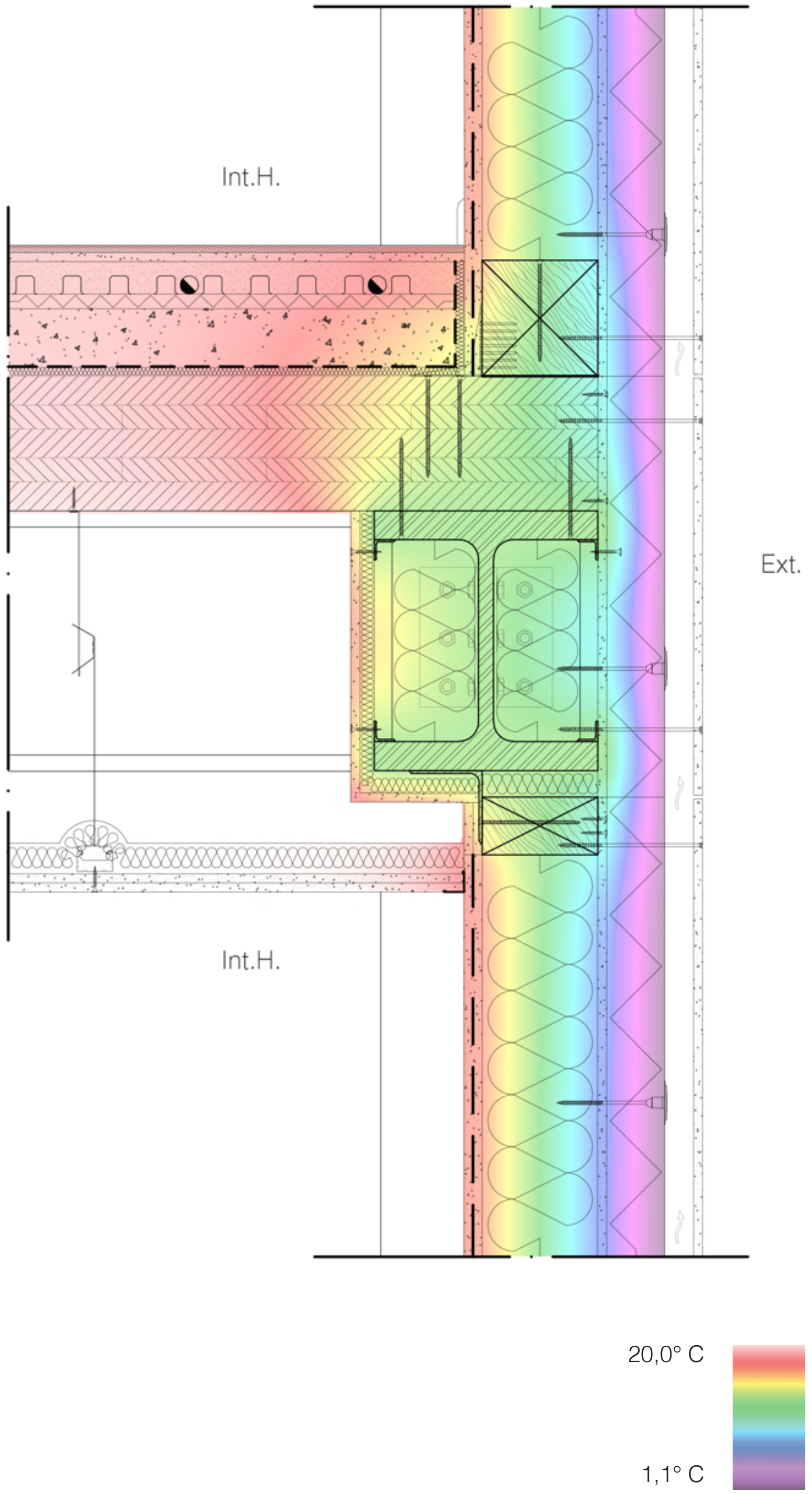

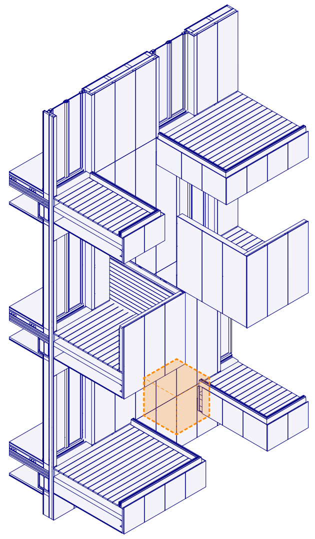

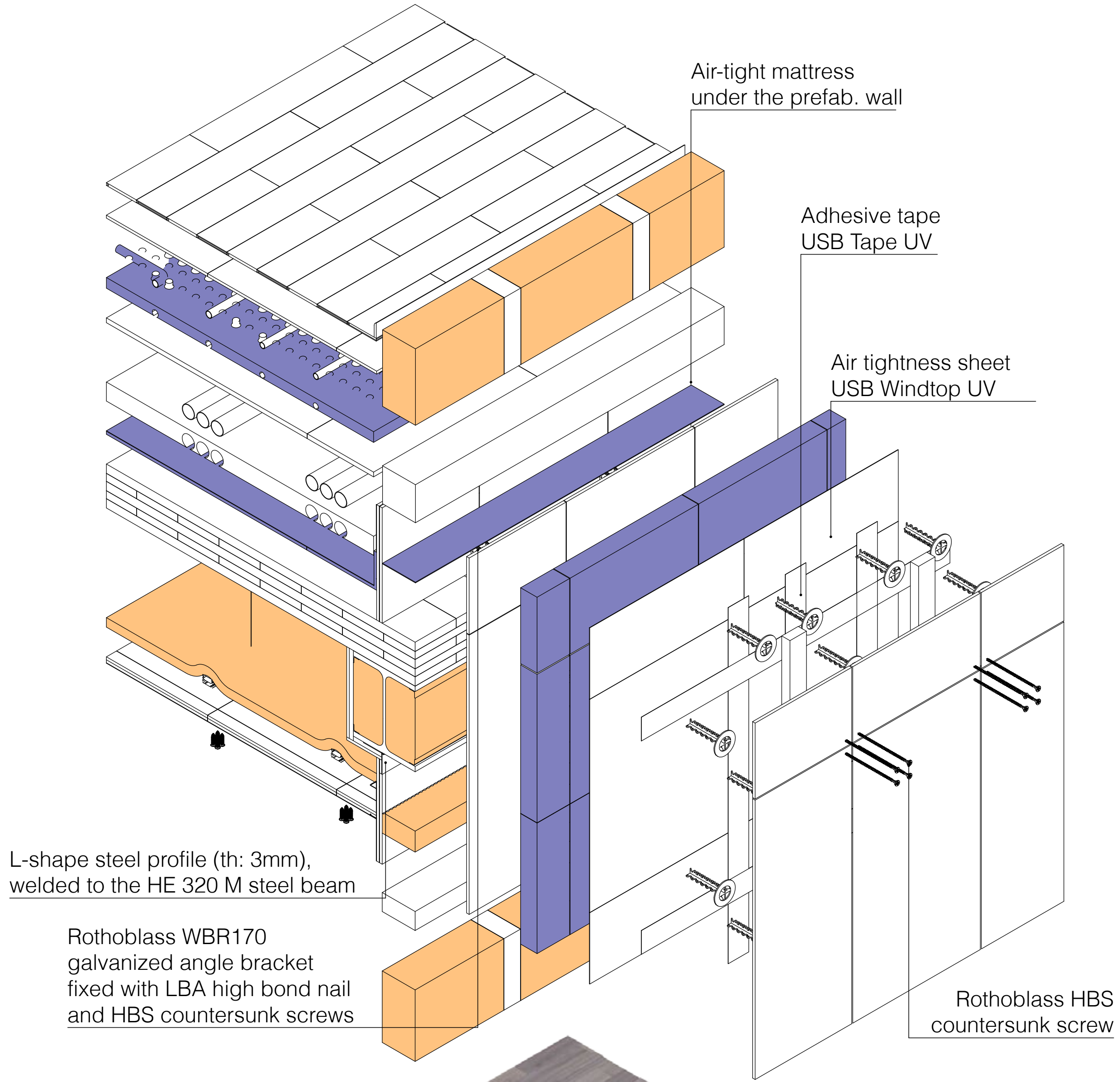

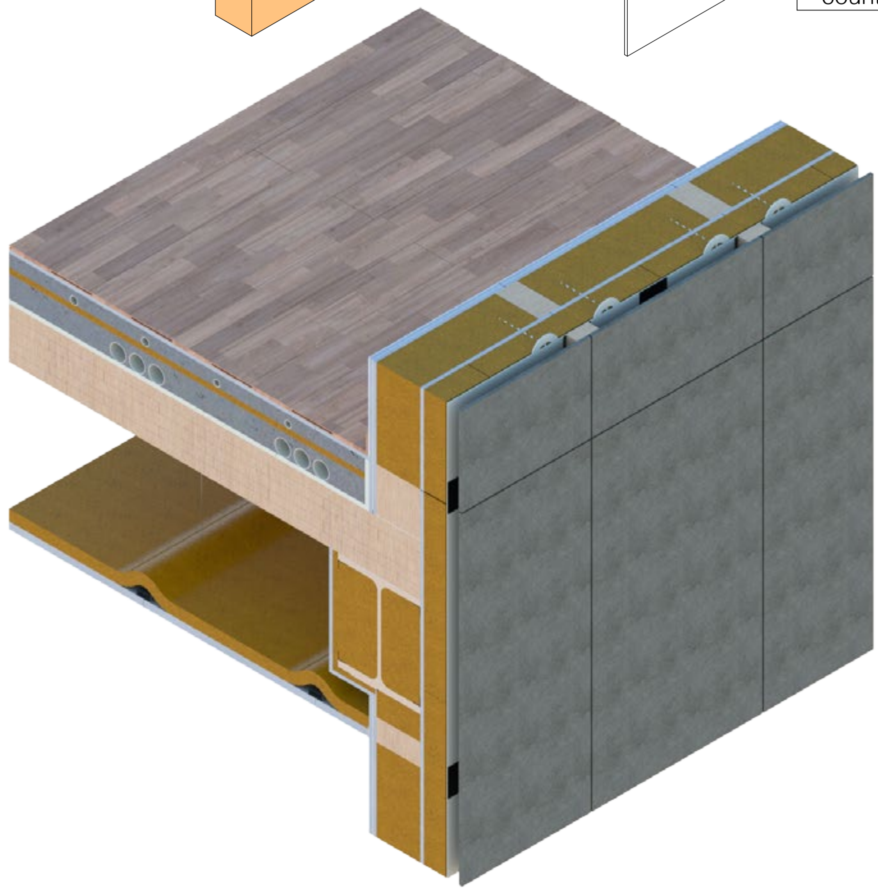

VERTICAL JOINT - INTERMEDIATE SLAB + EXTERNAL WALL + WINDOW

SCALE 1:10

The external prefabricated wall has already windows installed.
In this way, since the assembly of the windows is completed in the laboratory, there is no risk of having weak points from the point of view of thermal bridges or interstitial condensation on the window's perimeter.

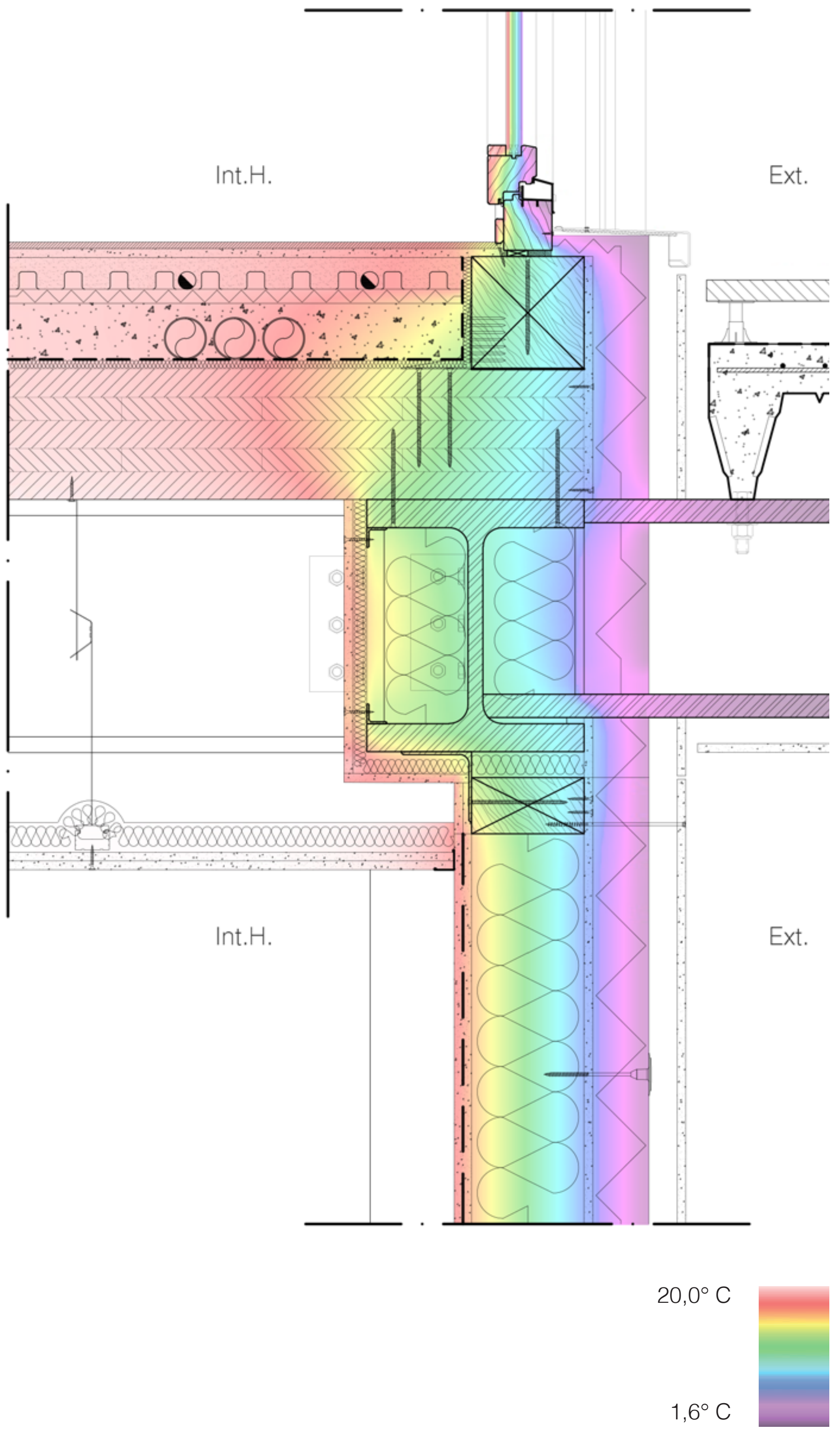

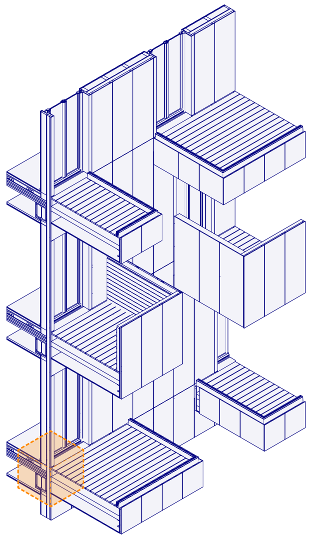

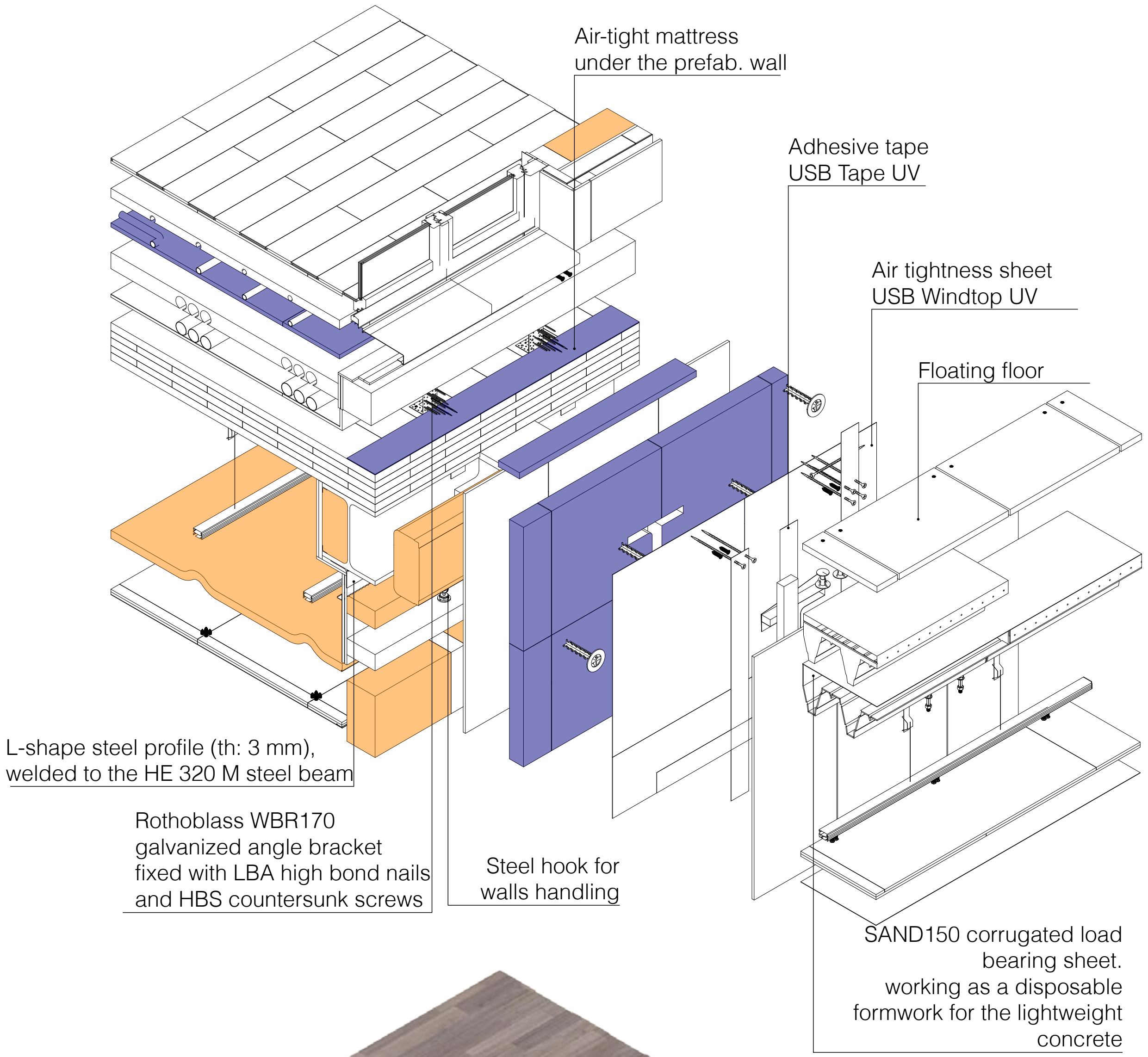

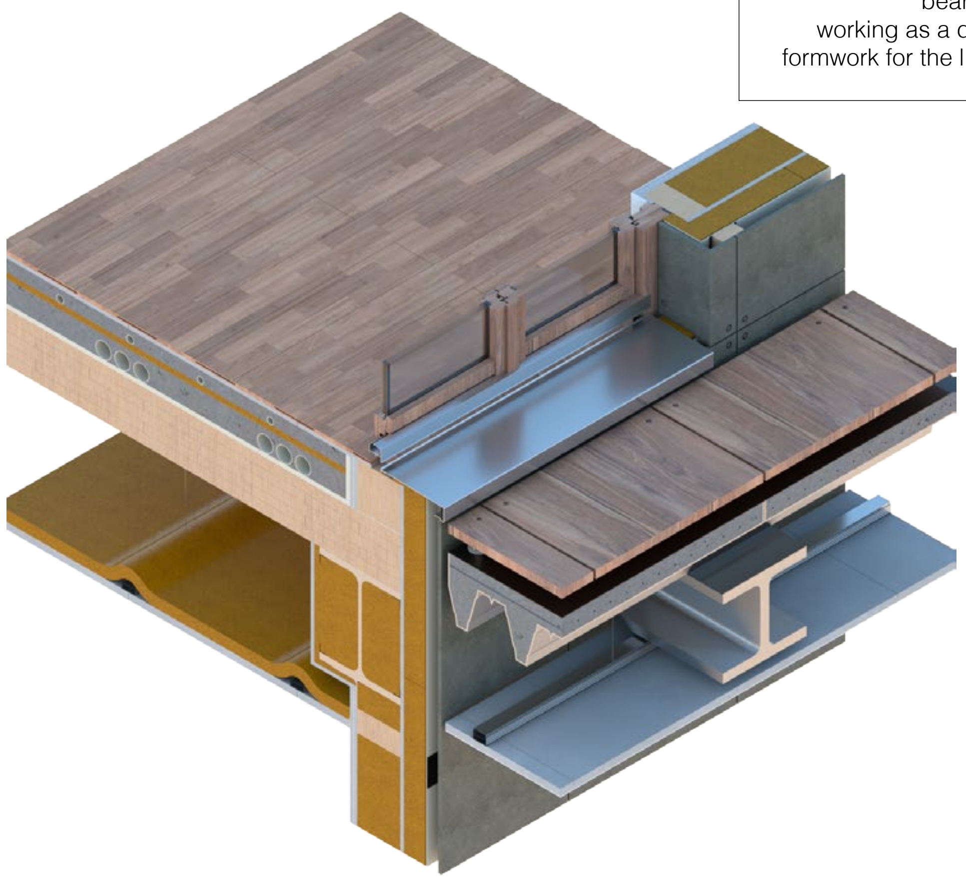

HORIZONTAL JOINT - COLUMN + EXTERNAL WALL

SCALE 1:10

The gap between the end of the prefab. wall and the steel pillar is filled with insulation and then sealed with gypsum fibre boards.
Externally, boards and external insulation are fixed to the pillar in order to ontinue the external insulation layer before applying the cladding.

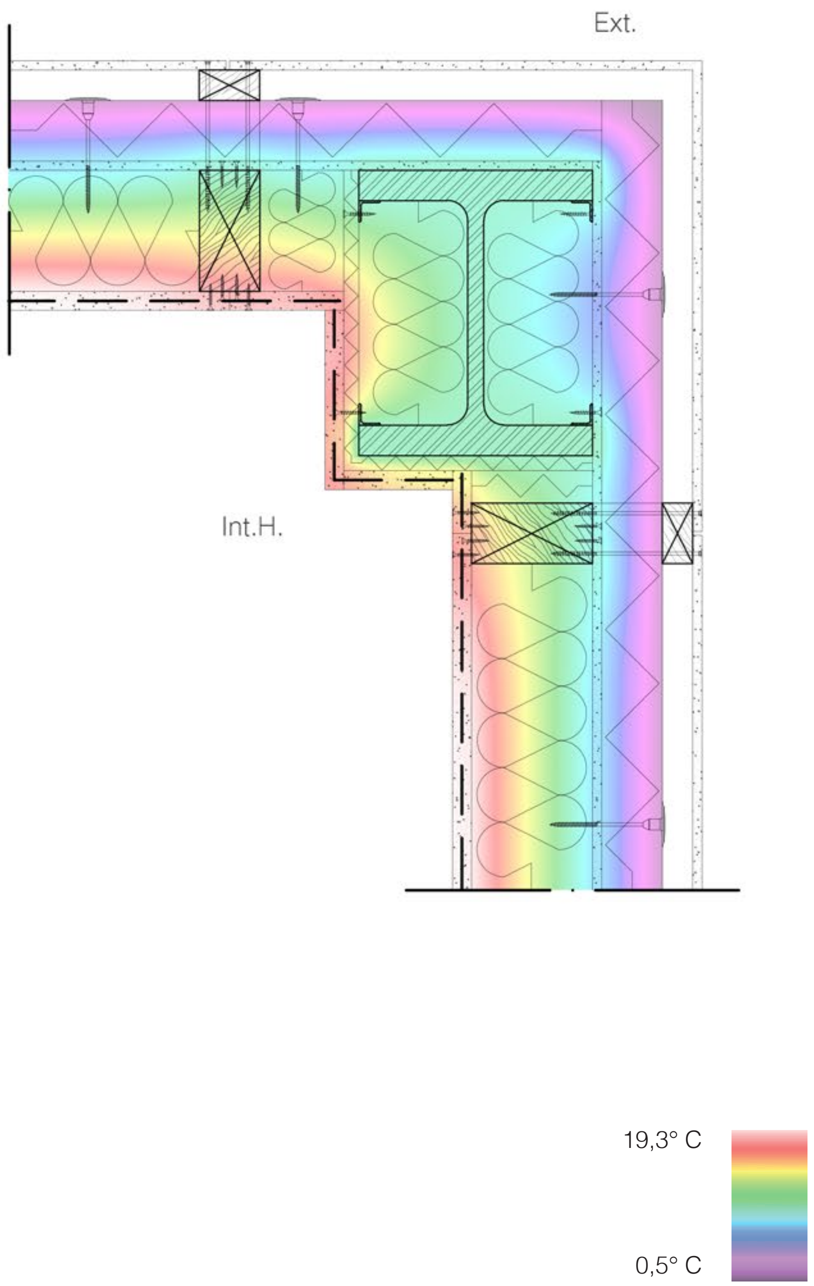

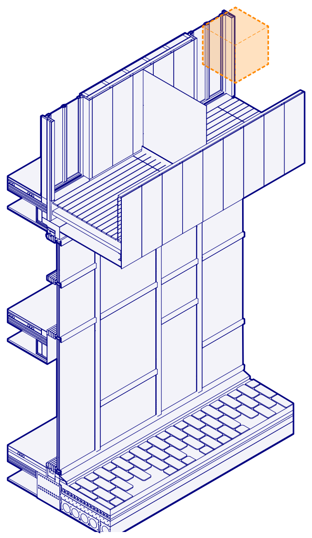

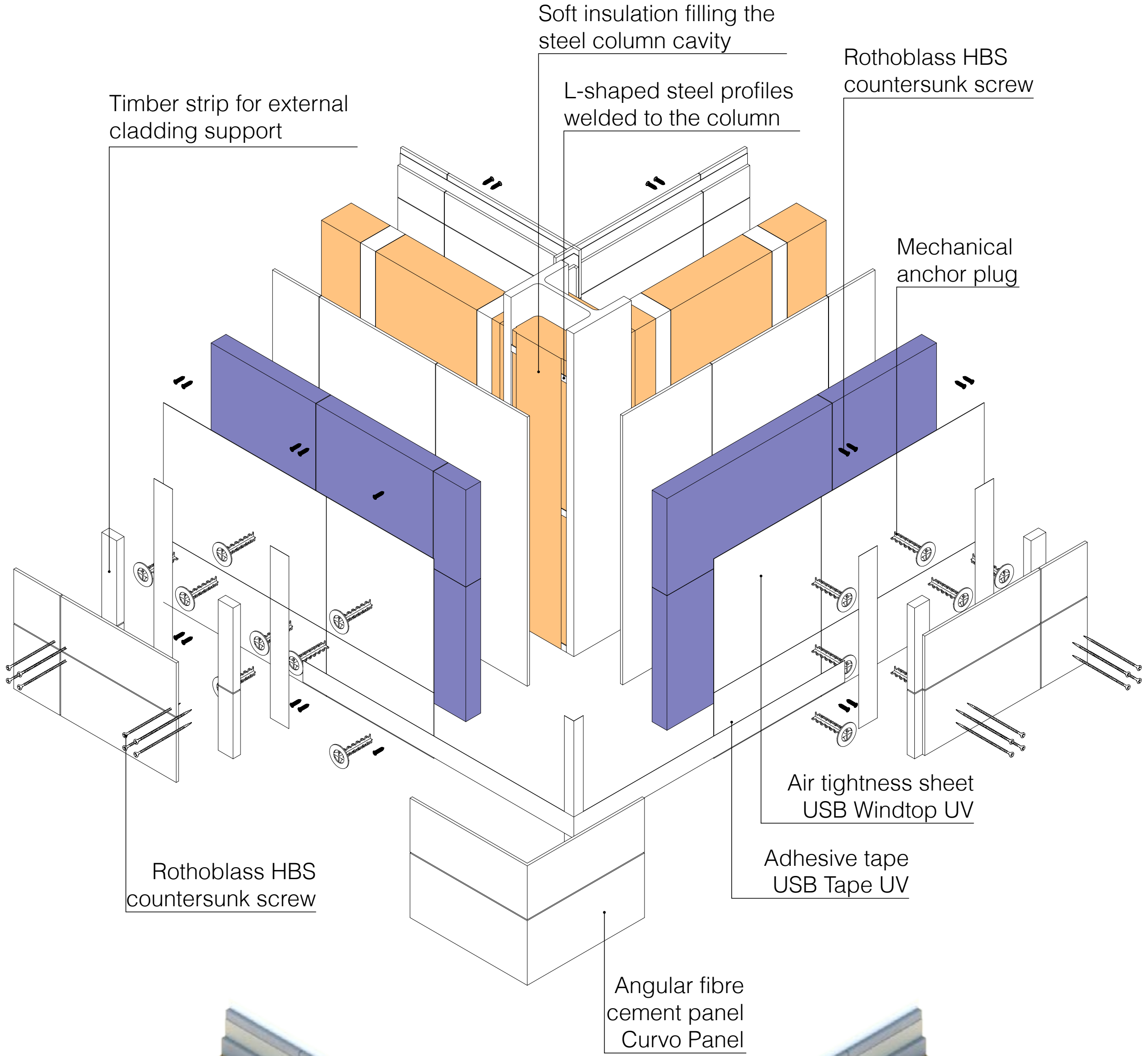

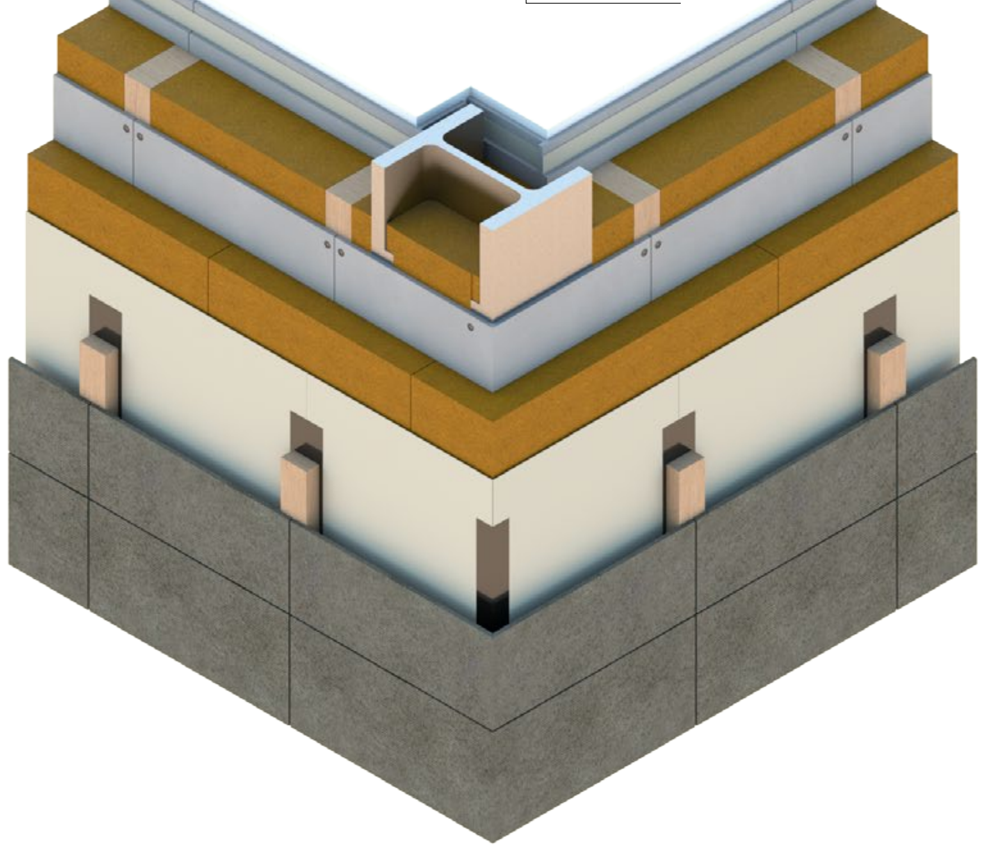

HORIZONTAL JOINT - COLUMN + EXTERNAL WALL + CURTAIN WALL

SCALE 1:10

In this case, since the curtain wall is kept on the external side of the pillar for architectural reasons, there is an external cavity which needs to be made rigid. For this purpose a timber I-joist is used, so that the mullion of the curtain wall can be horizontally fixed to it. The structural function of bearing the load of the curtain wall, though, is performed by a steel plate which is welded to the upper floor's border beam.
Finally, for thermal and acoustic reasons, the cavity is filled with soft insulation.

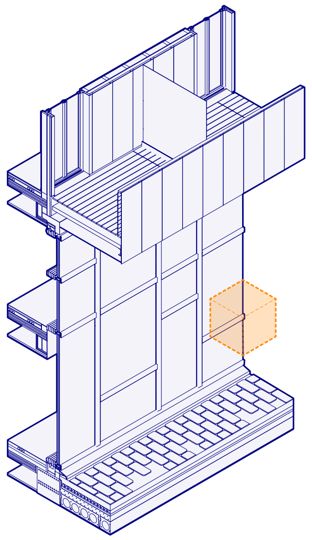

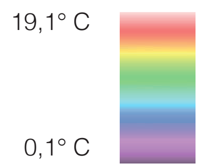

Politecnico di Milano, Master of Science in Building and Architectural Engineering
Steember - Steel and timber for a high rise building in Queens, New York
Chinnici Federico - **Maranesi** Marco

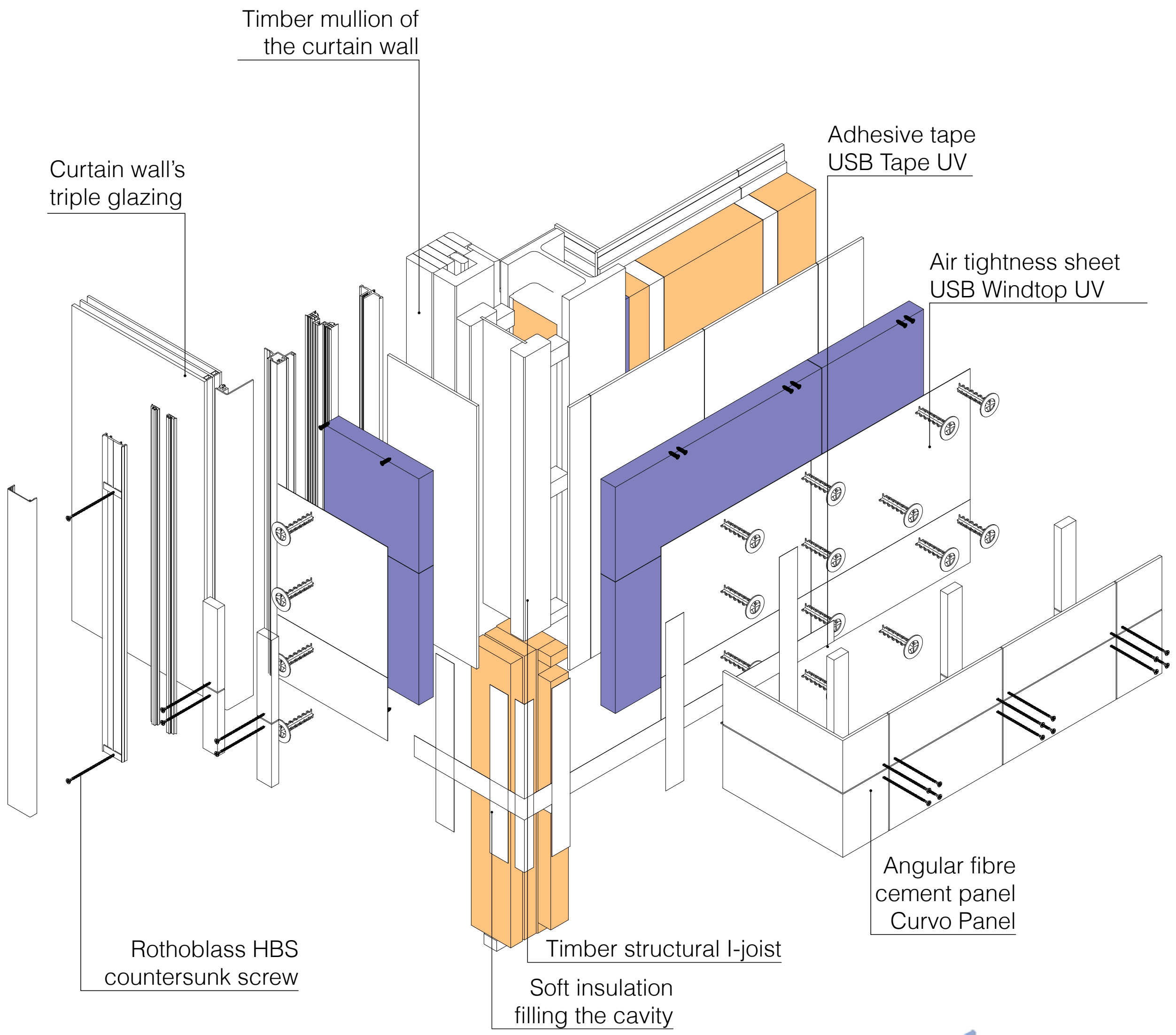

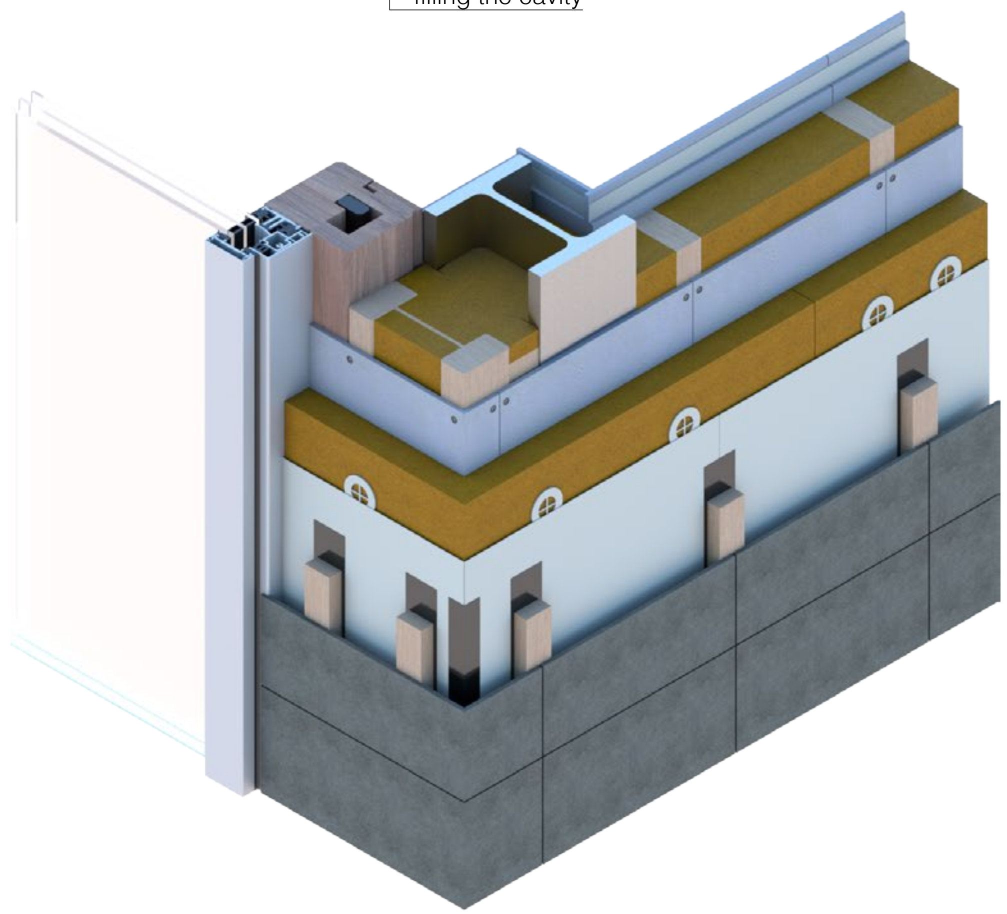

HORIZONTAL JOINT - EXTERNAL WALL + WINDOW

SCALE 1:10

The windows, as previously said, are completely installed in the wall in the prefabrication phase in laboratory. This allows workers to be more careful when placing every material and every element, decreasing a lot the risk of problems and mistakes.
In this way, the thermal insulation and the waterproofing can be better positioned, avoiding the risk of having interstitial condensation or mold in critical points such as the window outline.

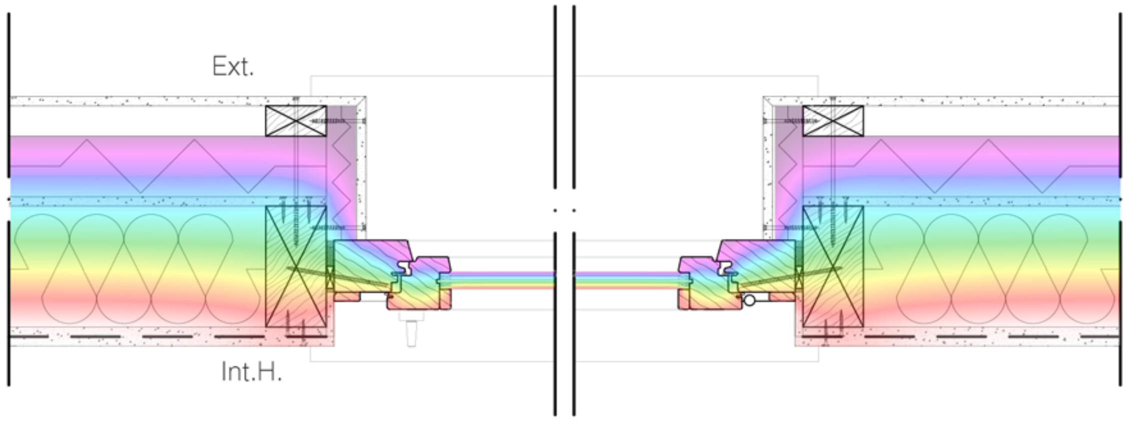

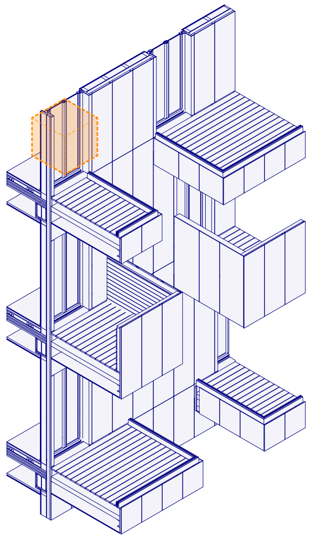

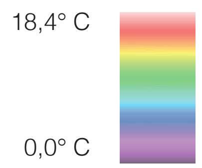

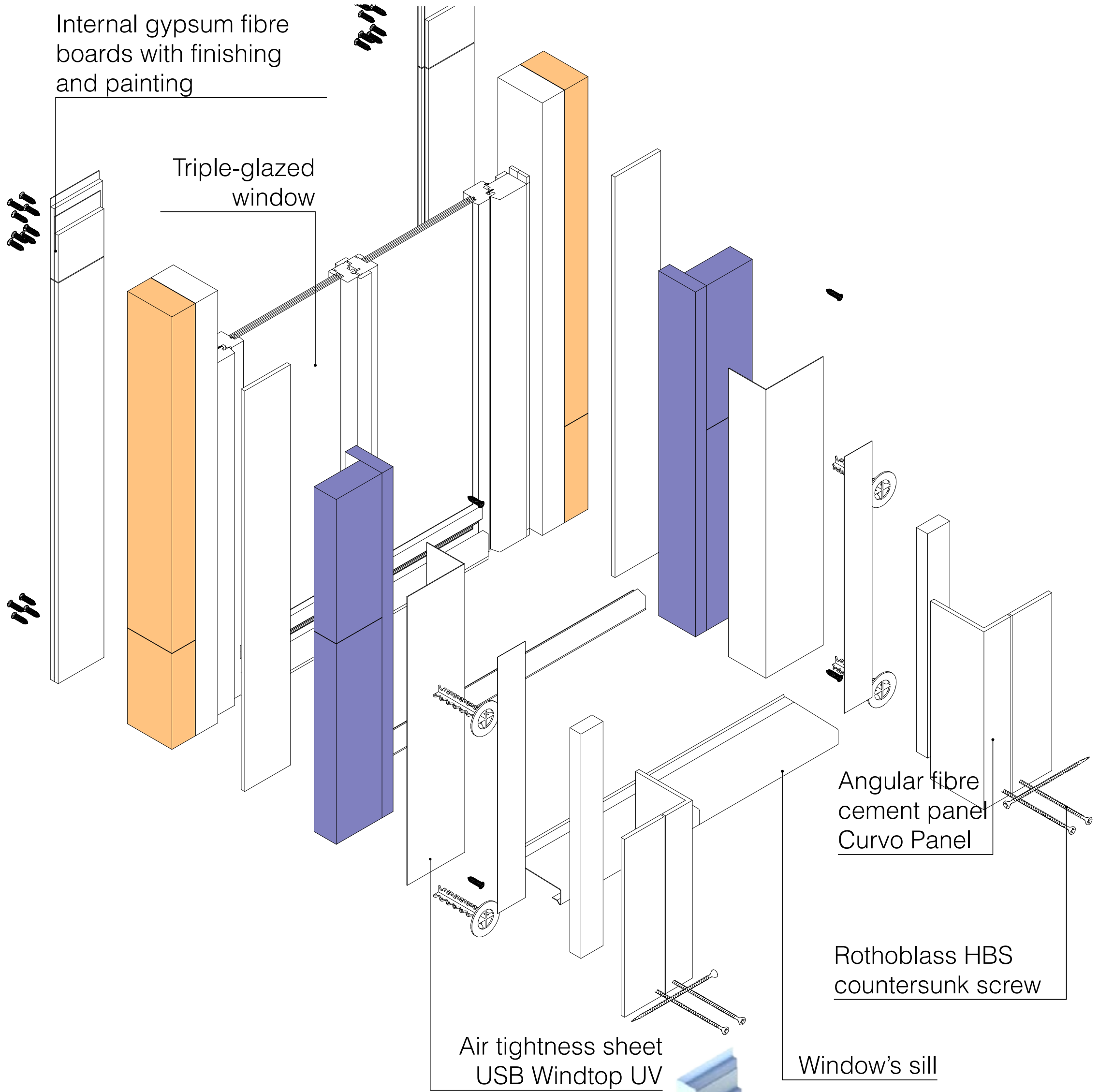

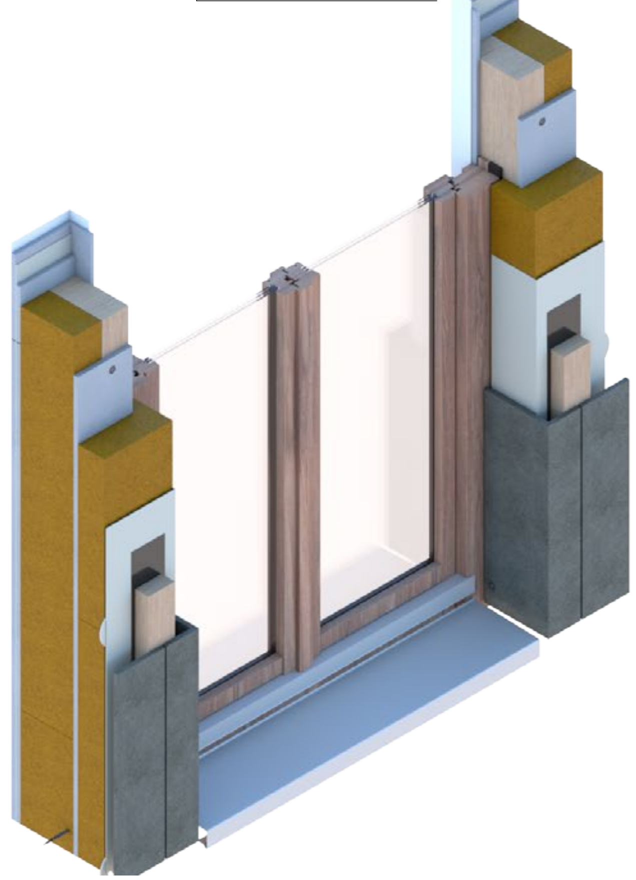

VERTICAL JOINT - INTERMEDIATE SLAB + EXTERNAL WALL WITH TWO WINDOWS + BALCONY

SCALE 1:10

Superiorly, the upper timber beam of the wall is anchored to an L shape steel profile using self/drilling screws even over a window. Under this beam there is the rolling-shutter box, which is completely insulated.

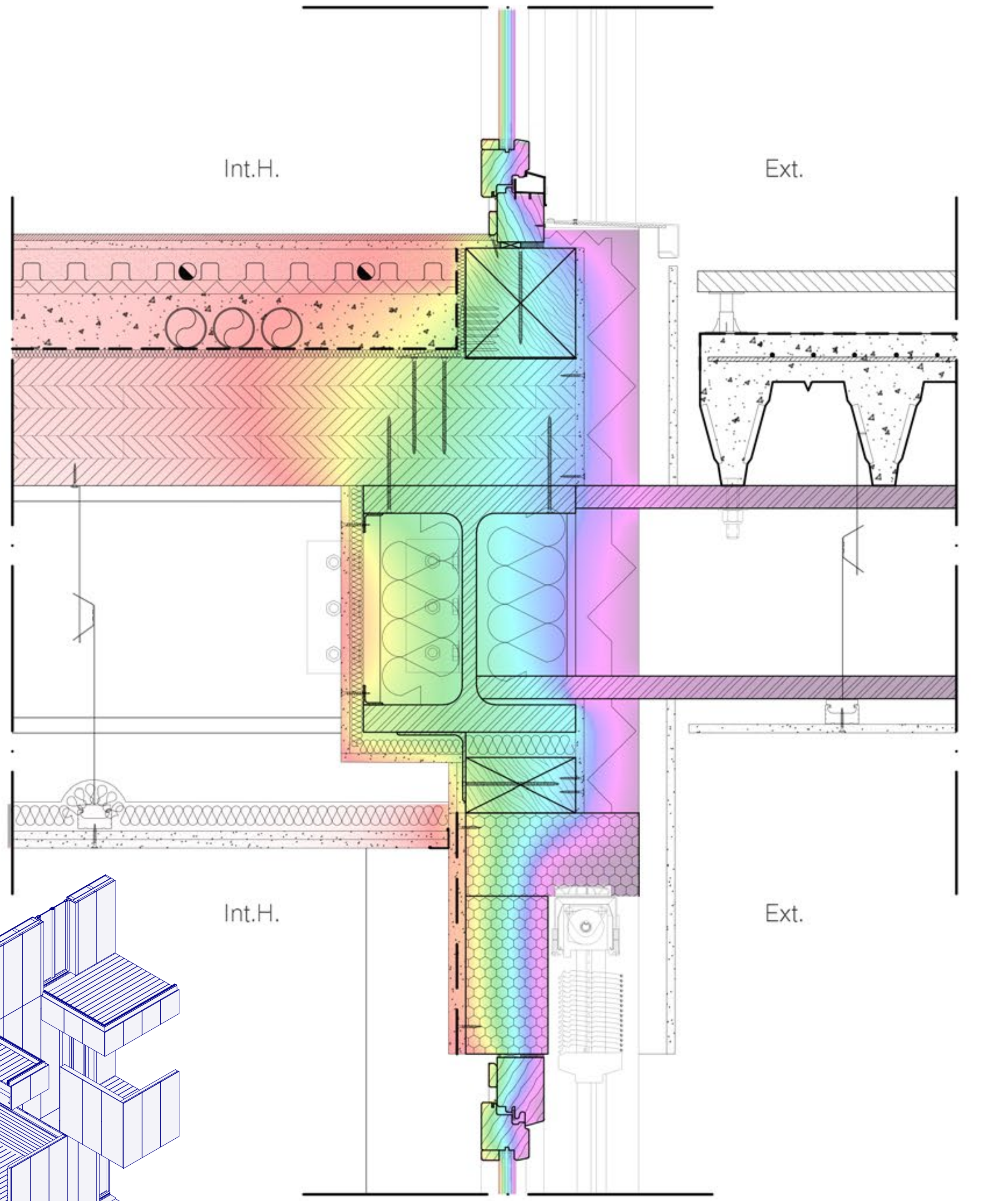

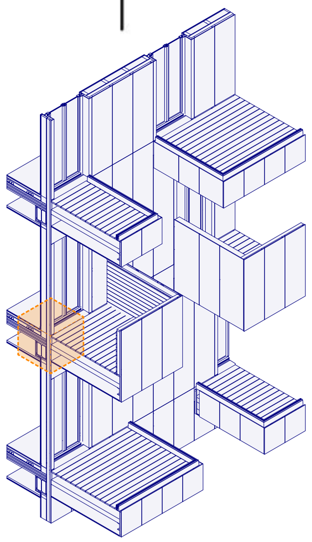

Politecnico di Milano, Master of Science in Building and Architectural Engineering
Steember - Steel and timber for a high rise building in Queens, New York
Chinnici Federico - **Maranesi** Marco

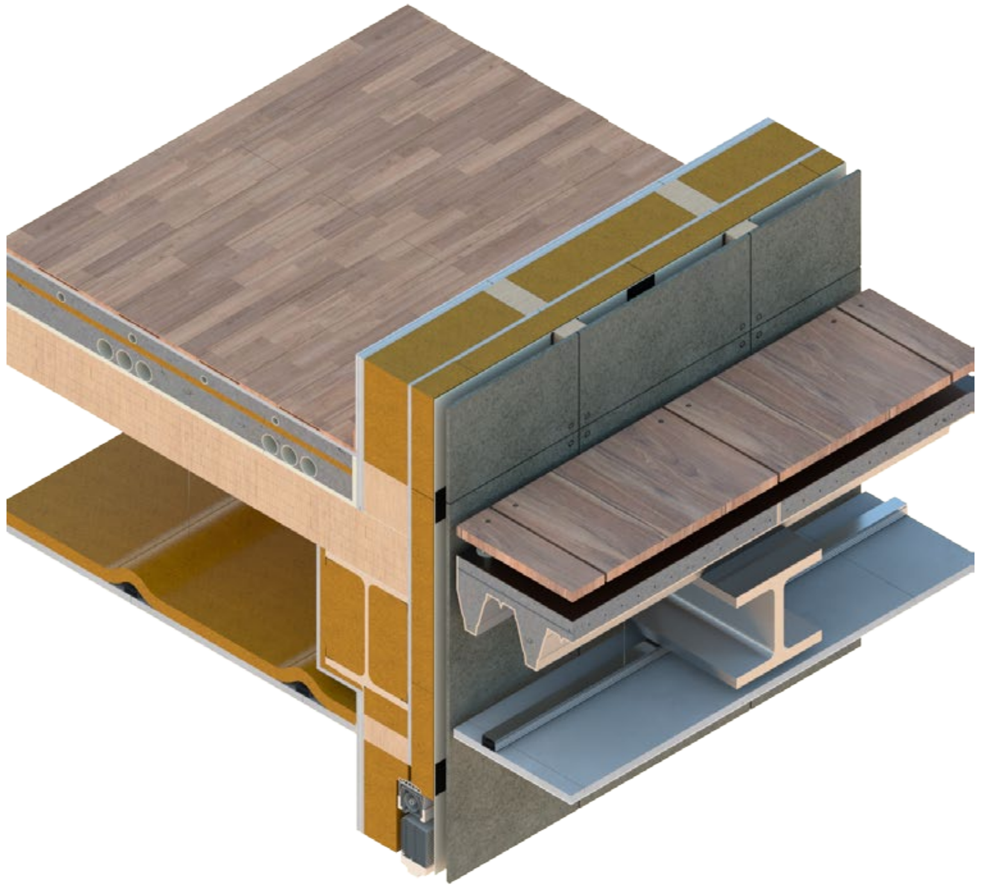

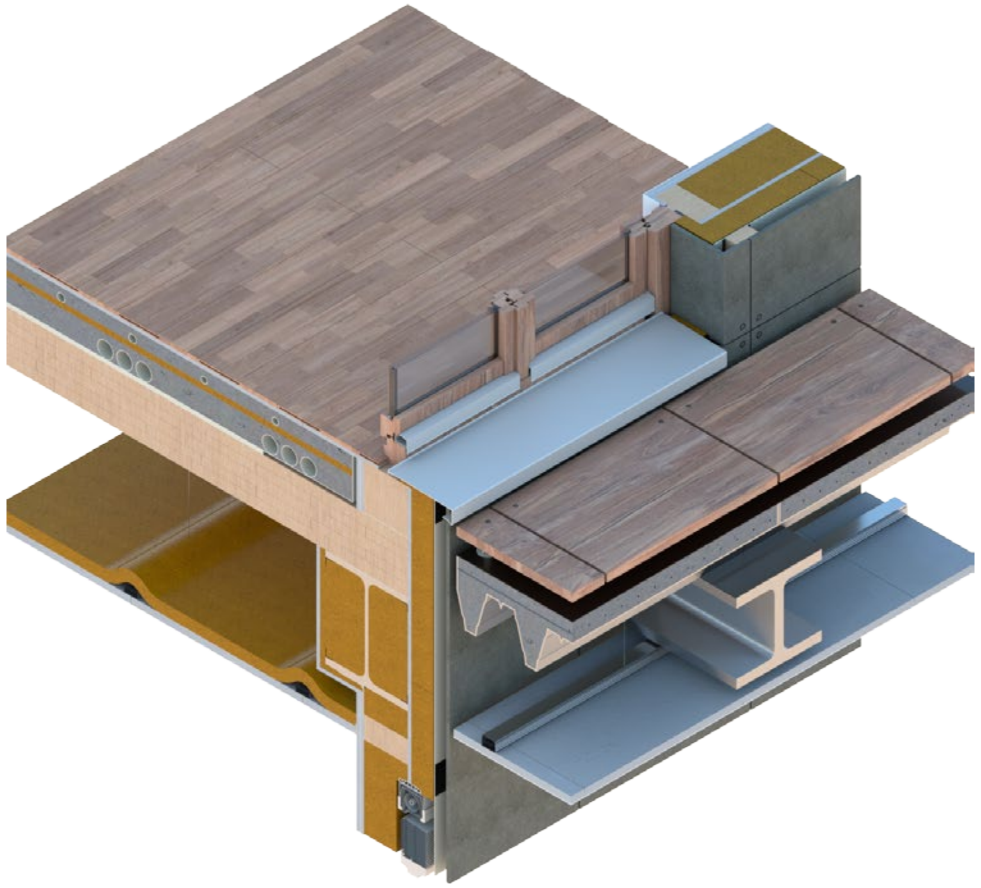

VERTICAL JOINT - GREEN ROOF + BALCONY

SCALE 1:10

On the rooftop the prefabricated wall and the balcony are fixed in the same way than on the other slabs. In this case the balcony is not accessible to residents but it is just present for architectural reasons.

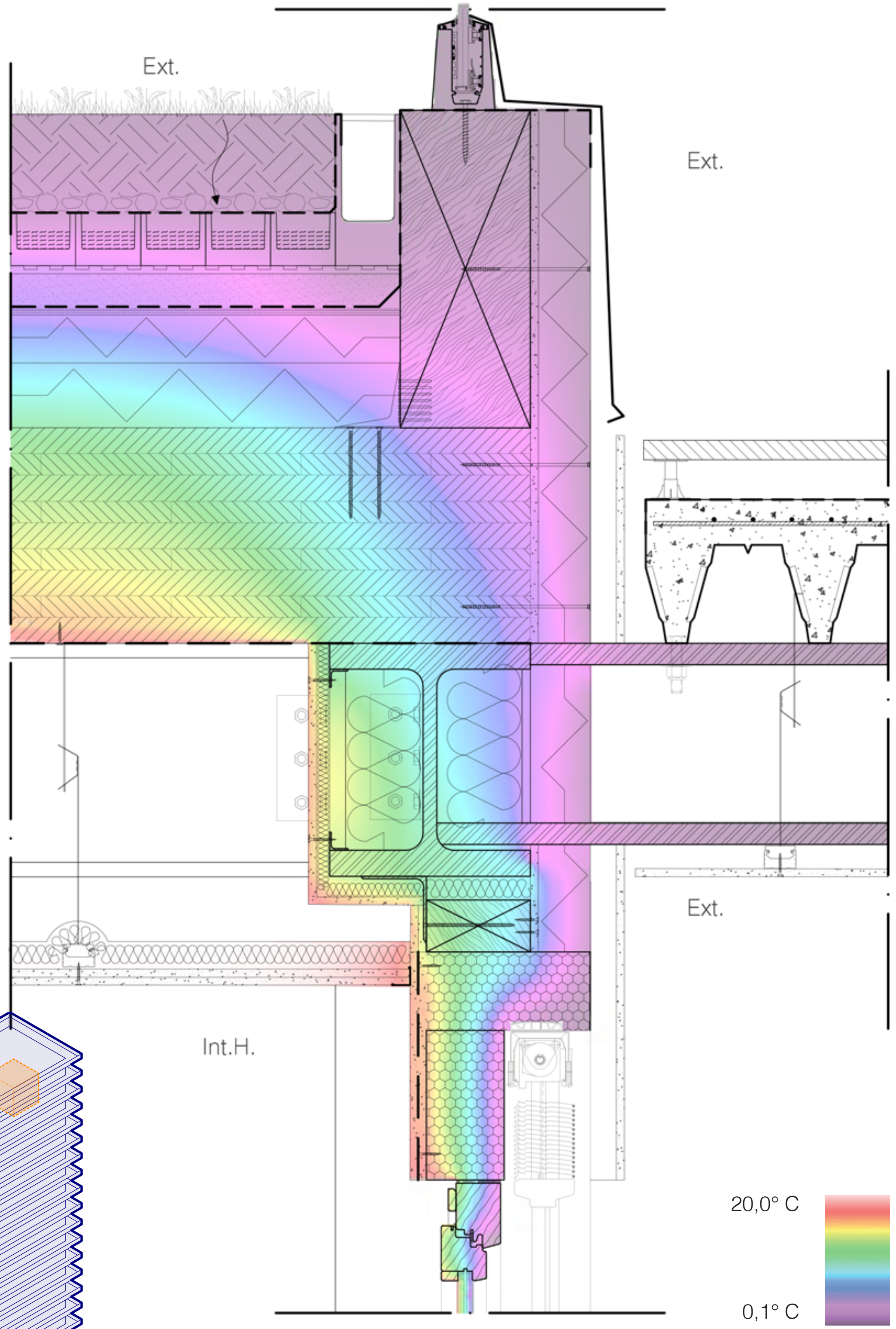

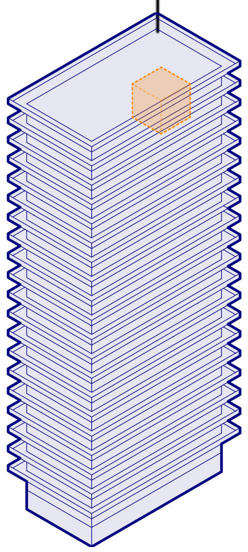

Politecnico di Milano, Master of Science in Building and Architectural Engineering
Steember - Steel and timber for a high rise building in Queens, New York
Chinnici Federico - **Maranesi** Marco

VERTICAL JOINT - CURTAIN WALL

SCALE 1:10

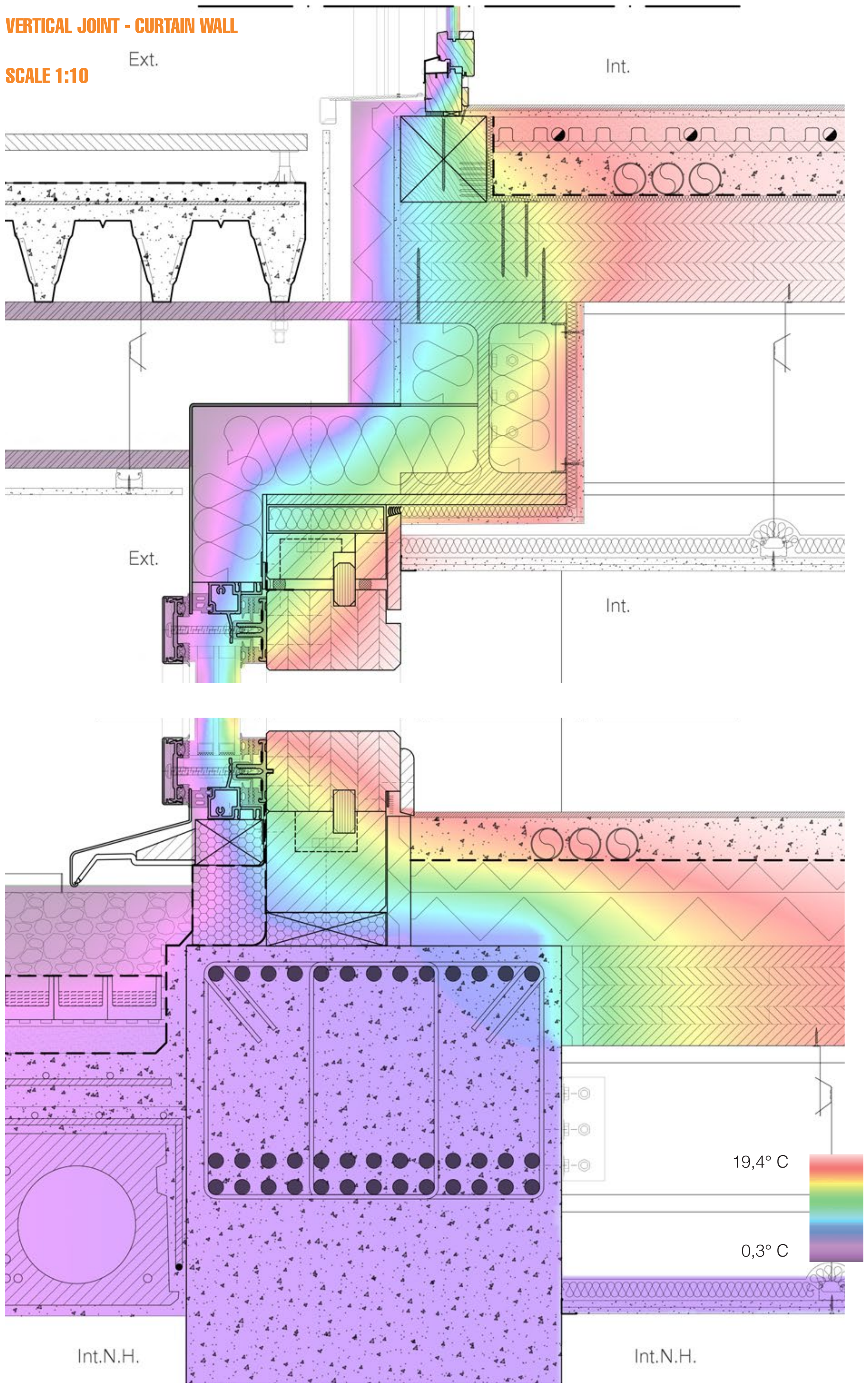

7.4 – THE BLOW-UPS

BLOW-UP 1 - OPAQUE

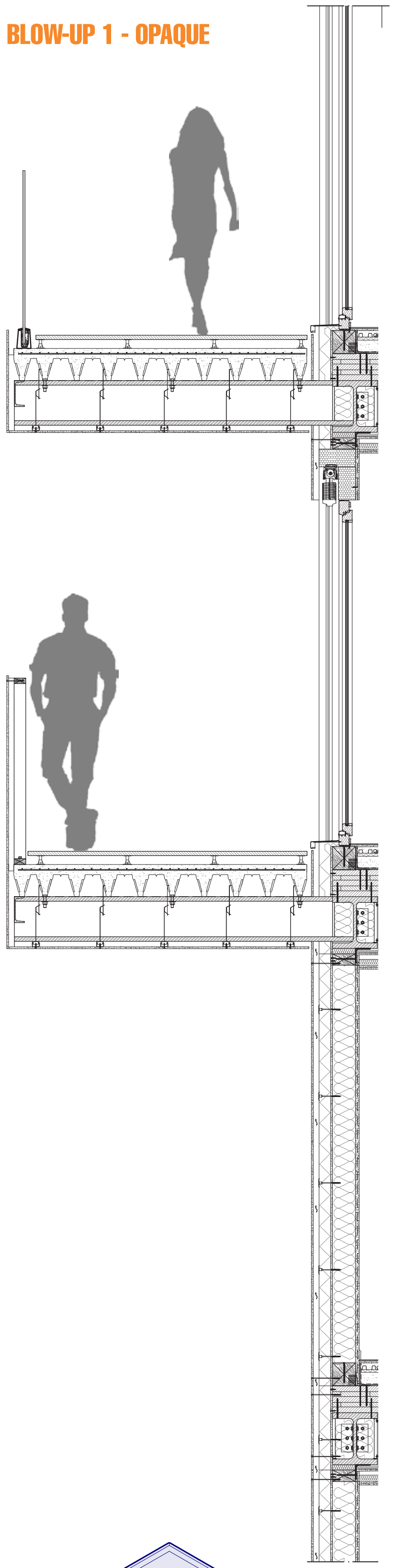

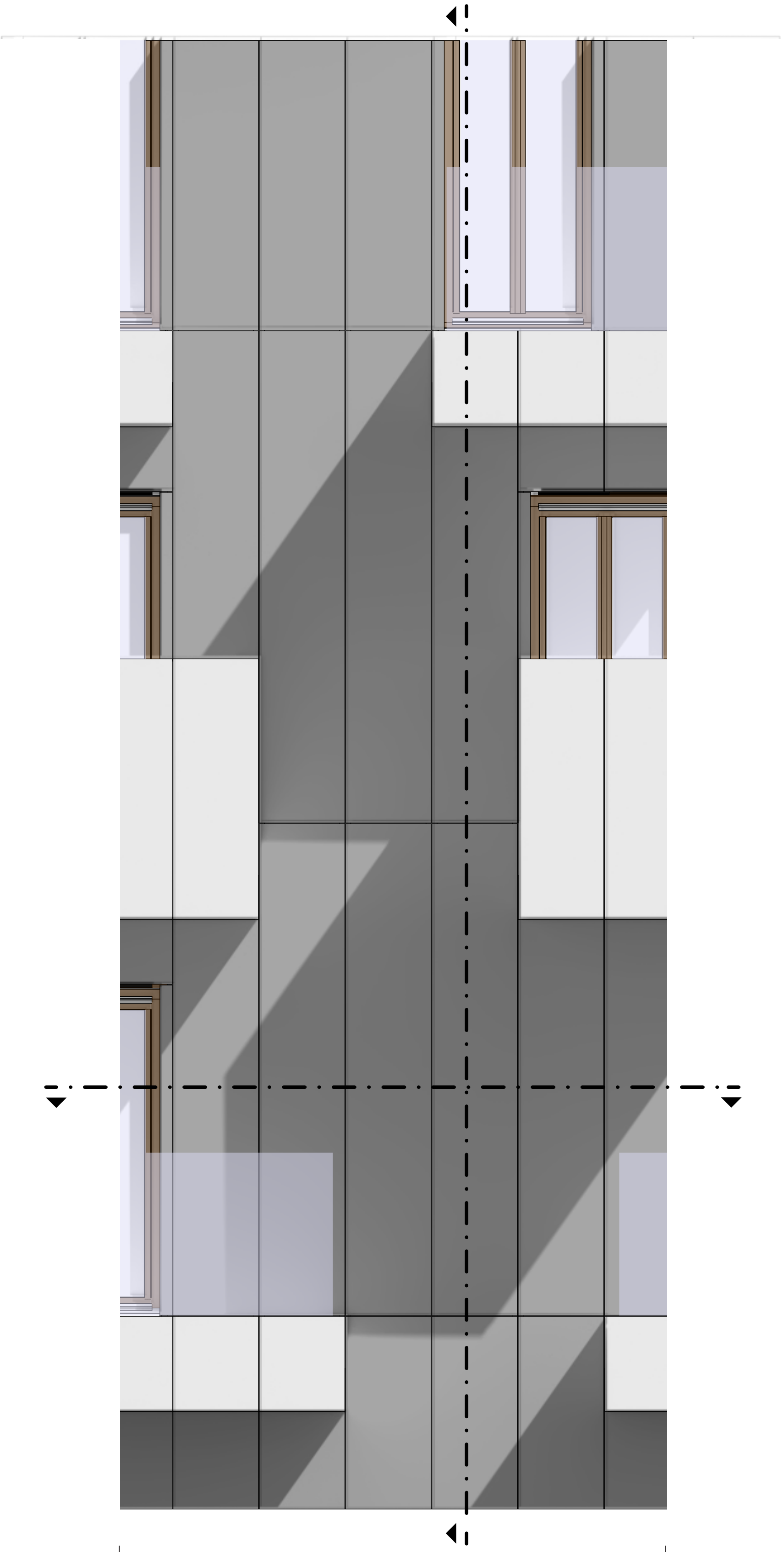

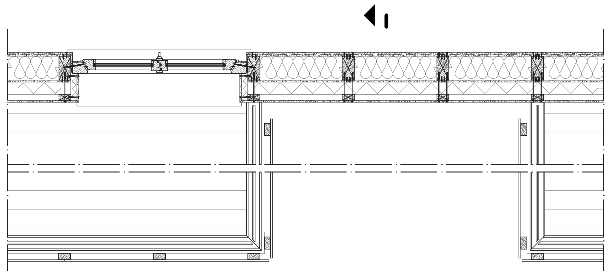

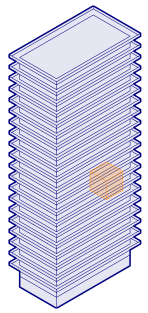

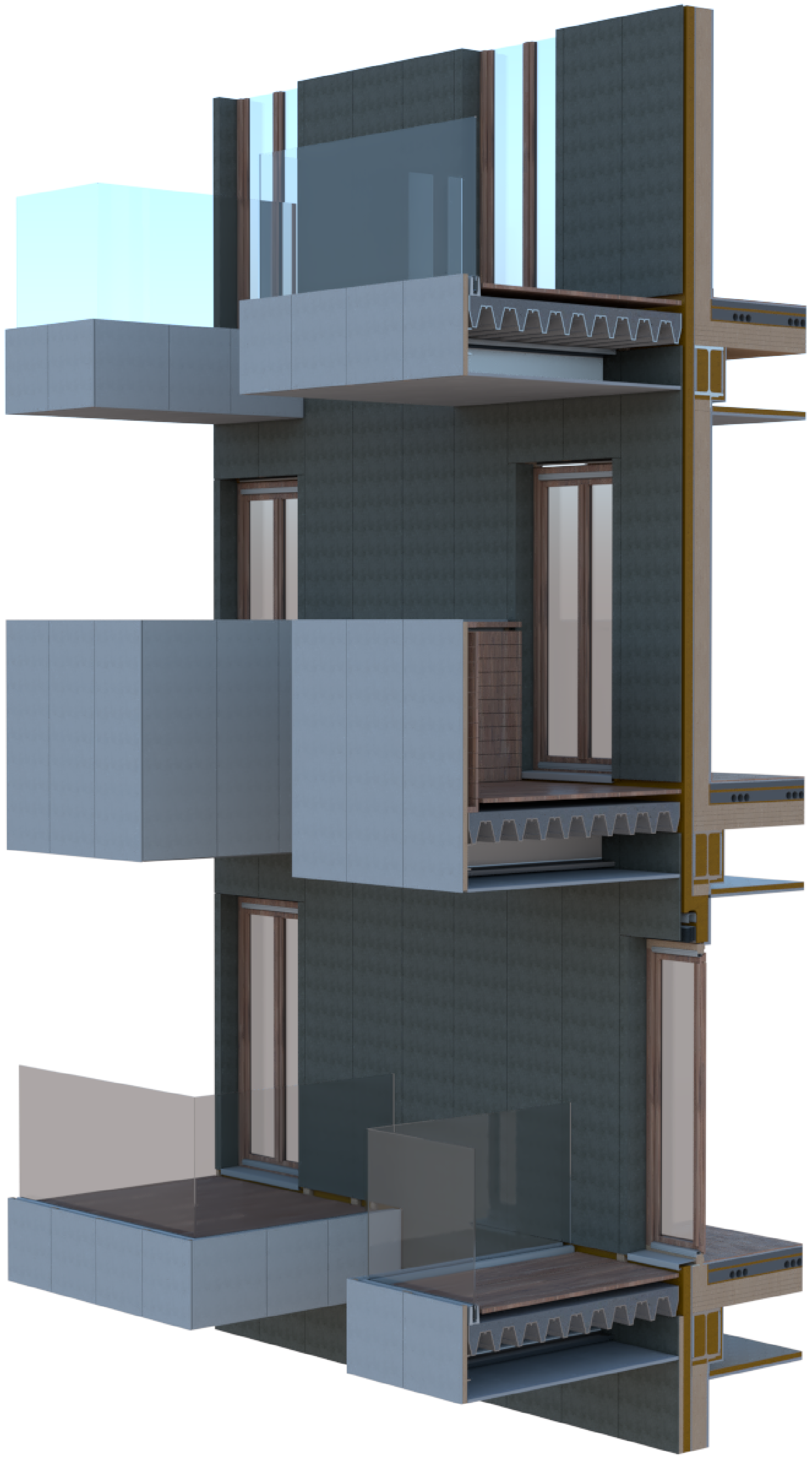

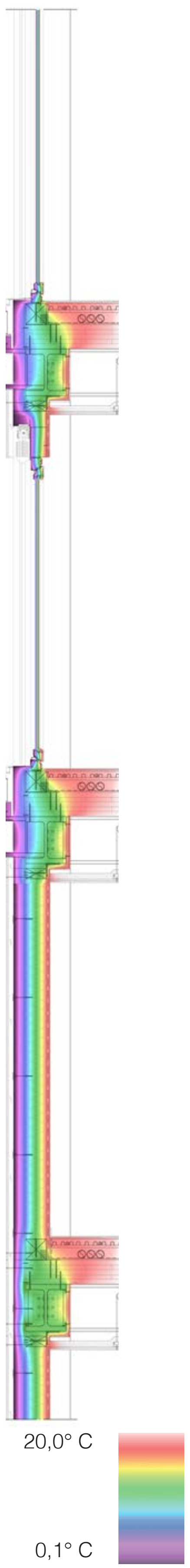

BLOW-UP 2 - TRANSPARENT

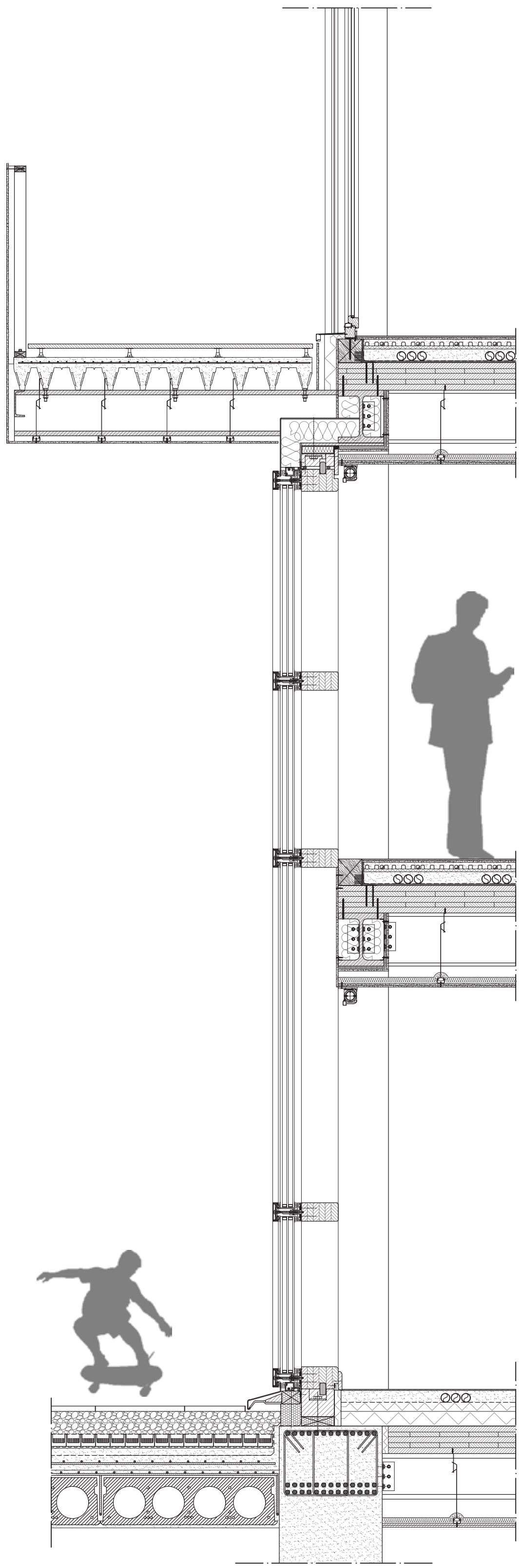

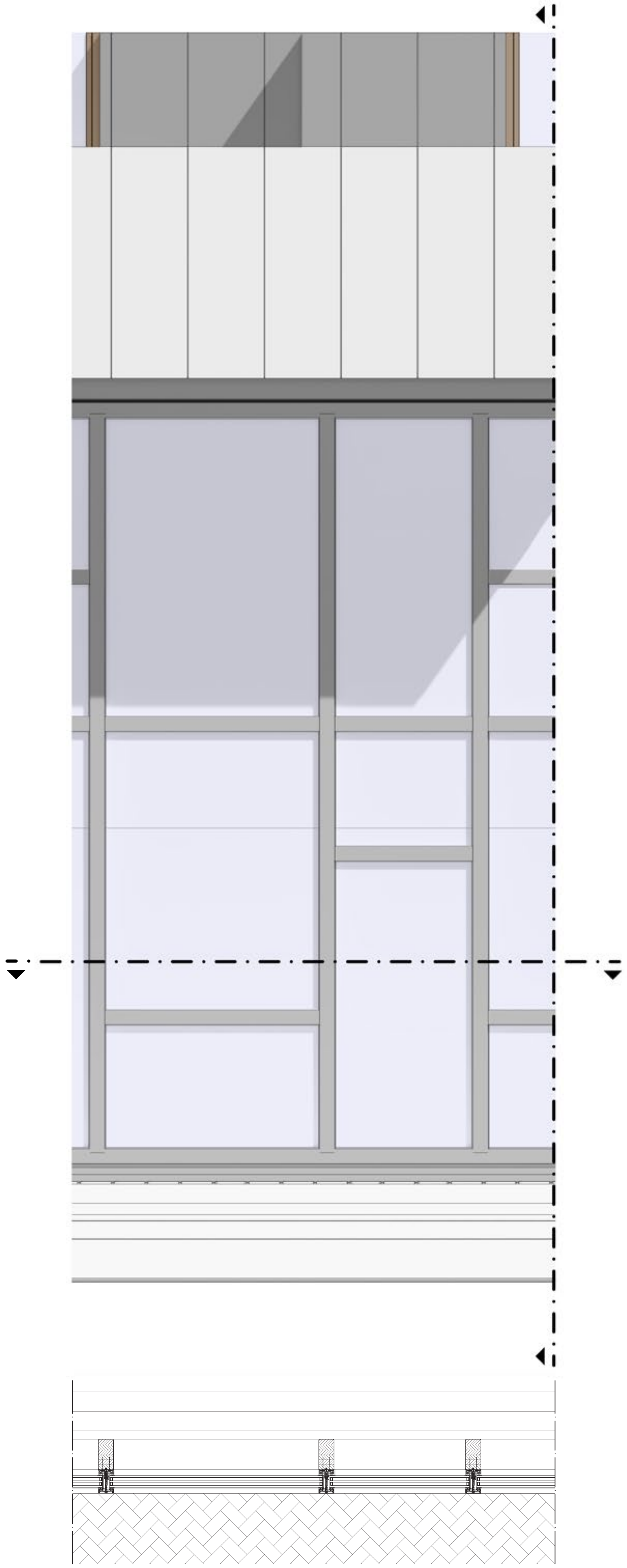

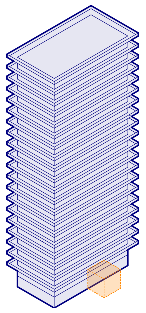

Politecnico di Milano, Master of Science in Building and Architectural Engineering
Steember - Steel and timber for a high rise building in Queens, New York
Chinnici Federico - **Maranesi** Marco

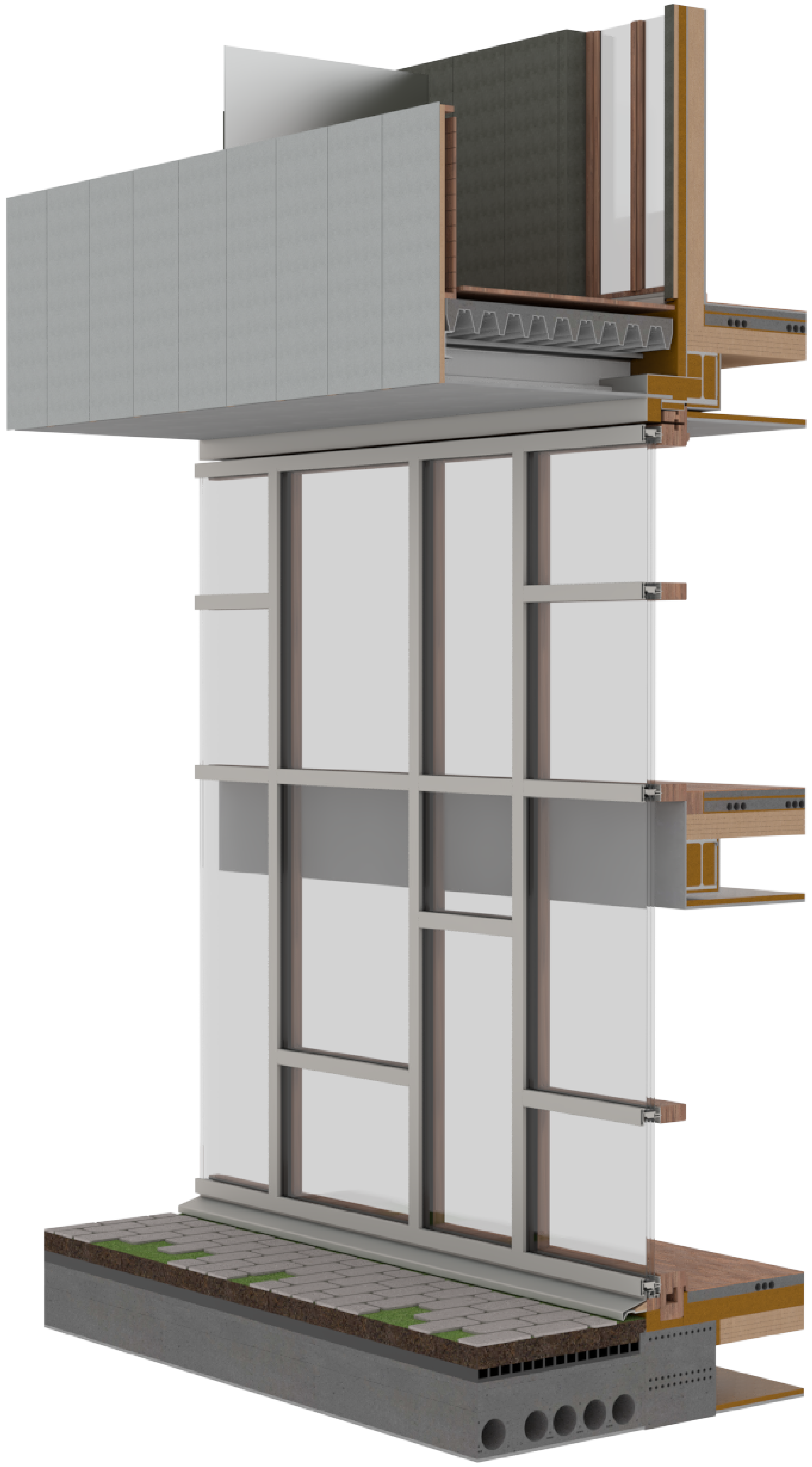

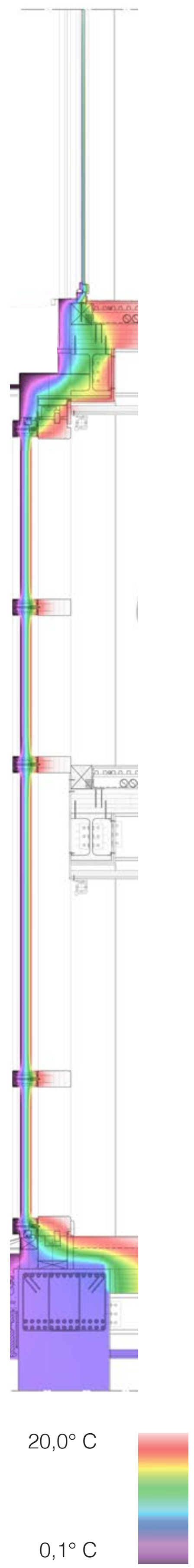

7.5 – THE CONSTRUCTION PROCESS

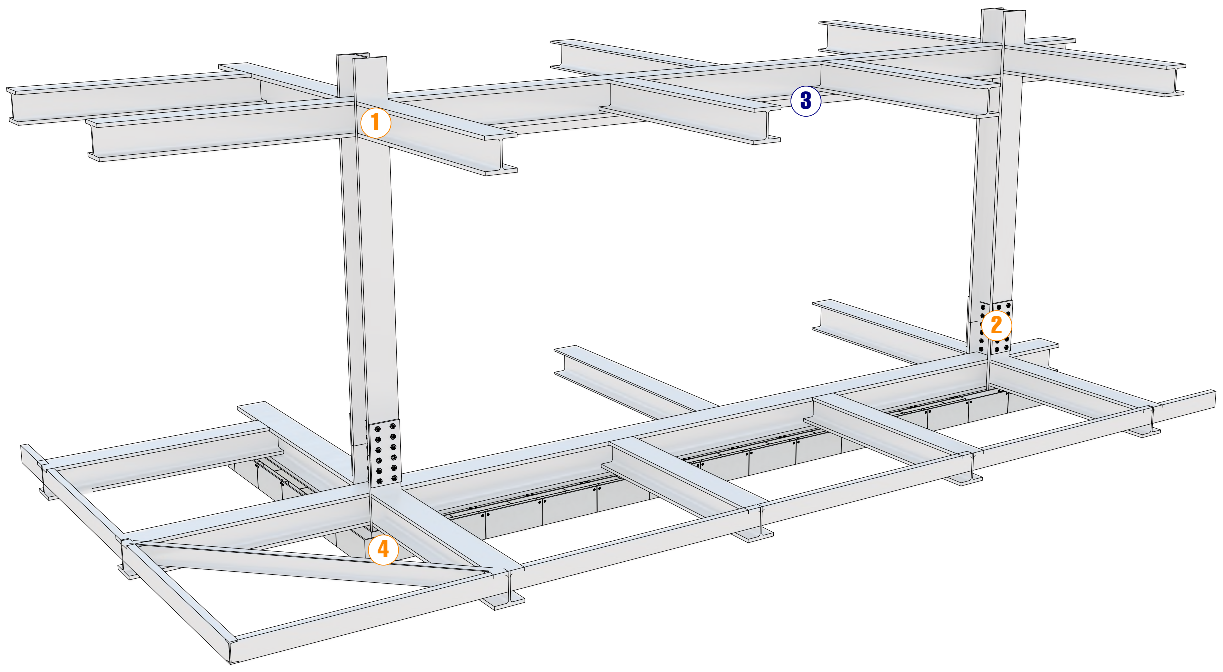

1 Steel structural frame, previously placed and assembled on-site

2 On-site fastening between the columns with steel plates

3 L-shape steel profile, welded to the beam off-site, for the wall's installation

4 Previously-placed on-site timber prefab. wall at the below storey

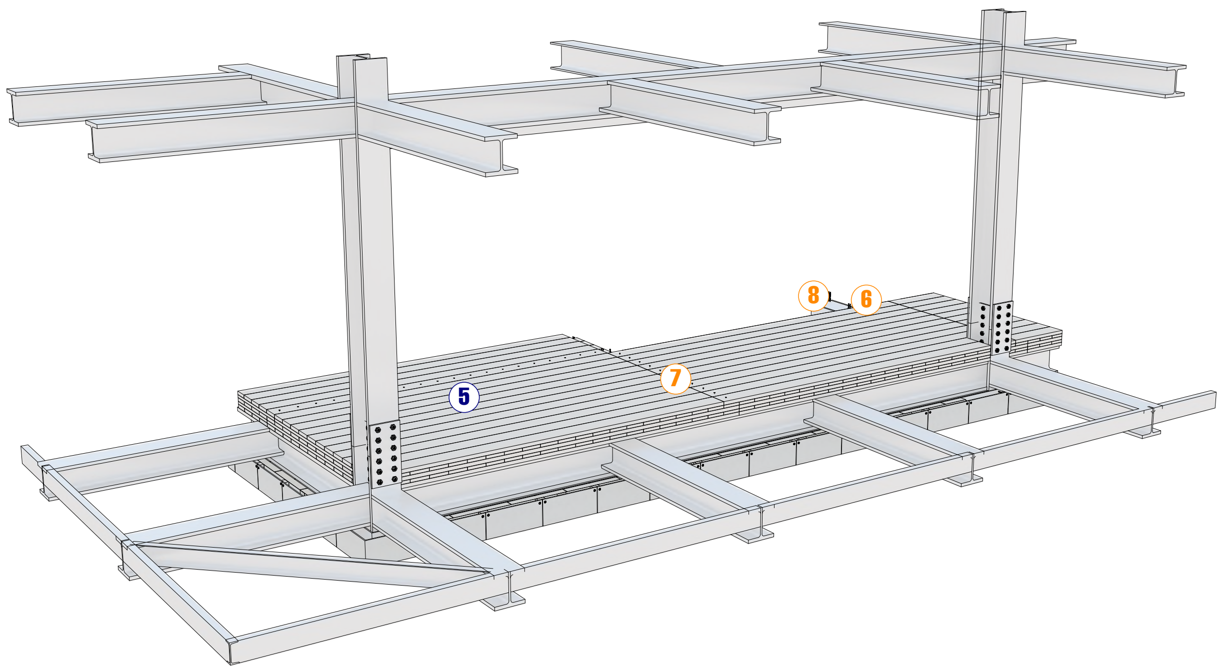

5 Off-site production of the CLT slabs with annexed vibration insulation pads on the edges

6 On-site CLT slab anchorage from below to the steel beam by means of self-drilling screws

7 On-site connection from above between CLT panels with self-drilling screws

8 On-site placement of the gypsum fibre board around the structural steel profiles under the CLT slabs

Politecnico di Milano, Master of Science in Building and Architectural Engineering
Steember - Steel and timber for a high rise building in Queens, New York
Chinnici Federico - **Maranesi** Marco

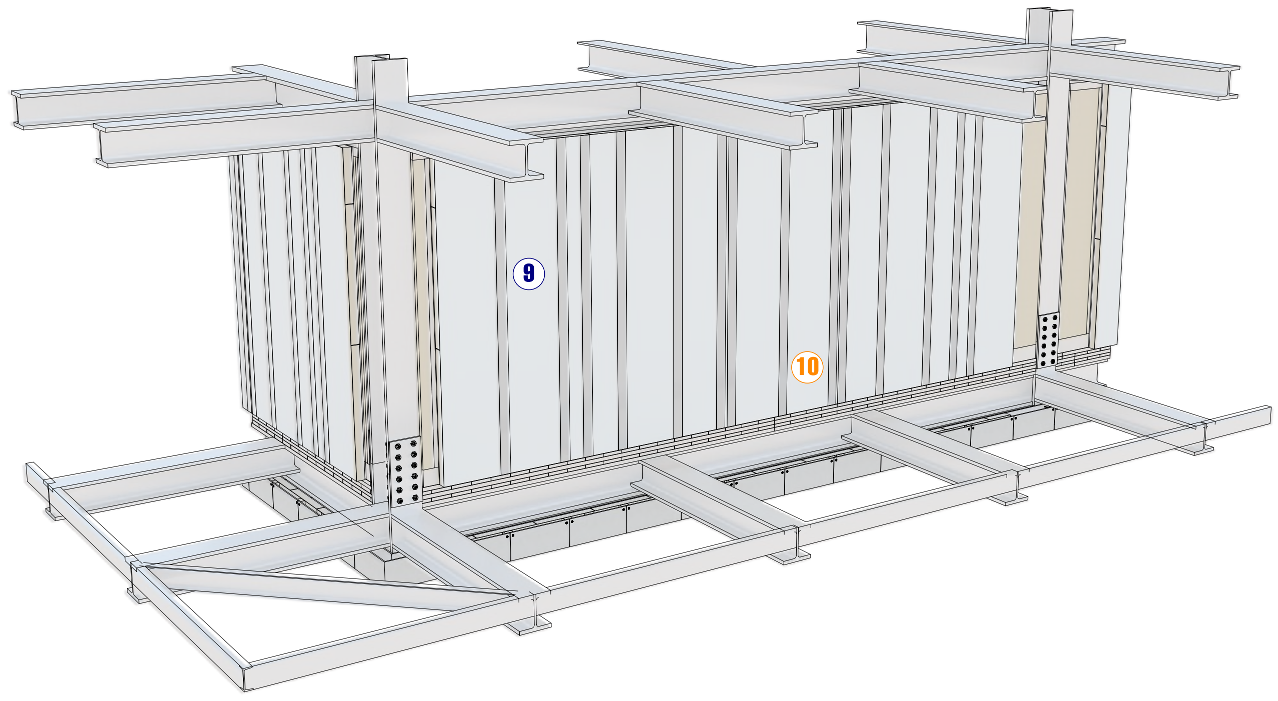

9 Off-site production of the prefab. timber frame wall

10 On-site handling and positioning of the prefab. timber frame wall, placed with a crane and pulled inside by means of lifting straps; the wall will be roughly placed on the belower CLT panel, matching the upper L-shape

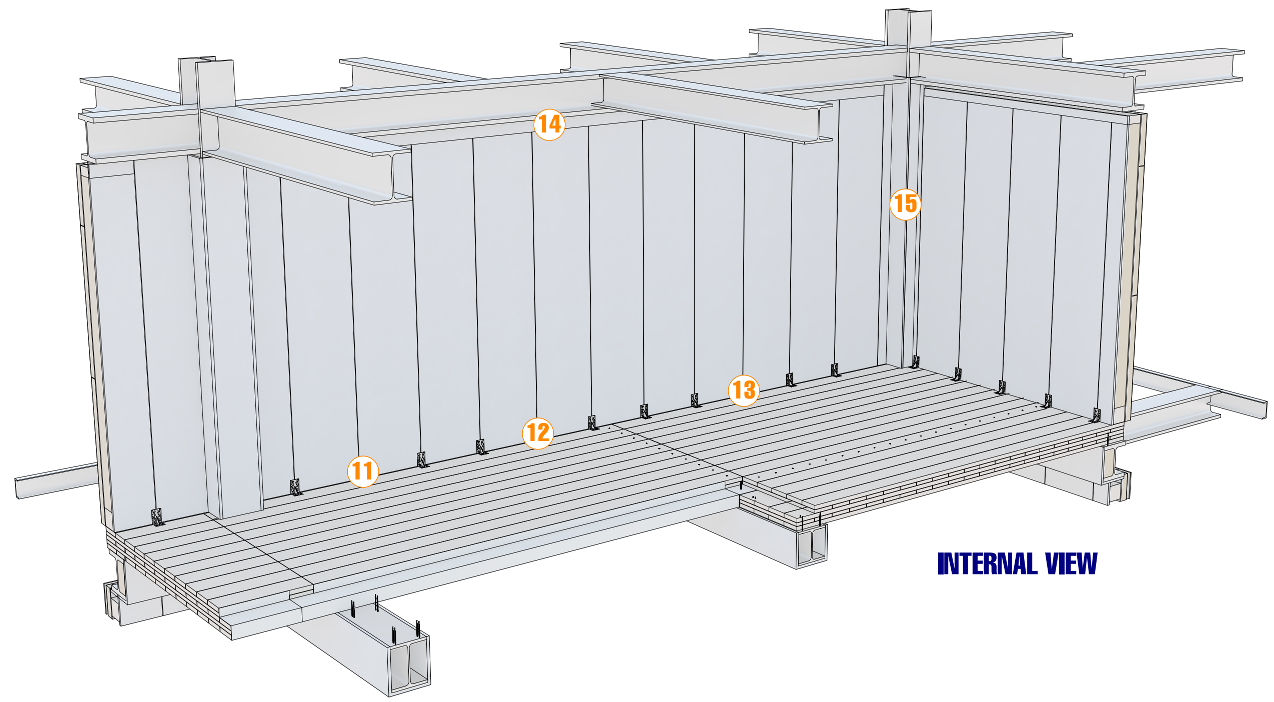

11 On-site positioning of angular brackets

12 On-site horizontal fixing of angular brackets with high bond nails to the wall

13 On-site vertical anchorage to the CLT slabs with self-drilling screws

14 On-site horizontal fixing of the wall with self-drilling screws to the L-shape steel profile

15 On-site columns convering with rigid insulation panels and screwed gypsum fibre boards

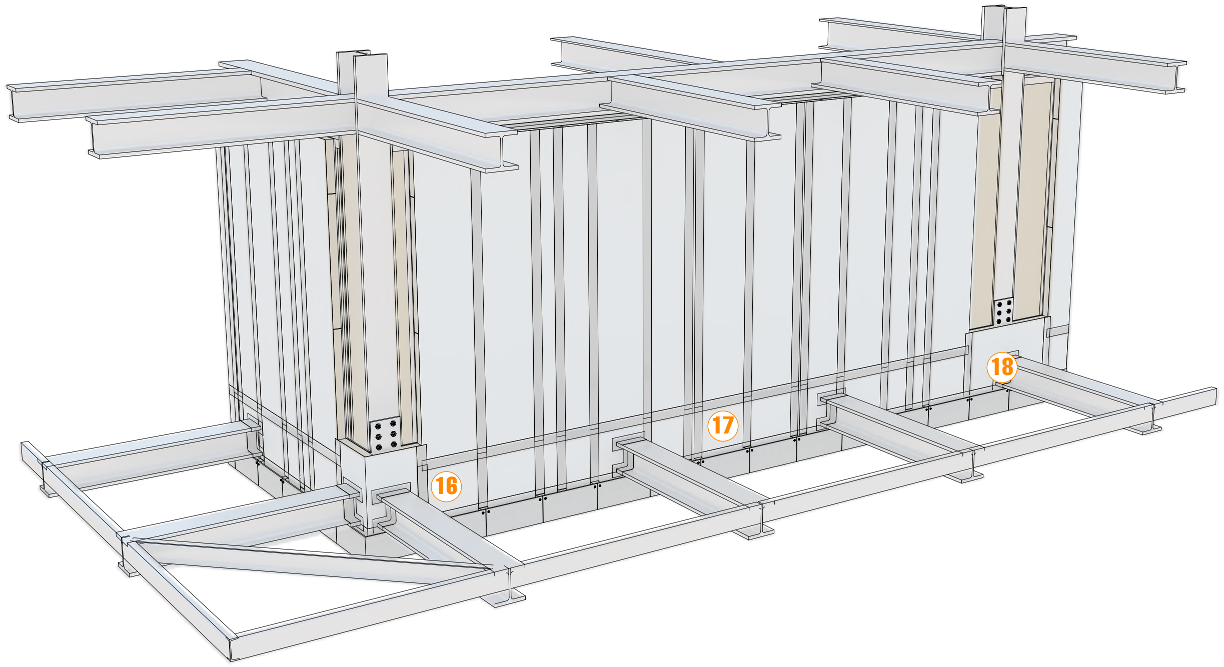

16 **On-site** fulfillment of cavities inside the string course with soft insulation and around the pillars

17 **On-site** closure with soft insulation, gypsum fibre boards and air-tight membrane

18 **On-site** sealing with air-tight adhesive tapes on the membrane's joints and around the cantilever steel beams

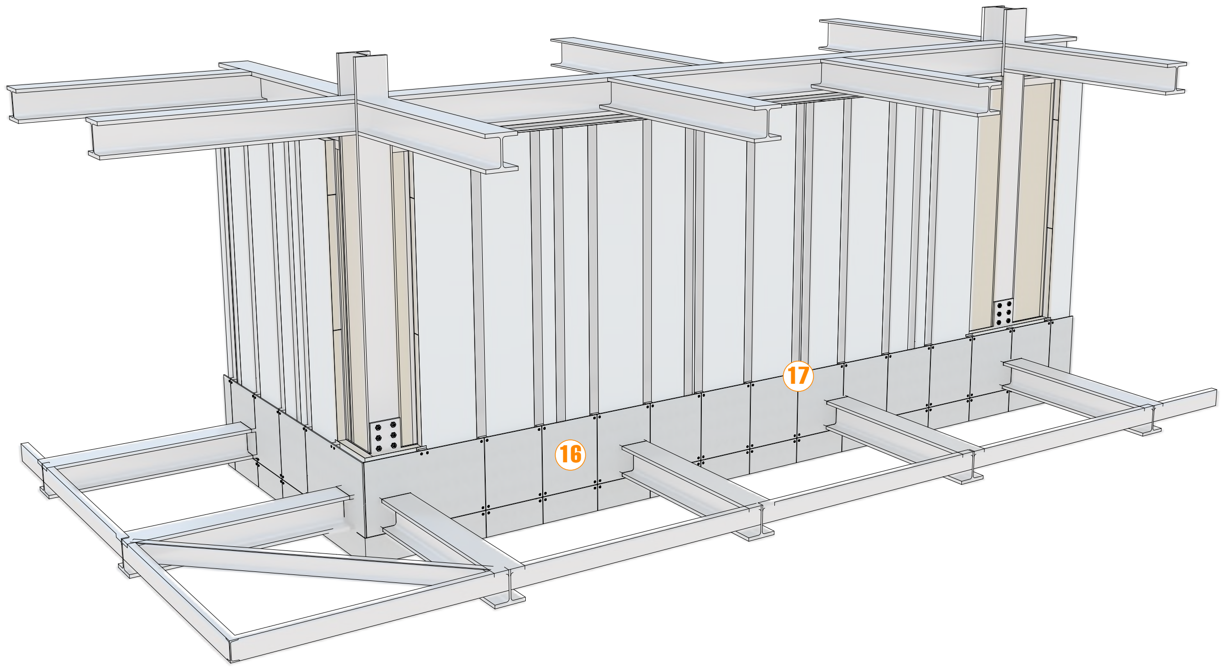

16 **On-site** positioning of timber strips to the timber frame wall mullions

17 **On-site** fastening of fibrecement cladding panels to the timber strips

Politecnico di Milano, Master of Science in Building and Architectural Engineering
Steember - Steel and timber for a high rise building in Queens, New York
Chinnici Federico - **Maranesi** Marco

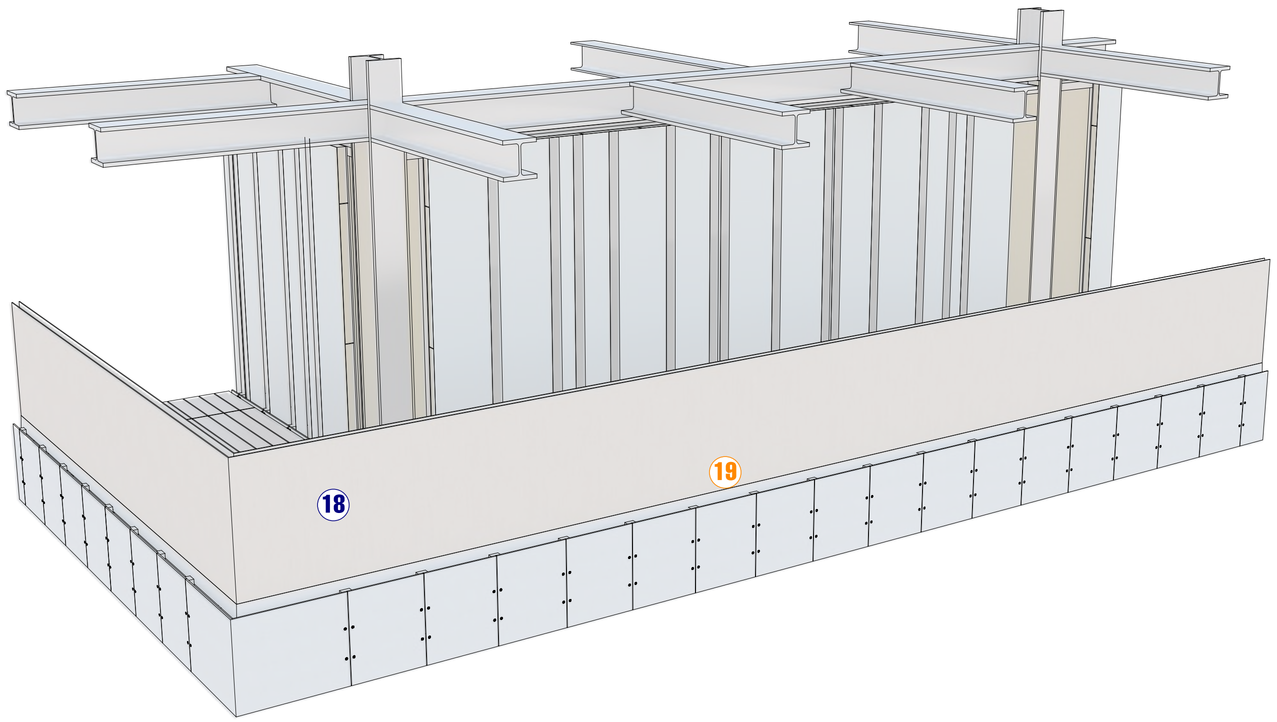

18 **Off-site** production and assembly of the prefab. balcony, complete with parapet, finishing, external cladding and wooden cover for the railing

19 **On-site** fastening of the balcony system by means of nuts, screwing the upper bolts, which are sealed in the concrete block, from below

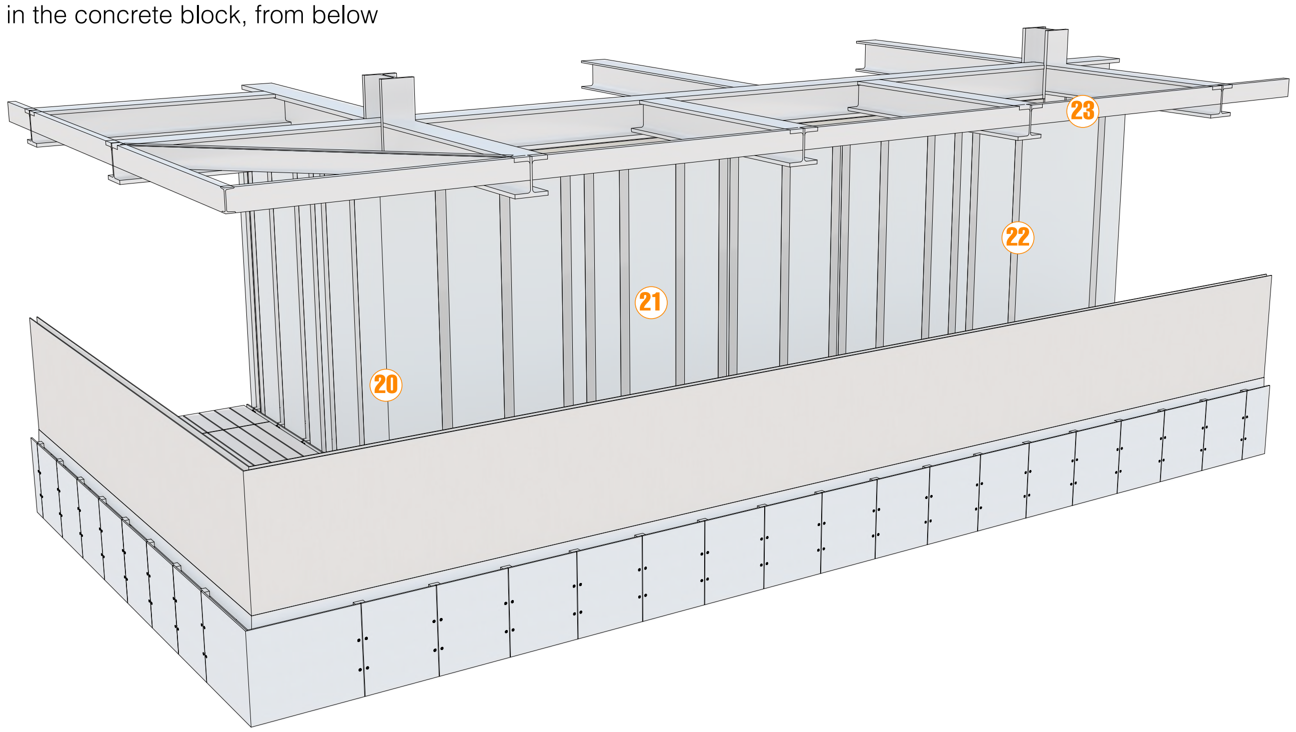

20 **On-site** fulfillment of cavities around the columns with soft insulation working from the balcony that can now be used as a working plane, without the needs of scaffolding

21 **On-site** closure with soft insulation, gypsum fibre boards and air-tight membrane

22 **On-site** sealing with air-tight adhesive tapes on the membrane's joints

23 **On-site** fastening of the upper structural steel frame for balconies

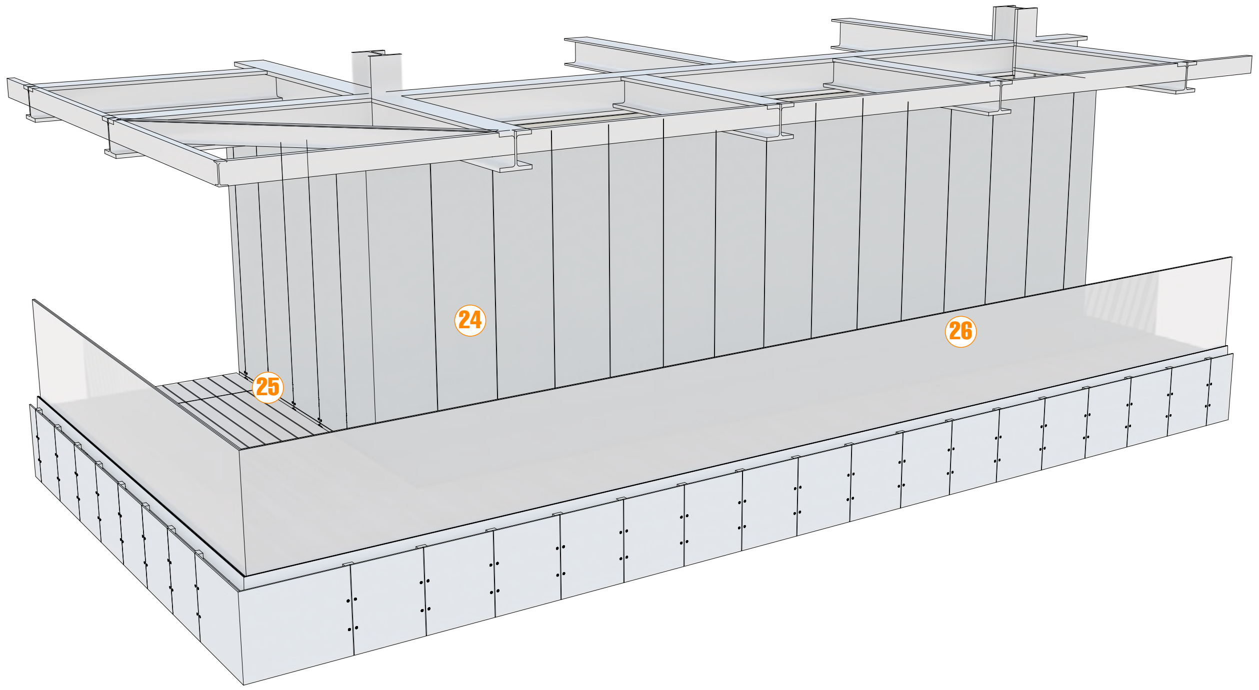

24 **On-site** positioning of timber strips to the timber frame wall mullions

25 **On-site** fastening of fibrecement cladding panels to the timber strips

26 **On-site** removal of the wooden safety protection for railings

The construction process is summarised and explained in these 8 steps.

By bringing all the prefabricated elements, the operations to be completed on-site are just the assembly and the composition of these ones, followed by the sealing of cavities and the application of the external cladding.

Having few and easy working procedures helps carpenters to work faster with lower risk of making mistakes.

This dry-assembled technology, together with lightweight materials, lends itself for different types of constructions, in particular for high rise buildings as in this case. The studied building has just 23 floors because of the number of apartmentes required in the competition. This technology, though, would allow to reach even higher heights and add other floors.

Politecnico di Milano, Master of Science in Building and Architectural Engineering
Steember - Steel and timber for a high rise building in Queens, New York
Chinnici Federico - **Maranesi** Marco

STARTING STAGE

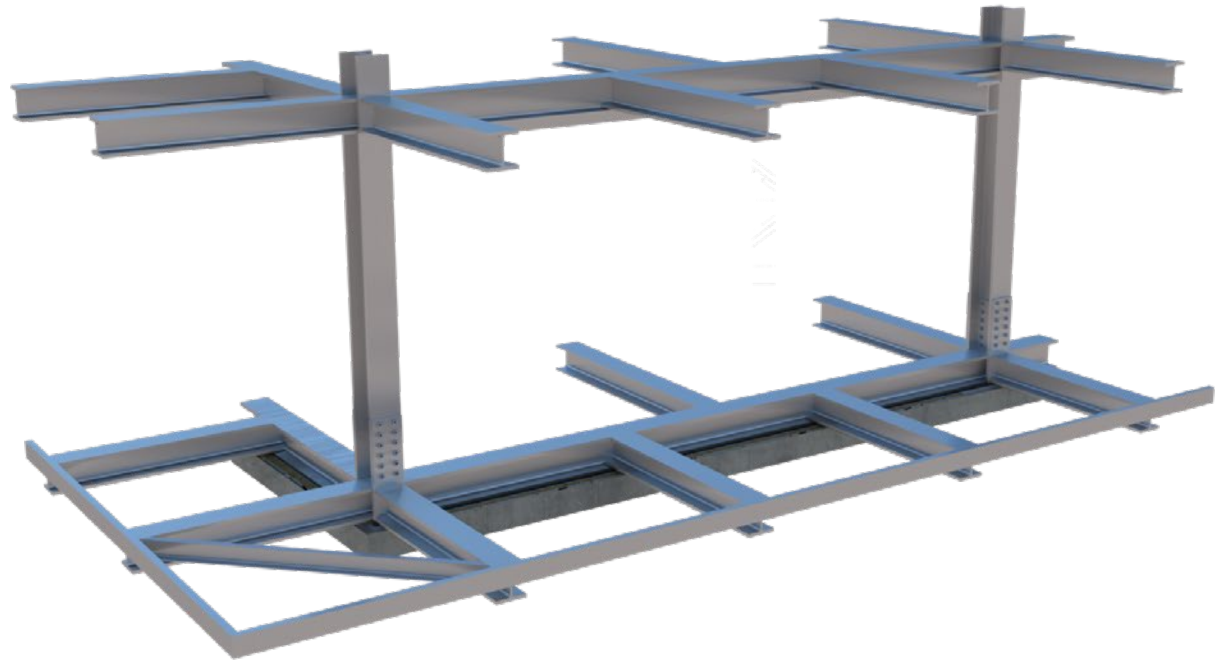

ENDING STAGE

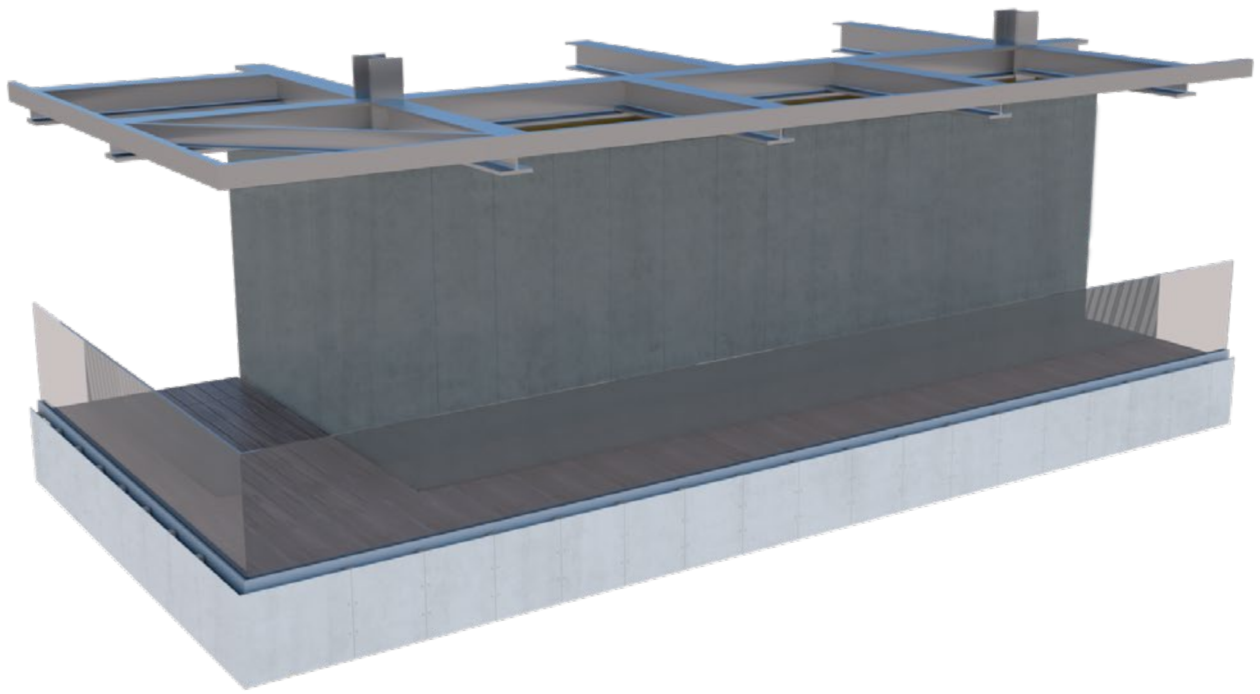

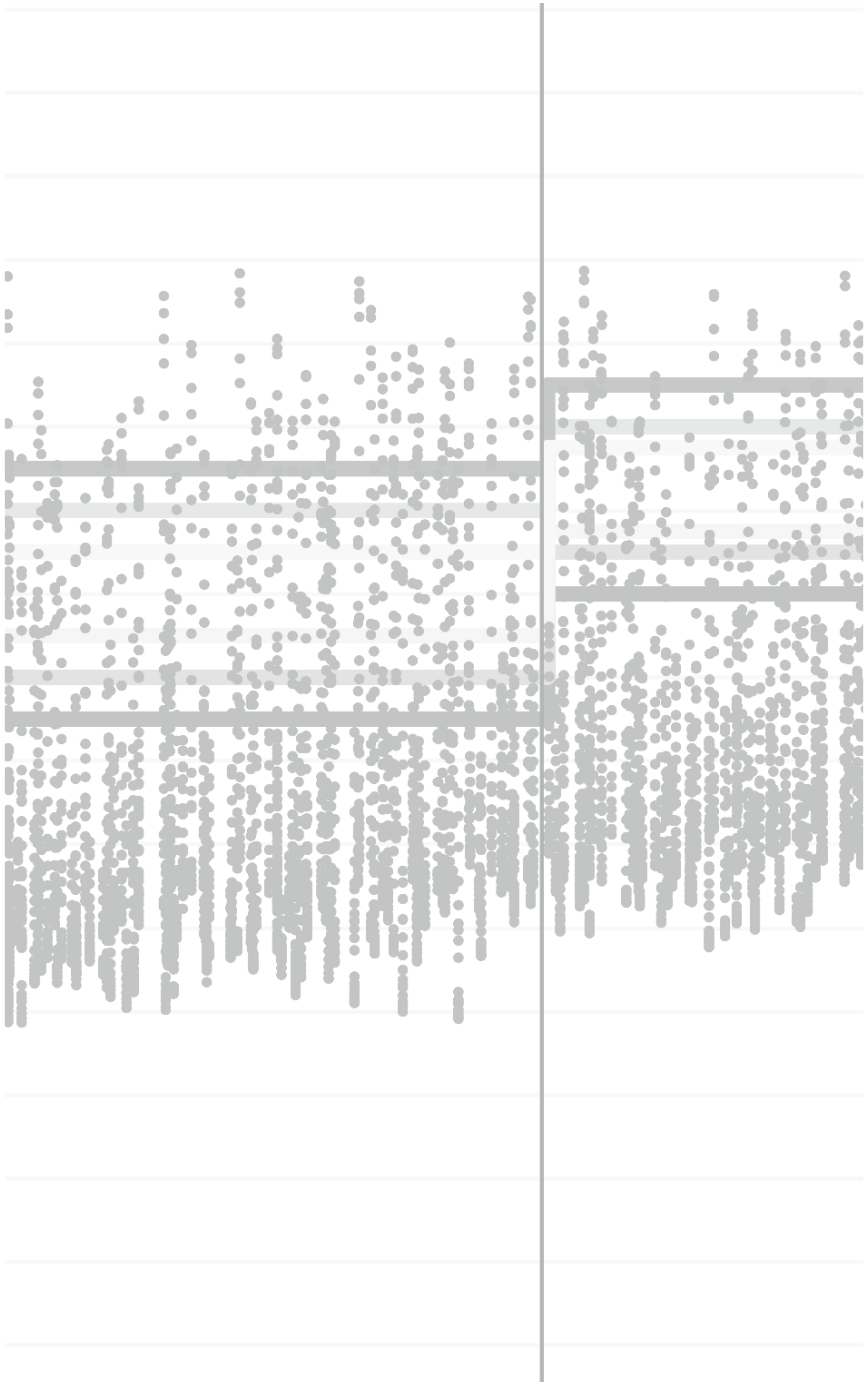

08 ENERGY DESIGN

8.1 – INTRODUCTION

Climate change and negative effects of pollution have focused people's attention on environmental issues. One of the aspects that arouses greater concern is the greenhouse effect, i.e. the increase in the average temperature of the planet caused by the emission into the atmosphere of some gases, generated above all by the combustion processes, the most significant of which is carbon dioxide (CO_2).

Figure 8.1 - Sustainability in buildings

Many countries are seeking a solution to these problems, adding regulatory restrictions and new parameters to be followed in many fields, particularly in the construction sector, in order to decrease pollution level and CO_2 emissions.

Considering that in many developed countries the construction and use of buildings is the leading consumer of energy and producer of greenhouse gas emissions, stabilizing and reversing emissions in this sector is the key to keeping future global warming under one-degree Celsius (°C) above today's level, in order to avoid increased global warming.

The European Union has adopted the 20/20/20 objective which foresees, by 2020, the reduction of greenhouse gas emissions by 20%, the increase of energy produced by renewable sources by 20% and energy consumption savings by 20%.

Another initiative is the "2030 challenge", by the American architect Edward Mazria and the Architecture 2030 organization. This asks the global architecture and construction community to adopt a series of greenhouse gas reduction targets for new and renovated buildings to save the environment, yearly increasing the fossil fuel standard reduction, aiming to have carbon-neutral buildings by 2030.

8.2 – THE ENERGY ANALYSIS OF THE BUILDING

The energy demand of a building and the thermal comfort of its rooms are two fundamental parameters to define the real performance of the building itself.

A smaller energy requirement means having a bigger economic saving in the building management through its life, a smaller power of the mechanical systems and bigger environmental sustainability.

In order to reach the best results of the above-written features, the design of the residential tower went through an integrated approach which, between the structural and technological aspects, included an optioneering process aimed to increase the overall building performance.

This optioneering started in the early stages of the design and went on until the end, putting together passive and active strategies, deeply studied to limit the energy consumption but at the same time, ensuring the internal thermal comfort for the residents.

The climate analysis of the site was fundamental and is the starting point to develop every strategic action while designing. The graphs and the results shown and discussed in section 3.4 represent the climate condition from which designers can take advantage or understand the obstacles.

Politecnico di Milano, Master of Science in Building and Architectural Engineering
Steember - Steel and timber for a high rise building in Queens, New York
Chinnici Federico - **Maranesi** Marco

8.3 – THE SOFTWARE USED AND THE 3D MODEL

Figure 8.2 - The logo of the software

The software used for the energy and comfort analyzes is Sefaira Systems.

The computer program uses the EnergyPlus calculation engine, which is the basis of the operation of many energy simulation programs on the market.

Sefaira Systems allows designers to carry out energy analyses of the entire building (WBEA: whole-building energy analysis) calculating, based on the chosen strategies, the used energy, CO_2 emissions, internal thermal comfort and the use of renewable sources. Storing these data is fundamental, while designing, to compare different strategies and finally decide for the best options.

The software is a dynamic simulation one. This means that, differently from a static regime simulation, in which the external conditions are considered stable during the hours of the day and the unit of time used is the heating or cooling season, a dynamic mode simulation uses hourly climate data and the unit of time considered is one hour or even one fraction of it. For energy and thermal comfort analyzes, the software performs a simulation every 60 minutes.

One of the main output data of the simulations is the annual energy used (EUI: Energy Use Intensity) which represents the building's annual energy consumption. This value considers, not only the thermal loads to be supplied or removed from the rooms, but also the efficiency of the considered plant systems.

The obtained number refers to the square meter of the surface so that it is comparable with that of other buildings and its unit of measurement is the kWh/m^2 year. The energy required by the building is broken down into various components: heating, cooling, fans, lighting, electrical equipment and pumps.

The necessary 3D model of the building is modelled with SketchUp and the Sefaira plug-in. In order to let the software manage to run the simulations, the model needs to be a very simplified one, where walls and slabs have no thickness and windows and other elements have no details. In the software it is then possible to specify the thermal properties of every building technological element, such as U values, the solar factor and type of construction. The surrounding buildings are modelled as simplified surfaces which are then considered as obstacles and shadings so that the software counts them when running the simulations and does not consider the solar radiation passing through them.

8.4 – THE THERMAL COMFORT

Thermal comfort is defined by UNI EN ISO 7730 standard as "the mental condition of satisfaction with the thermal environment " and it considers the thermo-hygrometric conditions of the internal environment. This parameter, together with the energy demand of the building, has been considered as the main drive force while choosing the best strategies since it is extremely important to guarantee the well-being of users when designing a new building.

8.4.1 – THERMAL BALANCE AND ITS FACTORS

The condition of thermal comfort is not unique, but its perception changes according to the individual person and it depends on the interaction between the human body and the environment. This thermal balance is influenced by various factors divided into objective variables (air temperature, average radiant temperature, airspeed and air humidity) and subjective variables (activity and thermal resistance of clothing).

- The air temperature (T_a) is the average air temperature of the room;
- The mean radiant temperature (T_{mr}) is the uniform temperature of the black walls of a hypothetical environment with which the person would exchange the same amount of radiant heat that would be exchanged with the real considered environment;

- The airspeed (v) is the airspeed relative to the body;
- Air humidity (RH) is the partial pressure of water vapour in the environment;
- The activity carried out by the person directly affects the metabolism and therefore the production of metabolic heat of the body (1 metabolic unit = 1 met = 58.2 W / m²);
- The thermal resistance of the clothes represents a unit of measure which expresses the thermal resistance of a piece of clothing (1 unit of clothing = 1 clo = 0.155 m² ° C/W).

The first two parameters can be expressed together in a single one, and this is the operative temperature. It is the uniform temperature of air and walls of the environment which make the subject have the same heat exchange, by convection and radiation, that it would have in the real environment. It is given by the combination of the air temperature and the mean radiant temperature. Often, for moderate thermal environments, it is possible to consider it equal to the arithmetic mean of the two temperatures.

8.4.2 – THE TECHNICAL REGULATIONS

The technical rules of reference are two:

UNI EN ISO 7730

Ergonomics of thermal environments. Analytical determination and interpretation of thermal well-being by calculating the PMV and PPD and of local thermal comfort criteria

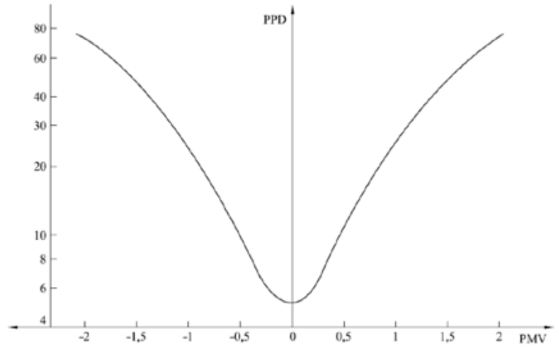

Figure 8.3 - The relative curve between PPD and PMV

This standard allows the designer to evaluate and predict the overall thermal sensation and the degree of discomfort (thermal dissatisfaction) of people in a given environment. It allows to have the analytical determination and interpretation of thermal well-being by calculating the PMV (predicted mean vote) and the PPD (predicted percentage of dissatisfied - expected percentage of dissatisfied people) and of the criteria of local thermal well-being, providing the environmental acceptable conditions for the global thermal well-being as well as those that represent local discomfort.

The PMV is an index which predicts the average value of the grades of a large group of people on a 7-point thermal sensation scale. This parameter, proposed by Fanger since the 1970s, is a function of the six variables previously defined.

The PPD index indicates the percentage of dissatisfied subjects. The correlation between the PMV and PPD index is expressed by a mathematical function and has been elaborated on the basis of experimental researches.

The PMV and the PPD express the hot or cold discomfort for the human body in his complex. However, thermal dissatisfaction can also be caused by local discomfort. The most common causes are the presence of an air current, a too high difference of air temperature, a floor too hot or cold and asymmetry of a too high radiant temperature.

The Fanger model, based on a static approach, defines a fixed band of acceptable temperatures that must be verified regardless of the external climatic conditions.

UNI EN 15251

Criteria for the design of the internal environment and for the evaluation of energy performance of buildings, in relation to the quality of indoor air, to the thermal environment, lighting and acoustics.

This regulation introduces the concept of “adaptation” by proposing a correlation between the comfort temperature for the occupants and the outside air temperature. The resulting comfort model is based on the fact that the human body adapts itself to external weather conditions, considering different internal temperatures as comfortable depending on season

and location. The information contained in the UNI EN 15251 standard refers to buildings without mechanical cooling system and naturally ventilated.

8.5 – THE STARTING POINT

For the first simulation, it was important to define the value of the parameters needed in the first specific case. Every parameter is then going to be optimized through a deep study and further simulations.

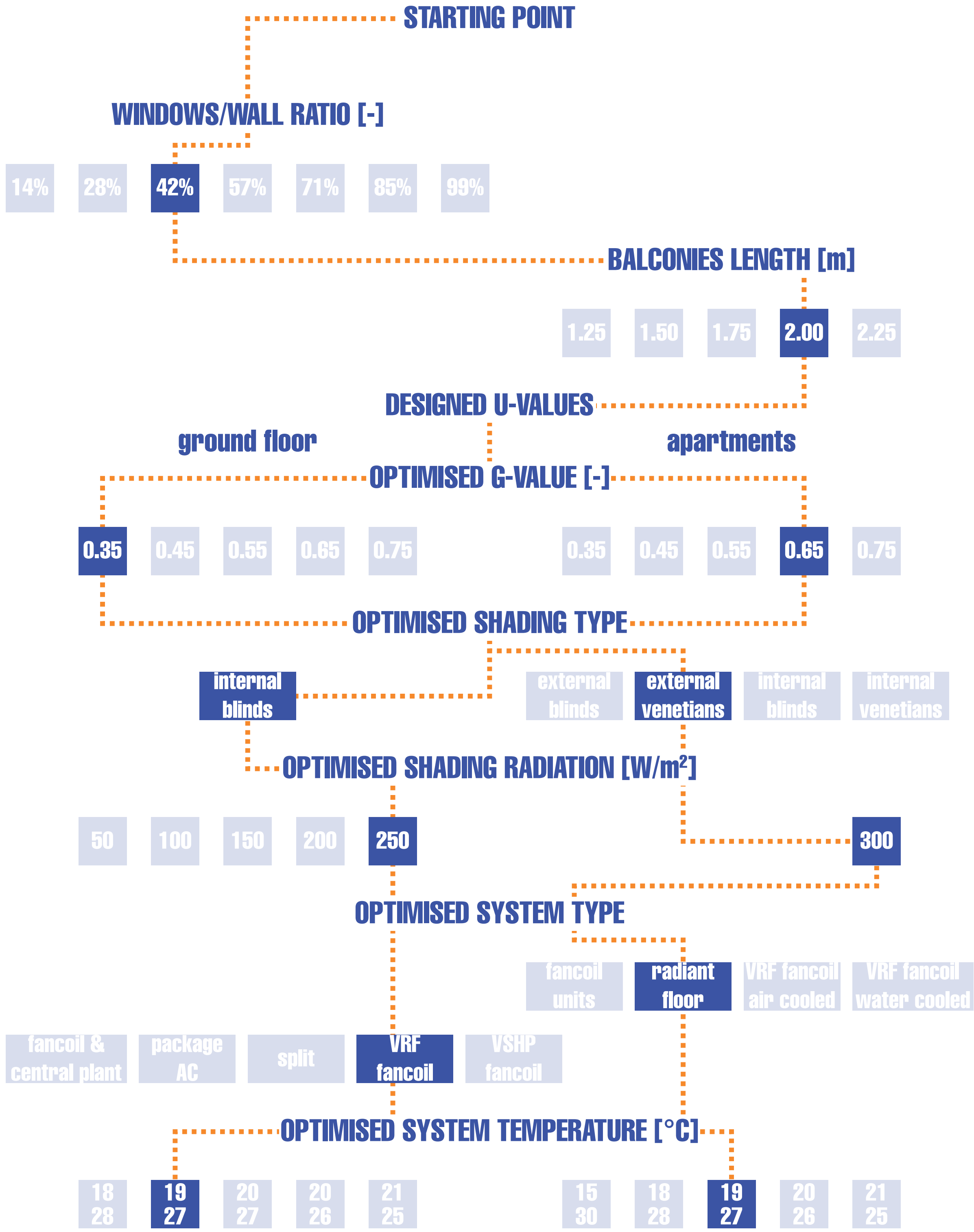

8.5.1 – THE U VALUES

The starting simulation has been done with the defined geometry of the building, with values of the thermal transmittance of opaque and transparent elements given by the requirements for energy efficient residential buildings in the New York Building Code (NYCECC). In this way, this first case would be the reference building, useful to compare the impact of every strategy and optimization.

In particular, the minimum values in the code are:

- U_{wall} = 0,465 W/m²K
- U_{floor} = 0,266 W/m²K
- U_{roof} = 0,170 W/m²K
- U_{window}= 1,98 W/m²K

8.5.2 – THE SPACE USE

If from the third floor upwards there are only apartments, on the first two levels the different rooms have various functions, such as co-working, gym, playroom and laundry. This difference is fundamental and it needs to be pointed out in the software in order to have realistic simulations.

The building has been divided into thermal zones according to the internal distribution of the rooms, both in the apartments and in the first two levels. Thanks to this division it was possible to specify the working hours of the systems and the internal gains due to electrical devices, lighting and people. These last ones are considered both as sensible and latent heat gain, according to the number of people, in fact, the software will consider 65 W/person as sensible part and 55 W/person as latent part.

The internal gains due to lighting and electrical devices have different values according to the function of the rooms, going from 2 W/m² and 5 W/m² for the apartments to 5 W/m² and 8 W/m² for the gym and the co-working rooms.

Also, the crowding index and the occupied hours have been specified, so that the systems would be working according to that schedule.

In particular, for the apartments, the rooms have been divided between night and day areas, changing the occupied hours. For example, the bedrooms have occupancy going from 11 pm to 7 am, while living rooms, kitchens and dining rooms have occupancy from 7 am to 10 pm but with different percentages, considering that from 8 am to 6 pm many flats could be empty due to the absence of people. In these hours the systems are set to keep the temperature at 20°C in winter and at 26°C in summer, while in the unoccupied hours they are set to work with lower intensity, due to the probable absence of people, and to keep temperatures of 18°C and 28°C.

Regarding the gym and the co-working rooms, the occupied hours are different in this case. The first rooms have a schedule which is similar to an office, considering the maximum possible occupancy to be reached from 9 am to 5 pm, while the gym has a 24 hours working system with a possible peak of occupancy reached from 5 pm to 11 pm.

8.5.3 – THE MECHANICAL SYSTEMS

Choosing the best mechanical system is a choice that affects the energy demand of the building, the maintenance cost and thermal comfort. Moreover, it can be determined according to the function inside the building itself.

The possibilities are all-air systems, fan coils and primary air systems and radiant floor and primary air systems.

The all-air system provides treated air both for air conditioning and for air quality control of the rooms. The other two types are mixed air-water systems. The latter uses an air system to

control and exchange air and hydronic terminals to manage heating and cooling loads in the various environments.

The hydronic terminals can be of various types and require a network distribution of hot and cold water. In the case of fan coils, the air is aspired through them to be heated or cooled and re-emitted in the environment where heat exchange occurs by convection. In radiant panels instead, hot or cold water flows into the pipes located in the radiant floor screed and the heat exchange with the environment mainly happens by radiation.

The primary air system is composed by an air handling unit (AHU), the channels of aeraulic distribution of supply and return, from the delivery diffusers and from the recovery grilles. Its main function in mixed systems is to provide fresh air to the internal environment ensuring the correct humidity level, in some cases, it can also provide conditioning of air.

A comparison between the three different kinds of systems can give an idea of which one is the most convenient to use, in terms of energy demand. In particular, the all-air system is the one with the higher energy consumption, while between the two mixed air-water systems, the radiant one is cheaper than the fan coils one.

As a result of this preliminary analysis, the radiant floor with a primary air system can be the right choice for the building, particularly for the residential apartments where the comfort temperature needs to be reached and then maintained for long periods. For the first two levels, a fan coils system can be used, so that according to the occupancy, it can be set to a needed temperature, which can be reached in a short period of time.

THE BENEFITS AND LIMITS OF THE RADIANT FLOOR

The radiant floor is not only convenient for energy reasons, but also for other important aspects that cannot be ignored by a designer, such as thermal comfort, air quality, no spatial constraints and low-temperature heat transfer fluid.

Radiant panels exchange heat mainly by radiation, as a consequence, there will not be convection current of hot air. If compared to a radiators system which has single and specific diffusers, the heat distribution is better, since this is a system "diffused" on the whole floor surface. This will result in a homogenous temperature distribution in the air, slightly warmer in the legs zone and slightly cooler in the chest zone, close to the heart and the respiratory system.

As a result of the heat exchange by radiation, the air moved by convection is less, avoiding the movement of dust and filth, having positive effects on the healthiness and wholesomeness of air. This system does not create spatial constraints since this is hidden in the slab thickness.

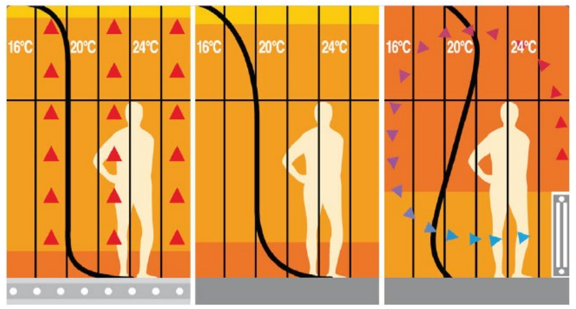

Figure 8.4 - Temperature distribution curves of radiant floor systems (left) and radiators (right) compared to the ideal one (centre).

It does not require any terminal like radiators or air vents, resulting in the freedom to furnishing an apartment as desired, without any limitations given by needed air circulation.

Finally, the water that needs to flow through the radiant floor pipes has a temperature range between 30-40°C, much lower than the 60-80°C range of a radiators system. The lower need for heating water results firstly in lower energy demand, as said before, but also in the possibility to use high efficient generators, like heat pumps, solar panels and condensing boilers.

However, this kind of system has some limits when it comes to cooling and dehumidifying air. As a matter of fact, lowering the temperature would mean having superficial condensation. In these cases, the primary air system starts working, conditioning air and keeping a healthy quality of air.

Anyway, all the first optimisations have been considered in free-run mode, without working systems.

8.6 – THE WINDOW/WALL RATIO

The first optimization had the goal to find the best quantity of transparent surface on the façade. To understand the best ratio between transparent and opaque, the floors have been considered without internal partitions and the façade of every level has been divided into regular modules. At each step, the number of transparent modules increased and a new simulation run.

To understand which one was the best solution, the results have been analyzed considering

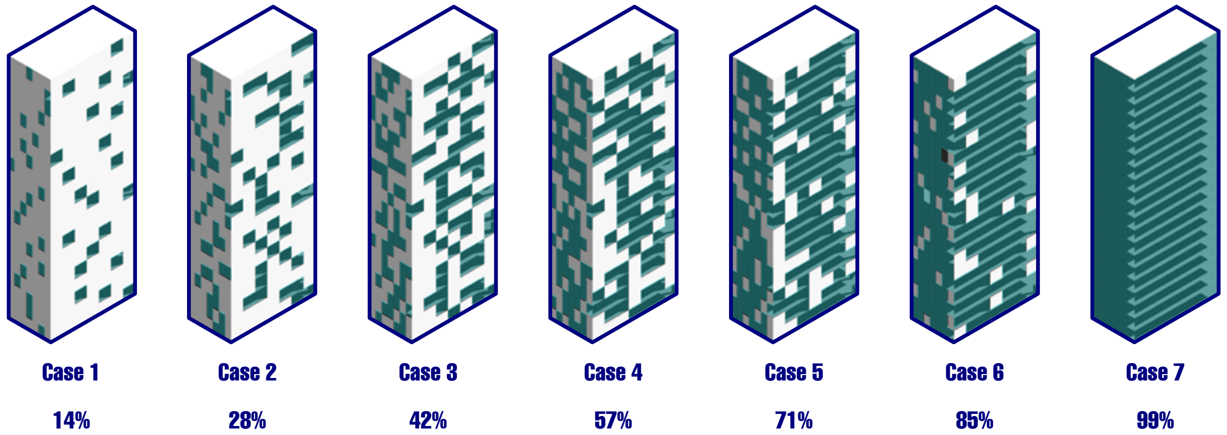

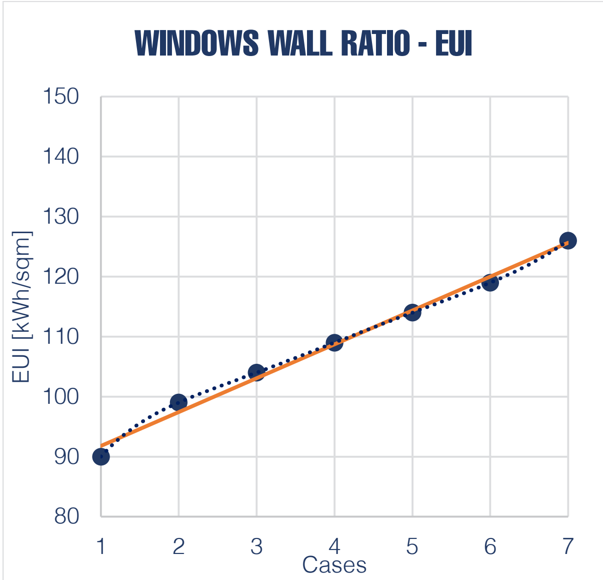

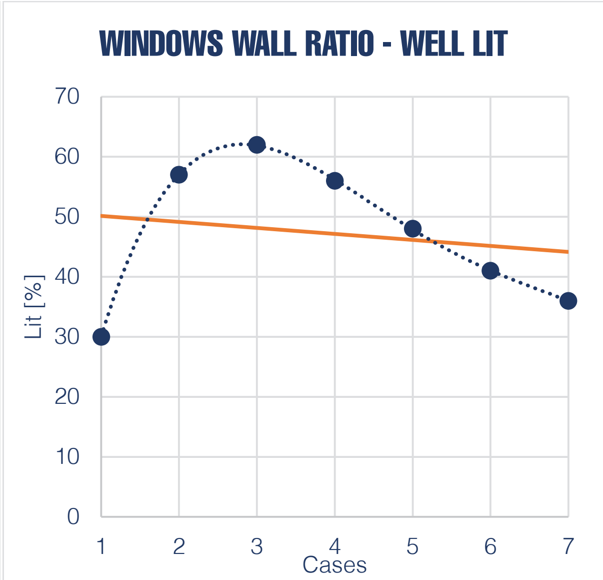

the EUI and the well-lit percentage, meaning that the best option would be the one that ensures the lowest EUI, paired with the highest well-lit percentage possible.

Obviously, adding transparent elements means increasing the EUI. The well-lit percentage does not have the same trend, in fact, adding too many glass elements would mean increasing the over-lit percentage, at the expense of the more important and more needed well-lit.

Matching the simulation results and the best options, the optimal quantity of transparent elements on the elevation is 42% of the total façade surface, corresponding to case 3.

Politecnico di Milano, Master of Science in Building and Architectural Engineering
Steember - Steel and timber for a high rise building in Queens, New York
Chinnici Federico - **Maranesi** Marco

8.7 – THE BALCONIES' LENGTH

Once the surface of glazing façade has been established, it is important to define how these elements are subject to solar radiation.

The amount of sunlight hitting the transparent elements needs to be controlled since it can have a positive effect on the cold season helping the building to naturally warm-up, but it can also have counteractive in the warm season, resulting in overheating for the internal rooms.

For this reason, the balconies, besides being useful for architectural and functional purposes, have been studied and developed as shading overhangs which would protect the windows.

By running various simulations it was possible to size the length of these elements in order to take advantage of the solar gain in the cold period of the year, but also to avoid the greenhouse effect and the overheating in the hottest months.

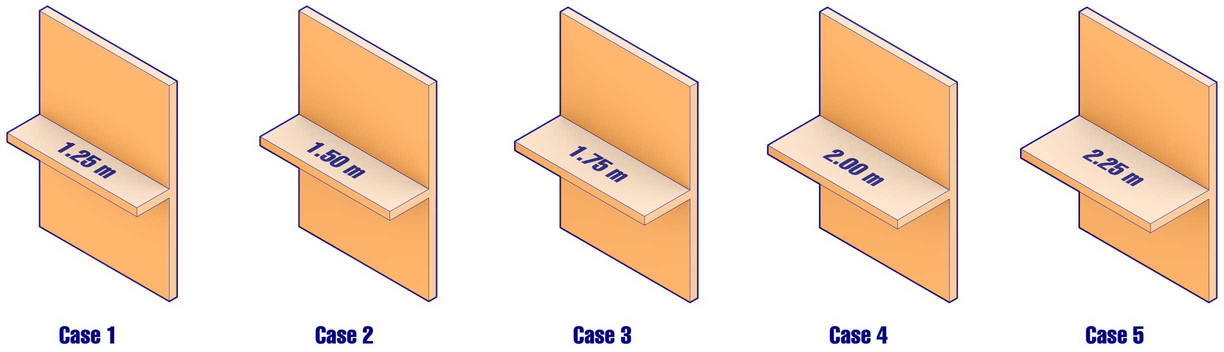

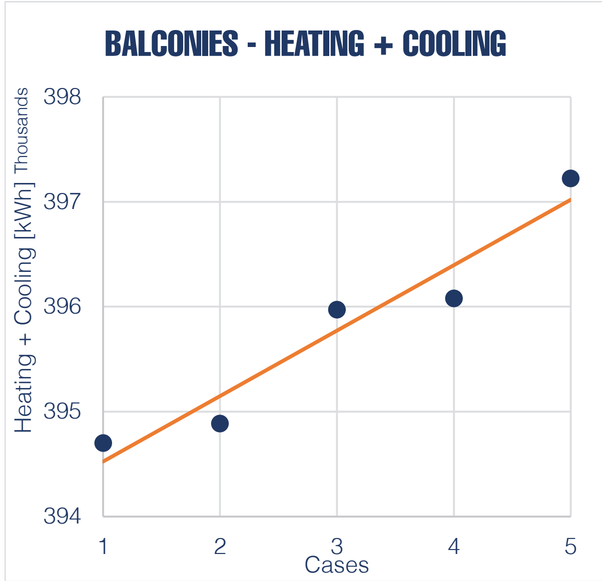

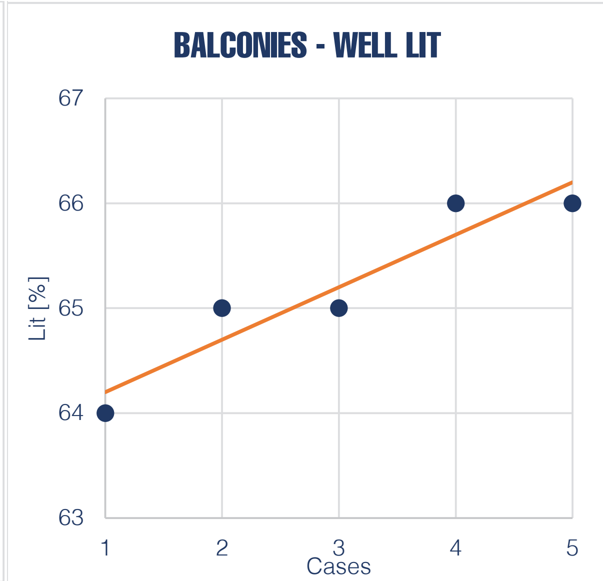

At the same time, the natural light has been established to be in a good amount for daylight reasons, with the purpose to have the best possible percentage of well-lit area on the floor plan.

As a consequence, the best result has been obtained by matching together the sum of heating and cooling demand with the well-lit percentage, resulting in an optimal length of these overhangs of 2,00 meters.

This length, other than being energetically helpful, is also an architectural advantage since a 2,00 m space is livable and enjoyable for the residents of the building.

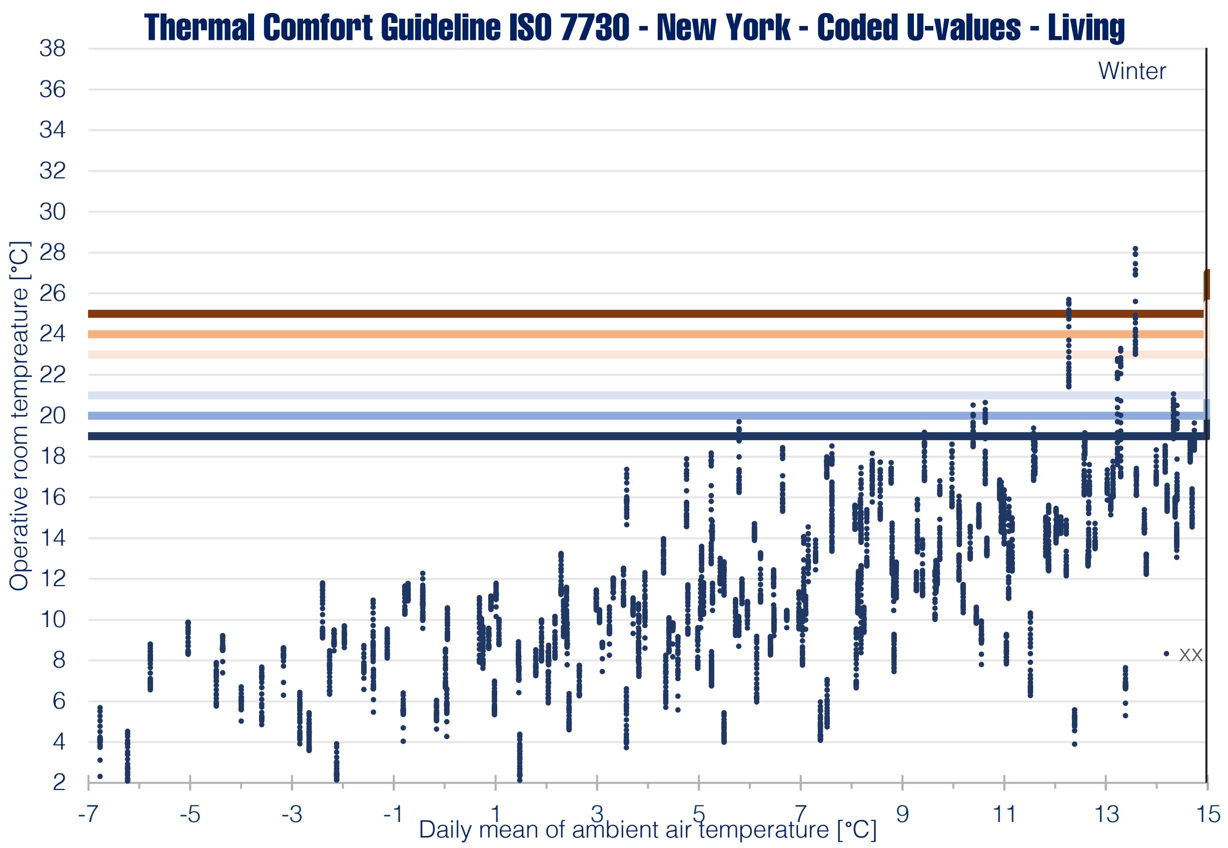

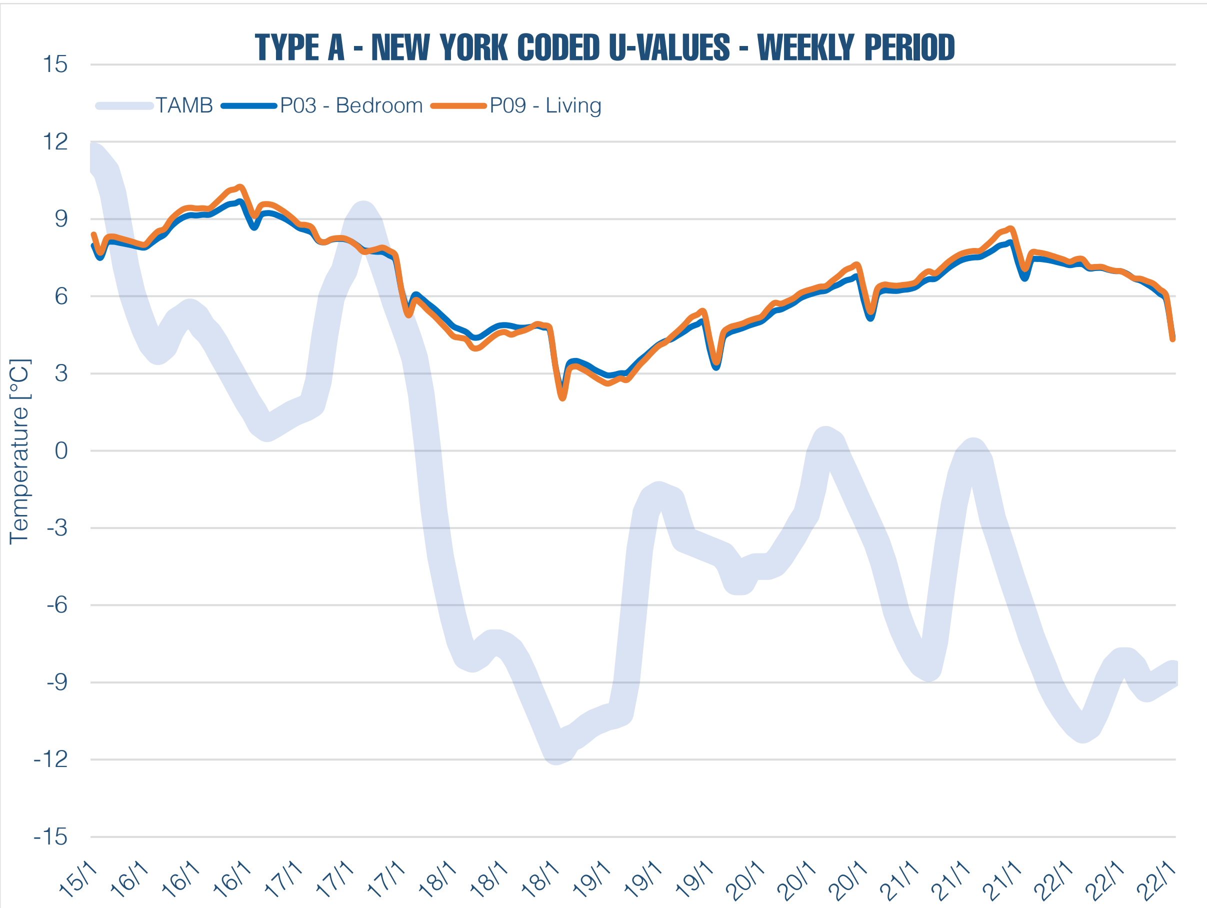

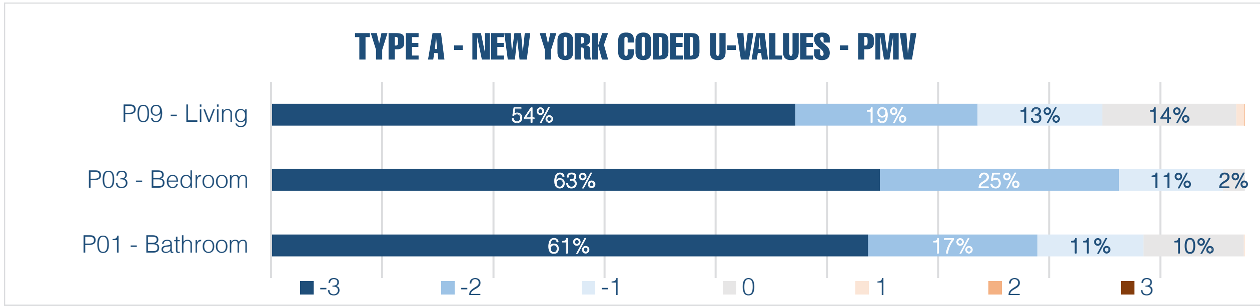

These first free run simulations consider a building with optimised balconies' lenght, optimised windows' size and New York minimum U-values.

This is to be considered as a starting point and as it is evident from the perceived comfort the internal conditions are very far from being satisfactory. In particular, most of the hours of the year are outside the comfort range because the temperature is too cold.The consider area, in this case, is the coldest apartment of the building, which is facing nort-west, in particular the living room, since it is the most representative room of the flat. In this way it is possible to state that the next passive strategies, focused to reduce the heating demand, will surely improve the overall internal comfort of the building.

8.8 – THE DESIGNED U VALUES

A further implementation of the building performance is given by the improvement of the thermal parameters of the technological elements. When designing the packages of the horizontal and vertical closures, the choice of every layer's material is done with the goal to reach the lowest possible U values, finding the right compromise between thermal performance and construction process.

The specific layers and thermal properties have been explained in the technological chapter, but they can be recalled here, to also be compared to the minimum required values of the New York Building Code.

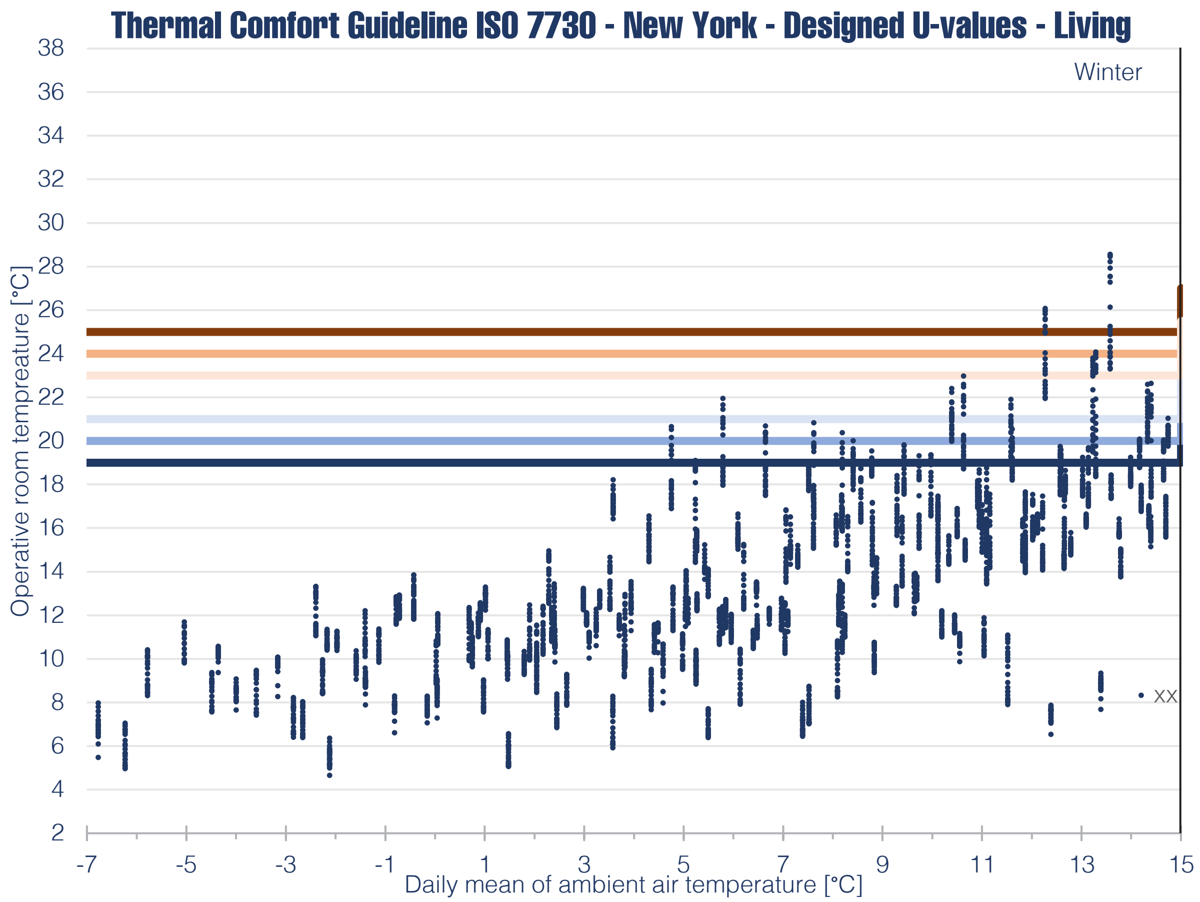

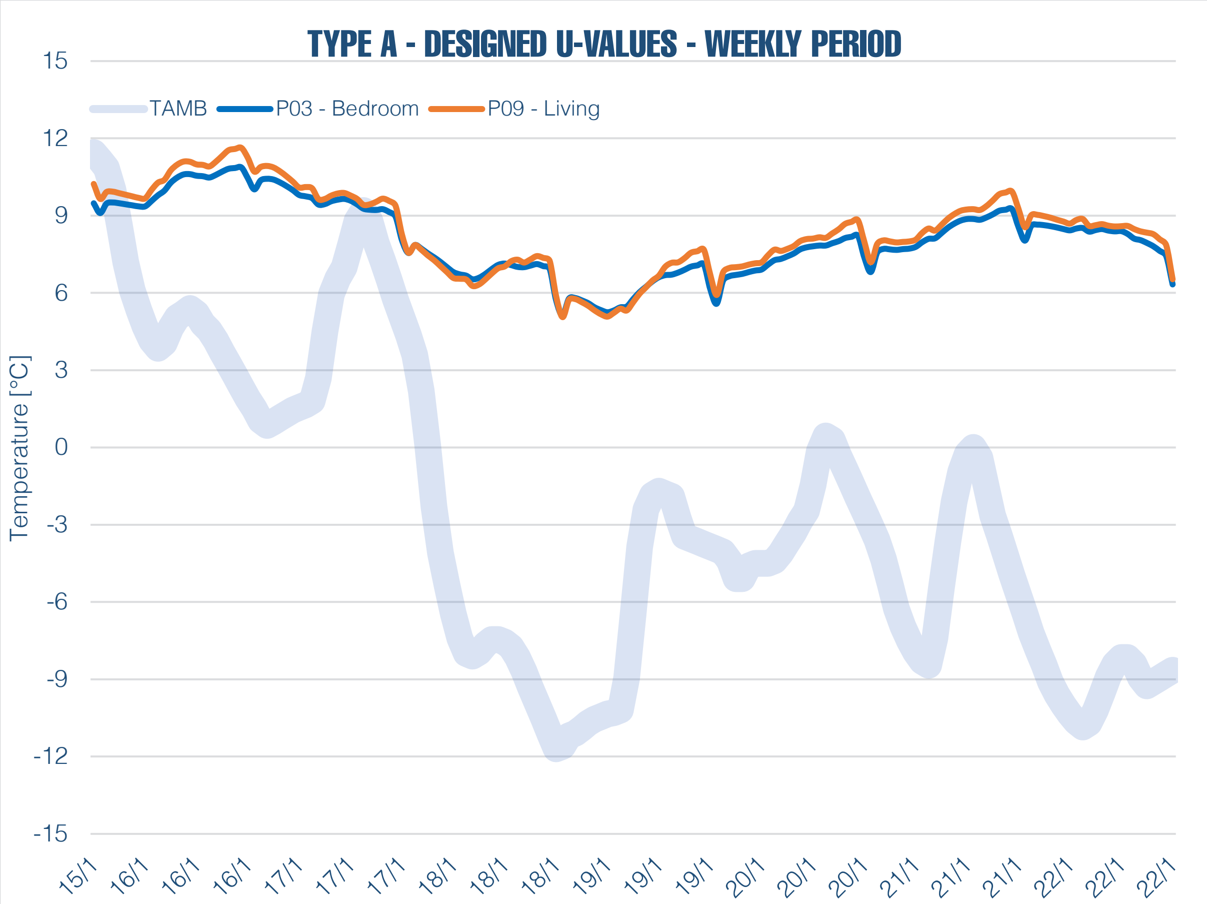

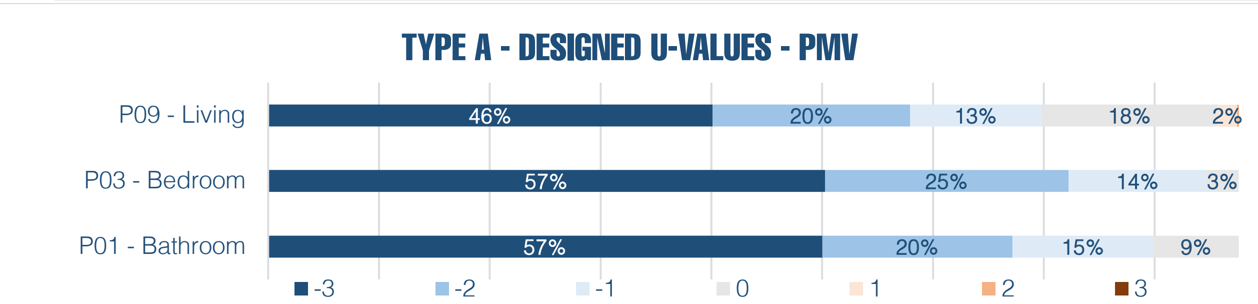

- U_{wall} = **0,150** < 0,465 W/m²K
- U_{roof} = **0,086** < 0,170 W/m²K
- U_{floor} = **0,129** < 0,266 W/m²K
- U_{window} = **1,235** < 1,98 W/m²K

At this point, the PMV index shows that the number of hours in the coldest range passes from 54% to 46%, while the comfort range (-0,5 < PMV < 0,5) has an overall improvement equal to 4%. Also, the coldest registered temperature, which was 2°C in the coldest week of the year, is now up to 5°C.

8.9 – THE SOLAR HEAT GAIN FACTOR (SHGC)

The glass of the windows and of the curtain wall requires an optimization too. The customization is about the solar gain factor (SHGC), a dimensionless index between 0 and 1 which is the ratio between the incoming solar energy (sum of the energy passed directly through the glass and the one absorbed by it and retransmitted inside) and the incident solar energy. This parameter can be referred to the glass only or to the combination of glass and solar control device.

To better understand how a different value of this parameter would affect the performance of the building, many simulations have been run and the results were analyzed in terms of energy demand and internal comfort of the environment, in order to find the best combination of the two. The same optimization has been made for the glass of the first two levels' curtain wall.

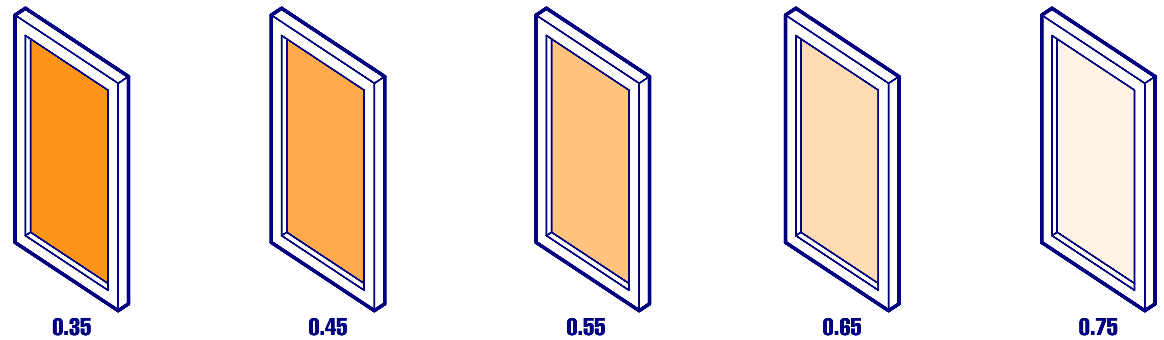

8.9.1 – THE APARTMENTS' WINDOWS

The results of the simulations of the north-west facing apartment (type A) show that this is the coldest zone of the building, as it is evident in the PMV graphs previously discussed.

A high value of the solar factor would mean increasing the temperature of the zone, but a too high number would create a too-warm apartment.

The other two apartments which were considered are the small studio facing south (resulted in the hottest one), and the attic at the last floor, that is the biggest and with many windows on every side of the building.

As a rebuttal that this g value works fine for the whole building, it is important to check if these two apartments get too hot with such a solar factor.

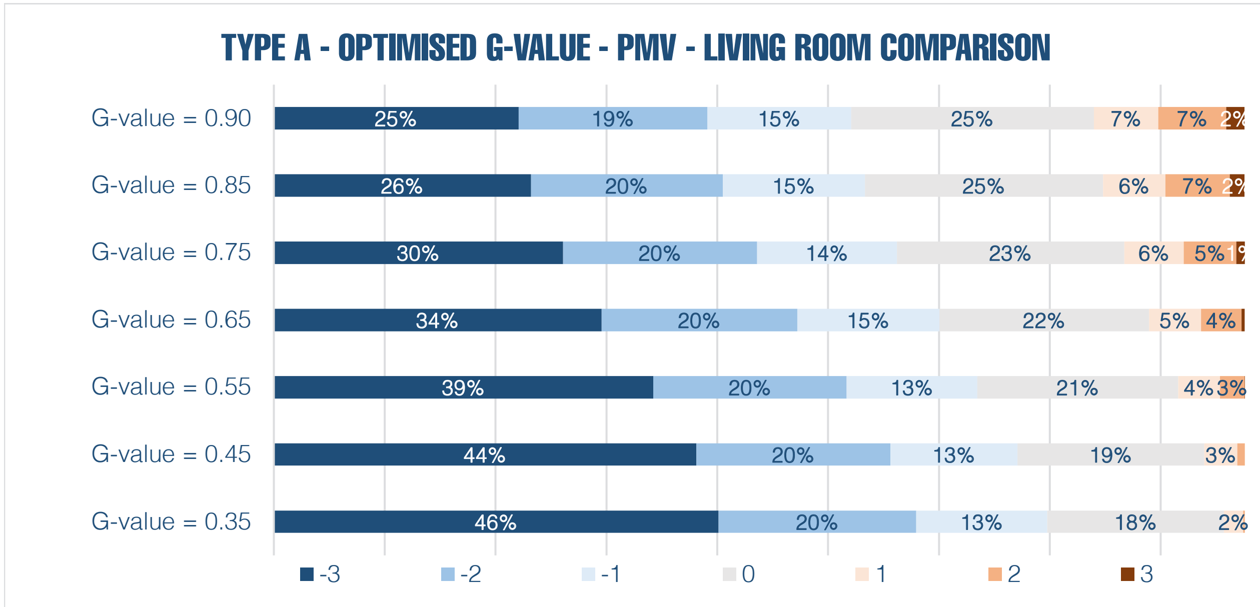

These data refers to the living room of the coldest apartment. The goal, in this case, is to reduce the heating demand and improve the overall comfort without creating overheating and cause too hot hours. Anyway, considering that the windows have been designe with a triple glass, it is obvious that a very high g value is not available.

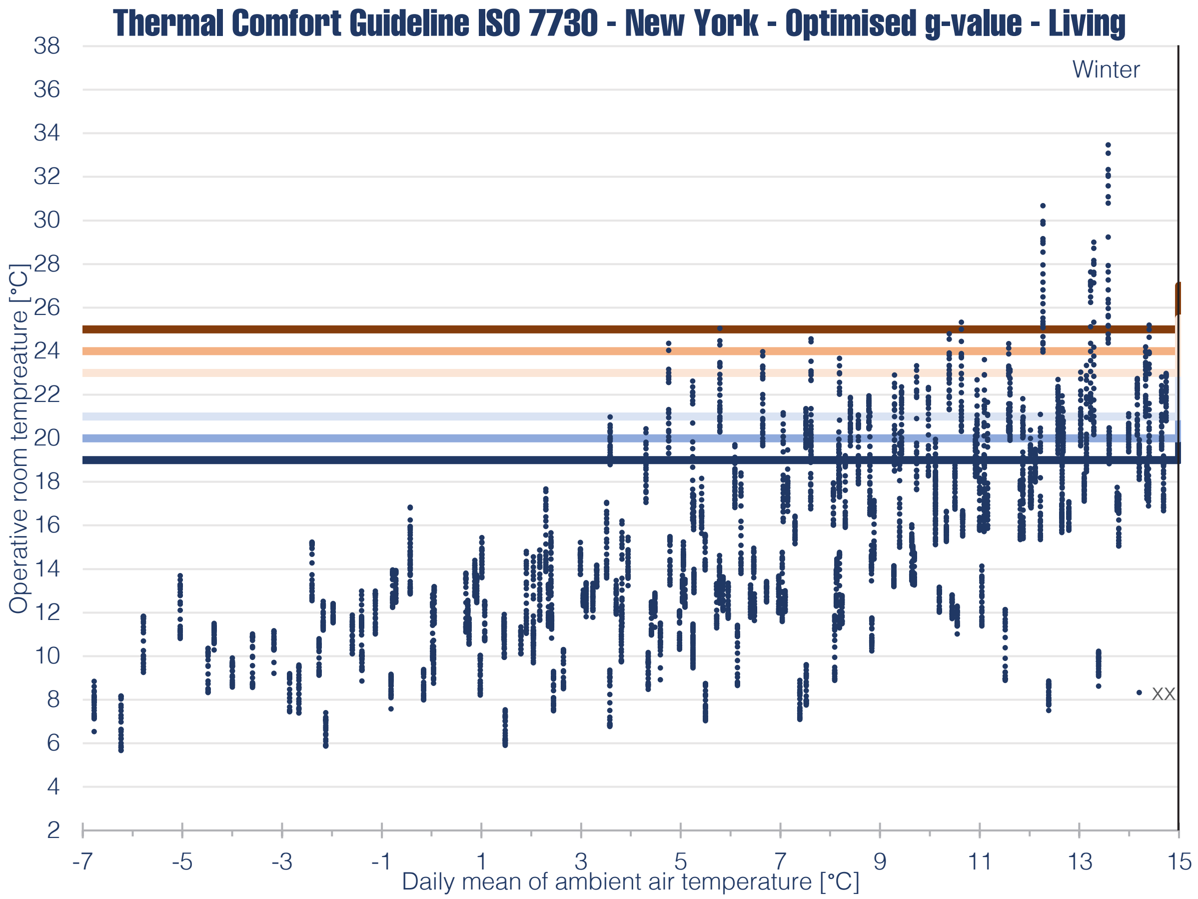

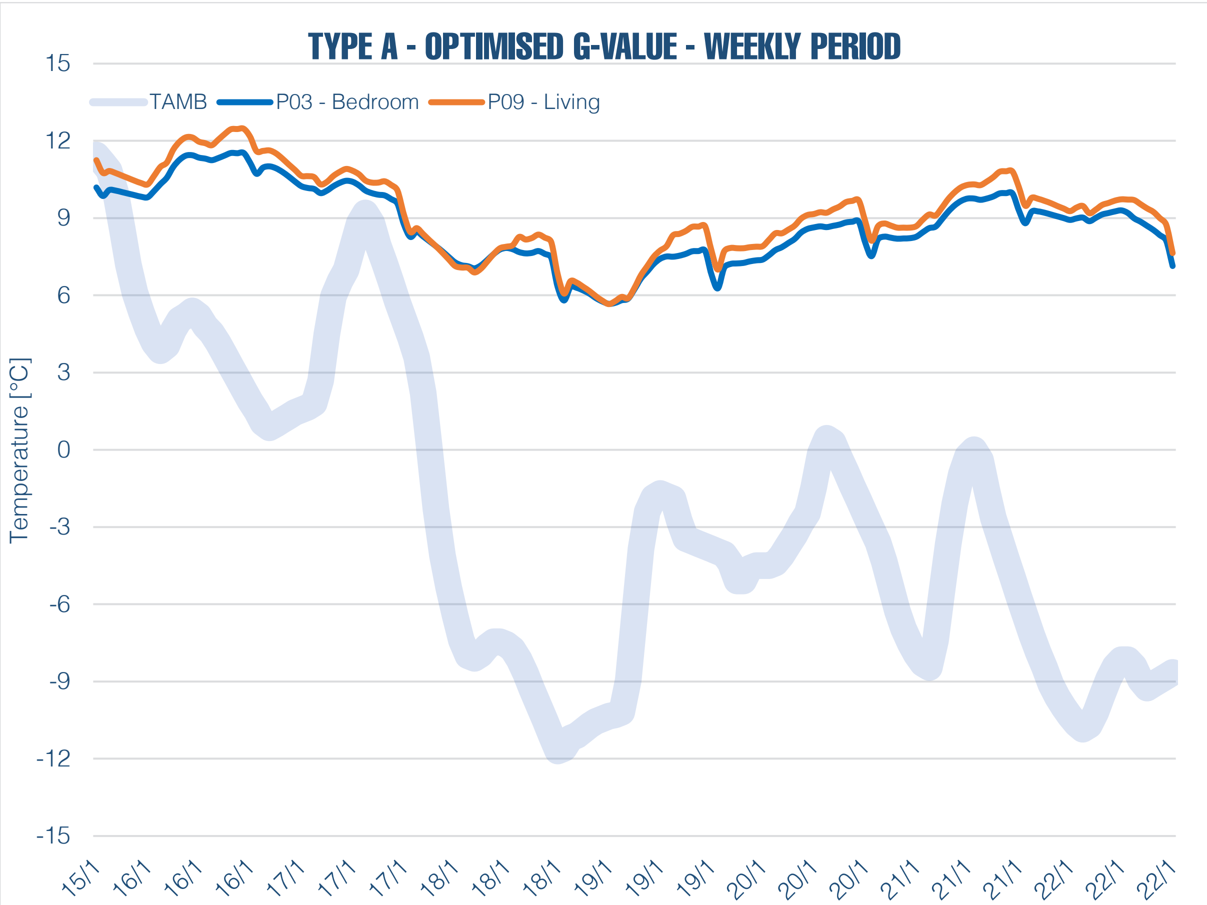

Politecnico di Milano, Master of Science in Building and Architectural Engineering
Steember - Steel and timber for a high rise building in Queens, New York
Chinnici Federico - **Maranesi** Marco

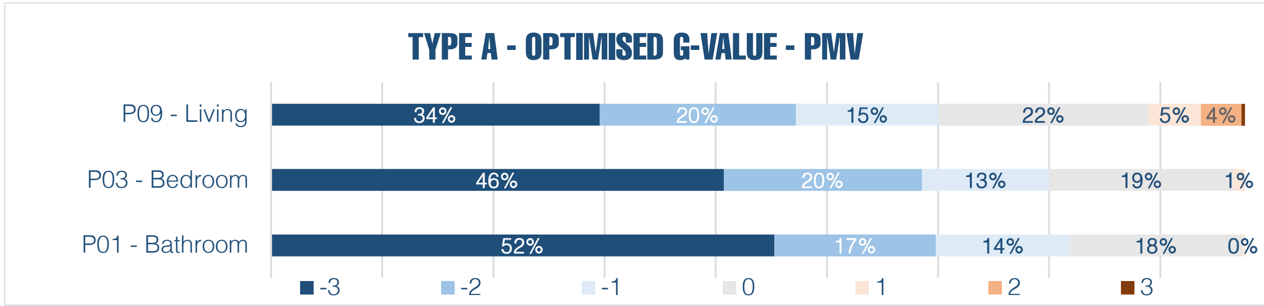

Considering the obtained results, the chosen g value is 0,65; commercial triple glazed windows can reach that value.

As a matter of fact, this number permits to increase the overall comfort from 18% to 22%, at the same time reducing the number of cold perceived hours of the 12% without increasing too much the number of hot hours.

As a verification, the same simulations have been analysed in the hottest apartment which faces the south (type B), proving that this value does not create over heating.

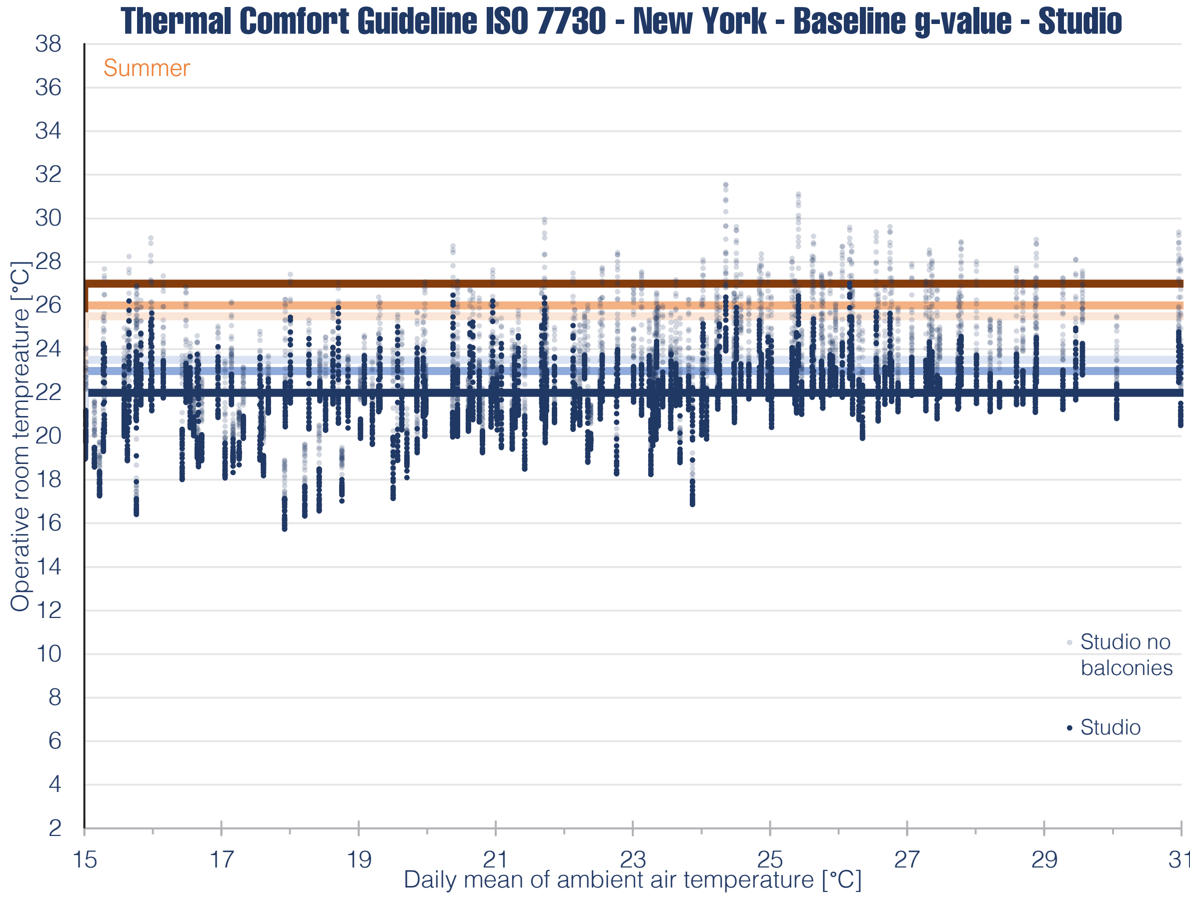

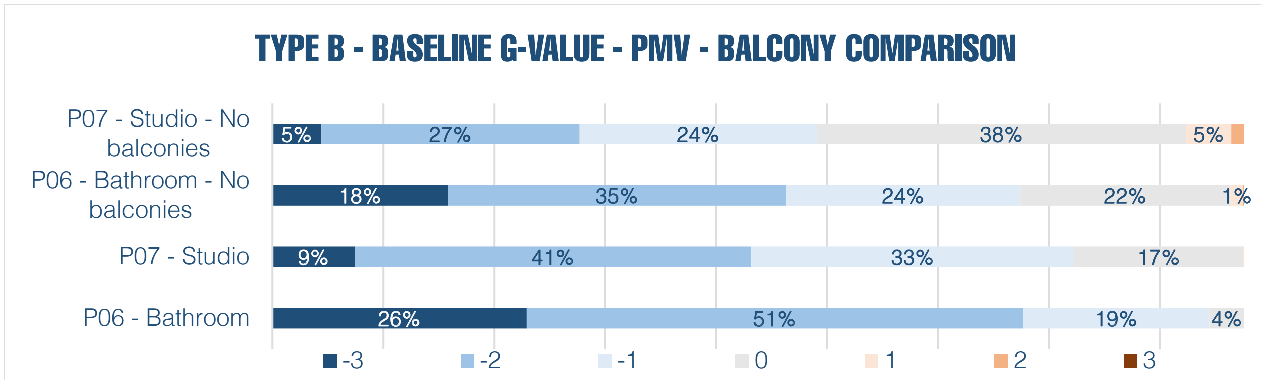

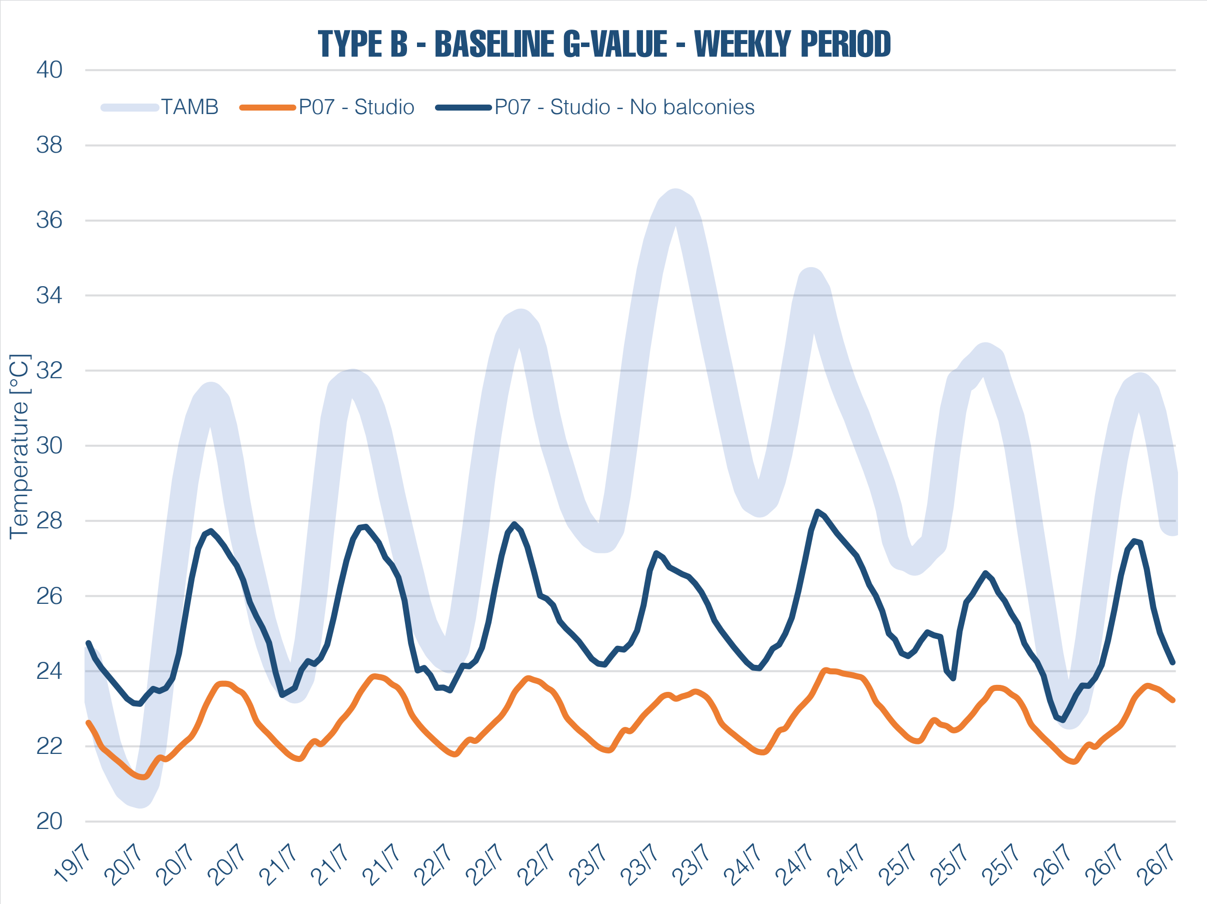

The graphs output that in the type B apartment there is no overheating despite the medium-high g value of 0,65. This is also achieved thanks to the presence of the balconies which were previously optimised and which help to cool down the internal temperature in the hot season.

The comfort chart demonstrates that the simulation run without the balconies would cause a considerable number of hours to be too hot for the comfort, in particular it is clear that without the balconies the internal temperature can reach 28°C in the hottest week of summer, which means using the cooling system. While, with the shadows projected by the balconies, the cooling system can be activated only in exceptional cases since the hottest temperature registered is 24°C.

8.9.2 – THE CURTAIN WALL

The first two levels have a big curtain wall on the whole façade. In this case, the solar radiation entering the rooms is much higher, resulting in higher solar gains. This, combined with the fact that the different intended use of these zones from the residential apartment has higher internal loads, makes the rooms hotter, as it is visible in the thermal comfort PMV graphs.

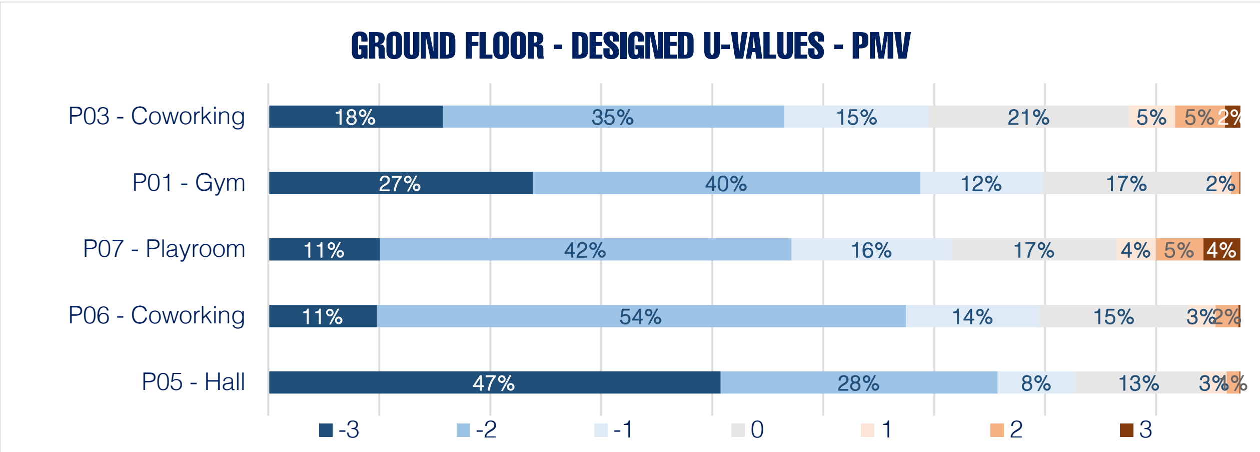

Politecnico di Milano, Master of Science in Building and Architectural Engineering
Steember - Steel and timber for a high rise building in Queens, New York
Chinnici Federico - **Maranesi** Marco

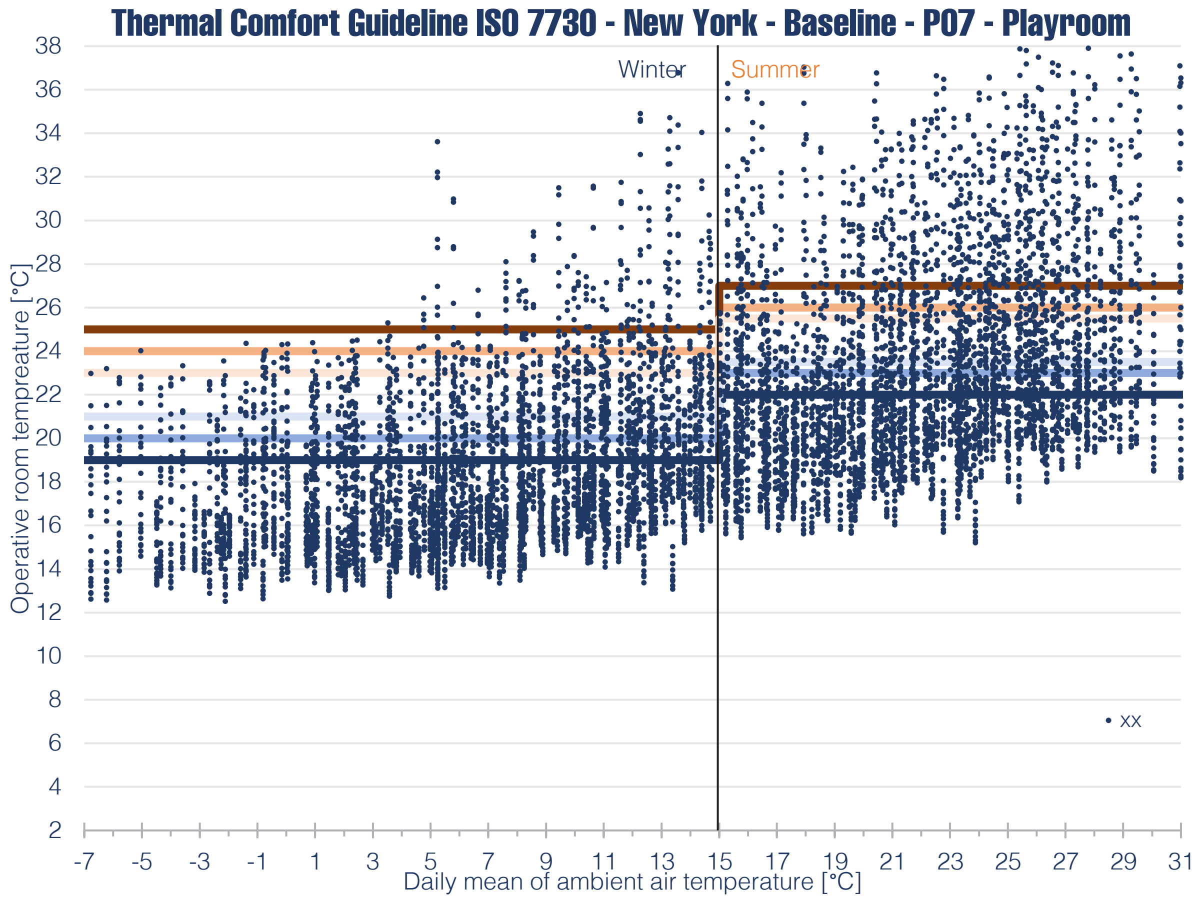

The playroom at the ground floor results to be the hottest room of the firts two floors. Considering that many hours through the year are outside the comfort range because too hot, it would not make sense to increase the g value more than 0,35, which is the first case considered.

In conclusion, there is no need of a passive strategy with the goal to reduce the heating demand.

8.10 – THE ACTIVE SHADING SYSTEM

After defining the best kind of glass, an active shading system is obviously required. This would be helpful in terms of energy efficiency, but it is also indispensable for the inhabitants since every resident of the building should have the freedom to decide how much light is wanted in the room, from fully enlightened to completely dark.

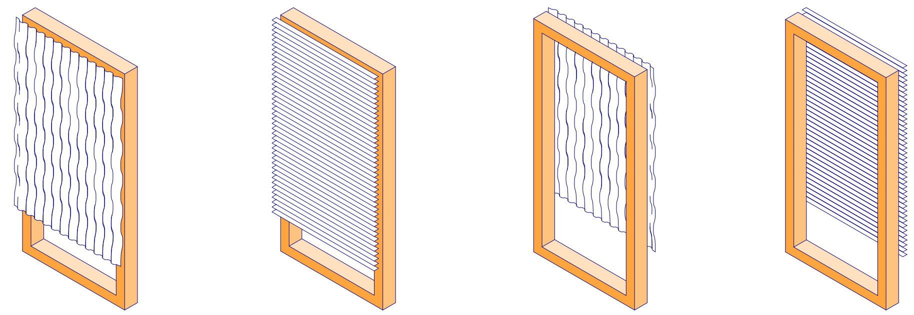

8.10.1 – THE APARTMENTS' WINDOWS

The goal is to find the best shading device, the one that more improves the internal comfort. At this stage, after optimising the g value of the windows, the considered apartment is the biggest one which faces all the four façades. In this way, it is possible to manage both the heating and cooling system since the apartment under investigation deals with both cold an hot zones. Furthermore, it is logical to use one unique shading type for the total building.

The considered room is the double bedroom, since it previously resulted as the hottest one.

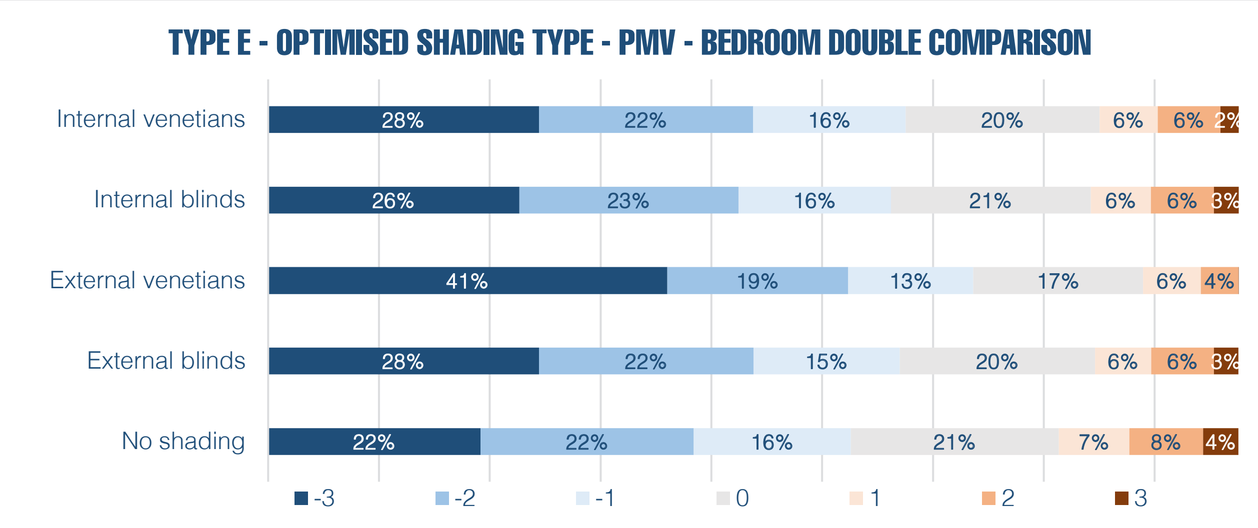

The external venetians are the ones which cause the highest number of cold hours, but, since the goal is to have the lower cooling necessity, they are the best solution because there are no hot perceived hours (PMV in class 3) throughout the whole year.

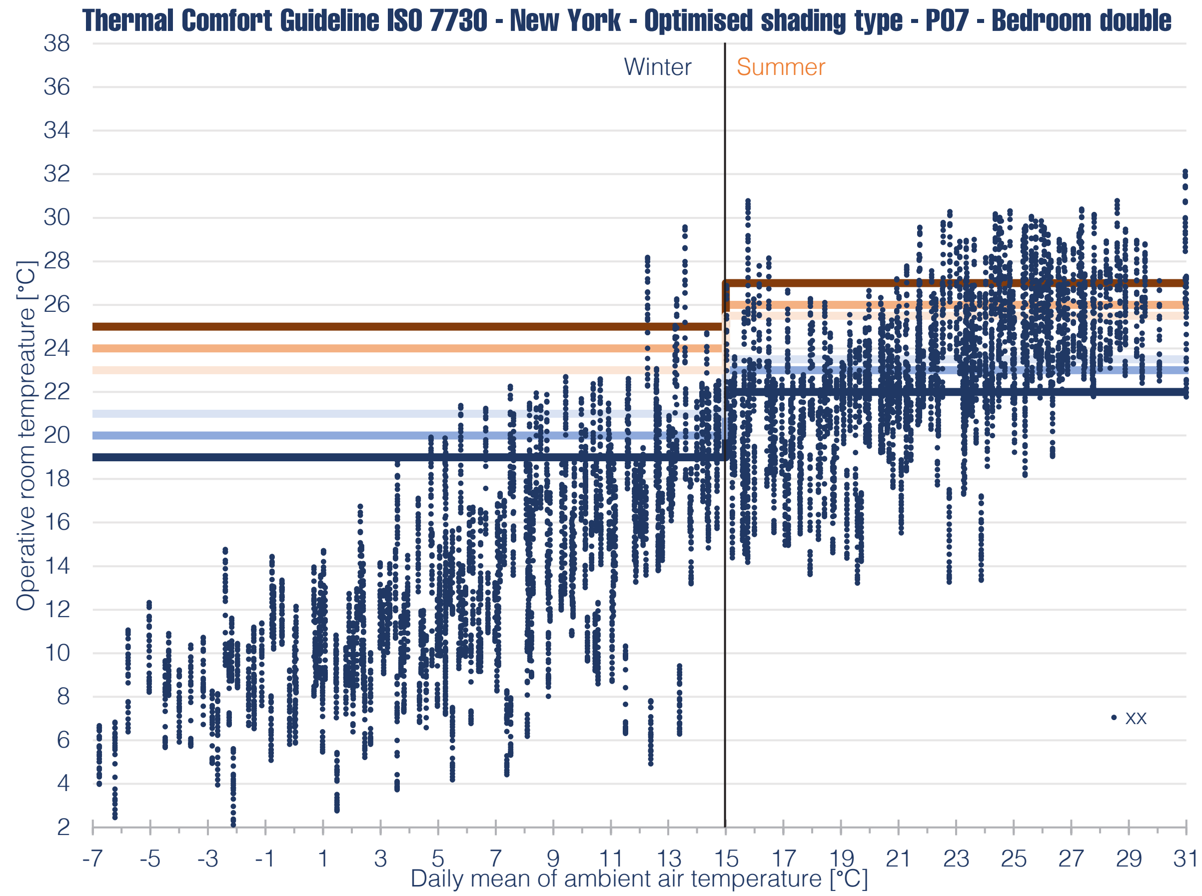

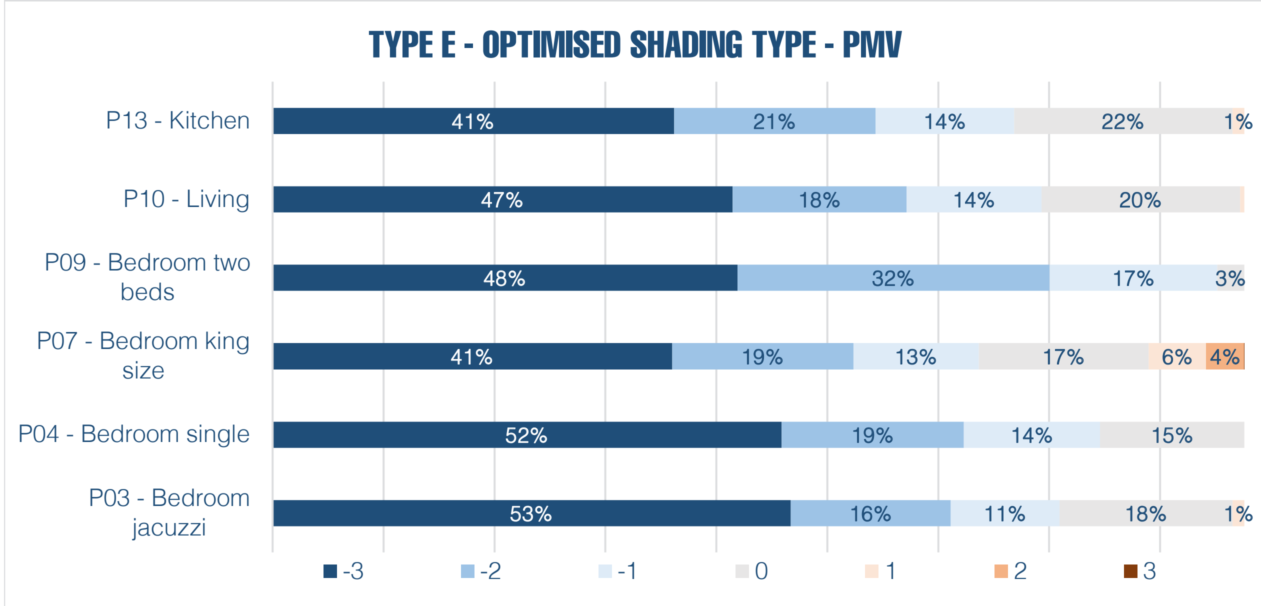

Also with the optimised shading system the double bedroom is the hottest one while the bedroom with two single beds results in being the coldest as it is evident in the temperature profiles registered in the hottest week of the year.

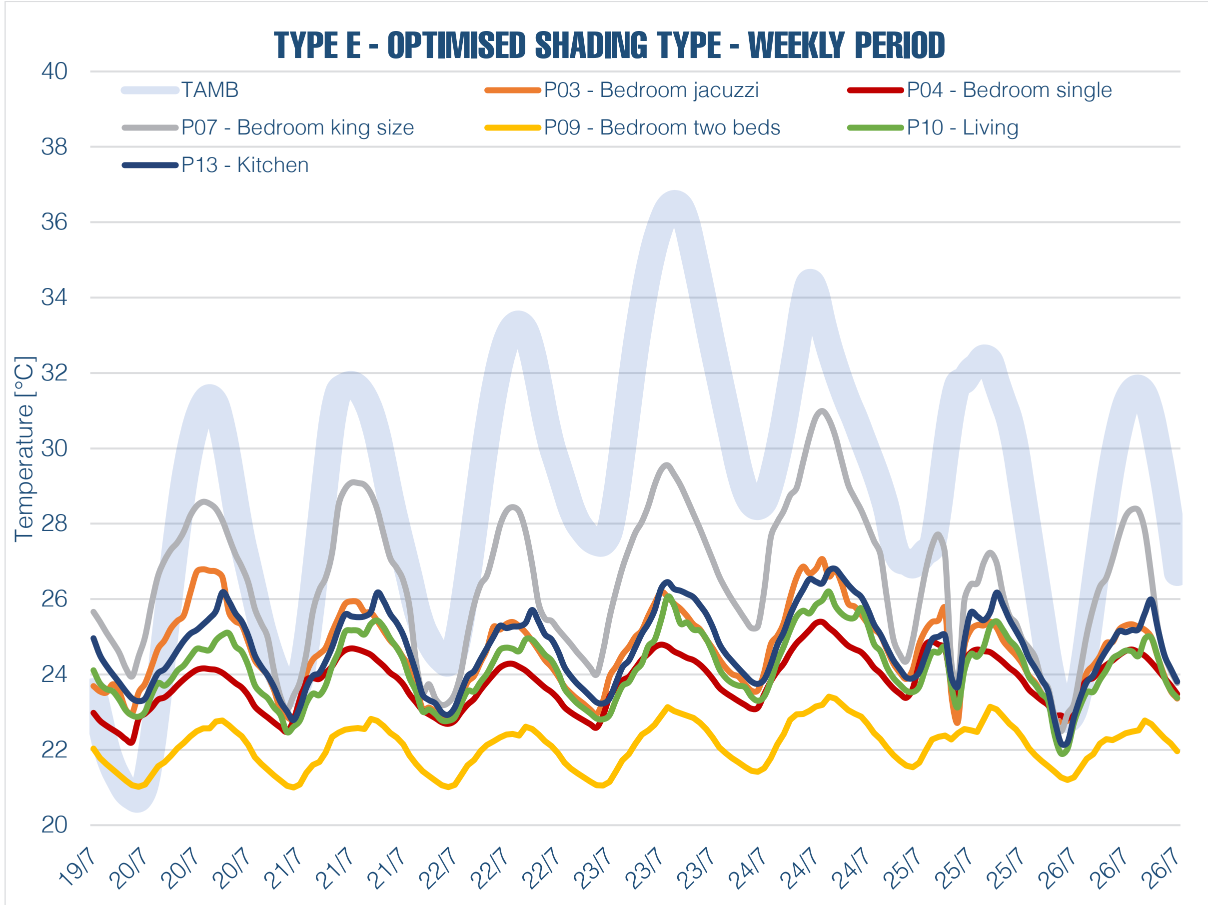

8.10.2 – THE CURTAIN WALL

The shading system of the curtain wall, instead, is not optimized and its choice did not go through a selection process. In this case, in fact, the choice was driven by an architectural aspect: having an external shading system in front of a curtain wall would not be appealing and would ruin the façade, without considering the problem of maintenance and dirt.

This is why internal blinds were chosen. This solution is internal and does not affect the exterior appearance of the façade.

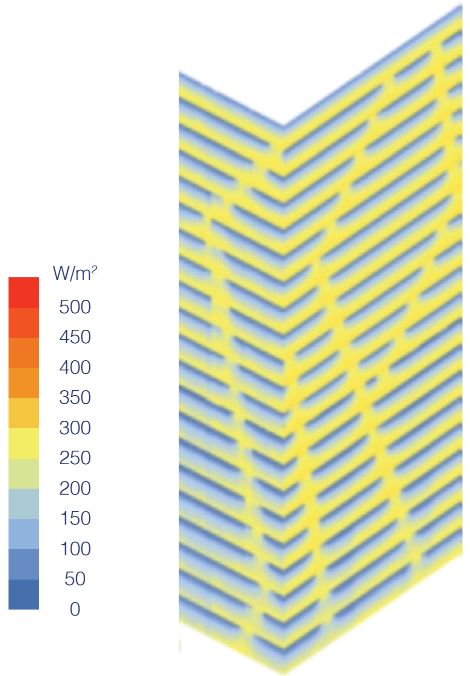

8.11 – THE SOLAR RADIATION ACTIVATING THE SHADING SYSTEM

The shading devices are going to be used as preferred by the users, according to their needs of light and privacy. Although, in periods of time in which people will not be present, it is important that the devices automatically activate to protect the internal rooms from the solar radiation.

To do so, it is important to select the correct solar radiation intensity [W/m²] at which they automatically activate. Thanks to a simulation run with Grasshopper and Ladybug it is possible to know the typical value of rays hitting the vertical surfaces of the four façades, and the maximum value reaches 350 W/m².

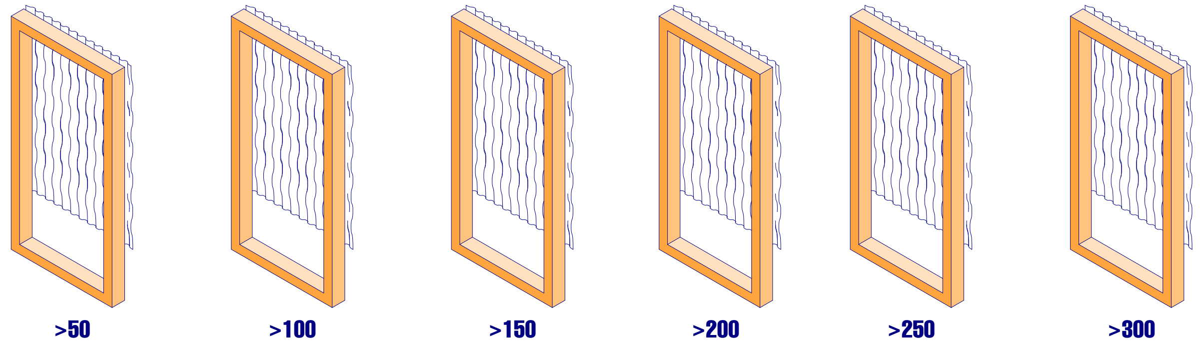

8.11.1 – THE APARTMENTS' WINDOWS

The apartments' windows are already enough shaded and protected by the balconies overhangs. So here the shading devices do not have an energy purpose, they will just be used by the users. Therefore, the automatic activation is set on 300 W/m², which is close to the maximum reached value.

8.11.2 – THE CURTAIN WALL

The internal blinds present on the first two levels are going to protect big and internally loaded rooms, so they need to be automatically activated not to let the solar gains negatively affect internal comfort.

Also in this case the considered room is the playroom, which is the hottest one.

The chosen value is 250 W/m² even if the difference with other values is not substantial. This selection is due to the fact that activating the shadings at ower values would mean having a sort of visual barrier towards the outside even in slightly cold periods of the year, affecting the emotional comfort of people inside who could be disturbed by not being free to watch out of the window.

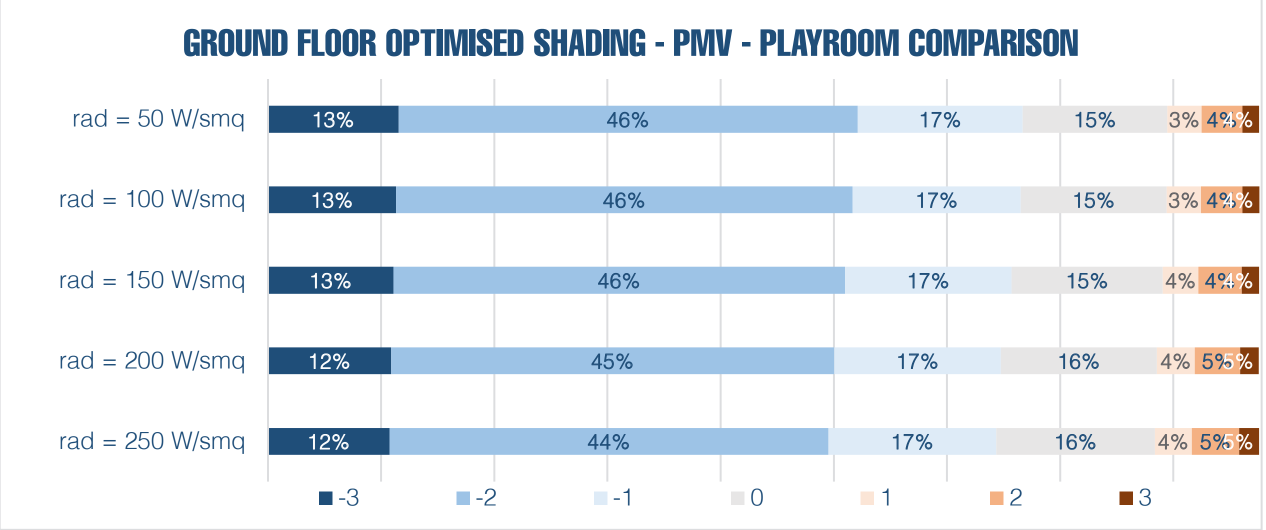

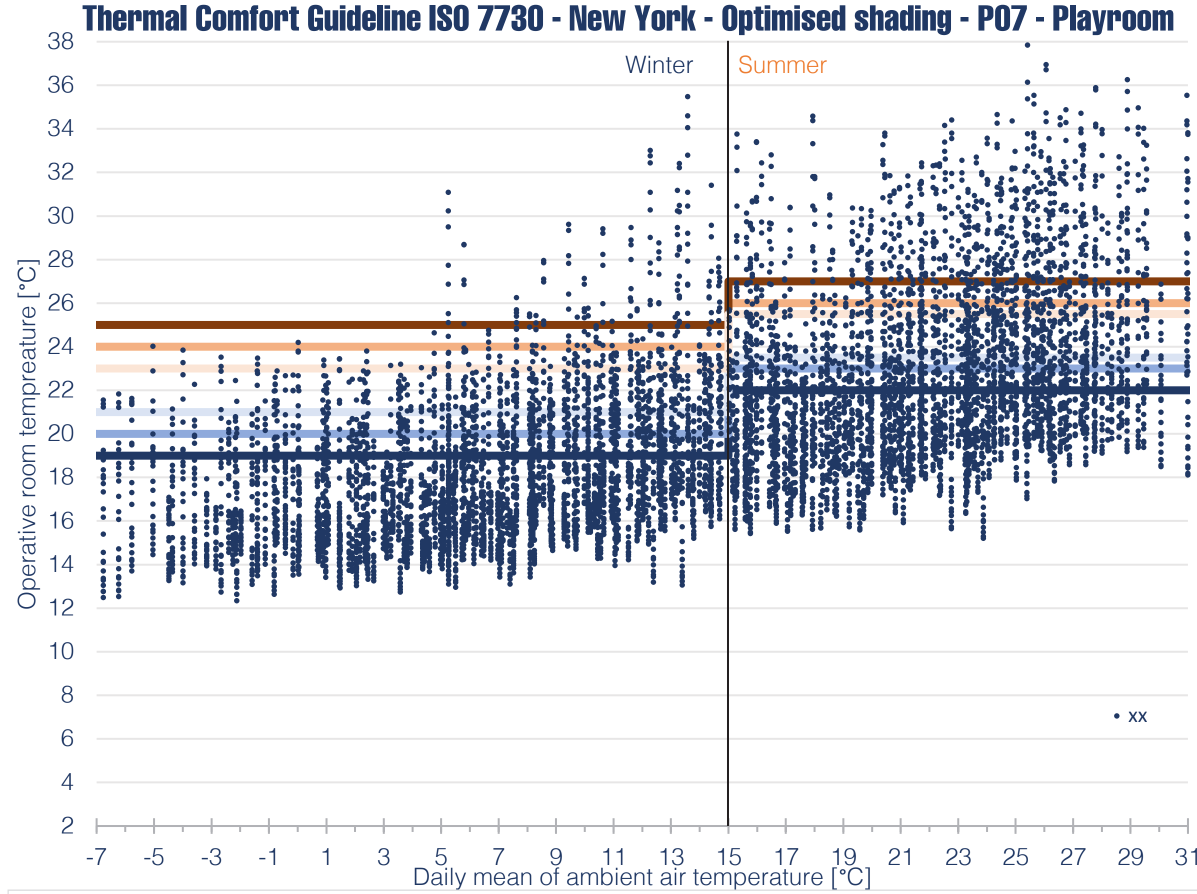

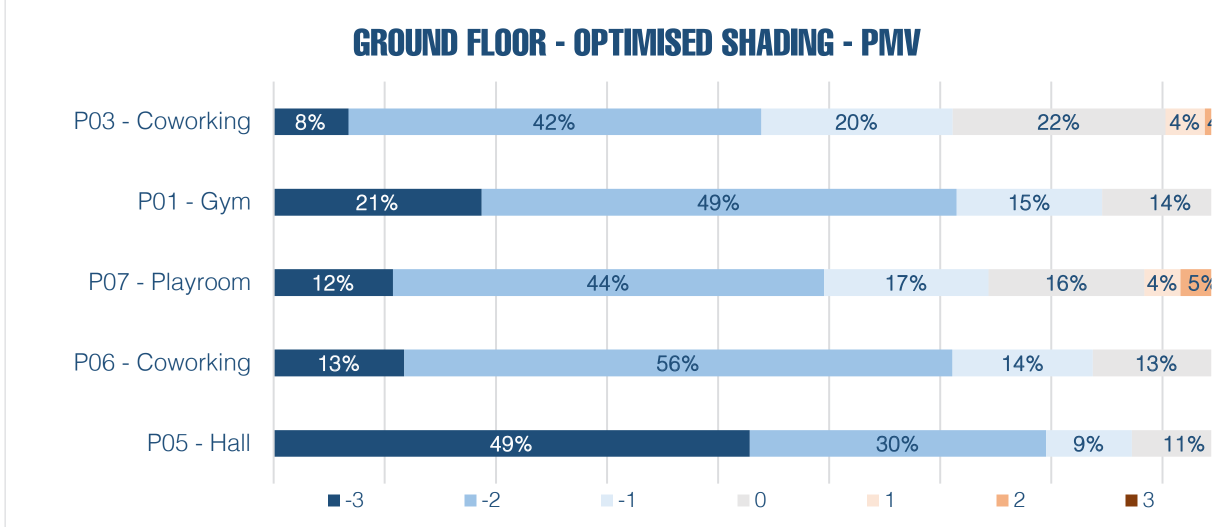

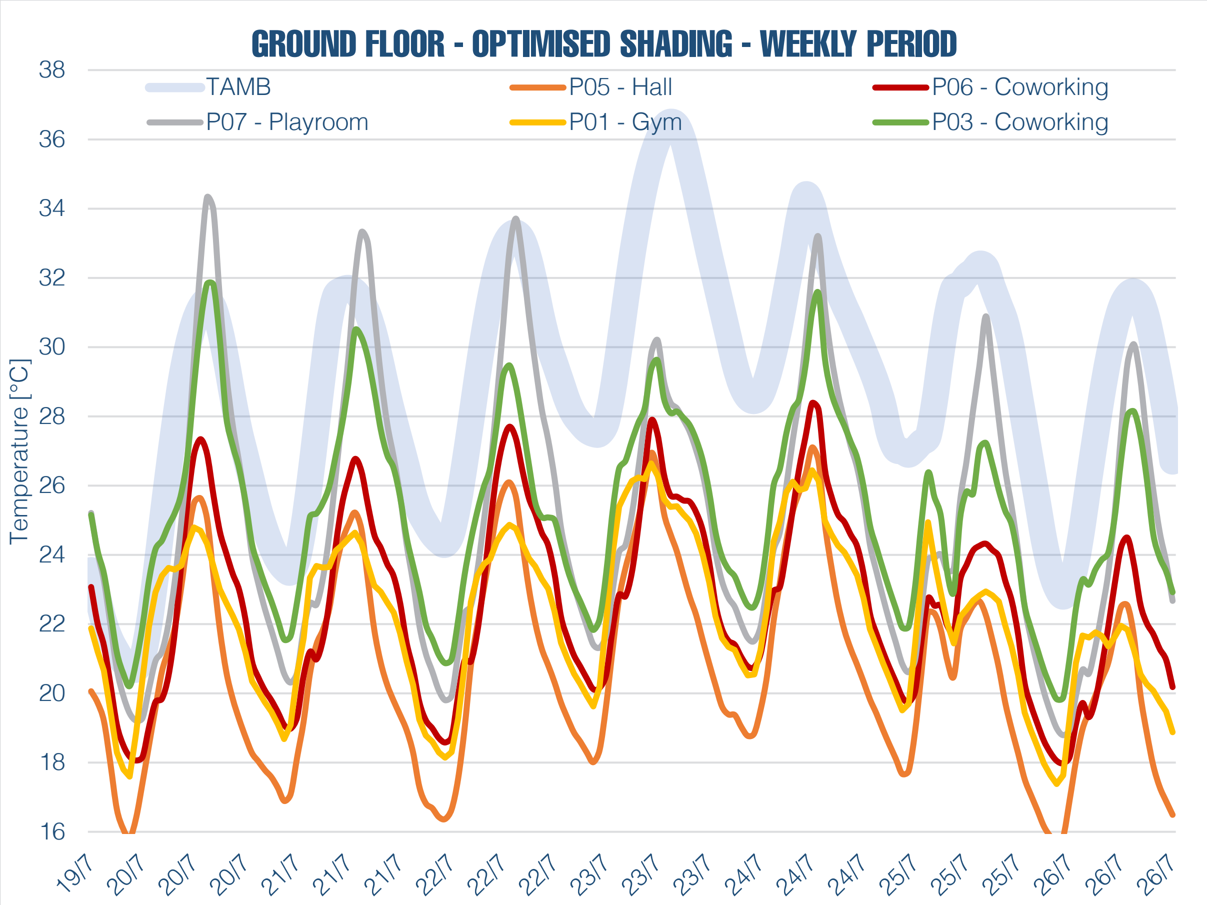

8.12 – THE MECHANICAL SYSTEMS

At this point, the mechanical systems have been switched on. No more free run simulations, it is important to quantify the energy demand of the building's systems and match it with the thermal comfort considered until now.

First of all, in order to choose the best kind of heating and cooling system, it is fundamental to compare the different energy demand that every typology requires.

8.12.1 – THE APARTMENTS

For the apartments' floors, from the 3rd to the 23rd, considering the residential use of the space, the choice is between hydronic terminals, meaning that the analyzed possibilities are fan coil units, radiant floor and variable refrigerant flow fan coils. These last ones have been simulated both air-cooled and water-cooled.

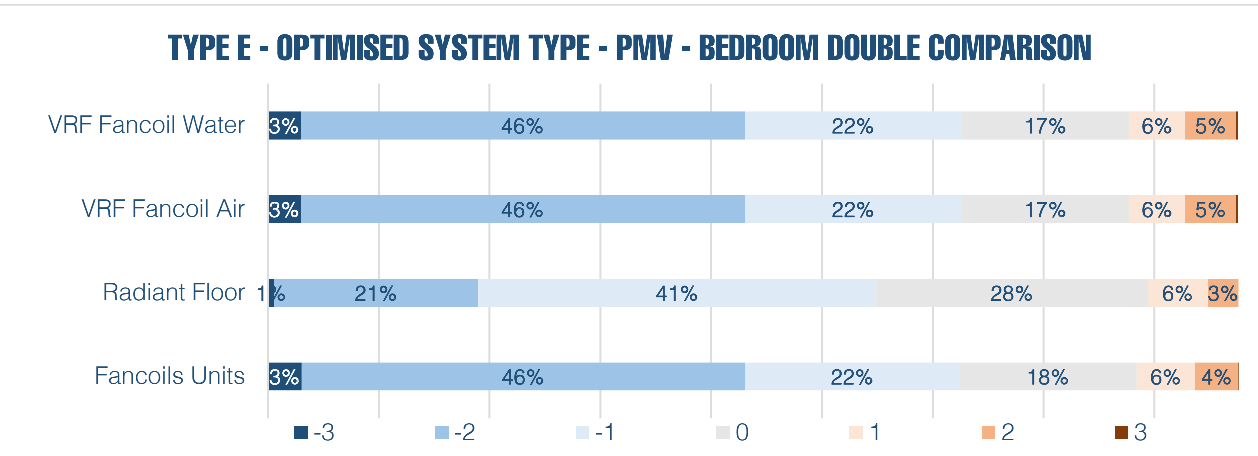

Politecnico di Milano, Master of Science in Building and Architectural Engineering
Steember - Steel and timber for a high rise building in Queens, New York
Chinnici Federico - **Maranesi** Marco

As it is visible in the graph, the radiant floor is not the best choice in terms of energy demand. However, given the considerable benefits that this system can give to the thermal comfort of the rooms, as previously explained, this is the chosen system, finding the best compromise between the two below graphs of the heating and cooling needs and of the internal comfort.

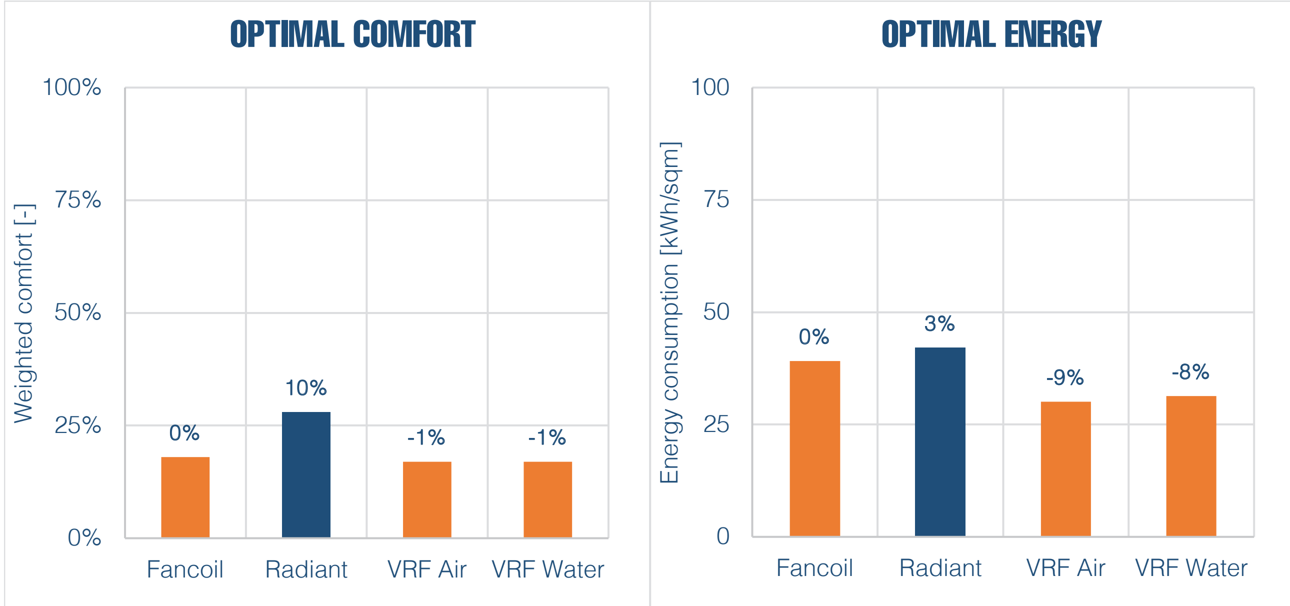

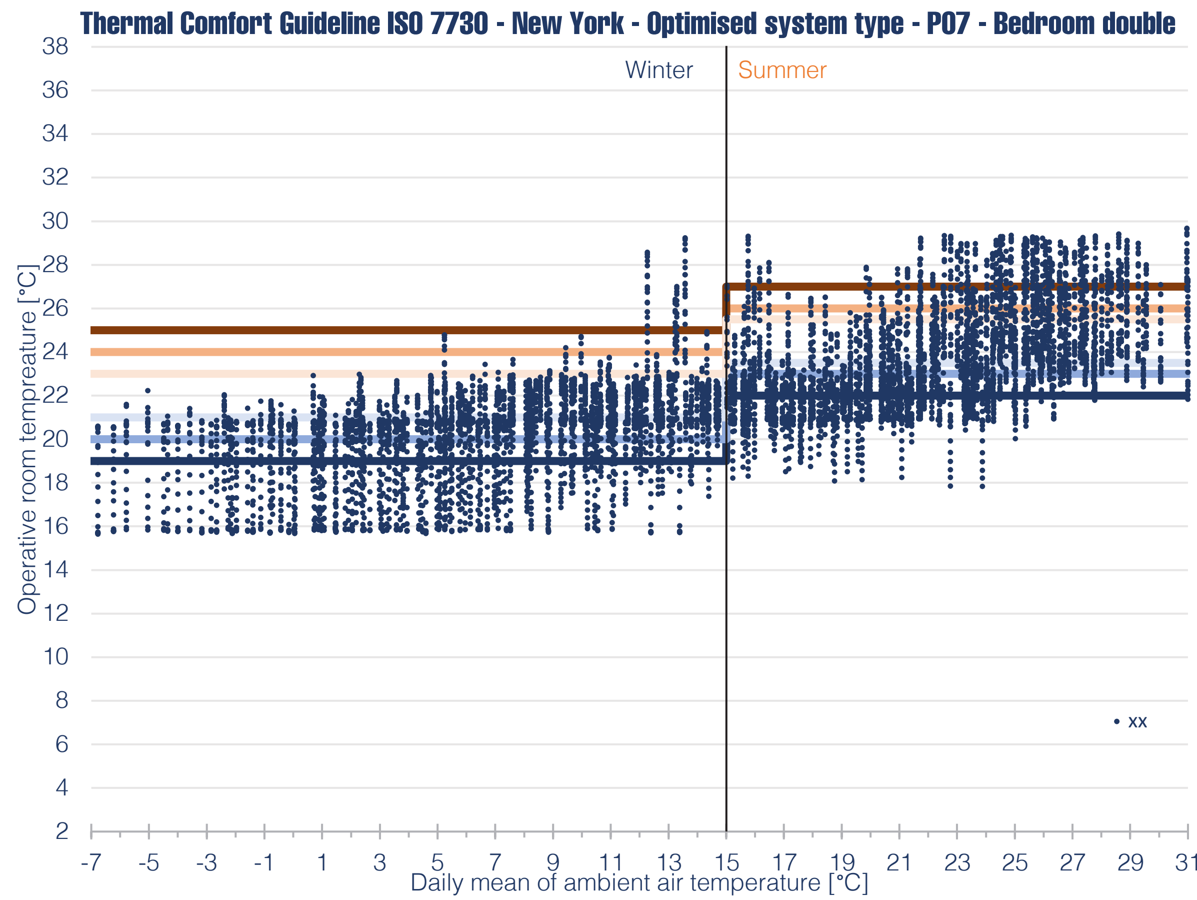

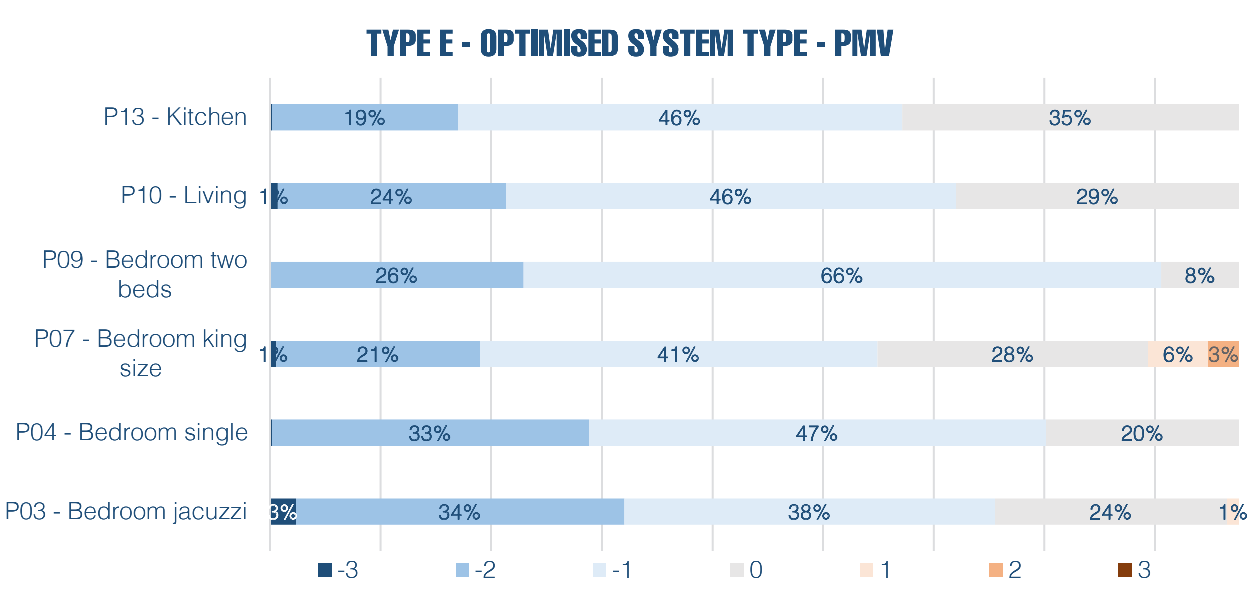

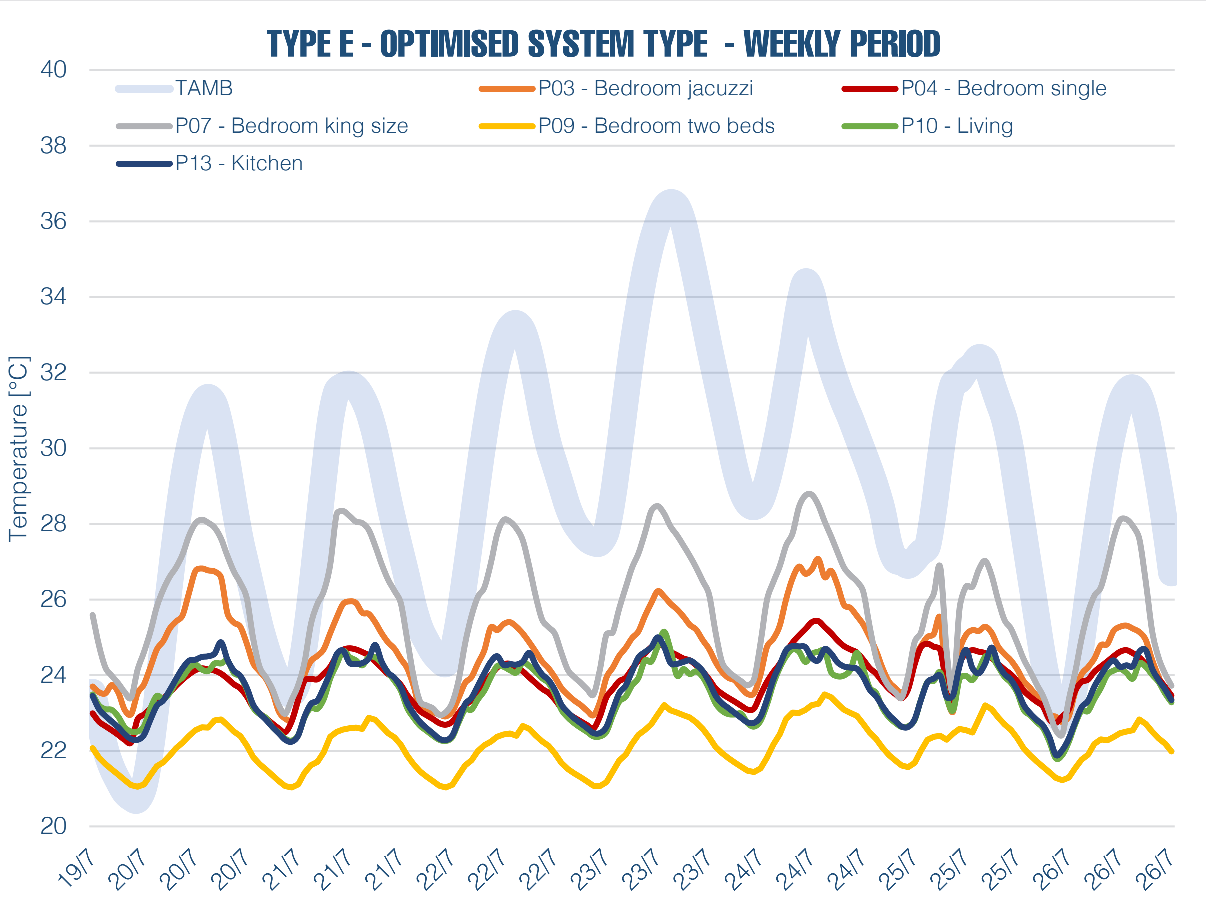

Politecnico di Milano, Master of Science in Building and Architectural Engineering
Steember - Steel and timber for a high rise building in Queens, New York
Chinnici Federico - **Maranesi** Marco

8.12.2 – THE BASEMENT

On the first two levels, the considered options are air systems, due to the different space use of the rooms and to the fact that in these areas the occupancy may be inconstant. Such plants, in fact, allow reaching the desired temperatures in a shorter period of time, if a change is suddenly needed.

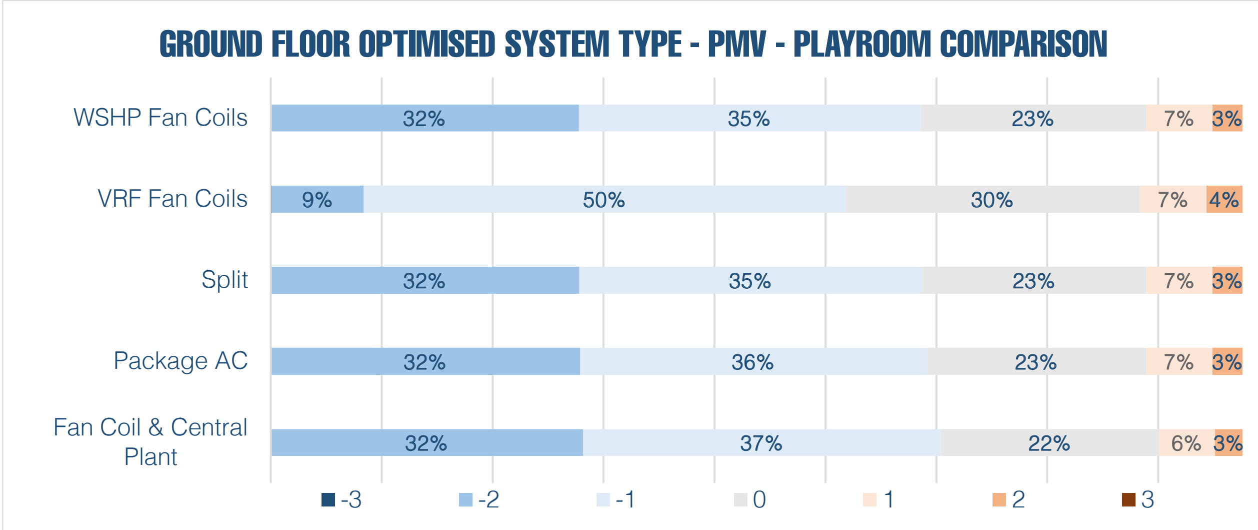

Matching the two hown graphs, in this case, the optimal solution is variable refrigerant flow fan coils, which manage to reach thermal comfort with low energy demand.

This type of system, even if slightly more consuming than the splits, guarantees a higher value of thermal comfort and this is why it is chosen kind of system.

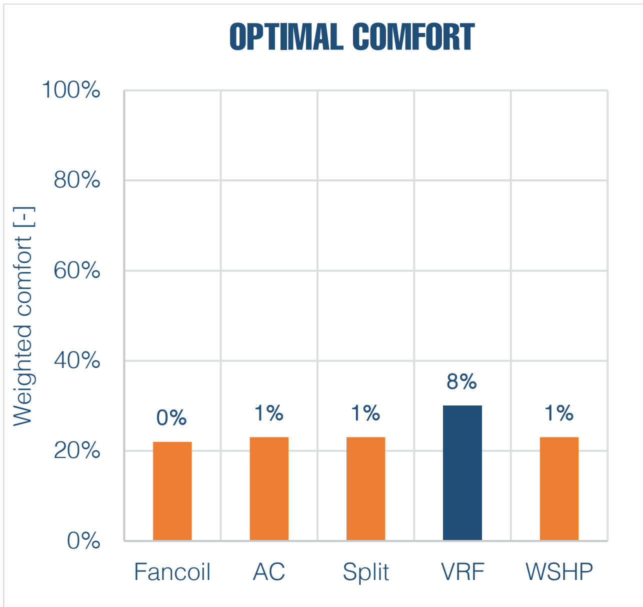

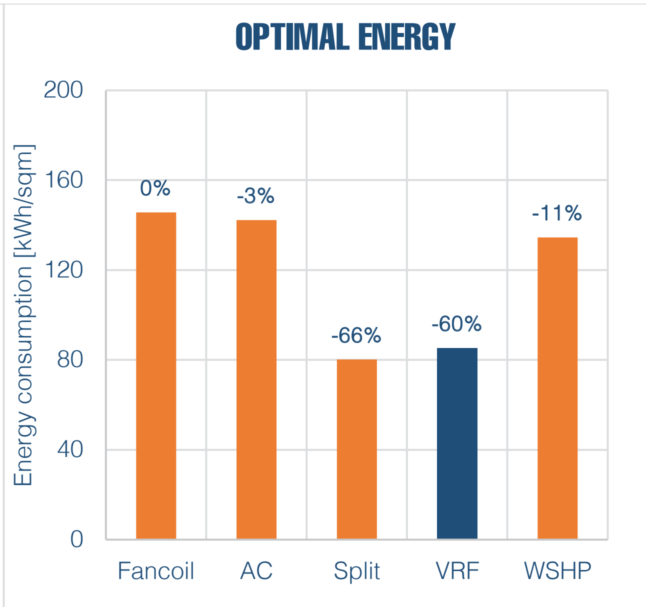

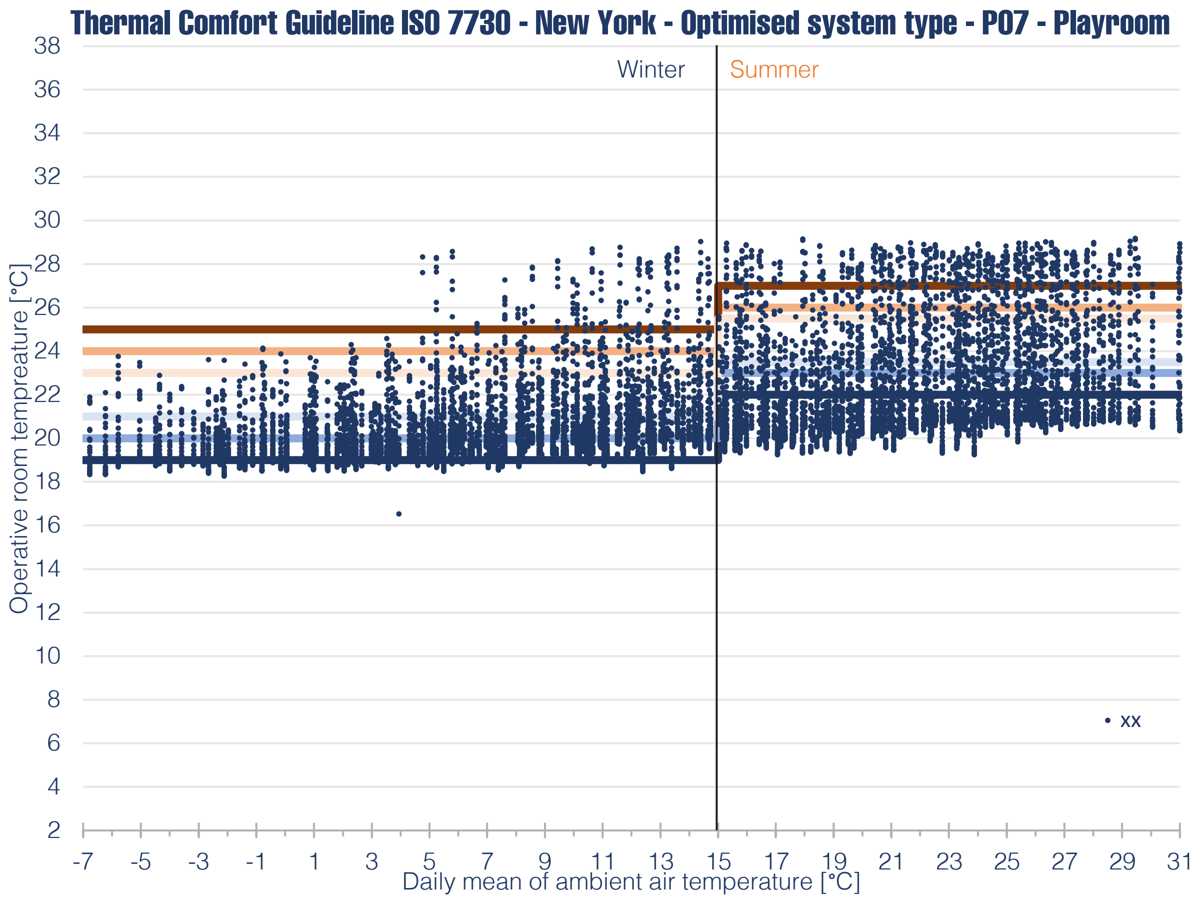

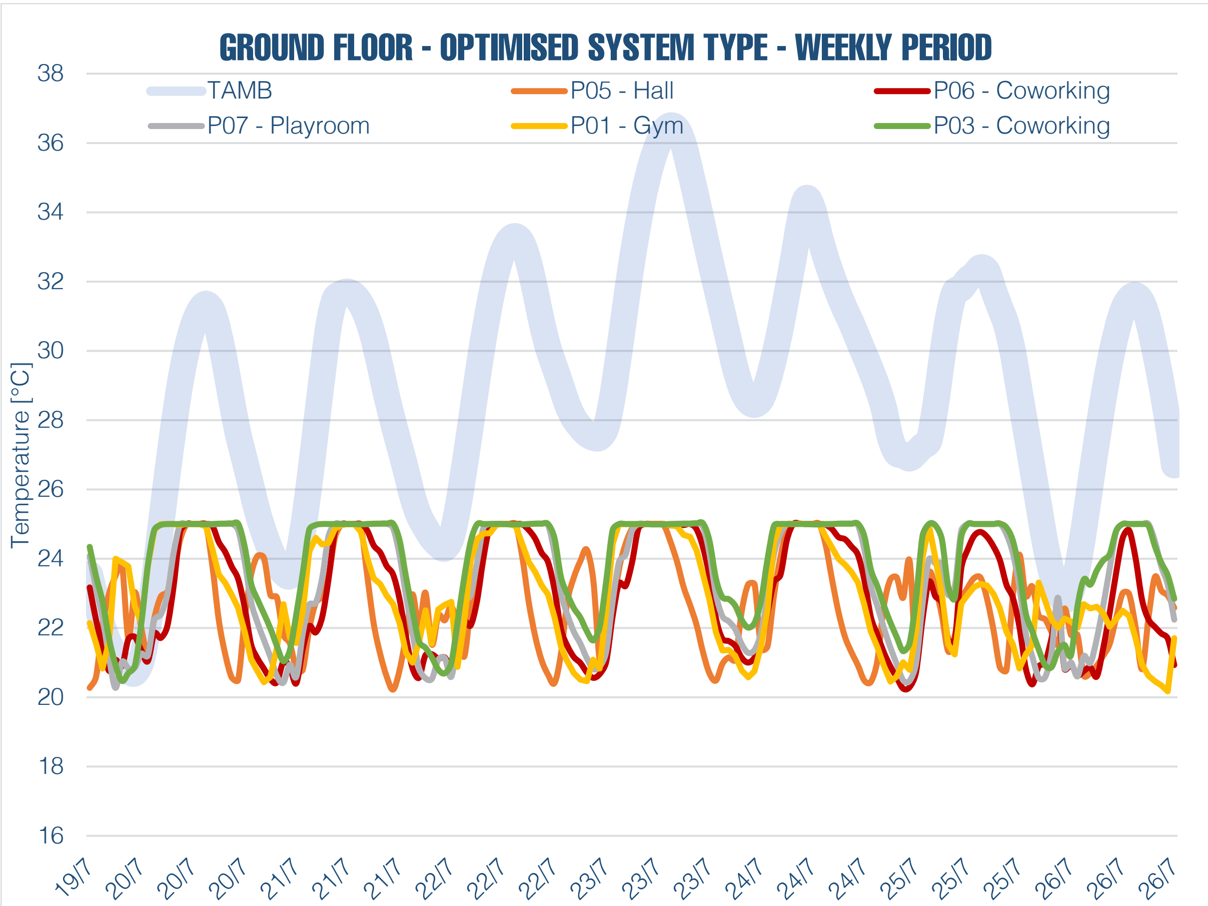

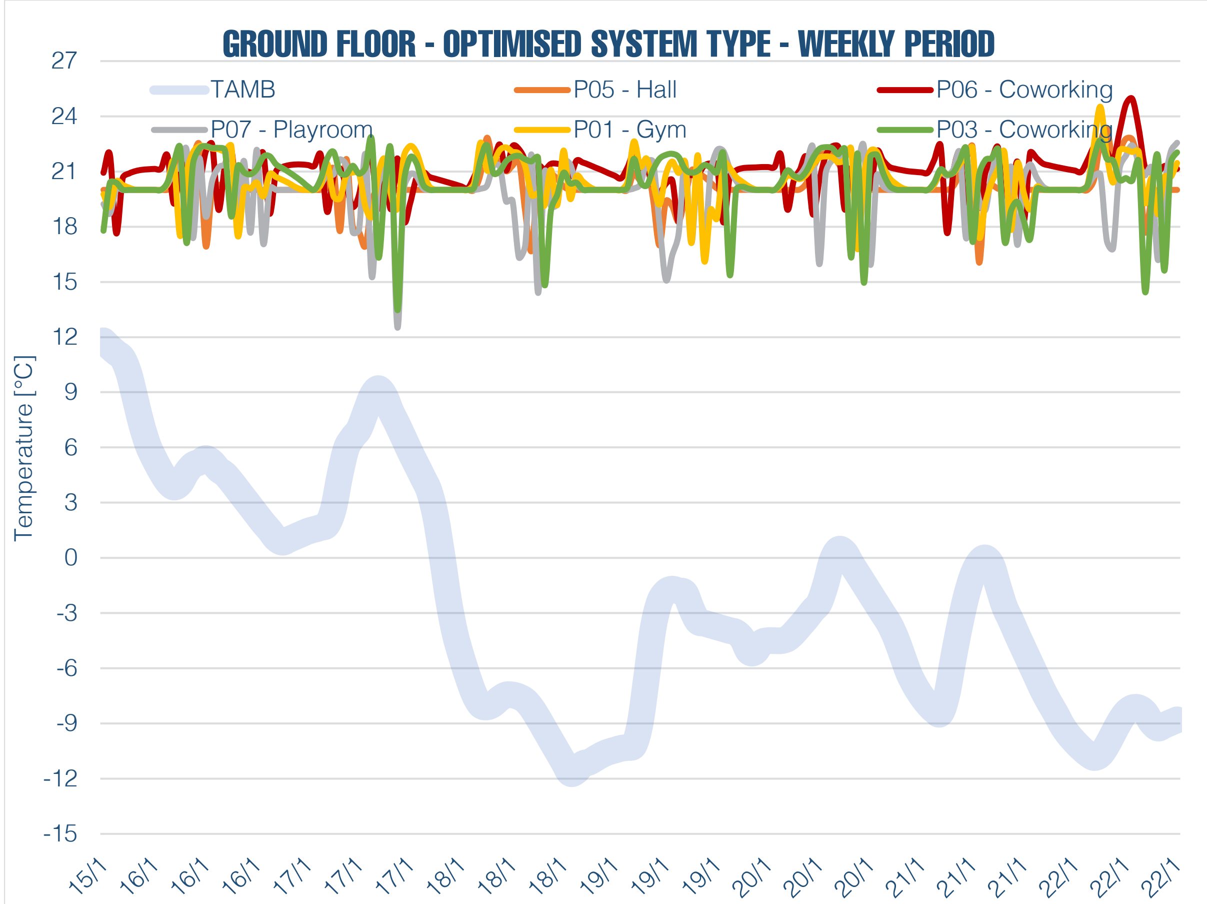

8.13 – THE WORKING TEMPERATURE

To further improve the thermal comfort through the year, the settings of the systems are fundamental. The software lets the designer set the setpoint and setback temperatures. The first ones are the temperatures that the heating and cooling system has to keep during the cold and warm season, while the second ones are the temperatures at which, once reached, the system understand it has to start again. For example, if the setpoint temperature of a heating system is 21°C and the setback is 18°C, as soon as the thermostat records that temperature, the system starts working until the ambient temperature reaches 21°C again.

Many simulations have been run with different values. Using higher temperatures in winter and lower ones in summer would be helpful in terms of thermal comfort since that would be easier to keep acceptable ambient temperatures. However, this would mean that the systems would be working harder and for more hours through the year, resulting in a higher EUI, due to increased heating and cooling needs.

8.13.1 – THE APARTMENTS

Considering the radiant floor, the starting setback temperatures were 18°C and 28°C. Other simulations have been done, considering that such a system does not need very high working temperatures.

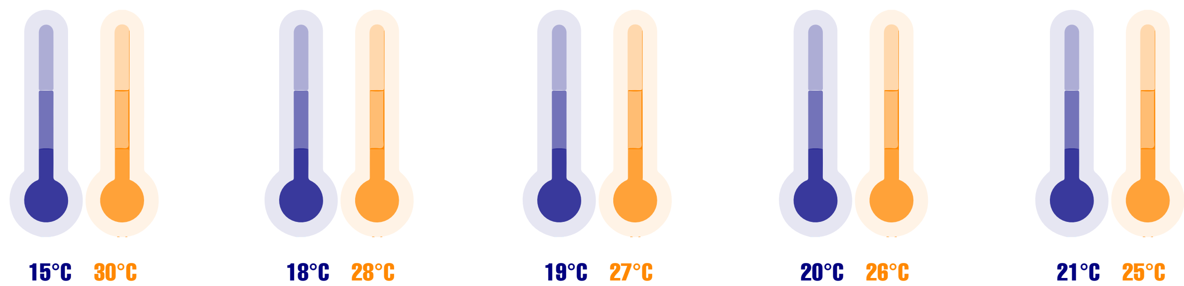

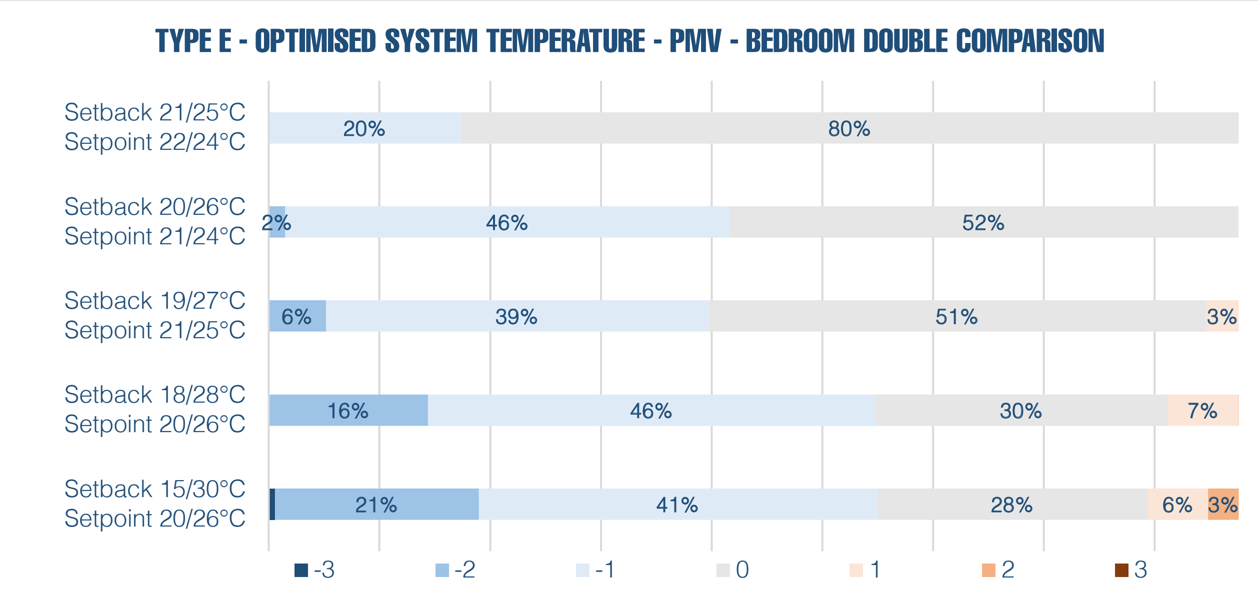

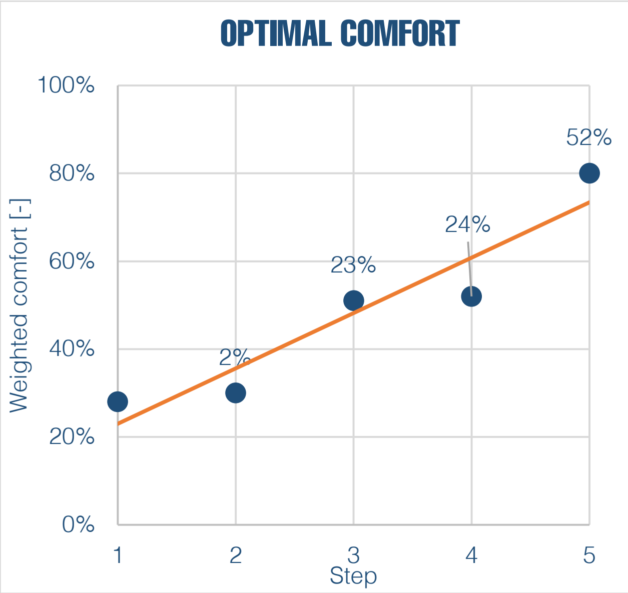

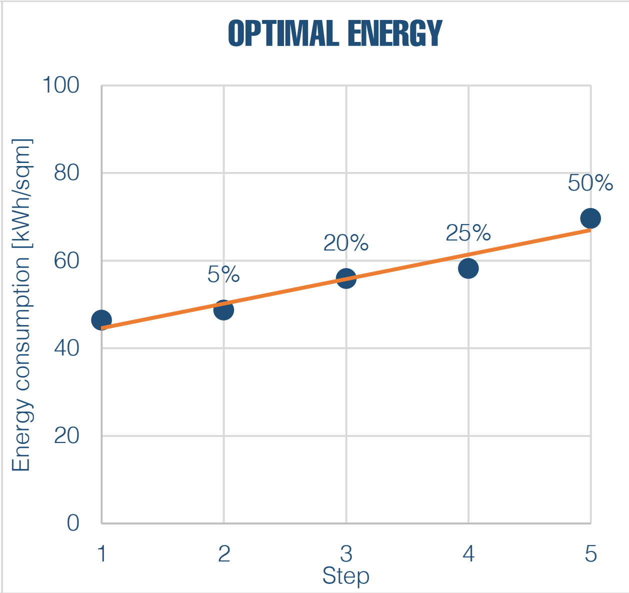

The target was to select the working temperatures so that the combination between these two values creates a positive delta.

Matching the thermal comfort and the consumptions of the building, the chosen setback temperatures are 19°C and 27°C. In fact, these values guarantee an increased comfort value (+23%) with respect to the starting point, but, of course, an higher energy demand (+20%).

Finally, in the annual profile temperature of the apartment, it can be seen how the optimal work of the systems guarantees the dry bulb temperature of every hour to stay within the comfort range.

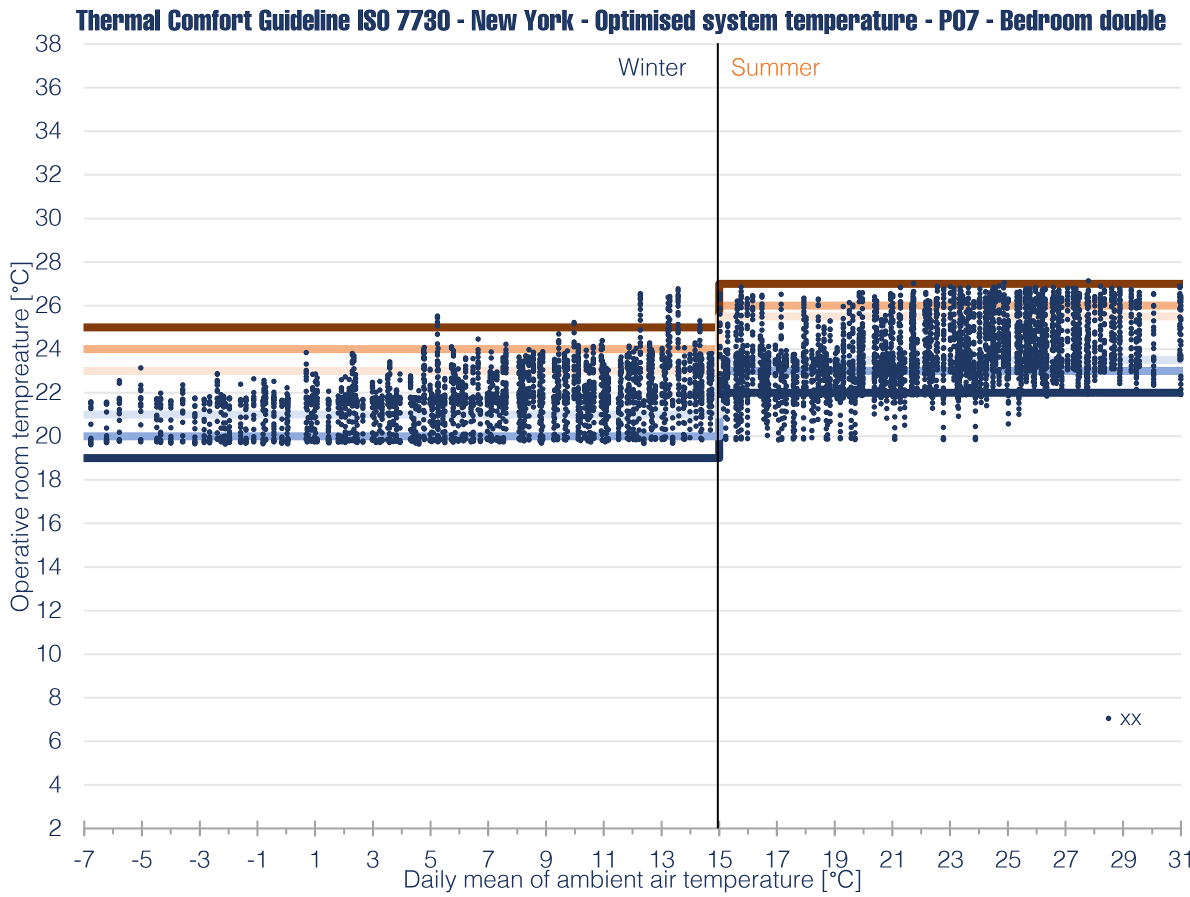

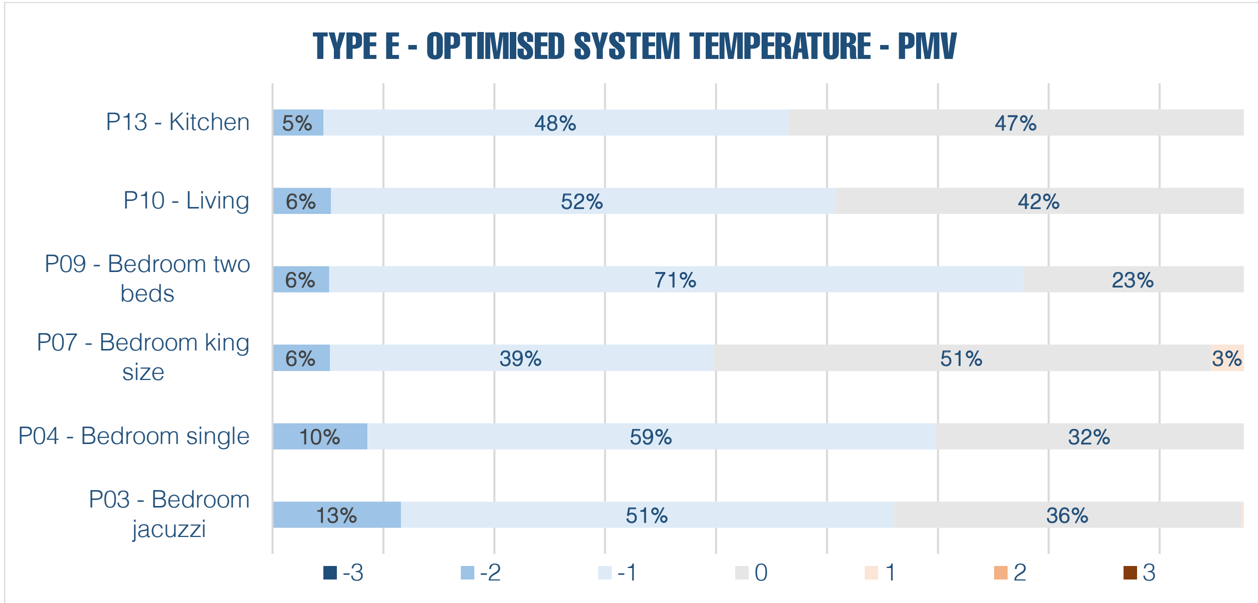

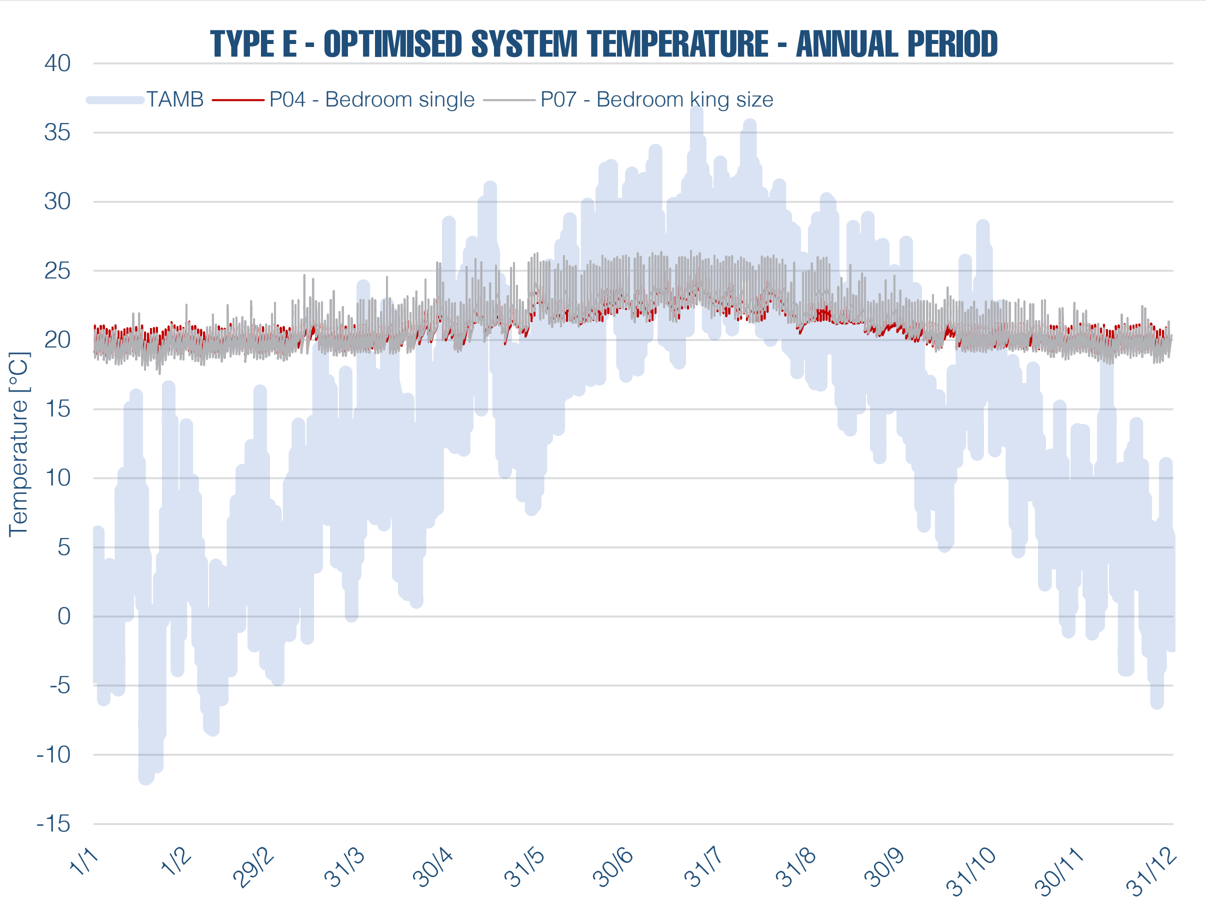

8.13.2 – THE BASEMENT

In this case, the system working system is VRF fancoils. As before, many simulations have been done to select the best range of temperatures in which it would optimally work.

The starting point has setback temperatures equal to 18°C and 28°C.

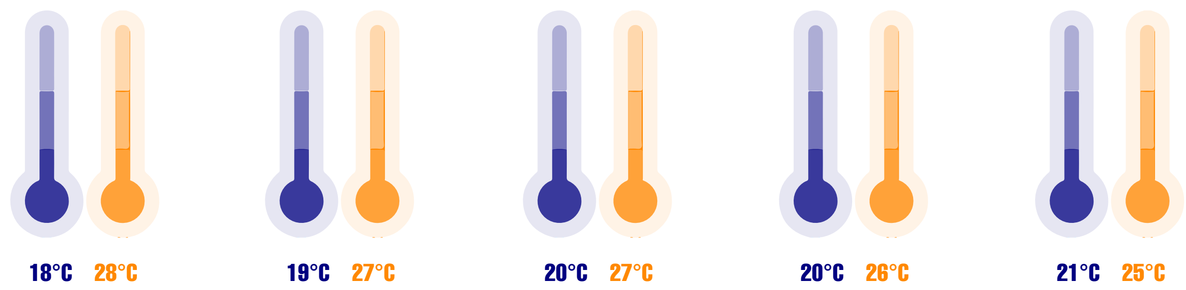

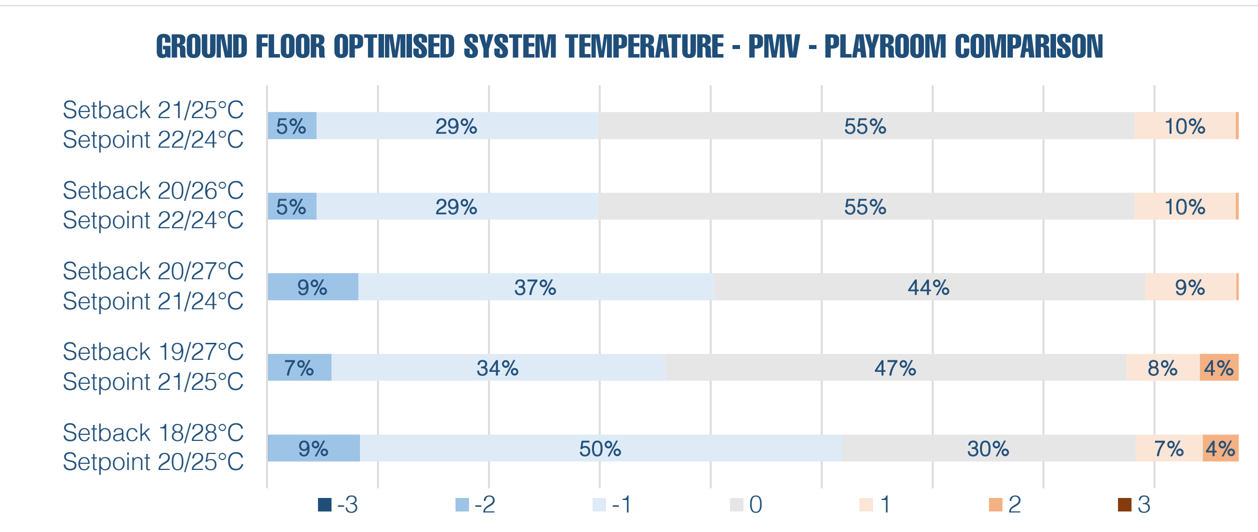

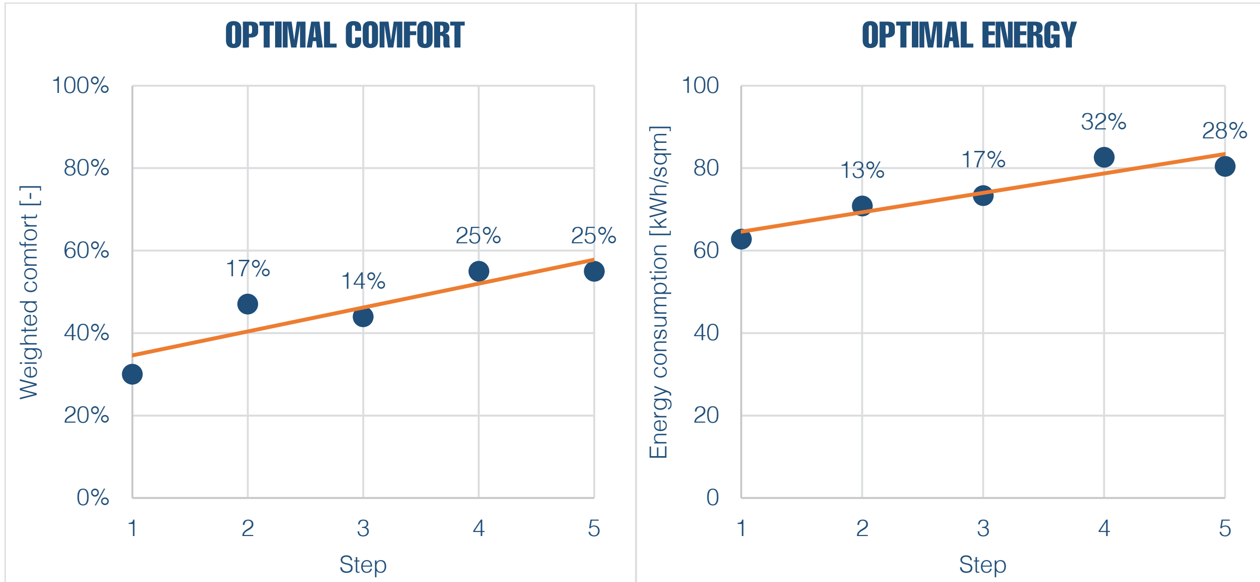

As previously done, the target was to select the working temperatures so that the combination between these two values creates a positive delta.

Finding a compromisebetween the thermal comfort and the consumptions of the building, the chosen setback temperatures are, also in this case, 19°C and 27°C. These values guarantee an increased comfort value (+17%) with respect to the starting point, but, of course, an higher energy demand (+13%).

Finally, in the annual profile temperature of the apartment, it can be seen how the optimal work of the systems guarantees the dry bulb temperature of every hour to stay within the comfort range.

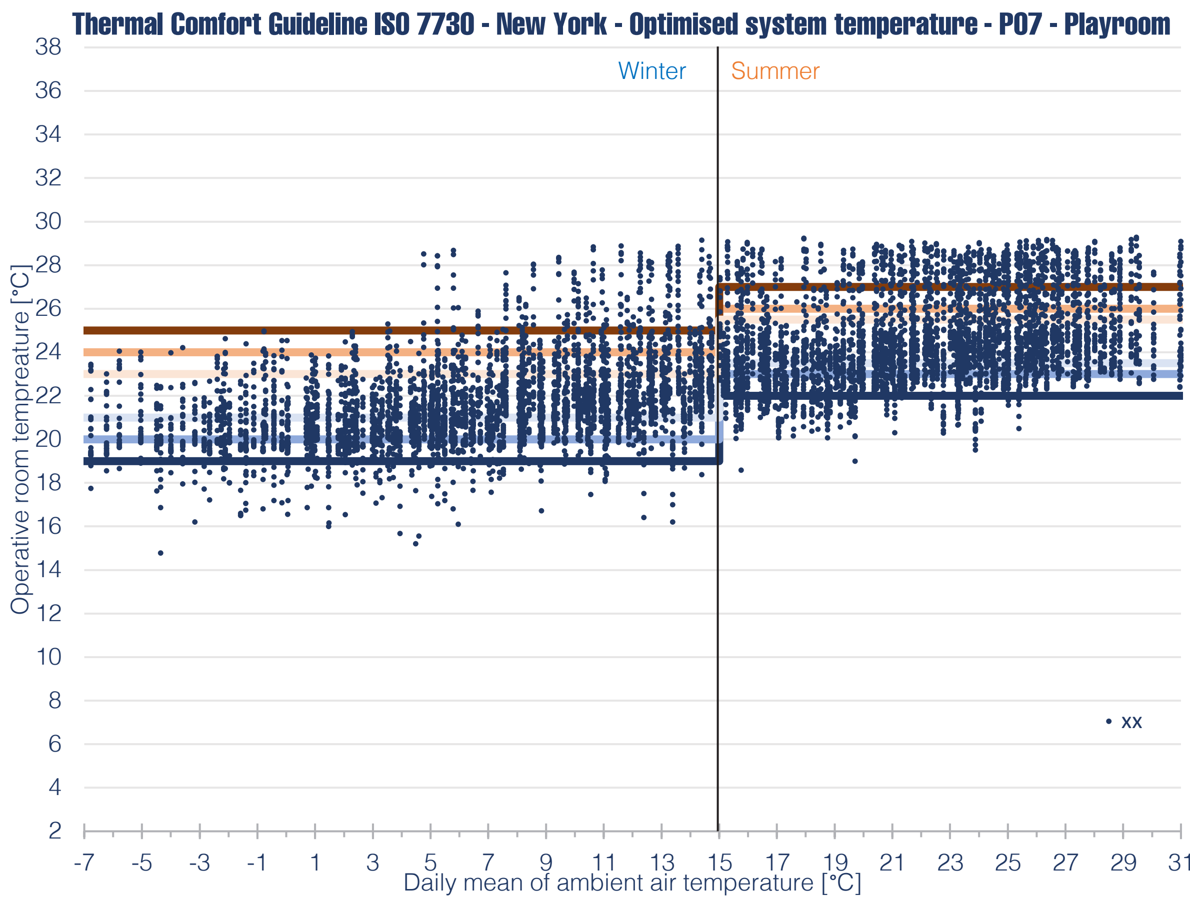

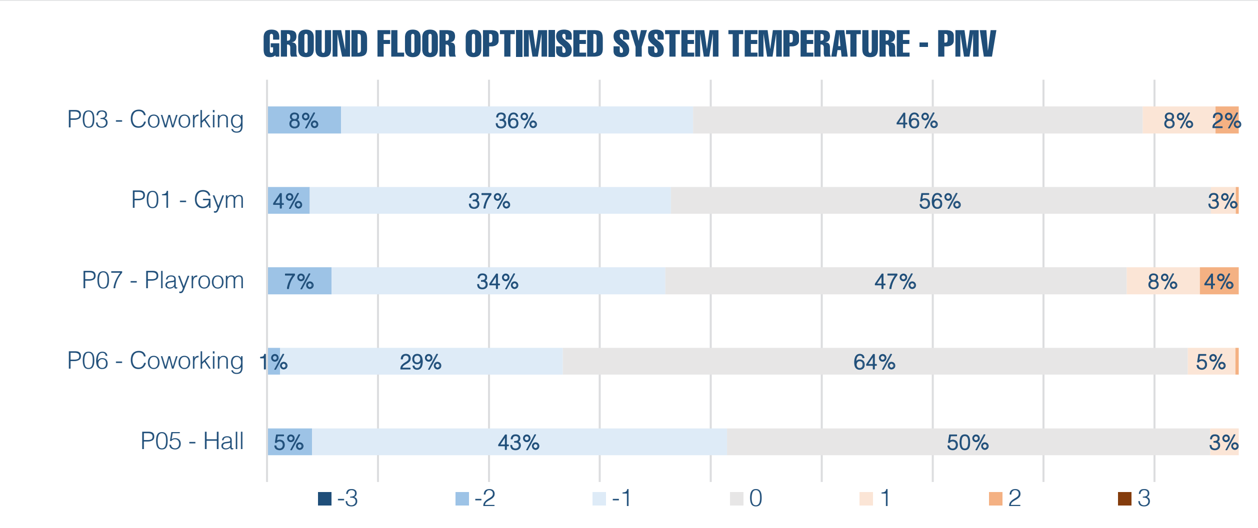

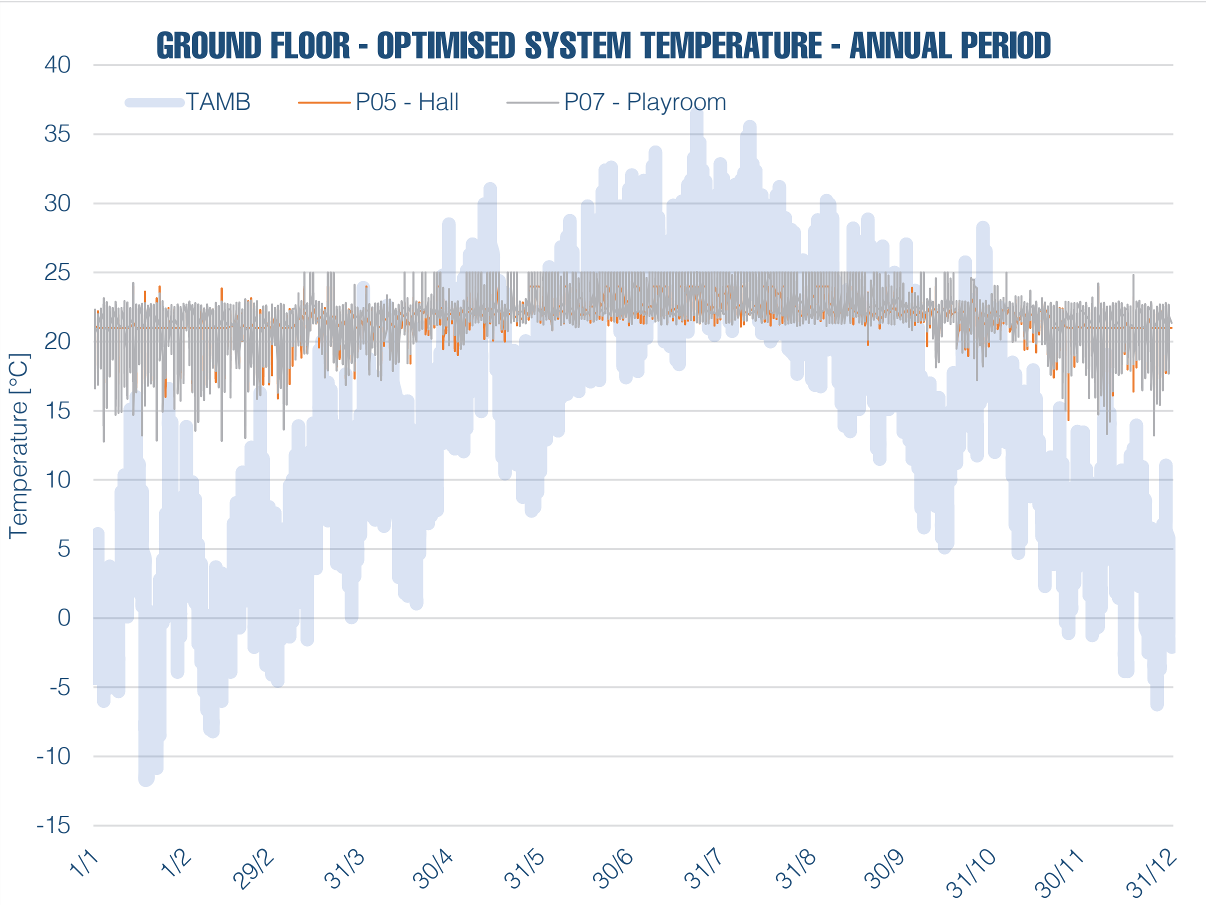

8.13.3 – FINAL ENERGY BREAKDOWN

As it is evident in final the Energy Use Intensity graph, every step of the optimisation improved the performance of the building by decreasing the amount of energy necessary to keep a constant thermal comfort.

In particular, considering the starting point, the sum of the passive strategies manages to almost halve the overall consumption through the year.

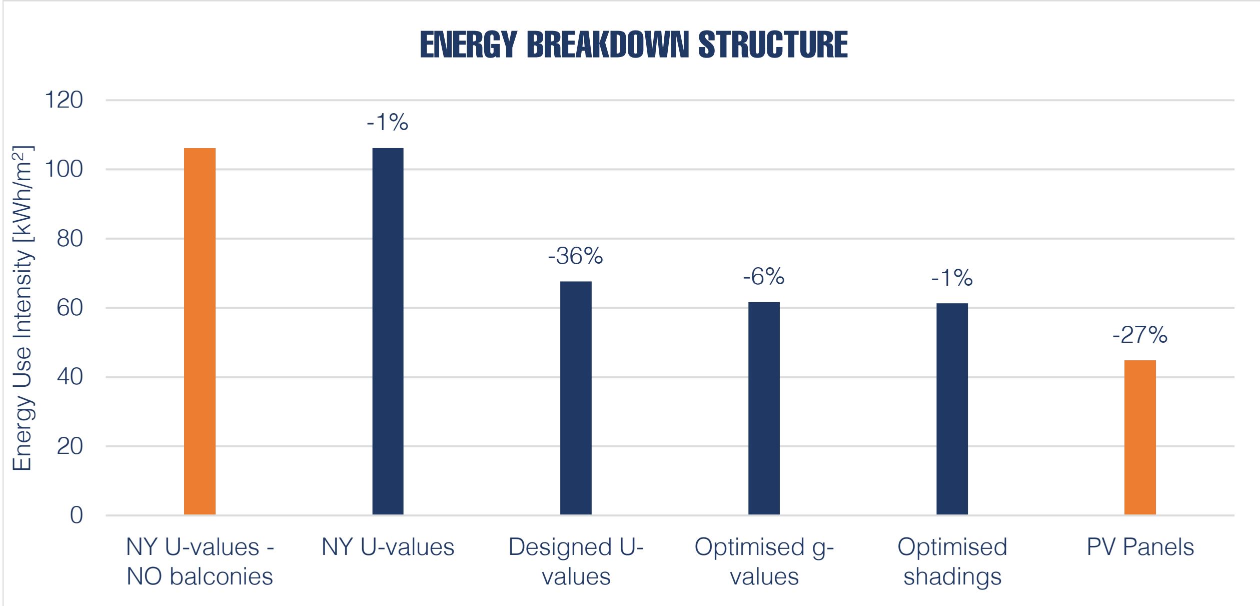

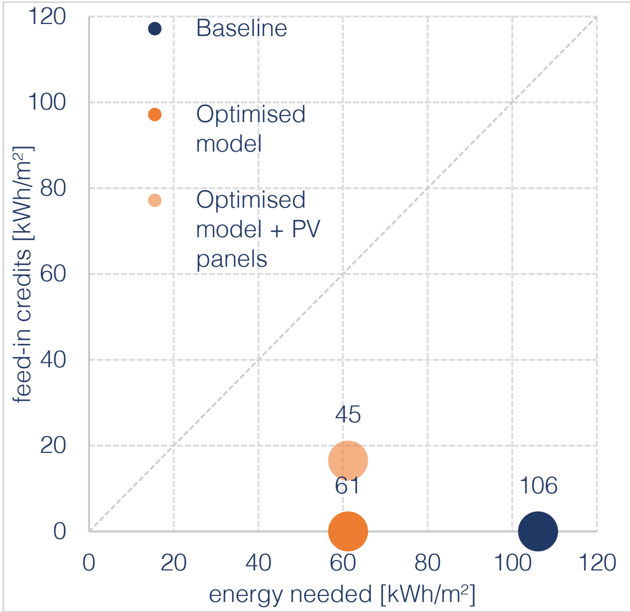

Finally, as a last optimisation, the introduction of a renewable energy source as the sun nstaling a PV panels system, gave the final result. In the end, the optimised solution plus the reneable energy sources allow to have a building which has an energy demand which is decreased by the 57% with respect to the initial condition.

09 CONCLUSIONS ACKNOWLEDGEMENT

CONCLUSIONS

At the end of this long and thorough thesis path, which started from the urban study of the area and ended with the architectural development of the residential centre, greater awareness in architectural and engineering design was reached. The work turns out to be the result of a multi-disciplinary study that has embraced different areas of architecture and engineering.

The different aspects, which have been deepened throughout the whole design process, helped us to develop every detail basing every choice on scientific results. Every characteristic of the building was developed and optimised, but particular attention has been paid to the technological aspects and energy efficiency.

The goal of having a building which can be mostly prefabricated and easily assembled on-site has been reached thanks to the use of light and versatile materials such as steel and timber. Following the instructions of the construction process, in fact, would be the perfect way to build the tower faster than any other buildings, with low risk of making mistakes. Being able to assemble the whole construction without making errors is also fundamental in order to guarantee the final performance of the building itself to meet the expectations during the design phase.

Furthermore, internal comfort has been deeply studied and optimised, and this is strictly related to the success of the assembly process. By running many simulations it was possible to halve the initial consumption of the total building guaranteeing, at the same time, a livable internal environment for the residents of the tower.

The greatest milestone reached with this work is the operational methodology and design process in the development of a complex architectural and engineering project, as a demonstration of the fact that architecture cannot exist without engineering and vice versa. This work, at the end of the two years of the Master of Science in Building and Architectural Engineering, taught us the basis of an integrated design method that will be useful for our future career in the building sector.

Politecnico di Milano, Master of Science in Building and Architectural Engineering
Steember - Steel and timber for a high rise building in Queens, New York
Chinnici Federico - **Maranesi** Marco

ACKNOWLEDGMENT

Our thanks to all the people who have guided and supported us in this thesis work and along the two-year long path of the master degree course through advice, suggestions and indications. Every Professor we had the pleasure to work with has been extremely useful for us to develop the right attitude and the best approach to the design work.

Our special thanks go to Professor Gabriele Masera, who spent his time and made efforts with us to create and develop our project, correcting our mistakes and helping us to improve and better define our intuitions and ideas.

Marco

I would like to thank all the people who have been on my side during my years at Politecnico di Milano: professors, colleagues and friends.

In particular, my warmest thanks are for my family, who always helped and encouraged me to never give up, even in the hardest times.

The most special gratitude is for my mother and my sister, who are my reference point. They taught me that all the sacrifices and efforts made are repaid in the end. Finally, a huge thank goes to my father who, being an Architect, firstly made me love the building sector and later gave me sound advice due to his long-term experience.

Federico

I would like to conclude this work with a special greeting to all the people who helped me complete this two-year course and, more in general, to all the people who made my educational path richer.

Lots of thanks go to my parents for their support.

I also address a special thought to Andrea, Michael and Alessandro, with whom I shared some parts of this thesis on different moments, receiving appreciations, hints and suggestions to further enhance the project.

REFERENCES

BIBLIOGRAPHY

- *C. Benedetti; "Costruire in legno. Edifici a basso consumo energetico", Bozen-Bolzano University Press, 2014*
- *S. Gagnon, C. Pirvu; "CLT Handbook", FP Innovations, U.S. edition, 2018*
- *M. Green; "The case for tall wood buildings", MGA, 2017*
- *S. Jones; "Mass timber: design and research", ORO editions, 2017*
- *J. Natterer, T. Herzog, R. Schweitzer, M. Volz, W. Winter; "Timber Construction Manual", Birkhaeuser - Detail, 2004*
- *A. Bernheimer; "Timber in the city"; ORO editions, 2015*
- *M. Hegger, M. Fuchs, T. Stark, M. Zeumer; "Energy manual", Birkhaeuser - Detail, 2008*
- *A. Athienitis, W. O'Brien; "Modeling, Design, and Optimization of Net-Zero Energy Buildings", Wiley, 2015*
- *K. Voss, E. Musall; "Net zero energy buildings", 2013*
- *L. Bertolini; "Materiali da costruzione – struttura, proprietà e tecnologie di produzione ", Città Studi Edizioni, 2010*
- *G. Salvalai; "2020. Edifici ad energia quasi zero (nZEB)", Maggioli Editore, 2015*
- *F. Hall, R. Greeno; "Building Services Handbook", Elsevier, 2008*
- *G. Toniolo; "Tecnica delle Costruzioni – Elementi strutturali in acciaio", Masson, 1990*
- *A. A. Bell Jr., "HVAC equations, data, and rules of thumb", McGraw-Hill, 2000*

ARTICLES

- *M.H. Ramage et al.; "The wood from the trees: The use of timber in construction. Renewable and Sustainable Energy Reviews", 2017*
- *K. Mahapatra, L. Gustavsson; "Multi-storey timber buildings: breaking industry path dependency", Journal Building Research & Information, Volume 36, 2008 - Issue 6*
- *V. Ž. Leskovar, M. Premrov; "An approach in architectural design of energy-efficient timber buildings with a focus on the optimal glazing size in the south-oriented façade", 2011*
- *V. Ž. Leskovar, M. Premrov; "Influence of glazing size on energy efficiency of timber-frame buildings", Construction and Building Materials,Volume 30, May 2012, Pages 92-99*
- *T. Kalamees, Ü. Alev, M. Pärnalaas; "Air leakage levels in timber frame building envelope joints", Building and Environment, Volume 116, 1 May 2017, Pages 121-129*
- *J.F.Nicol, M.A.Humphreys; "Adaptive thermal comfort and sustainable thermal standards for buildings", Energy and Buildings,Volume 34, Issue 6, July 2002, Pages 563-572*

STANDARDS AND REGULATIONS

- *NYC Codes, Buildings, 2014 Construction codes; Rules*
- *NYC Codes, Buildings; 2.1.12 - Residential Envelope Module*
- *NYC Codes, Buildings; 2.1.13 - Commerciall Envelope Module*
- *NYC Department of housing preservation & development; HPD design guidelines*
- *UNI EN ISO 13788:2013 - Prestazione igrotermica dei componenti e degli elementi per edilizia - Temperatura superficiale interna per evitare l'umidità superficiale critica e la condensazione interstiziale - Metodi di calcolo*
- *UNI EN ISO 7730, 2006 - Ergonomics of the thermal environment - Analytical determination and interpretation of thermal comfort using calculation of the PMV and PPD indices and local thermal comfort effects.*
- *EN 15251, 2007 - Indoor environmental input parameters for design and assessment of energy performance of buildings addressing indoor air quality, thermal environment, lighting and acoustics*

Politecnico di Milano, Master of Science in Building and Architectural Engineering
Steember - Steel and timber for a high rise building in Queens, New York
Chinnici Federico - **Maranesi** Marco

- *Eurocode 1: Actions on structures. EN 1991-1-1*
- *Eurocode 2: Design of concrete structures. EN1992-1-1*
- *Eurocode 3: Design of steel structures. EN 1993-1-1*
- *Eurocode 5: Design of timber structures. EN 1995-1-1*
- *D.M. 17 gennaio 2018: "Norme tecniche per le costruzioni"*
- *ASCE 7: Minimum design loads for buildings and other structures; 49 CFR 193.2013*
- *ANSI/ASHRAE Standard 55-2017: Thermal environmental conditions for human occupancy*

SITOGRAPHY

- https://up.codes/codes/new_york
- https://www.britannica.com/place/New-York-City
- http://www.aianys.org/rules-regulations
- http://www.oasisnyc.net
- https://www.dos.ny.gov/cnsl/lg03.htm
- http://www.immdesignlab.com
- http://www.promolegno.com
- https://www.galimberti.eu
- http://www.oppo.it
- http://www.alveox.it
- https://www.fermacell.it
- https://gutex.de
- https://www.mapei.com
- https://www.rothoblaas.com
- https://www.klh.at/it
- https://www.hoepli.it
- https://www.riwega.com
- https://www.leca.it
- https://www.xlamdolomiti.it
- https://www.unitherm.it
- https://www.schueco.com
- http://bituver.it
- https://sefaira.com/
- https://meteonorm.com/
- https://energyplus.net/weather